SOUTHAMPTON OCEANOGRAPHY CENTRE

CRUISE REPORT No. 37

RRS *DISCOVERY* CRUISE 253
04 MAY - 20 JUN 2001

Faeroes, Iceland, Scotland Hydrographic and
Environmental Survey (FISHES)

Principal Scientist
J T Allen

2001

George Deacon Division for Ocean Processes
Southampton Oceanography Centre
University of Southampton
Waterfront Campus
European Way
Southampton
Hants SO14 3ZH
UK

Tel: +44 (0)23 8059 6382
Fax: +44 (0)23 8059 6204
Email: jta@soc.soton.ac.uk

DOCUMENT DATA SHEET

AUTHOR
ALLEN, J T et al

PUBLICATION DATE
2001

TITLE
RRS *Discovery* Cruise 253, 04 May-20 Jun 2001. Faeroes, Iceland, Scotland Hydrographic and Environmental Survey (FISHES).

REFERENCE
Southampton Oceanography Centre Cruise Report, No. 37, 206pp.

ABSTRACT

The FISHES 2001 cruise, RRS *Discovery* Cruise 253, was split into two legs. A large scale CTD survey of the Iceland Basin and Rockall Trough was carried out during the first and longer leg, 4 May – 21 May. The second leg, 1 June – 20 June, concentrated on repeated high resolution SeaSoar surveys of the Iceland Faeroes Front (IFF). A wide range of measurements were made alongside each scale of physical survey techniques used for the two legs of the cruise. These ranged from traditional biological sampling using net hauls to fast repetition fluorometric techniques for the underway determination of primary productivity parameters. Deck phytoplankton incubation experiments under controlled light environments involved both the usual measurements of N^{15} uptake and measurements of Si^{32} uptake. During the second leg of the cruise, a regional multi-disciplinary process model was used to forecast observations in near real-time.

KEYWORDS
ACRONYM, ATLNENROC, ATLNN, CRUISE 253 2001, CTD OBSERVATIONS, *DISCOVERY*, FISHES 2001, ICELAND BASIN, ICELAND FAEROES FRONT, ROCKALL TROUGH, SEASOAR

ISSUING ORGANISATION
Southampton Oceanography Centre
Empress Dock
European Way
Southampton SO14 3ZH UK

Copies of this report are available from: **National Oceanographic Library, SOC** *PRICE*: £43.00
Tel: +44(0)23 80596116 Fax: +44(0)23 80596115 Email: nol@soc.soton.ac.uk

Contents

SCIENTIFIC PERSONNEL

ALDERSON, Steven	Legs 1 and 2	SOC-JRD
ALLEN, John (Principal Scientist)	Legs 1 and 2	SOC-GDD
AVGOUSTIDI, Vallia	Leg 2	SOC-SOES
BENEY, Martin	Leg 2	SOC-OED
BENSON, Jeff	Legs 1 and 2	SOC-OED
BROWN, Louise	Leg 1	Queens Univ, Belfast
CORNELL, Vic	Leg 2	SOC-ITG
CRISP, Nick	Legs 1 and 2	SOC-GDD
CUNNINGHAM, Stuart	After 19/5 Leg 1	SOC-JRD
DUCKLOW, Hugh	Leg 1	VIMS, Virginia, USA
FEIGHERY, Lisa	Leg 1	Univ of Galway, Eire
FIELDING, Sophie	Legs 1 and 2	SOC-GDD
HARLE, James	Leg 1	SOC-GDD
HARRIS, Andy	Leg 2	SOC-OED
HYDES, David	Leg 2	SOC-GDD
HOLLIDAY, Penny	Legs 1 and 2	SOC-GDD
IRIGOIEN, Xabier	Leg 1	SOC-GDD
JOHNSON, Martin	Leg 1	Env Chem, UEA
JOHNSON, Helen	Leg 2	Univ of Reading
KEOGH, Bob	Legs 1 and 2	SOC-OED
LLOYD, Rob	Leg 1	SOC-OED
LUCAS, Mike	Legs 1 and 2	SOC-GDD
McCALLISTER, Leigh	Leg 1	VIMS, Virginia, USA
MOORE, Mark	Legs 1 and 2	SOC-SOES
MUSTARD, Alex	Legs 1 and 2	SOC-GDD
NELSON, Paul	Leg 1	Env Chem, UEA
NOLAN, Glen	Leg 2	Univ of Galway, Eire
O'HIGGINS, Tim	Legs 1 and 2	Dublin, Eire
O'REILLY, Naoise	Leg 1	SOC-JRD
PHIPPS, Ritchie	Legs 1 and 2	SOC-OED
POLLARD, Raymond	Before 19/5 Leg 1	SOC-GDD
POND, Dave	Leg 1	SOC-GDD
POPOVA, Katya	Leg 2	SOC-GDD
RIGGS, James	Leg 2	SOC-OED
RIXON, Michel	Leg 2	SOC-GDD
ROBERTS, Rhys	Legs 1 and 2	SOC-OED
SANDERS, Richard	Leg 1	SOC-GDD

SMEED, David	Leg 2	SOC-JRD
SMITHERS, John	Legs 1 and 2	SOC-OED
SROKOCZ, Meric	Leg 2	SOC-JRD
WYNAR, John	Legs 1 and 2	SOC-OED

SOC - Southampton Oceanography Centre
GDD - George Deacon Division
JRD - James Rennell Division
SOES - School of Ocean and Earth Sciences
OED - Ocean Engineering Division
UEA - University of East Anglia
VIMS - Virginia Institute of Marine Sciences

SHIP'S PERSONNEL

CHAMBERLAIN, Roger	Master
WARNER, Richard	Chief Officer
OLDFIELD, Phil	2nd Officer
REYNOLDS, Peter	3rd Officer
KISHORKUMAR, Jet	Chief Engineer
GREENHORN, Alex	2nd Engineer
CONNOR, Keith	3rd Engineer
BELL, Steve	3rd Engineer
STEWART, Dave	Electrical Engineer
TREVASKIS, Mike	CPO(D)
LEWIS, Greg	PO(D)
SMYTH, John	Motorman 1.A. (Leg1)
STEWART, Terence	Motorman 1.A. (Leg2)
WYNESS, Martin	S.1.A.
MACLEAN, Andy	S.1.A.
DICKINSON, Bob	S.1.A.
HEBSON, Harry	S.1.A.
COOPER, Gerry	S.1.A.
HAUGHTON, John	S.C.M.
CONNELLY, Dave	Chef
KUJAWIAK, Andy	M/S
ORSBORN, Jeff	STWD
STEPHEN, Mick	STWD

LIST OF FIGURES

RRS *Discovery* Cruise 253 (legs 1 and 2) 4th May 2001-20th June 2001. FISHES (Færœs, Iceland, Scotland Hydrographic and Environmental Survey), physical, biological and chemical observations in the Iceland Basin, Rockall Trough and Iceland-Færœs Front regions of the NE Atlantic.

J T Allen and R T Pollard

ABSTRACT

The FISHES 2001 cruise, RRS *Discovery* cruise 253, was split into two legs. A large scale CTD survey of the Iceland Basin and Rockall Trough was carried out during the first and longer leg, 4th May - 31st May. The second leg, 1st June to the 20th June, concentrated on repeated high resolution SeaSoar surveys of the Iceland Færœs Front (IFF). A wide range of measurements were made alongside each scale of physical survey techniques used for the two legs of the cruise. These ranged from traditional biological sampling using net hauls to fast repetition flourometric techniques for the underway determination of primary productivity parameters. Deck phytoplankton incubation experiments under controlled light environments involved both the usual measurements of N^{15} uptake and measurements of Si^{32} uptake. During the second leg of the cruise, a regional multi-disciplinary process model was used to forecast observations in near real-time.

1. INTRODUCTION

The FISHES 2001 cruise repeated the occupation of a number of hydrographic lines between Scotland and Iceland (Figure 1) and carried out detailed multidisciplinary surveys of the northern ends of the Iceland Basin (including the Iceland Færœs Front - IFF) and Rockall Trough to resolve both basin- and meso-scale physical, chemical and biological structure. Two scales of survey were undertaken, one with full-depth CTDs at 20-50 km intervals, the other with the towed SeaSoar vehicle to resolve scales of variability at the IFF from a few km up to 100 km. The SeaSoar surveys were repeated three times to examine temporal change.

A wide range of measurements were made alongside each scale of physical survey technique. These ranged from traditional biological sampling using net hauls to fast repetition flourometric techniques for the underway determination of primary productivity parameters. The number of scientific staff required to support all of the measurements made exceeded the number of berths available on RRS *Discovery* and thus the cruise was split into two legs. The large scale survey of the Iceland Basin and Rockall Trough was carried out during the first and longer leg, 4th May - 31st May. The second leg, 1st June to the 20th June, concentrated on the repeated high resolution surveys of the IFF.

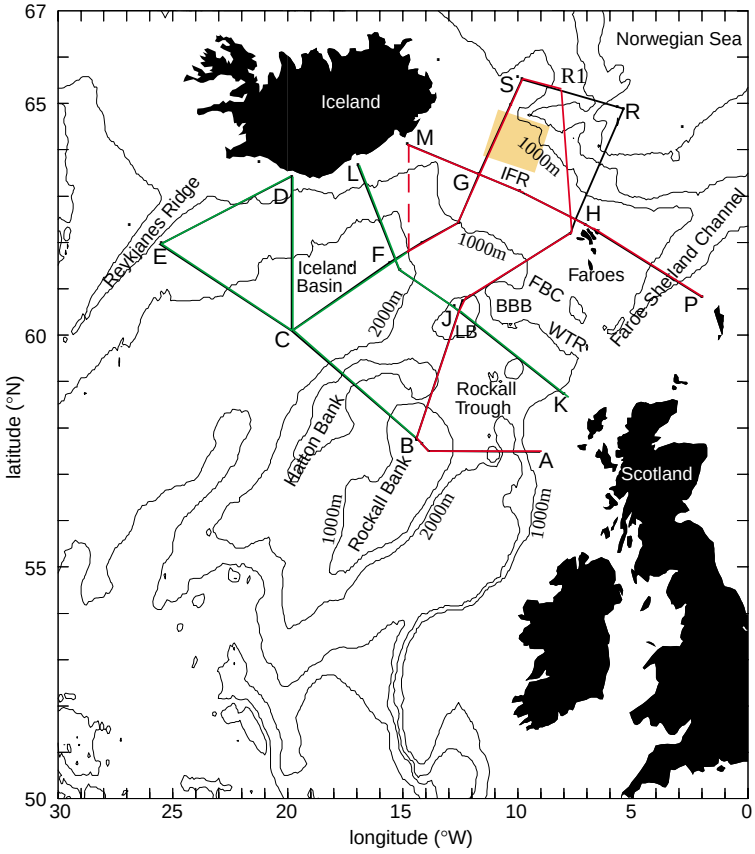

Figure 1: Cruise track for FISHES, green lines are the CTD sections prior to the boat transfer on the 19th May, red lines are the CTD sections after the 19th May but prior to the end of leg 1 of the cruise and the orange box shows the location of the three high resolution SeaSoar surveys during leg 2 of the cruise.

During the first leg of D253, a detailed comparison between two CTD systems was made. The timing of the FISHES cruise caught the SOC in a transition period between Neil Brown and SeaBird CTD systems. The cruise provided an ideal opportunity to inter-calibrate the two systems over a number of hydrographic sections for which the SOC holds a significant time series of CTD measurements. An optical particle counter (OPC) had been added to the Neil Brown instrumented CTD frame and data from this and the CTD were handled using two superimposed FSK signals that could be separated at the deck unit. Deck incubations under controlled light environments were carried out using samples from early morning CTD stations. However, the usual measurements of N^{15} uptake were paralleled by measurements of Si^{32} uptake. These latter measurements are quite novel and provide a new insight to primary productivity in diatom dominated regimes. In total, 132 CTD and net haul stations were completed in 24 days.

The three repeat high resolution multi-disciplinary SeaSoar surveys that dominated the second leg of D253 covered an area of approximately 100 km * 100 km. The position for these surveys was determined from an analysis of satellite IR and ocean colour images. A regional multi-disciplinary process model was used to forecast the observations in near real-time. The design of repeated SeaSoar surveys, in terms of cross track spacing, the direction of the survey relative to the propagation of instabilities and the primary direction of survey legs, was determined using a genetic algorithm technique to optimise sampling patterns according to

mapping error. The reliability of model forecasts was extended by assimilating data from the SeaSoar surveys in near real time, creating a feedback loop to improve the efficiency of our observing capability. A 24 hour gap between each SeaSoar survey provided time for targetted station sampling; the positions of these stations were also closely related to model forecast structures.

2. OBJECTIVES

The objectives of RRS *Discovery* cruise 253, FISHES, remained very similar to those in the original cruise proposal and were:

i. to continue our examination of inter-annual variability by reoccupation of Scotland-Rockall-Iceland sections. Occupying survey lines under altimetric satellite tracks, wherever possible, so that sub-seasonal temporal change of surface currents can be resolved over the lifetime of the satellites.

ii. to establish the fate of North Atlantic Current (NAC) pathways from the North Atlantic to the Norwegian Sea (at the time of the survey) and the extent to which upper ocean NAC waters are transported into the Norwegian Sea by eddies.

iii. to map the properties of winter mode waters and to examine whether, for example, saline Eastern North Atlantic Water (ENAW) crosses mean flow paths to circulate from the Rockall Trough to the Reykjanes Ridge.

iv. to map nutrient concentrations, phytoplankton biomass and zooplankton distributions on a basin scale and in relation to physical regimes (eddies, fronts, seamounts, ridges etc). This objective seen as a first step to examining, explaining and modelling their basin scale variability.

v. to investigate the mesoscale spatial patchiness of nutrient concentrations, phytoplankton biomass and zooplankton distributions with a view to interpreting and quantifying their interactions and response to physical forcing. Specifically, to determine the effect of grazing pressure on the spring phytoplankton bloom.

vi. to contribute to Techniques for Optimising Environmental Surveys (TOES, an MOD/NERC Joint Grant Scheme project) by testing algorithms to optimise sampling strategies and objectively design surveys according to measurement error and logistic constraints.

vii. to compare the properties of the deep outflows through the Færœ Bank Channel and over the Iceland Færœs Ridge and their downstream modification.

viii. to utilise new sensors and test their ability to enhance observation at the mesoscale.

3. BACKGROUND

Many surveys had been conducted in the area in the past, so we here summarise the understanding of the circulation and structure of the region which was important to our specific objectives.

Bathymetry

The area lies at the very north-eastern corner of the North Atlantic Ocean (Figure 1). It is bounded to the north by the Iceland Færœs Ridge (400-500 m deep) between Iceland and the Færœ Islands and by the Wyville-Thomson Ridge extending from south of the Færœs to the Scottish continental shelf. The 800m deep Færœ Bank Channel between the Wyville-Thomson Ridge and the Færœs is the only deep channel between the Atlantic and Norwegian Seas. The Iceland Basin is bounded by Iceland and the Reykjanes Ridge to the north and west and by the Rockall-Hatton Plateau to the east. The Rockall Trough is bounded by the Rockall-Hatton Plateau to the west, by Lousy Bank, Bill Bailey's Bank and the Wyville-Thomson Ridge to the north and by the Scottish shelf to the east. Channels between Bill Bailey's Bank, Lousy Bank and the Rockall-Hatton Plateau reach depths of 1200m, but in general both the Iceland Basin and the Rockall Trough are closed below about 1000m on all sides but the south. Thus the deep circulation is severely constrained by the bathymetry. While water in the upper 1000m (which was the primary focus of FISHES) can circulate freely, it too is constrained by the bathymetry beneath and by how much geostrophic shear can be supported by contrasting water masses in the top 1000m.

Transport

The region has relatively weak circulation and strong eddies, making the mean circulation hard to quantify. Work prior to the early 1990s is described by van Aken and Becker (1996) , who state that "the large-scale circulation pattern and its variability in the north-eastern North Atlantic Ocean was not well established until now". From the NANSEN surveys (1988-1991) van Aken and Becker conclude that 7 Sv (1 Sverdrup = 1 Sv = $10^6 m^3 s^{-1}$) of upper layer water (σ_0<27.7kg m^{-3}) from the North Atlantic Current (NAC) passes north through the Iceland Basin and 3 Sv through the Rockall Trough. However, they also remark that their transport scheme, derived by inverse analysis, "only shows the mean transport per basin, since distinction of flow around eddies from recirculation within the basin could not be achieved". Bacon (1997), from a synoptic data set in 1991, derives 16 Sv of northward flow through the Iceland Basin just west of Hatton Bank, and Pollard et al. (1999), from a synoptic data set in 1996, derive 14 Sv of northward flow through the Iceland Basin and a further 3 Sv through the Rockall Trough. The

cause of the substantial differences between these estimates is not clear. There may well be temporal variability in the position of the subpolar gyre, as shown recently by Bersch et al. (1999) . Indeed, van Aken and Becker, Bacon and Pollard et al. find 23 Sv, 25 Sv and 27 Sv respectively for the total transport of the NAC across 54°N, which are not so different. The differences arise in the split between the transports through the Irminger Basin (13, 9 and 10 Sv) and the Iceland Basin (7, 16 and 14 Sv).

However, Pollard et al.'s estimate of the transport into the Norwegian Sea between Iceland and Scotland (14 Sv) definitely seems too large. Van Aken and Becker's estimate of 7 Sv is supported by moored measurements (as part of Nordic WOCE and VEINS). Hansen et al. (1999) show 4 Sv passing north of the Færœs and 3 Sv through the Færœ-Shetland Channel. Further downstream, Orvik et al. (1999) find 7.8 Sv crossing the Svinøy section west of Norway.

Also, despite recent observations as part of Nordic WOCE and VEINS, the pathways for the flow between the Iceland Basin and the Norwegian Sea are not fully clear. Shelf-edge flow west of Scotland is well documented, but is it augmented further north by water that has flowed through the Iceland Basin and turned east to the south of the Færœs? Where exactly does the flow that enters the Norwegian Sea west then north of the Færœs crosses the Iceland-Færœ Ridge? Hansen et al. (1999) sketch the flow close to the west of the Færœs. Pollard et al. (1999) show the flow close to the Iceland coast. Of course, their choice of reference level is suspect, because of the deep flow of Iceland-Scotland Overflow waters (ISOW) in the opposite direction as described by Saunders (1990). On the other hand, north-eastward flow in the surface layer close to the Iceland coast is consistent with the path and strength of Modified North Atlantic Water (MNAW) in the Iceland Færœs Front as documented by Read and Pollard (1992) and by Allen et al. (1994).

Our near-synoptic survey grid was designed to cross all possible flow pathways in order to quantify the transports at one moment in time (with CTD, ADCP, Lowered ADCP and inverse modelling) and to seek to distinguish mean and eddy components using satellite altimetry.

Mode Water

Deep winter mixed layers are found over the majority of the survey area, so that varieties of winter mode water are the dominant upper ocean water masses. These are generically called Subpolar Mode Water (SPMW) following McCartney and Talley (1982), and locally are varieties of North Atlantic Water, such as Eastern North Atlantic Water (ENAW) and MNAW. North of the Iceland Færœs Front (IFF), fresh Arctic surface water reduces mixed layer depths considerably, though Read and Pollard (1992) found a patch of mode water, Norwegian North Atlantic Water (NNAW), north of the front.

The accepted picture of the formation of SPMW in the northern North Atlantic until now has been that given by McCartney and Talley (1982). Talley (1999) states that "The SPMW was depicted therein as moving smoothly eastward and then northward and thence cyclonically around the subpolar gyre into the Labrador Sea". Recent work challenges that interpretation. Talley (1999) argues that the deep mixed layers are confined to the boundary regions and that large areas of coherently low potential vorticity terminate abruptly switching to another density, particularly across the NAC. Pollard et al. (1999) find the most weakly stratified mode water to the east of each of two major currents, the Irminger Current up the western flank of the Reykjanes Ridge and the NAC extension through the Iceland Basin on the western flank of the Hatton Plateau. They give three reasons for this distribution, the import of high salinities in the surface layer that weaken the stratification, the anticyclonic circulation in both regions and the preference for mode water to form where currents are weak. This is because, conversely, where there are strong surface currents there is the potential to maintain the stratification of the surface layer by advection. Read (2001) also finds patchiness in the distribution of mode waters. Indeed, she finds that the inflowing Western North Atlantic Water in the NAC is relatively well stratified compared to the more saline ENAW whose recent formation by winter mixing was documented by Pollard et al. (1996).

Pollard et al. (1999) point out the enigma in the circulation of the north Iceland Basin. Their transport estimates showed no tendency for, widely assumed, cyclonic circulation around the northern margins of the basin, yet mode water properties, salinity in particular, on the eastern flank of the Reykjanes Ridge suggest an origin further east, such as the Rockall Trough. A possible explanation is that eddies breaking off the northward flow, from the Atlantic to the Norwegian Sea, can transport properties across it. Our survey was designed to compare the properties of mode waters, nutrients as well as temperature and salinity, to pin down the circulation of the north Iceland Basin.

Biological implications of weak advection

Pollard et al. (1999) , Read (2001) and Talley (1999) are all agreed that winter mode water is likely to be found where mean currents are weak, and that strong currents actually act as barriers, or at least boundaries, to SPMW distribution. This lack of continuity between different varieties of mode water may have biological implications. If there is rather little advective exchange between different water masses, then phytoplankton and zooplankton community succession may develop quite differently. However, zooplankton which migrate vertically may be able to move indirectly between water masses. Bryant (1999) reports that the Trans-Atlantic Study of *Calanus* (TASC) has observed and modelled the copepod, *C. finmarchius*, moving seasonally between the Norwegian Sea and the North Atlantic. This is achieved through upward migration into the northward surface flow during the summer and downward migration in winter, returning southwards in the ISOW flowing through the Færœ-Shetland Channel.

Nevertheless, plankton in different mode water areas of the north Iceland Basin and Rockall Trough, where mean currents are weak, will be isolated at least during their spring and summer growing season. Satellite images such as those presented by Holligan et al. (1993) frequently show evidence for high biomass south of Iceland with a sharp transition to lower values in the middle of the Iceland Basin. Do these correlate with SPMW on the flank of the Reykjanes Ridge transitioning to stronger currents (remnants of the NAC) in the middle of the Basin ? To gain information on chemical and biological distributions on the large area CTD survey, we mounted a Chelsea Instruments fluorimeter and Focal Technologies OPC on the CTD frame (both in deep pressure cases) in addition to sampling routinely for nutrients.

Mesoscale (~100 km) eddies and their biological implications

Energetically, eddies dominate over mean currents in the north Iceland Basin; White and Heywood (1995) documented this using altimetric satellite variability. Eddy-resolving ocean circulation models such as OCCAM (1/8° x 1/8°) also show this. An interesting phenomenon is the tendency towards long-lasting standing eddies. During PRIME (Plankton Reactivity In the Marine Environment), in 1996, an eddy was studied near 59°N, 20°W which Martin et al. (1998) showed to have existed for at least several months since the previous spring. Read and Pollard (1999) have reported another eddy at virtually the same place during ACSOE (Atmospheric Chemistry Studies in Ocean Environments) in 1998. A satellite tracked drogue showed that the ACSOE eddy precessed by about 100 km, and it lasted for at least six months. OCCAM also shows standing eddies, though their characteristics have yet to be diagnosed. A likely explanation is that standing eddies are topographically trapped wakes, and OCCAM plots do indicate that eddies at the PRIME/ACSOE position could be trapped downstream of where the NAC is turned sharply north-west by the Hatton-Rockall Plateau. Alternatively, eddies might form annually at the end of winter, related to the formation of deeply mixed (over 500m) winter mode water. This hypothesis has yet to be examined.

Whatever, their explanation, long-lived eddies certainly exist, and may, like mode waters, have consequences for plankton trapped within them. Indeed, PRIME and ACSOE deliberately examined the biological and chemical consequences of water trapped in eddies. In our first experiment using an Optical Plankton Counter (OPC) mounted on SeaSoar, Pollard et al. (2000) showed that the distribution of zooplankton carbon was strongly related to fronts in the Southern Ocean, and that different zooplankton size classes had different spatial distributions, possibly relating to their different depth distribution, tendency to vertical migration, and utilisation of ageostrophic circulations near the fronts. Also Read et al. (2000) showed that the largest concentrations of zooplankton were found in an eddy. Fielding et al. (2001) , using acoustic backscatter data, found layers of zooplankton associated with a tongue of subducted phytoplankton at the Almeria-Oran front in the W. Mediterranean. OPC data measuring smaller

zooplankton than the acoustic instruments found the highest abundances in the fast-flowing geostrophic jet associated with the front.

Smaller mesoscale (~10-100 km) eddies and the Iceland Færœs Front (IFF)

In the summer of 1990, RRS *Charles Darwin* cruise 51 (CD51) made a series of high resolution SeaSoar surveys of the IFF. From these surveys Read and Pollard (1992) identified the characteristic T/S relationships between the water masses of Nordic Seas and Atlantic Ocean origin. At the western end of the Iceland Færœs Gap, where the Jan Mayen Front and the IFF are juxtaposed, there is a very steep front between East Icelandic Water (EIW) and MNAW. Further east the front is less well defined: the water mass boundaries become increasingly more convoluted and the presence of a third major upper layer water mass, NNAW, separating the Atlantic and Nordic water masses was observed. On a smaller scale the IFF is perturbed by meanders and small scale (15-30 km) cyclonic and anticyclonic eddies. Repeated surveys allowed Allen et al. (1994) to observe the time development of a few of these structures and make estimates of salt and heat fluxes due to eddy transport. Moreover, the temporal and spatial resolution of the CD51 surveys were sufficient to allow Allen and Smeed (1996) to make a full three dimensional diagnosis of the vertical circulation associated with mesoscale meanders and eddies. These analyses confirmed the conclusions of previous authors such as Pollard and Regier (1992) and Tintoré et al. (1991) that significant vertical circulation of the water column could be driven by eddies and baroclinic frontal instability.

The IFF marks a boundary between plankton communities of temperate and sub arctic origin. Whilst Fraser (1961) identified the presence of patches of Atlantic and Boreal species in the water above the Iceland Færœs Ridge there has not been a study of zooplankton distributions with specific reference to the IFF. Roe et al. (1996), used ADCP acoustic backscatter data from CD51 to identify columns of high zooplankton abundance associated with the edges of eddies and fronts, in addition to conventional diel migratory behaviour. However this data was not supported by net samples. Long running Icelandic studies have described regional characteristics of the surrounding waters as part of their fisheries assessment, although these are biased towards the shelf. None of this research has been able to resolve the effect of mesoscale physical processes on the pelagic communities, however it provides background information on the water masses found in the region of the shelf and IFF. In the spring northern waters are colder and fresher than the Atlantic origin water found in the south. These northern waters may contain slightly lower nutrient concentrations (12.9 as opposed to 13.9 μM NO_3; Stefánsson and Olafsson, 1991), and support lower primary production during the spring bloom (4.3 as opposed to 7.1 mg C m^{-3} h^{-1}; Gudmundsson, 1998).

At these latitudes the spring bloom will start to develop in mid-March (Sakshaug and Slagstad, 1991) , although this is frequently delayed by as much as a month, and usually peaks in late April to mid-May (Gudmundsson, 1998). Gudmundsson (1998) and Thórdardóttir (1984) report a variation in timing of the bloom between the water masses. The decline in the bloom is less well understood: Stefánsson and Olafsson (1991) and Gudmundsson (1998) state that the bloom declines, usually in May and June, as nutrients are depleted in the surface layer. The spring diatom blooms in these areas normally collapse, firstly because of silicate depletion, followed secondly by nitrate and possibly phosphate depletion. This has strong implications for phytoplankton community succession and may result in a population shift from diatoms to large blooms of the coccolithophore *Emiliania huxleyi* (Tyrrell and Taylor, 1996) by June /July of most years (Brown and Yoder, 1994). Such blooms have a considerable impact on ocean-atmosphere pCO_2 gradients (Holligan et al., 1993; Robertson et al., 1993) and on the interpretation of satellite imagery and the light environment of the upper ocean. They dramatically change the light backscattering and absorption qualities of the water. Increased scattering and reflectance reduces the euphotic depth at all PAR wavelengths. This may also help to drive phytoplankton community succession.

However, Gislason and Astthorsson (1998a) observed a reduction in phytoplankton standing stock in northern waters while "nutrients were still high". This decrease was correlated with an increase in zooplankton biomass, especially the herbivorous copepod *Calanus finmarchicus*, and they suggest that "increased grazing pressure" may be reducing phytoplankton standing stock. This species numerically dominates the mesozooplankton in spring, especially at offshore stations, accounting for more than 60% of the abundance in northern waters, and more than 80% in southern waters (Astthorsson et al., 1983; Gislason and Astthorsson, 1998b).

Techniques for Optimising Environmental Surveys (TOES)

At the mesoscale, the balance between scale resolution and synopticity of an individual survey as a one time observation, becomes critical to understand the errors in the diagnosed dynamics of the flow. Recent research results by Allen et al. (2001) can be used to quantify potential sampling errors. This cruise was timely for the use of early results of the TOES project (Crisp et al., 2000). Through simulation and the development of active multi-variate data analysis techniques (Rixen et al., 2001) a more accurate diagnosis of the dynamics of mesoscale flow and the patchiness of biogeochemical parameters is made.

Grazing

Previous SOC cruises have shown that the fluorimeter and the OPC, when mounted on SeaSoar, are capable of resolving clear variability in the distribution of phytoplankton and mesozooplankton. Conspicuous features of these distributions were patches in the euphotic

zone where phytoplankton and mesozooplankton biomass were inversely correlated reported from the Southern Ocean by Pollard et al. (2000) and from the Strait of Hormuz by A Mustard (PhD thesis, in press). A plausible hypothesis to explain these observations is that zooplankton grazing was exerting a top down control on the phytoplankton population. In order to understand these observations we attempted to estimate the herbivorous grazing pressure of zooplankton from the population density and the ingestion rate per animal. The OPC data were to provide the zooplankton population density and allow us to identify the size of zooplankton that show the strongest inverse correlation with the phytoplankton. Similar data were to be collected using TUBA (Towed Undulating BioAcoustic sensor). This was to allow inter-comparison between the instruments and a chance to test the new TUBA design. In addition we took net samples to verify the OPC and acoustic data, to identify the dominant herbivore species and to calculate the herbivorous ingestion rate from the gut fluorescence and the gut clearance rate following Mackas and Bohrer (1976), Dam and Peterson (1988) and Morales et al. (1991). Note, however, that this method does not measure other non-photosynthetic food sources (such as heterotrophic microzooplankton) and is suitable for calculating herbivorous consumption, but not secondary production. Zooplankton grazing can be assessed by comparison with the phytoplankton standing stock and primary production, to determine if it is responsible for producing the observed distributions and also to evaluate the expected time scales of these processes.

Long term change

A hydrographic line from Scotland to Rockall was occupied by David Ellett of Dunstaffnage Marine Laboratory several times a year from 1975 and by SOC annually (and extended to Iceland) since 1996. Holliday et al. (2000) describe the long-term changes that have taken place. In particular, interannual to decadal changes in upper ocean salinity affect the salinity, stratification and depth of winter mixing of the north Rockall Trough and Iceland Basin. The occupation of this line in its entirety, A-B-C-D (**Figure 1**), was a core component of FISHES.

Bottom Water

Saunders (1990; 1996) has described the outflow of Iceland Scotland Overflow Water (ISOW) through the Færœ Bank Channel and its transport along the deep slope southeast of Iceland. In between, ISOW may be joined by intermittent pulses of bottom water flowing through two 500m deep channels in the Iceland Færœs Ridge. ISOW is also found more centrally in the Iceland Basin, apparently inconsistent with circulation confined to the boundary. Surveys during RRS *Discovery* cruise 242 (Cunningham et al., 2000) suggest that the bottom water may be steered away from the slope along deep channels revealed by the Smith and Sandwell (1997) satellite derived bathymetry. For this reason, during FISHES we ensured that deep CTDs were located in bathymetric hollows where they existed.

4. NARRATIVE

PSO's Diary

4th May (Day 124)

Discovery slipped from the Southampton Oceanography Centre on time at ~12:00 hrs. A substantial crowd came to watch us depart and wish us well, this was much appreciated by all on board. The weather down the English Channel was fine, with a gentle sea. A little way down Southampton Water we were closely passed by a helicopter carrying the Granada Television documentary film crew that had been on board the ship the day before. The footage was to be used in a Documentary about Climate Variability and its impact on the British Isles.

Our first destination was the centre of the Rockall Trough and we had decided to pass to the west of Ireland. This gave us plenty of deep continental shelf for three separate bottom track ADCP calibrations. During refit, the ship's 150 KHz RDI vessel mounted acoustic Doppler current profiler (VM-ADCP) had been turned through ~45° and a 75 KHz RDI phased array VM-ADCP had been fitted in the ship's second transducer space. The potential for harmonic interference between these instruments made it desirable to carry out individual calibrations with one or other instrument turned off and a combined calibration with both instruments operating.

5th May (Day 125)

A science meeting was held at 10:00 hrs for all the scientists and technicians on board. After a number of housekeeping items had been dealt with, CTD rosette bottle sampling was the primary topic of discussion. Both the volumes of water needed and the order in which they were to be drawn were carefully identified. This would later result in three different types of station sampling, early morning primary productivity stations in water depths exceeding 1800 m, similar stations in water depths less than 1800 m and routine CTD stations at other times of the day. The main constraints imposed by the sampling for primary productivity incubations were, that an upper ocean light profile was obtained prior to the determination of firing depths for the bottle stops in the top 100 m, and that two 10 litre bottles were required at each of these shallow stops to provide enough water for the subsequent filtering.

6th May (Day 126)

At 02:00 the ship moved to GMT to match the science reference time. Somewhat later in the morning the weather was still very pleasant and warming with more continuous sunshine than that experienced during the previous 24 hours. However, a building but gentle swell from the west warned us of a moderately deep depression some 300-400 miles west of our position. We reached our first station in the centre of the Rockall Trough (Discovery Stn 13965#1-4, 55 °N

13 °W) at ~15:30. The station was nicknamed Palace1, after the first operation on station. At a ship's speed of ~1 knot, the first Palace float of the cruise, part of the ARGO float programme, was launched over the stern into a very calm sea (#4); watched by several scientists and technicians sporting their finest designer sunglasses in the afternoon sunshine. After a half mile steam into wind, the ship hove to and the triple net, Fast Repetition Rate Flourimeter (FRRF) and self-contained CTD (SC-CTD) system was deployed from a deck winch and the aft-starboard crane (#2). The main CTD was launched (#1) from the mid-ships gantry and conducting hydro-winch whilst the net system was still in the water, but, it was held at 5-10 m, soaking the oxygen sensor, until the net system had reappeared at the surface ready for recovery. Before recovery of the CTD, whilst carrying out the final, near surface, bottle stop, the net system was re-deployed (#3) and recovered following CTD recovery at ~19:05. This station served both to calibrate the Palace float and provide an operational test for the various instruments to be deployed on the FISHES cruise track stations. Henceforth, #2 would always be used as an identifier for a standard net deployment whether it preceded or succeeded the full depth CTD cast, which similarly was always given the identification #1. Further # numbers would be given to additional work on station as required.

A water track ADCP calibration, comprising 6 zig-zag legs at ±45° to the mean direction of steaming to point B (Figure 1), was carried out at a speed of 8 knots following our departure from the Palace1 station. Normal cruising speed of ~12 knots and a direct heading to point B was resumed before midnight.

7th May (Day 127)

A small detour to Rockall preceded our arrival at point B. This was much appreciated by all and many photographs were taken as Discovery closed to within 900 m of the island. The weather was deteriorating and the sea becoming rather more lumpy, some of the early sea legs were now beginning to be tested !

At 11:15 station 13966 #2/#1 (point B) was begun. At this point it was already clear that the triple net system had too high a drag/weight ratio: over the next few stations, the 50 µm nets would be exploded by the drag exerted during heave caused by the pitching of the ship. At that point the net system was simplified to a single 250 µm net.

Following completion of station 13967 #2/#1 (BC1) at ~15:25, it was apparent that the times allocated for stations had been rather optimistic, at least at this early stage of the cruise with deteriorating weather. A number of solutions were discussed including firing bottles "on the fly" during CTD upcasts rather than the usual bottle stops. Following discussions both on board and over email, this option was only used on two stations; but no published studies were quoted and it seems imperative that this is tested in the future as many of the reasons for bottle

stops are historically related to instrument limitations that no longer exist. The key arguments were:

1) There is substantial suspicion that bottle stops are primarily a historic artifact of instrumental limitation.

2) On deep, >2000m, CTD casts bottle stops may add 30 minutes to the duration of an oceanographic station.

3) There are arguments on both sides for suggesting that firing water bottles on the fly may be a better or worse technique for final calibration of the CTD instrument data. However, we have little published knowledge to hand to support any of these.

4) WOCE standard calibrations were all made with bottle stops.

5) The previous occupations of ABCD, with which we primarily wished to compare our results, were made using traditional bottle stops for CTD calibration.

In the end, station spacings were increased slightly, where possible, to make up the anticipated time offset between the original plan and the actual times on station being achieved. Three more stations, 13968 (BC2), 13969 (BC3) and 13969 (BC4), were completed during the day.

8th May (Day 128)

Early in the morning, our atmospheric and ammonium chemist, Martin Johnson, cut his scalp open badly on the door frame to the Chemistry laboratory. Having been well attended to by the 2nd Officer, Phil Oldfield, Martin was helped to his cabin to rest. Martin had remained conscious throughout and was reasonably comfortable after he had been given medical attention, but nevertheless the apparent severity of the injury required that he was monitored on an hourly basis. Happily, Martin felt fully recovered within 24 hours and was allowed back on watch; a full and severe haircut was duly offered and accepted following the medically necessary shaving that he had undergone earlier! The whole experience served as a salutary reminder of the dangers of youthful exuberant movement at sea. During the day, the Master, Roger Chamberlain, had a brief word with all the younger members of the scientific staff reminding them to slow down a little and think about how they might move safely between laboratories rather more than they might on land.

Three stations, 13970 (BC5), 13971 (BC6) and 13972 (BC7), were completed before 09:00. From the appearance of first and second generation copepods in the net samples, it was clear that the spring bloom had already passed in this region. Furthermore it appeared as though the

silicate had been taken up from the surface water by diatoms. Two more stations, 13973 (BC8) and 13974 (BC9) were completed over lunch and early in the afternoon before, on station 13975 (BC10), the net system deployments were abandoned due to deteriorating weather. Station 13975 was further delayed by a 'cats paw' in the hydro-wire as the cable grabbers were released. A new termination was made very efficiently and the station was completed before 22:00 hrs. The inclement weather now forced sampling on station before the ship could get underway.

9th May (Day 129)

Stations 13976 (BC11) and 13977 (BC12) were occupied before 09:20; however, the heavy swell was beginning to cause severe problems during CTD recovery into the frame guide slots in the deck track carriage. It took many hours of careful course changes and slow steaming to reach point C. On arrival, another cats paw in the CTD cable, near the cable haulers, required another re-termination of the CTD cable. Station 13978 (C) comprised a net haul and a shallow CTD cast, the dangerous recovery of the latter forced us to abandon a further, full depth, CTD deployment. One more CTD station, 13979 (IB13) was deployed in the evening using a technique developed on a number of WOCE cruises. Here the ship is brought into the swell for deployment and recovery of the CTD frame into/out of the water and then turned just a little off head to wind during the descent and ascent of the CTD. Station 13979 (IB13) was completed at ~00:30 on the 10th May.

10th May (Day 130)

Hove to on station 13980 (IB14) by 04:45. The wind had begun to drop but there was still a heavy and confused swell. By 08:40 the wind had dropped considerably, a bright blue sky heralded a change in the weather and we began steaming back to station. At station 13981 (IB16) the second PALACE float was deployed at 14:56 prior to a CTD cast and the first net haul from a pennant winch on the CTD gantry. As the CTD gantry is nearly mid-way along the ship, the heave was less and the the net system could be more quickly, reliably and less weather dependently deployed from there. To facilitate this method of deployment, Ritchie Phipps and Bob Keogh had spooled some 200 m of 6 mm hydro wire onto one of the CTD gantry pennant. This was a great success and all further net deployments were carried out this way.

On station 13982 (IB17) the EK500 was brought in to check the towing cable and tail cone. The tail cone was replaced but ironically most of the damage to the original tail cone occurred on recovery. The CTD and net haul were completed by 22:55.

11th May (Day 131)

Stations 13983 (IB19), 13984 (IB20), 13985 (D-IB21), 13986 (DE1) were completed routinely by mid afternoon (~15:40). On station 13987 (DE2), the EK500 was recovered again to carry out a second check on its security during sustained 11-11.5 knot transits. Once again it was clear that the recovery procedure itself was responsible for most, if not all, of the damage sustained to the tail cone. A long boat hook helps to keep the EK500 fish away from the side of the ship, but a longer davit arm assembly would be a more sensible modification to the dedicated winch system.

By station 13988 (DE3), completed at ~23:52, the wind had dropped completely and the sea had taken on an almost almost glass like appearance.

12th May (Day 132)

Stations 13989 (DE4), 13990 (DE5), 13991 (E), 13992 (EC1) and 13993 (EC2) were completed routinely. Approaching station 13991 a large run of pilot whales were spotted; they appeared to remain within the vicinity of the ship until we had left station.

13th May (Day 133)

Station 13994 (EC3) was intended to be sampled for primary productivity incubations but at ~02:00 in the morning there was insufficient light at this latitude to determine a PAR (Photosynthetically Available Radiation) profile prior to the main CTD cast. These profiles were obtained using the FRRF and PAR sensor on the net deployment frame. Therefore having completed the CTD cast at EC3, an extra shallow station, 13995 (EC3P), was carried out after steaming along track for a suitable time towards EC4, our next planned station. This extra station was the idea of Richard Sanders, and when the weather allowed sampling whilst underway stations like this were employed a number of times to provide suitable timing for primary productivity sampling with minimal time cost to the overall CTD survey. They were frequently referred to as the Sanders stations.

At this point in the cruise, the Chief Officer, Richard Warner, raised the alarm regarding our fresh water consumption. Fresh water consumption had substantially exceeded our ability to produce fresh water since leaving Southampton. One major cause of excess consumption was the Milli-Q water purification system. This system backwashes its filters using approximately 30 litres of water every half an hour if it is used at all since the last backwash. To overcome this a large carboy was set up near the chemistry lab sink to hold purified water. This was filled just once per day and therefore we were able to reduce the backwash wastage from around 1000 litres per day to 30-60 litres per day.

Stations 13996 (EC4), 13997 (EC5), 13998 (EC6) and 13999 (C) were completed routinely by 23:53.

14th May (Day 134)

RRS *Discovery* station 14000 (CG1) finished at 05:46 and was followed by a small PSO's RPC in the saloon bar to mark the passing of a millennial station in the centenary anniversary year of Scott's *Discovery*, where the scientific station numbers began, and the 40th anniversary year of the laying of the keel of the present RRS *Discovery*. All members of the ship's complement were invited to sign the visitors' book in commemoration.

Stations 14001 (CG2), 14002 (CG3), 14003 (CG4) and 14004 (CG5) were completed routinely by 00:40 on the 15th.

15th May (Day 135)

Station 14005 (CG6) was completed by 06:18. Small depressions were rapidly coalescing and therefore, in an attempt to out play the weather, we abandoned the rest of the line up to point G until later in the cruise and turned towards Iceland to begin line F-L starting at FL1. Stations 14006 (FL1), 14007 (FL2) and 14008 (FL3) were completed routinely by 22:35. The sky was relatively cloud free near Iceland but the wind was fresh, force 7 gusting 8.

16th May (Day 136)

Station 14009 (L), was followed by an extra station on the Iceland shelf 14010 (L1) before steaming back to point F to begin line F-J-K. Stations 14011 (F) and 14012 (FJ1) were completed routinely by 23:48.

17th May (Day 137)

Stations 14013 (FJ2), 14014 (FJ3), 14015 (J), 14016 (JK1), 14017 (JK2) and 14018 (JK3) were completed routinely by 22:02.

18th May (Day 138)

Stations 14019 (JK4), 14020 (JK5), 14021 (JK6) and 14022 (K) were completed routinely by 12:38. Two new stations, K1 further on shelf from K, and JK56 between JK5 and 6 were added to create a repeated occupation of a line across the shelf edge. Thus, stations 14023 (K1), 14024 (K), 14025 (JK56) at which all 24 rosette bottles were fired on the fly and 14026 (K) were completed by 21:48. At this point we set a course for Stornoway to carry out a boat transfer.

19th May (Day 139)

At 08:30, Raymond Pollard was taken ashore at Stornoway in *Discovery*'s rigid inflatable boat (RIB). This had been pre-arranged in order that Raymond could present the George Deacon Division's core strategic proposal to NERC. Stuart Cunningham, who had been waiting for our arrival, was picked up from Stornoway and joined the ship on return of the RIB. Stuart was welcomed on board and by 09:20 *Discovery* was steaming back out to sea. During the afternoon we sailed between the Flannan Islands and, in the evening, we passed through the St Kilda group on our way to point A (Figure 1).

During the day, we swapped CTD frames to begin using the SeaBird 911 plus CTD system. Swapping CTD frames is a tricky task, requiring careful and awkward use of the main starboard crane. An aft extension to the CTD launching rail system to allow CTD frames to be moved out of launch position in either direction would be a simple solution to make dual CTD frame operation easier.

20th May (Day 140)

At station 14027 (A-ADT), the PES and EK500 fishes were re-deployed before making the routine net haul. The CTD cast was yo-yo'd once to examine and pre-empt any drift in the first deployment of the SeaBird CTD. Station 14027 was completed by 03:00. Stations 14028 (15G), 14029 (ADD), 14030 (ADR), 14031 (ADQ), 14032 (ADP) and 14033 (ADO) were completed routinely by 15:23.

At station 14034 (ADN), the third PALACE float was launched before making two CTD casts swapping between CTD frames to make a deep station intercomparison between Neil Brown Mk III and SeaBird 911 plus CTDs. Finally the CTD frames were swapped back again to continue the leg with the SeaBird CTD. At this point we discovered that beam 2 on the 30° RDI 150 KHz LADCP, fitted to the SeaBird instrumented frame, had failed; but we decided to continue the leg without LADCP data until a convenient time could be found to swap LADCP instruments between CTD frames. Station 14035 (ADM) was completed routinely by 23:45.

21st May (Day 141)

Stations 14036 (ADL), 14037 (ADK), 14038 (ADJ), 14039 (ADI), 14040 (ADH), 14041 (ADG) and 14042 (ADF) were completed routinely by 17:45. The 20° beam angle RDI 150 KHz LADCP instrument was swapped into the SeaBird instrumented CTD frame before station 14043 (ADE). Station 14044 (ADD) was completed routinely by 23:26.

22nd May (Day 142)

Stations 14045 (ADC), 14046 (ADB) and 14047 (B-ADA) were completed routinely by 03:56. We then negotiated Rockall for a second time, in poorer weather than before but still with a reasonable view of the rock. Heading north we began leg B-J, and stations 14048 (BJ1), 14049 (BJ2), 14050 (BJ3), 14051 (BJ4) and 14052 (BJ5) were completed routinely by 00:42 on the 23rd.

23rd May (Day 143)

Stations 14053 (BJ6), 14054 (J), 14055 (JH1), 14056 (JH2), 14057 (JH3) and 14058 (JH4) were completed routinely by 23:48.

24th May (Day 144)

To make a better crossing of the IFF and the Jan Mayen Front (JMF), point R was replaced by point R1 in the cruise plan with the respective creation of new stations in between point H and R1. Stations 14059 (JH5), 14060 (JH6), 14061 (H) and 14062 (HR1) were completed routinely by 12:54. At which point we held on station to swap CTD frames back to the Neil Brown MkIII instrumented frame. The Neil Brown instrumented frame had also been equipped with a deep pressure case optical plankton counter (OPC) for this cruise. John Smithers had developed a method to get both the OPC data and the Neil Brown data up the sea cable using two superimposed FSK signals that could be separated at the deck unit. At the beginning of the cruise this worked for one downcast and two thirds of an upcast and then mysteriously failed thereafter. The problem had now been solved, water leaking into the OPC lead had created a high resistance current drain.

On station 14063 (HR2), the CTD cast had to be abandoned due to an electronics failure within the Neil Brown CTD. However, John was able to fix the instrument quickly and station 14064 (HR3) was completed routinely by 21:50.

25th May (Day 145)

Station 14065 (HR4) was completed routinely by 01:52. Station 14066 (HR5) was then chosen for a second inter-calibration between the Neil Brown MkIII and SeaBird 911 plus CTDs. After making one net haul, one shallow CTD cast for primary productivity incubation sampling and two deep inter-calibration CTD casts, the Neil Brown instrumented CTD frame was swapped back onto the launch rails and we left station.

Stations 14067 (R1), 14068 (RS1) and 14069 (S) were completed routinely by 21:43. All biological measurements showed highly productive regions whilst crossing both the IFF and the JMF.

26th May (Day 146)

Stations 14070 (SG1), 14071 (SG2), 14072 (SG3), 14073 (SG4), 14074 (SG5), 14075 (SG6) and 14076 (G-CG9) were completed routinely by 22:32. During the afternoon, the two Chelsea Instrument MiniPak CTD instruments failed their communications under test, despite having been working on the bench several times previously. These had been purchased for use on the newly re-developed SeaSoar (leg 2 of the cruise) and integrated with the PENGUIN data handling system. So began a period of regular telephone and facsimile communication with Chelsea Instruments that would continue well into the second leg of the cruise.

27th May (Day 147)

Stations 14077 (CG8), 14078 (CG7) and 14079 (CG6) were completed routinely before we turned north west and steamed towards point M to begin the final line of the first leg of the cruise, along the Iceland Færœs Ridge and across the Færœ Shetland Channel.

28th May (Day 148)

Stations 14080 (M), 14081 (MH1) and 14082 (MH2) were completed routinely by 10:56. Just moving off station, at ~11:00 the EK500 parted from its tow cable. On investigation of the data, it appeared as though everything was normal until a matter of minutes before the signal became pure noise. On recovery of the cable it was clear that the Kevlar strength layer had failed inside the brass towing sheath. Strangely the failure occurred just after CTD recovery as the ship began to move off station, ie when the towing load would be expected to still be low: however, this was probably just coincidence. Two images of the cable are given in Figure 2 for future reference. To that point the fish had towed with apparently little vibration at speeds up to 11.5 knots. Poor weather the previous night and during the morning had in fact reduced towing speeds to 7.5 knots at times, although greater snatch loadings during pitching might have been set up. From a science point of view Sophie Fielding and Nick Crisp took things very constructively and immediately began drawing up plans for increased TUBA usage to overcome the loss of the EK500 on the second leg of the cruise.

Stations 14083 (MH3), 14084 (MH4), 14085 (MH5) and 14086 (MH6) were completed routinely by 23:59.

29th May (Day 149)

Stations 14087 (MH7), 14088 (H) and 14089 (HP1) were completed routinely by 09:17. The most direct route to the next station involved a passage through Kalso Fjord in the Færœ Islands. This enabled us to take a welcome short break from station sampling and appreciate

the dramatic scenery of these spectacular islands. Back on station by 15:37, stations 14090 (HP2), 14091 (HP3) and 14092 (HP4) were completed routinely by 23:00.

Figure 2: Two images of the failed EK500 tow cable.

30th May (Day 150)

Ahead of schedule for our arrival in Lerwick, three extra stations were added to our section across the Færœ Shetland Channel. Stations 14093 (HP45), 14094 (HP5), 14095 (HP56) and 14096 (HP6) were completed by 09:06.

Although no long term solutions to the failed CI MiniPak CTD units had been found, Nick Crisp had managed to put the working stand alone communications board on a real time end-cap. Thus we could deploy the one remaining working CTD unit on SeaSoar using its internal batteries but communicating via a real time RS232 signal. The latter was critical for SeaSoar deployment as real time pressure information is necessary to know where the vehicle is in the water column. Two test SeaSoar deployments followed station HP6 but these were not successful. The first failed because the keyway was missing between the propeller and the hydraulic shaft leaving the propeller to freely rotate. The second deployment failed due to a wet connector within the MiniPak CTD - this had occurred during battery replacement and caused the pressure sensor to drift badly.

Station 14097 (HP7) was carried out routinely before 14:39, by which time everything was ready for a third SeaSoar test deployment. This time the MiniPak CTD worked fine, but still the vehicle failed to respond to wing command. It was later discovered, near the beginning of the second leg of the cruise, that the hydraulic ram could sometimes stick and would then require a very large command signal to shift it. Finally station 14097 (P) was completed routinely by 18:24 and having brought in the PES fish we began our overnight steam to Lerwick and the end of the first leg of the cruise. It was fitting that the PSO should hold a well deserved RPC to celebrate the end of a very successful leg 1 of D253.

31st May (Day 151)

Arrival in Lerwick around 07:00 heralded a busy day attempting to organise the transportation of essential electronics spares for the MiniPak CTDs. 13 members of the scientific party left the cruise during the day as planned and were replaced by 12 others who had stayed in Lerwick the previous night, waiting for the ship to arrive. It was very strange to have so many people leaving, particularly when the whole ship's company had worked together so well as a team. However, the new crowd were offered a warm welcome and began to fit in very quickly.

1st June (Day 152)

Delays waiting for electronics spares seemed to drag on interminably. Finally, the last of the essential spares arrived on the 19:25 (BST) flight from Aberdeen and RRS *Discovery* slipped from her dock in Lerwick at ~19:30 (GMT) to begin leg 2 of the cruise. Some less important spares failed to make it to the ship in time, but it was paramount for the scientific objectives of the cruise that we did not spend a second night in port. The weather was grey and overcast, a poor forecast, but light winds at this time. A scientific meeting during the afternoon concluded that the second leg of the cruise should focus on fine scale SeaSoar surveys of a region of the IFF. Close analysis of recent satellite images continued through the evening to identify an ~100 km square box over which we would carry out our observations.

2nd June (Day 153)

Heading out across the Færœ Shetland Channel, it was our initial intention to repeat the CTD station at HP6 and then carry out a test SeaSoar deployment in the channel before proceeding to the IFF. By 06:30, lumpy seas creating 6 metre waves were forcing our speed down. The barometer was rising and skies were bright and sunny by mid-morning, however force 8, gusting 9, winds sustained a heavy sea; it became apparent that we would have to abort our proposed test SeaSoar deployment and head straight for our chosen survey region on the IFF.

By approximately 19:30 we were able to achieve our highest transit speeds all day, ~4 knots, as we continued to edge slowly towards the Færœ Islands.

3rd June (Day 154)

By early morning the sea state had dropped significantly and we were able to steam at ~10.5 knots. The weather forecast was changeable but hopeful and the wind speed had dropped to a 6. The newly developed data handling PC for SeaSoar, PENGUIN, failed to boot during the afternoon, presenting a little more technical frustration. By 22:30 we slowed our steaming to ~4 knots to arrive on a re-occupation of station SG2 (Figure 3) in time for a primary productivity CTD cast early in the morning of the 4th.

4th June (Day 155)

Station 14099 (SG2) was completed by 05:20, but on recovery of the CTD frame the cable cats pawed badly and therefore required a retermination. A number of large whales, tentatively identified as hump back whales, were spotted at ~05:50. Station 14100 (SG1) was completed routinely by 09:49.

SeaSoar was deployed at 11:14 (*Discovery* station 14101) and towed north towards point S at 8 knots. This was a test deployment, but the vehicle flew perfectly from the beginning of the tow, reaching a repeatable depth of 330 m on just 500 m of faired cable paid out. After reaching point S, ~14:50, we turned back south along the reverse track and recovered SeaSoar at 17:15. Although the sea conditions appeared generally flat calm, a single swell wave just at the point of hauling the SeaSoar vehicle out of the water caused us to lose control of the recovery and the vehicle hit the back of the ship with significant force. The Fast repetition Rate Flourimeter (FRRF), mounted in the lower nose position took most of the impact and appeared to be badly damaged. However further investigation indicated that movement in the clamps and a cushioning effect from the connectors on the rear of the instrument may have saved the instrument from more than superficial damage. Indeed the FRRF was removed from SeaSoar and began to work again on the bench upon restart. However, the impact had compromised the seals around the light chamber and sheared two bolts holding the O'ring seal / perspex window retaining plates in position. These were replaced and the O'ring seals re-positioned but it was felt prudent to swap this instrument with one currently in use on the underway non-toxic supply and not subject it to a pressure cycle until its case had been re-tested after the cruise.

Station 14102 (F1p1) was completed routinely by 22:37 in a cold filament of water from north of the IFF. Following recovery of the CTD, the LHPR towing swivel was load tested on the conducting warp as we steamed gently north in preparation for an LHPR tow south across this filament of cold water.

5th June (Day 156)

At 00:38, the LHPR was deployed (14103) from the conducting warp and towed across a filament of cold water intruding southwards in the north west corner of our survey area. The tow lasted ~1.5 hours and the LHPR was recovered at ~02:05. CTD and net station 14104 (F1p2) was completed routinely by 05:26.

At 09:50, SeaSoar was fully deployed to begin the first fine scale SeaSoar survey (FSS1, Figure 3), *Discovery* stn 14105. However, an ADSL modem failure just an hour or so later required a full power down re-boot. After powering up, the CI MiniPak CTD failed to restart and therefore SeaSoar had to be recovered. The vehicle was inboard by 12:23.

Station 14106 (F1P3) was completed routinely by 13:56 before we were forced to heave to in rapidly deteriorating seas, wind speed 8 gusting 9 frequently.

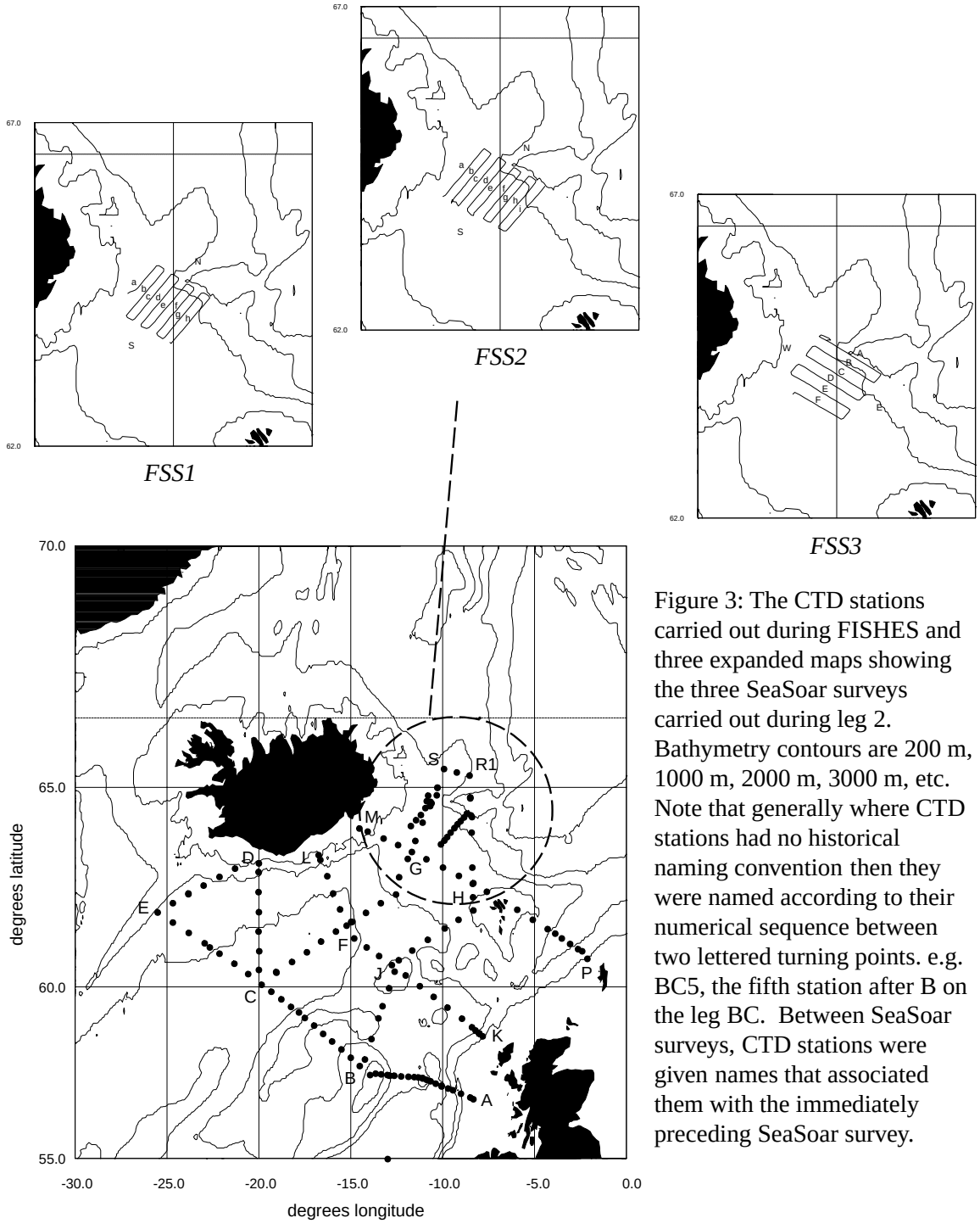

Figure 3: The CTD stations carried out during FISHES and three expanded maps showing the three SeaSoar surveys carried out during leg 2. Bathymetry contours are 200 m, 1000 m, 2000 m, 3000 m, etc. Note that generally where CTD stations had no historical naming convention then they were named according to their numerical sequence between two lettered turning points. e.g. BC5, the fifth station after B on the leg BC. Between SeaSoar surveys, CTD stations were given names that associated them with the immediately preceding SeaSoar survey.

6th June (Day 157)

Force 10, gusting 11 winds overnight left us hove to all day. By mid-day, the air pressure was rising fast but 8 gusting 9 winds kept feeding the big seas. The bad weather was used to technical advantage however. The PENGUIN underwater PC was programmed to effect

modem reboots and self reboots/shut downs (unix halts) where necessary so that it would be more robust to deck side user communication which is limited to remote terminal access and power cycling for the whole SeaSoar system. In addition some new I^2C firmware (see detailed report later) was added to PENGUIN so that it could also handle the rather delicate power cycling required by the CI MiniPak CTD.

7th June (Day 158)

With bright sunny weather and wind speeds dropping below 10 ms^{-1} *Discovery* was turned into the wind at ~10:30 to test her steaming capability in the decreasing but still choppy seas. At 7 knots the ship was still taking too much water breaking over the bow and so the decision was made to wait for a little longer.

After lunch, a similar steaming test was more successful and so SeaSoar was fully deployed at 14:36 to restart FSS1 (Figure 3) from the south west corner (F1aS) of the survey box (*Discovery* stn 14107). At 19:19 we began our turn at the northern end of leg a (F1aN).

8th June (Day 159)

Light winds and warmth in the bright morning sunshine. FSS1 continued without incident during the day, making turning point F1eS by 19:30. All the technicians and engineers on board seemed to have been roped into making brackets and modifications for the LHPR. This followed the suggestion that the Towed Undulating BioAcoustic instrument (TUBA) would benefit from a good calibration data if it could be fitted to the LHPR. However the most sensible way to achieve this would entail towing the LHPR from the faired SeaSoar cable; TUBA needs a minimum four conductors in its deployment cable. Therefore work began on a SeaSoar mandrel style mechanical termination block to be fitted to the existing LHPR towing bridle. In addition the fabrication of brackets was begun to fit TUBA, the OPC and PENGUIN2 on the LHPR frame. PENGUIN2 was a spare for the SeaSoar PENGUIN data handling system and would be used in this case simply to log the OPC data. The results were to remain a credit to all the scientists and engineers on board for their unbounded enthusiasm towards new and novel applications of instruments and platforms.

9th June (Day 160)

Vivid sunrise by 03:00, and a setting moon on the other side of the ship. Not a breath of wind and striking cloud-scapes in all directions. Sadly, by ~13:00 the sky was overcast with light cloud, but the temperatures were still pleasant in light winds. FSS1 continued throughout the day, making our final turning point F1hN at 18:43.

10th June (Day 161)

The hydrographic data from SeaSoar FSS1 seemed to indicate a remarkable similarity to the patterns of eddies and frontal meandering observed 11 years ago and published by Allen et al. (1994); now with concurrent high resolution biological data we were observing dramatic changes in both phytoplankton and zooplankton distributions across the boundaries between cold waters of sub-arctic origin and warm Modified Atlantic Waters (MAW). SeaSoar FSS1 (14107) ended, at point F1hS, at 01:36 and SeaSoar was fully recovered by 02:23. We then began a line of CTD and net haul stations back up line h, with the first and last stations suitably timed for early morning primary productivity samples for on deck incubation. Thus stations 14108 (F1hS), 14109 (F1h1), 14110 (F1h2), 14111 (F1h3), 14112 (F1h4), 14113 (F1h5) and 14115 (F1h6) were completed routinely by 16:43.

Following a further 2 mile steam along track, the LHPR was deployed from the conducting warp (14115) at 17:18. It was towed at ~4 knots north eastwards towards and just past F1h7 before recovery at 19:27. During LHPR tows, the cable is paid out to allow the vehicle to sink to some prescribed depth. During the upcast, the cable is hauled in stages to allow the LHPR to sample discreet depths. Following the LHPR recovery, CTD/net stations 14116 (F1h7) and 14117 (F1hN) were completed routinely by 23:21.

11th June (Day 162)

At primary productivity station 14118 (F1iN), three different nets (50, 200 and 500 µm mesh) were fished and a calibration dip for the TUBA instrument was organised before the usual CTD cast. All were completed by 04:09 and SeaSoar was deployed to begin FSS2 (14119) at 04:23. This time the survey would have an extra leg, i, and run east to west with otherwise the same turning points at the end of each leg as in FSS1 (Figure 3). FSS2 continued throughout the day, making turning point F2gN by 20:44. Overnight the sea became quite choppy with winds gusting 7/8 at times.

12th June (Day 163)

At ~05:30, it was noticed that the OPC data were poor. This had happened at the end of the first survey, but following a restart on deck and re-deployment for FSS2 the instrument had worked well for 24 hours or so. The instrument continued to provide a good time stamp, but the attenuance values had jumped to a very high level and there were virtually no particle counts. The sea-state was dropping but it was still too rough to risk a deployment and recovery cycle for just one instrument failure. Turning point F2eN was made by 12:16.

At 15:43, the PENGUIN system was halted to plug the SeaSoar system into an Un-interruptable Power Supply unit (UPS). By 15:50 the SeaSoar system was back up and

running but this did not effect any change to the OPC data failure. Quit a sudden increase in wind speed, force 8, soon whipped up a lumpy sea and reduced our steaming speed to 7 knots. Turning point F2dS was made by 20:55 and the weather began to improve again by midnight.

13th June (Day 164)

During the early hours of the morning, the OPC began to work again for no apparent reason. By 05:18 we had made turning point ~05:30. However, at ~05:30 the FRRF instrument stopped sending data to PENGUIN and the OPC began to register slightly high attenuance values and somewhat fewer particle counts. The weather was still too rough to risk a recovery.

By 12:00 we had made turning point F2cS. The weather had become bright and calm and the sea-state had dropped to 3 or less. SeaSoar was recovered and inboard by 13:05. It was immediately apparent that SeaSoar had struck the bottom at some point. As before, the FRRF had taken the brunt of the impact and looked fairly severely damaged. The OPC had a mouth-full of stones and would require a strip down and clean - we were incredibly lucky not to have lost the whole vehicle. Coral samples were removed and preserved. Examination of the data streams showed that at the time of loss of data from the FRRF (~05:30), both the Precision Echo Sounder (PES) and the MiniPak CTD agreed on a depth of 398 m. It was assumed that a mis-reading of the minimum depth alarm setting may have caused this incident. It was a salutary reminder that protective alarms can create a false sense of security. The FRRF pressure case had not been compromised, but on opening, plastic retaining spacers fell out revealing loose circuit boards. Clearly the impact had dislodged the circuit boards and broken their retaining structures. After plugging the boards back in, the instrument appeared to work, however, since a third FRRF was available it was felt prudent to replace it.

SeaSoar was re-deployed to complete the final two legs of FSS2 at point F2bS at 17:34.

14th June (Day 165)

SeaSoar FSS2 (14119) ended at point F2aS and SeaSoar was fully recovered by 09:03. The hydrographic data from SeaSoar FSS2 confirmed the HOPS (Harvard Ocean Prediction system) model forecast (detailed report given later) and indicated that there were also significant differences to the patterns of eddies and frontal meandering observed 11 years ago and published by Allen et al. (1994); the varability appeared dominated by large anticyclones (30-50 Km) rather than small cyclones - possibly because of the lack of surface capping, vorticity not constrained etc. The Biology was apparently controlled by mixed layer depths causing light stress in deeply mixed anticyclonic circulations and high growth in stratified cyclonic cold tongues. Then vertical velocities were clearly apparent at depth drawing phytoplankton down along steeply sloping isopycnals.

We began a line of CTD and net haul stations up line b, with the last station suitably timed for early morning primary productivity samples for on deck incubation. Thus stations 14120 (F2bS), 14121 (F2b1) and 14123 (F2b2) were completed routinely by 14:52. *Discovery* station 14122 was reserved for the first LHPR tow off the faired SeaSoar cable; which was delayed by technical problems until after the CTD station at F2b2. This LHPR deployment was eventually aborted on deck due to a failure with the TUBA instrument.

CTD and net haul stations 14124 (F2b3) and 14125 (F2b4) were completed routinely by 20:42. Following station 14125, the LHPR was finally deployed (14126) on the faired SeaSoar cable at 21:26 and towed north at 3 knots along line b until its recovery at 23:45. Not surprisingly, the faired cable allowed much greater depths to be achieved for a given length of cable paid out.

15th June (Day 166)

The early morning productivity CTD station at 14127 was completed routinely by 03:28. By 04:44, SeaSoar was fully deployed to begin FSS3 (Figure 3). Following some careful survey design ideas and mapping error optimisation as part of the TOES (Techniques for Optimising Environmental Sampling) project, FSS3 was designed with six legs running perpendicular to those of FSS1 &2. The corners of the box covered were the same. The survey began at point F3AW which was the same point as F2aN and F1aN. FSS3 continued throughout the day, reaching turning point F3BW by 00:03 on the 16th.

16th June (Day 167)

FSS3 continued throughout the day without incident, reaching turning point F3EW by 19:15.

17th June (Day 168)

Approximately 17 miles before the end of F3F, point F3FW, FSS3 (14128) was stopped and SeaSoar was recovered without incident by ~11:30. The weather had begun to deteriorate and the scientific justification for a final LHPR tow had become of sufficiently high priority to require some flexibility in the SeaSoar survey. It was generally felt that the last 17 miles of the survey track at the south west corner of the survey region would not add significantly to the overall data set. After steaming to position F2dS, also on line F3F (Figure 3), the LHPR was deployed (14129) on the SeaSoar faired cable at 13:35 and towed at 3 knots towards F2eS. Following recovery of the LHPR in force 5/6 seas, we steamed to position F2eS for our last CTD station and net haul (14130). Station 14130 was completed routinely by 17:06, the PES fish was recovered and the ship's TSG (thermosalinograph) and non-toxic supply turned off. We set course for home at full speed to try to out run a large depression that threatened to cut us off near the Færœ Islands.

18th/19th June (Days 169/170)

Continued steaming for Govan on the Clyde. Thankfully we had reached the shelter of The Minch before the gale force winds hit us hard. During the 19th we took further sheltered passages through the Sounds of Mull and Islay to avoid the worst of the rough seas.

20th June (Day 171)

Arrival in Govan, demobilisation all day.

J. Allen

Master's Diary (Summary)

04/05/01	0800-0900	Familiarisation briefing completed for all Non-RSU personnel joining in Southampton. Sailing preparations continue.
	0900-0930	All ships personnel attend Emergency and lifeboat muster.
	1045	Pilot embarked.
	1107	All gone fore and aft.
	1306	Cleared Needles and Fairway Buoy. Full away on passage.
	1545	PES fish deployed, continuing passage.
05/05/01	0800-0900	Cruise Planning meeting held in Officers' Lounge.
	1100	Noon Position 50 15.9N 007 57.9W.
06/05/01	0200	Vessel reverts to GMT.
	1534	**Pallas Float** deployed **Station 13965#4** 55 00.1N 012 59.9W. (Figure 3)
	1553-1609	**Net** cast outboard **Station 13965#2** 55 00.8N 012 59.9W.
	1600-1830	**CTD** cast outboard **Station 13965#1** 55 01.1N 012 58.8W.
	1830-55	**Net** cast outboard **Station 13965#3** 55 01.7N 012 57.8W.
	1855-2253	ADCP calibration along base course of 346 T.
07/05/01	1110-56	Hove to on **CTD/NET Station 13966#1&2** 57 32.6N 013 56.9W.
	1426-1521	Hove to on **CTD/NET Station 13967#1&2** 57 48.7N 014 29.7W.
	1521	EK500 Fish deployed.
	1733-1824	Hove to on **CTD/NET Station 13968#1&2** 58 03.1N 014 59.8W.

	2044-2158	Hove to on **CTD/NET Station 13969#1&2** 58 17.4N 015 30.1W.
08/05/01	0020-0141	Hove to on **CTD/NET Station 13970#1&2** 58 30.6N 016 00.0W.
	0357-0523	Hove to on **CTD/NET Station 13971#1&2** 58 43.8N 016 30.3W.
	0737-0859	Hove to on **CTD/NET Station 13972#1&2** 58 57.5N 016 58.6W.
	1107-1218	Hove to on **CTD/NET Station 13973#1&2** 59 10.2N 017 29.2W.
	1352-1544	Hove to on **CTD/NET Station 13974#1&2** 59 20.1N 017 47.8W.
	1725-2200	Hove to on **CTD Station 13975#1** 59 29.1N 018 14.7W.
	1730-1912	DOWN TIME - CTD Cable Kinked and re-terminated.
09/05/01	0029-0252	Hove to on **CTD/NET Station 13976#1&2** 59 41.2N 018 46.0W.
	0548-0915	Hove to on **CTD Station 13977#1** 59 53.9N 019 18.8W.
	1506-1854	Hove to on shallow **CTD Station 13978#3** 60 06.0N 019 50.5W.
	2200-0125/10	Hove to on **CTD Station 13979#1** 60 29.4N 019 59.2W.
10/05/01	0442-0918	Hove to near **CTD Station 13980#1 -** unworkable due to swell.
	0918-1135	Hove to on **CTD Station 13980#1** 60 58.9N 019 58.2W.
	1456	**Pallas Float** deployed **Station 13981#3** 61 30.0N 020 01.4W.
	1515-1737	Hove to on **CTD/NET Station 13981#1&2** 61 29.8N 020 00.3W.
	2038-2255	Hove to on **CTD/NET Station 13982#1&2** 61 59.6N 019 59.3W.
11/05/01	0159-0340	Hove to on **CTD/NET Station 13983#1&2** 62 30.4N 020 00.1W.
	0630-0750	Hove to on **CTD/NET Station 13984#1&2** 63 00.4N 020 01.0W.
	0912-1050	Hove to on **CTD/NET Station 13985#1&2** 63 12.8N 019 59.9W.

	1426-1546	Hove to on **CTD/NET Station 13986#1&2** 63 05.3N 021 17.5W.
	1816-1939	Hove to on **CTD/NET Station 13987#1&2** 62 52.8N 022 08.3W.
	2215-2352	Hove to on **CTD/NET Station 13988#1&2** 62 40.1N 022 59.9W.
12/05/01	0232-0515	Hove to on **CTD/NET Station 13989#1,2&3** 62 27.4N 023 49.2W.
	0800-0948	Hove to on **CTD/NET Station 13990#1&2** 62 13.3N 024 39.9W.
	1231-1406	Hove to on **CTD/NET Station 13991#1&2** 61 59.2N 025 30.2W.
	1652-1819	Hove to on **CTD/NET Station 13992#1&2** 61 44.0N 024 40.7W.
	2123-2322	Hove to on **CTD/NET Station 13993#1&2** 61 27.7N 023 48.7W.
13/05/01	0202-0330	Hove to on **CTD Station 13994#1** 61 11.5N 022 56.7W.
	0433-0548	Hove to on **CTD/NET Station 13995#1&2** 61 05.2N 022 39.9W.
	0746-0952	Hove to on **CTD/NET Station 13996#1&2** 60 55.1N 022 07.5W.
	1237-1439	Hove to on **CTD/NET Station 13997#1&2** 60 39.1N 021 19.6W.
	1700-1906	Hove to on **CTD/NET Station 13998#1&2** 60 22.6N 020 34.8W.
	2132-2353	Hove to on **CTD/NET Station 13999#1&2** 60 05.0N 019 50.6W.
14/05/01	0246-0546	Hove to on **CTD/NET Station 14000#1,2&3** 60 24.6N 019 02.1W.
	0824-1043	Hove to on **CTD/NET Station 14001#1&2** 60 42.2N 018 11.7W.
	1304-1518	Hove to on **CTD/NET Station 14002#1&2** 60 57.5N 017 23.0W.
	1750-1952	Hove to on **CTD/NET Station 14003#1&2** 61 14.4N 016 36.5W.

	2234-0040/15	Hove to on **CTD/NET Station 14004#1&2** 48.0W.	61	29.7N	015
15/05/01	0316-0618	Hove to on **CTD/NET Station 14005#1,2&3** 57.6W.	61	44.7N	014
	0850-1134	Hove to on **CTD/NET Station 14006#1&2** 34.6W.	62	03.9N	015
	1549-1740	Hove to on **CTD/NET Station 14007#1&2** 57.1W.	62	28.3N	015
	2047-2235	Hove to on **CTD/NET Station 14008#1&2** 16.6W.	62	53.8N	016
16/05/01	0212-0312	Hove to on **CTD/NET Station 14009#1&2** 38.7W.	63	18.0N	016
	0406-57	Hove to on **CTD/NET Station 14010#1&2** 44.9W.	63	24.9N	016
	1736-1928	Hove to on **CTD/NET Station 14011#1&2** 13.1W.	61	38.9N	015
	2148-2348	Hove to on **CTD/NET Station 14012#1&2** 48.3W.	61	18.9N	014
17/05/01	0201-0340	Hove to on **CTD/NET Station 14013#1&2** 07.1W.	61	05.1N	014
	0551-0721	Hove to on **CTD/NET Station 14014#1&2** 27.6W.	60	51.3N	013
	0942-1046	Hove to on **CTD/NET Station 14015#1&2** 45.8W.	60	36.9N	012
	1323-1416	Hove to on **CTD/NET Station 14016#1&2** 00.4W.	60	20.4N	012
	1648-1811	Hove to on **CTD/NET Station 14017#1&2** 13.9W.	60	03.2N	011
	2042-2202	Hove to on **CTD/NET Station 14018#1&2** 28.9W.	59	45.6N	010
18/05/01	0042-0202	Hove to on **CTD/NET Station 14019#1&2** 43.2W.	59	27.9N	009
	0442-0612	Hove to on **CTD/NET Station 14020#1&2** 56.7W.	59	09.1N	008

	0900-1036	Hove to on **CTD/NET Station 14021#1&2** 58 49.4N 008 12.3W.
	1138-1238	Hove to on **CTD/NET Station 14022#1&2** 58 44.5N 007 59.5W.
	1346-1431	Hove to on **CTD/NET Station 14023#1&2** 58 39.5N 007 48.4W.
	1544-1619	Hove to on **CTD Station 14024#1** 58 44.3N 007 59.8W.
	1817-1920	Hove to on **CTD Station 14025#1** 58 54.9N 008 23.5W.
	2101-48	Hove to on **CTD Station 14026#1** 58 44.3N 008 00.0W.
	2120-32	EK500 and PES Fishes inboard.
	2148	Set Course for Stornoway.
19/05/01	0800-0930	Boat Transfer underway Stornoway.
	0954	CTD Frames Changed.
	0954	Proceeding for working Area.
20/05/01	0158	EK500 & PES Fishes outboard.
	0158-0300	Hove to on **CTD/NET Station 14027#1&2** 56 49.9N 008 19.2W.
	0352-0432	Hove to on **CTD Station 14028#1** 56 52.8N 008 29.6W.
	0540-0625	Hove to on **CTD/NET Station 14029#1&2** 56 57.1N 008 47.1W.
	0711-53	Hove to on **CTD Station 14030#1** 56 59.9N 008 59.5W.
	0848-0950	Hove to on **CTD/NET Station 14031#1&2** 57 02.8N 009 13.4W.
	1038-1206	Hove to on **CTD Station 14032#1** 57 05.9N 009 25.3W.
	1319-1523	Hove to on **CTD/NET Station 14033#1&2** 57 09.0N 009 41.4W.
	1637	**Pallas Float** deployed **Station 14034#3.**
	1637-2026	Hove to on **2 X CTD Stations 14034#1&4** 57 13.8N 010 03.5W.
	2143-2345	Hove to on **CTD/NET Station 14035#1&2** 57 17.4N 010 22.6W.
21/05/01	0103-0247	Hove to on **CTD Station 14036#1** 57 21.7N 010 39.2W.
	0346-0446	Hove to on **CTD Station 14037#1** 57 24.1N 010 51.1W.
	0545-0643	Hove to on **CTD/NET Station 14038#1&2** 57 27.1N 011 04.8W.
	0743-0836	Hove to on **CTD Station 14039#1** 57 28.3N 011 18.6W.

	0934-1135	Hove to on **CTD/NET Station 14040#1&2** 57 29.2N 011 31.9W.
	1256-1433	Hove to on **CTD Station 14041#1** 57 29.7N 011 50.9W.
	1600-1745	Hove to on **CTD Station 14042#1** 57 30.7N 012 14.6W.
	1905-2101	Hove to on **CTD/NET Station 14043#1&2** 57 31.7N 012 37.4W.
	2157-2326	Hove to on **CTD Station 14044#1** 57 31.7N 012 51.8W.
22/05/01	0011-51	Hove to on **CTD/NET Station 14045#1&2** 57 33.0N 012 59.9W.
	0204-23	Hove to on **CTD Station 14046#1** 57 34.0N 013 20.0W.
	0328-56	Hove to on **CTD/NET Station 14047#1&2** 57 35.1N 013 38.1W.
	0654-0734	Hove to on **CTD/NET Station 14048#1&2** 58 00.2N 014 13.2W.
	1038-1219	Hove to on **CTD/NET Station 14049#1&2** 58 34.8N 013 51.7W.
	1547-1707	Hove to on **CTD/NET Station 14050#1&2** 59 10.1N 013 29.0W.
	1909-2034	Hove to on **CTD/NET Station 14051#1&2** 59 30.1N 013 15.6W.
	2337-0042/23	Hove to on **CTD/NET Station 14052#1&2** 59 59.8N 012 54.9W.
23/05/01	0332-0454	Hove to on **CTD/NET Station 14053#1&2** 60 26.4N 012 36.7W.
	0700-49	Hove to on **CTD/NET Station 14054#1&2** 60 44.9N 012 23.0W.
	1022-1146	Hove to on **CTD/NET Station 14055#1&2** 61 00.0N 011 38.1W.
	1433-1556	Hove to on **CTD/NET Station 14056#1&2** 61 16.8N 010 47.6W.
	1846-2008	Hove to on **CTD/NET Station 14057#1&2** 61 34.5N 009 53.0W.
	2247-2348	Hove to on **CTD/NET Station 14058#1&2** 61 48.0N 009 07.4W.
24/05/01	0243-0316	Hove to on **CTD/NET Station 14059#1&2** 62 02.2N 008 18.9W.

	0528-0622	Hove to on **CTD/NET Station 14060#1&2** 20.6W.	62	22.3N	008
	0838-0937	Hove to on **CTD/NET Station 14061#1&2** 19.7W.	62	43.6N	008
	1154-1416	Hove to on **CTD/NET Station 14062#1&2** 22.5W.	63	07.1N	008
	1652-1745	Hove to on **CTD/NET Station 14063#1&2** 26.2W.	63	32.6N	008
	2036-2150	Hove to on **CTD/NET Station 14064#1&2** 24.5W.	63	57.7N	008
25/05/01	0014-0152	Hove to on **CTD/NET Station 14065#1&2** 27.7W.	64	22.3N	008
	0414-0800	Hove to on **CTD/NET Station 14066#1,2&3** 29.7W.	64	47.0N	008
	0910-1112	**Station 14066 - CTD Change & Cast for comparison.**			
	1407-1517	Hove to on **CTD/NET Station 14067#1&2** 32.1W.	65	17.3N	008
	1656-1857	Hove to on **CTD/NET Station 14068#1,2&3** 13.5W.	65	21.6N	009
	2040-2143	Hove to on **CTD/NET Station 14069#1&2** 55.3W.	65	26.1N	009
26/05/01	0018-0107	Hove to on **CTD/NET Station 14070#1&2** 17.0W.	65	00.7N	010
	0332-0432	Hove to on **CTD/NET Station 14071#1&2** 41.5W.	64	35.4N	010
	0652-0735	Hove to on **CTD/NET Station 14072#1&2** 04.6W.	64	11.8N	011
	1022-1107	Hove to on **CTD/NET Station 14073#1&2** 28.4W.	63	45.7N	011
	1354-1438	Hove to on **CTD/NET Station 14074#1&2** 53.7W.	63	19.4N	011
	1728-1825	Hove to on **CTD/NET Station 14075#1&2** 21.2W.	62	52.5N	012
	2111-2232	Hove to on **CTD/NET Station 14076#1&2** 34.5W.	62	26.6N	012

27/05/01	0110-0230	Hove to on **CTD/NET Station 14077#1&2** 62 13.3N 013 21.7W.
	0500-0628	Hove to on **CTD/NET Station 14078#1&2** 61 58.7N 014 09.8W.
	0919-1112	Hove to on **CTD/NET Station 14079#1&2** 61 44.3N 014 57.9W.
28/05/01	0425-55	Hove to on **CTD Station 14080#1** 64 03.8N 014 31.9W.
	0628-47	Hove to on **CTD Station 14081#1** 63 59.0N 014 04.3W.
	0952-1056	Hove to on **CTD/NET Station 14082#1&2** 63 49.0N 013 12.0W.
	1056	**Estimated time of EK500 Fish Loss 63 49.5N 013 12.8W.**
	1328-1415	Hove to on **CTD/NET Station 14083#1&2** 63 39.6N 012 25.3W.
	1621-1711	Hove to on **CTD/NET Station 14084#1&2** 63 29.5N 011 40.0W.
	1939-2028	Hove to on **CTD/NET Station 14085#1&2** 63 19.2N 010 52.7W.
	2311-59	Hove to on **CTD/NET Station 14086#1&2** 63 06.9N 009 58.9W.
29/05/01	0227-0311	Hove to on **CTD/NET Station 14087#1&2** 62 54.6N 009 05.5W.
	0527-0621	Hove to on **CTD/NET Station 14088#1&2** 62 42.8N 008 21.4W.
	0845-0917	Hove to on **CTD/NET Station 14089#1&2** 62 30.8.8N 007 35.4W.
	1038	PES recovered 62 28N 007 10.9W.
	1200-1400	Passage through the Faeroes (Kuno Passage).
	1458	PES re-deployed 62 05N 006 08W.
	1537-1611	Hove to on **CTD/NET Station 14090#1&2** 62 03.5N 005 56.0W.
	1849-1926	Hove to on **CTD/NET Station 14091#1&2** 61 48.3N 005 05.0W.
	2153-2300	Hove to on **CTD/NET Station 14092#1&2** 61 33.6N 004 16.2W.
30/05/01	0032-0131	Hove to on **CTD Station 14093#1** 61 26.5N 003 52.0W.

	0259-0411	Hove to on **CTD/NET Station 14094#1&2** 61 19.0N 003 30.3W.
	0552-0645	Hove to on **CTD Station 14095#1** 61 10.4N 003 04.2W.
	0822-0920	Hove to on **CTD/NET Station 14096#1&2** 61 02.5N 002 37.3W.
	0933	Commenced deploying SeaSoar 61 03.5N 002 37.0W.
	1042	SeaSoar inboard 61 05.8N 002 46.8W.
	1234	Commenced deploying SeaSoar 61 02.6N 002 37.2W.
	1251	SeaSoar inboard 61 03.4N 002 38.7W.
	1352-1439	Hove to on **CTD/NET Station 14097#1&2** 60 59.0N 002 24.0W.
	1449	Commenced deploying SeaSoar 60 59.4N 002 23.0W.
	1602	SeaSoar inboard 61 02.8N 002 33.9W.
	1746-1816	Hove to on **CTD/NET Station 14098#1&2** 60 47.0N 002 07.5W.
	1824	PES recovered 60 47.0N 002 07.2W Set Course for Lerwick.
31/05/01	0718	Arrival Lerwick.
01/06/01	1945	Sailed Lerwick.
02/06/01	0015	PES re-deployed 60 47.3N 000 35.5W. Slow steaming due to weather.
03/06/01		Steaming to work area.
04/06/01	0300-0520	Hove to on **CTD/NET Station 14099#1&2** 64 35.3N 010 40.1W.
	0750-0949	Hove to on **CTD/NET Station 14100#1,2&3** 65 00.6N 010 16.1W.
	1110-1703	SeaSoar Cast outboard. 65 00.0N 010 15.0W **Station 14101**.
	1450-1508	Altered course to 198. 65 25.5N 009 51.2W.
	1703	SeaSoar Inboard 65 11.8N 009 58.9W.
	2145-2237	Hove to on **CTD/NET Station 14102#1&2** 64 39.2N 010 35.6W.
05/06/01	0038-0205	LHPR cast Outboard **Station 14103.** 64 40.8N 010 34.0W.
	0205	LHPR inboard 64 35.2N 010 39.1W.

	0417-0526	Hove to on **CTD/NET Station 14104#1&2** 64 49.8N 010 46.9W.
	0920	SeaSoar Cast outboard. 64 51.4N 010 48.9W **Station 14105.**
	1223	SeaSoar Inboard 64 42.7N 010 50.8W.
	1259-1356	Hove to on **CTD/NET Station 14106#1&2** 64 42.0N 010 51.6W.
	1900-2130/06	Hove to - wind & sea - Wind reaching Force 9-10 at times.
06/06/01	2130	Set Course186 64 57N 011 49W.
07/06/01	0130-1436	Hove to - steep sea - 64 18N 12 00W.
	1436	SeaSoar Cast outboard. 64 29.3N 011 35.3W Co. 060 **Station 14107.**
	1924-2020	Altered Course 10 degrees/minute 64 54N 010 34W.
08/06/01	0303-0411	Altered Course 10 degrees/minute 64 07N 011 42W.
	1052-1146	Altered Course 10 degrees/minute 64 43N 009 49W.
	1832-1930	Altered Course 10 degrees/minute 63 56N 010 54W.
09/06/01	0154-0259	Altered Course 10 degrees/minute 64 33N 009 15W.
	0950-1037	Altered Course 10 degrees/minute 64 46N 010 35W.
	1743-1843	Altered Course 10 degrees/minute 64 24N 008 45W.
10/06/01	0136	End of Survey 63 41N 010 05W.
	0223	SeaSoar Inboard.
	0331-0429	Hove to on **CTD/NET Station 14108#1&2** 63 40.8N 010 05.0W.
	0525-0625	Hove to on **CTD/NET Station 14109#1&2** 63 46.3N 009 54.4W.
	0715-0817	Hove to on **CTD/NET Station 14110#1&2** 63 51.3N 009 44.5W.
	0923-1020	Hove to on **CTD/NET Station 14111#1&2** 63 57.4N 009 33.5W.
	1124-1223	Hove to on **CTD/NET Station 14112#1&2** 64 04.0N 009 21.8W.
	1319-1428	Hove to on **CTD/NET Station 14113#1&2** 64 09.2N 009 10.7W.
	1522-1643	Hove to on **CTD/NET Station 14114#1&2** 64 14.0N 009 00.7W.

	1718	LHPR cast Outboard **Station 14115** 64 15.3N 008 57.7W.
	1927	LHPR inboard 64 20.5N 008 48.4W.
	2000-2113	Hove to on **CTD/NET Station 14116#1&2** 64 19.2N 008 49.7W.
	2212-2319	Hove to on **CTD/NET Station 14117#1&2** 64 24.7N 008 40.3W.
11/06/01	0100-0409	Hove to **CTD/NET/TUBE Station 14118#1,2,3,4** 64 19.9N 008 23.5W
	0423	SeaSoar Cast outboard. 64 20.0N 008 23.2W Co. 220 **Station 14119.**
	1130-1238	Altered Course 10 degrees/minute 63 39N 009 56W.
	1949-2044	Altered Course 10 degrees/minute 64 26N 008 45W.
12/06/01	0332-0440	Altered Course 10 degrees/minute 64 47N 010 28W.
	1116-1225	Altered Course 10 degrees/minute 64 36N 009 24W.
	2006-40	Altered Course 10 degrees/minute 63 54N 011 05W.
13/06/01	0417-0518	Altered Course 10 degrees/minute 64 46N 009 59W.
	1418-1710	SeaSoar recovered.
	1710	SeaSoar re-deployed 64 08N 011 42W.
14/06/01	0014-0120	Altered Course 10 degrees/minute 64 55N 010 53W.
	0818	End of Survey 64 11N 012 00W.
	0845	SeaSoar Inboard.
	0903-1051	Hove to on **CTD/NET Station 14120#1&2** 64 06.8N 011 43.7W.
	1200-45	Hove to on **CTD/NET Station 14121#1&2** 64 15.2N 011 26.7W.
	1353-1452	Hove to on **CTD/NET Station 14123#1,2&3** 64 22.8N 011 10.9W.
	1524-1633	Hove to on **CTD/NET Station 14122** 64 19.7N 011 17.3W - **aborted.**
	1700-1843	Hove to on **CTD/NET Station 14124#1&2** 64 32.4N 010 55.5W.
	1956-2042	Hove to on **CTD/NET Station 14125#1&2** 64 41.0N 010 39.2W.
	2126	LHPR cast Outboard **Station 14126** 64 41.2N 010 38.9W.
	2345	LHPR inboard 64 46.4N 010 27.4W.

15/06/01	0237-0328	Hove to on **CTD/NET Station 14127#1&2** 64 50.4N 010 19.2W.
	0420	SeaSoar Cast outboard. 64 51.8N 010 21.5W **Station 14128.**
	0642	Course 120 SeaSoar Survey Begins 64 54.8N 010 37.0W.
	1423-1548	Altered Course 10 degrees/minute 64 20N 008 25W.
16/06/01	0002-0136	Altered Course 10 degrees/minute 64 47N 010 48W.
	0908-1032	Altered Course 10 degrees/minute 64 03N 008 58W.
	1757-1928	Altered Course 10 degrees/minute 64 29N 011 21W.
17/06/01	0241-0417	Altered Course 10 degrees/minute 63 47N 009 32W.
	1030	End of Survey 64 03N 011 29W.
	1129	SeaSoar Inboard.
	1335	LHPR cast Outboard **Station 14129** 63 57.5N 011 12.7W.
	1540	LHPR inboard 63 55.7N 011 02.6W.
	1624-1706	Hove to on **CTD/NET Station 14130#1&2** 63 55.1N 010 54.9W.
	1706	PES Fish Inboard -**SCIENCE ENDS** - 63 55.4N 010 54.1W. Set Course for Govan, Glasgow.
20/06/00	0900 (BST)	Arrival KG5 Dock, Govan, Glasgow.

5. TECHNICAL SUPPORT

Deck Operations - *Rhys Roberts, Bob Keogh, Ritchie Phipps and Jeff Benson*

General Introduction

RRS *Discovery* Cr 253 'FISHES' was conducted in the north east Atlantic for the Southampton Oceanography Centre. The equipment supported during the cruise were the CTD, LHPR (Longhurst Hardy Plankton Recorder, or more affectionately referred to as the Laurel & Hardy !), SeaSoar (affectionately considered to be the 'dredge version' for reasons that become obvious in the narrative !, section 4), and Plankton net with FRRF (Fast Repetition Rate Fluorimeter). A total of 162 CTD deployments were made with the CTD wire. 2 deployments of the LHPR were made with the conductor wire.

Starboard Gantry

Used for the deployment and recovery of the CTD and nets equipped with FRRF. This worked well throughout the cruise, but it was noted that both the CTD extension, and roller extension were noisy in operation, possibly due to air in the rams. The handrail around the gantry fouls when the gantry is fully out, adding to the interesting noises and vibrations that travel throughout the ship when the gantry is in use.

The aft Rexroth winch was used for most deployments of plankton nets and FRRF. It worked without problems throughout the cruise, but could do with some adjustment to the valves to give smoother operation. Two of the handles for the stbd gantry local control are broken and need to be replaced.

Stern Gantry

Used for the deployment and recovery of the LHPR and SeaSoar. The Gantry functioned as normal without any problems for the duration of the cruise.

Midships Scientific Powerpack

Used to power the stbd gantry. The cooling fan for the electrical cabinet was found to be very hot due to a seized bearing. The fan was replaced. The gantry powerpacks cut out twice during use, this coincided with bulbs blowing on the gantry start buttons in the winch cab.

Aft Scientific Powerpacks

Used to power the aft gantry and two deck winches. The cooling fan in this powerpack was also found to have stopped due to a seized bearing. The fan was removed, and a new one was to be fitted in port.

Simrad EA-500

The Simrad EA-500 echo sounder had no operational problems; the HP colour printer was tested and briefly used during a particular area of benthic interest during the first half of the cruise.

PES Winch, Davit and Power Pack

The PES fish was deployed from the beginning of the cruise, and operated successfully throughout. Approximately four metres of fairing will need replacement clamps prior to the next deployment.

Chernikeef EM Log

The Chernikeef EM log functioned properly throughout the cruise.

Shipborne Wave Recorder

The shipborne Wave Recorder was tested and operated throughout the cruise with no reported problems.

300KW Power Pack, 20T and 10T Cobra Unit

Used periodically throughout the cruise with no problems encountered.

10T Storage System, Including 37KW Power Pack, Inboard Compensator and Diverter Sheaves

Used throughout the cruise for deployment of CTD's without problems, however it was noted that the inboard compensator ram seals are leaking. Three CTD terminations were made during the cruise, with a loss of 60 metres of wire, all were tested to 1.5 T.

20T Storage System, Including 37KW Powerpack, Inboard Compensator and Diverter Sheaves

Was used for the deployment of the LHPR. Worked well throughout the cruise. It was noted that the scroll counter for the conducting and core drums is not working. The unit has been disconnected for some reason, no sign of dangling wires or lost multimeters though! A Tobi termination was made on the conducting wire for use with the LHPR, and tested to 2.5T.

10T and 20T Cable Hauler Assemblies and Power Pack

The 10T & 20T cable haulers were used throughout the cruise, and operated satisfactorily, however several problems were noted.

The cooling water valve handles on the powerpack need to be replaced with locking type handles, one of the handles has rusted away, and the other was partially turned off by accident by staff working on the hanger top. There would appear to be a problem with a relief valve in the powerpack which makes the operation of the 10T cable haulers erratic in haul. The 20T haulers only generate the correct load when the cable is in haul, when in veer the load drops to about 0.15T. It was decided that as the unit was still operating satisfactorily, and that any time spent trying to find and rectify the problem would mean a loss of scientific time, that the problem would be best addressed in port.

10T Outboard Hanger Deck Diverter Sheaves

Used for the deployment and recovery of the CTD, with no problems encountered.

20T System Hanger Deck Diverter Sheaves and Roller Assembly

Used for the deployment and recovery of the LHPR, with no problems encountered.

30Tm Crane, Port Aft and Power Pack

Not used during the cruise.

30Tm Crane, Aft Stbd and Power Pack

Used for the deployment of plankton nets, with no problems encountered.

Non Toxic Water System

Used for the duration of the cruise, with no problems encountered. It was noted that Number 2 pump remains disconnected for some reason.

Workshop

The workshop was used extensively during the cruise for the manufacture of a variety of brackets and supports. In particular, there was a requirement to attach the TUBA (Towed Underwater Bio-Acoustic instrument), OPC (Optical Plankton Counter), and PENGUIN (Practical Environmental Networks for Grouping Underwater Instrument Nodes) to the LHPR. Several brackets were made, and fitted to the LHPR for this purpose. As TUBA requires a multi-channel conductor wire, a SeaSoar type towing adaptor was made, tested to 1 Tonne, and fitted to the LHPR. As a result, two successful deployments of the LHPR were made using the SeaSoar winch and cable.

Winch Control Cab

All controls functioned as usual. The quick stop was used at the start of the cruise to make safe the CTD winch whilst nets were being deployed. It was found by chance that the winch could still be driven with the quick stop on! All subsequent sampling and net deployments were made with the CTD winch turned off.

Two of the winch cab aft windscreen wipers were not working. Several bulbs were replaced on the winch control panel, it is much more homely up there now.

Clam System

System working well, however on three occasions the wire out could not be zeroed, and no wire out or load displayed. The problem was resolved with a power cycle and light thumping. It was also noted that there was no water depth reading on the clam display throughout the cruise.

Seismic Compressors

The Hamworthy seismic compressors were inspected for signs of damage which may have occurred due to condensation, since their use on D251. The second stage valve was removed from each compressor. Signs of rust due to condensation in the upper cylinder were clearly visible.

CTD Operations - *John Smithers and Jeff Benson*

During cruise D253, CTD stations were occupied using both the GO/Neil Brown MkIIIc CTD and the SeaBird 911 CTD. The cruise was begun using the MkIIIc and the first deployment began on the 7th May 2001. The Neil Brown CTD equipment used during cruise D253 was as follows:

CTD DEEP04

FSI Rosette Pylon 24 Bottle	SN 01
Chelsea Instruments Aquatracka	SN 161/2642/003
Chelsea Instruments Fluorometer	SN 88/2360/108
Simrad 200 metre Altimeter	SN 9607048
RDI LADCP	20 degree Beam
RDI LADCP	30 degree Beam
SIS Reversing Thermometers	T795,1684,1545
SIS Reversing Pressure Meters	P6394,6751, 6534

Pascal Oxygen Sensor

All equipment functioned satisfactorily. The 20° beam angle LADCP was mounted on the frame for most of the CTD stations. Stations 13966-14034 were occupied using the MkIIIc with little problem other than a requirement to re-terminate the sea cable due to damage

sustained in heavy swells. A total of three terminations were carried out over a short period of time, with no further occurrence of cable problems during the cruise.

The Pascal Oxygen sensor was fitted for station 13981. This used a SeaBird pump to create the required flow over the sensor head, driven by a separate battery pack. The sensor output was digitised within the CTD. The results observed during the casts provided graphical plots that suggested either the pump or the sensor were intermittent. This sensor was still under development and data were being collected for evaluation back at SOC.

During the intervals between casts, attempts were made to interface a full ocean depth Optical Plankton counter. This interface had been built and tested at SOC but not used on the CTD wire. A number of problems with interference between the Rosette Pylon and the OPC and overall signal levels were experienced. These were solved and the OPC fitted for station 14011. The OPC performed correctly during the down cast but failed at 600 metres on the up cast. The OPC was removed and casts continued using the MkIIIc until station 14026.

A number of casts were made firing Niskin bottles “on the fly”. This was attempted on a few repeat stations to verify the quality of calibration that could be obtained this way. Although considerable time per cast can be saved, 30 seconds/bottle fired, there were concerns expressed about how satisfactory the results would be and so a normal operation of the firing system was later resumed.

From station 14027 the Seabird system was used. A new Pascal oxygen sensor head was fitted and transferred to the SeaBird system. This appeared to work in the expected manner and data was collected for later evaluation. During this series of casts the 20° beam angle LADCP was swapped to the SeaBird system.

A total of 40 SeaBird CTD casts (consisting of 38 files) were completed during this cruise, station numbers 14027 through 14066. Two casts were not recorded to the hard drive, (station numbers 14029 and 14031), as a faulty ZIP drive resulted in the data being corrupted and not recoverable from the personal computer. Station number 14049 was divided into two casts, (14049 and 14049A), as a software problem caused a required reboot during data collection. SeaBird for Windows version 1.22 was used for real-time data collection, and SeaBird DOS version 4.248 was used for all post-processing, as a Windows software error made operating the SeaBird Windows post-processing inoperable. All casts were simultaneously recorded to the DAPS, thus no raw data was lost. The calibration file used for all casts was D253MAIN.CON and the cast files configuration was as follows:

24-way rosette frame

CTD underwater unit: Sea-Bird 9+ (s/n 09P24680-0636)

Primary Premium Temperature Sensor 3P (s/n 03P-4107)

Primary Conductivity Sensor 4C (s/n 04C-2573)

Primary Submersible Pump 5T (s/n 05T-3002)

Digiquartz Temperature Compensated Pressure Sensor (s/n 83008)

Secondary Premium Temperature Sensor 3P (s/n 03P-4116)

Secondary Conductivity Sensor 4C (s/n 04C-2580)

Secondary Submersible Pump 5T (s/n 05T-3090)

Pylon: Sea-Bird 32 Carousel/24-bottle position (s/n 32-24680-0345)

Aux 0) Sea-Bird Oxygen Sensor 43B (s/n 43B-0008)

Aux 2) Benthos/Datasonics PSA-916T Altimeter (s/n 875)

Aux 3) Chelsea MKIII Aquatracka Fluorimeter (s/n 88-2360-108)

Aux 4) Pascal micro-electrode oxygen sensor (s/n I)

Aux 6) SeaTech Light Scattering Sensor (s/n 339)

Aux 7) Chelsea MKII Alphatracka 25cm path Transmissometer (s/n 161047)

The Chelsea fluorimeter was the same instrument used as on the Neil Brown CTD frame, as continuity of measurements was required for all CTD casts. The SeaBird oxygen sensor was pumped through the secondary pair of temperature and conductivity sensors for all CTD casts. The Benthos/Datasonics altimeter did not give adequate height off bottom readings for many of the casts. Numeric data fluctuated between "real" values and "false" values randomly, and frequently at critical moments nearing full depth. Various positions were tried on the frame, limited by the location and amount of other instruments installed, as was the powering down of all other acoustic sources: by trial and error over many stations, it was determined that acoustic interference was not the cause, and that the location of the altimeter was not ideal. The installation near the outer stainless steel ring was reflecting the altimeter signal prior to receipt by the instrument. Lowering the unit below the frame assisted in better height off bottom data, but did not fully solve the problem. In future these altimeter models need to be installed as close to the centre of the frame as possible. As a final check, the spare altimeter (s/n 876) was

installed from station number 14048 onwards, with no noticeable improvement in bottom detection.

From cast 14063 onwards the Neil Brown MkIIIc CTD was used again and the OPC tried once more. A number of problems were experienced with the first cast which was traced to a fault in the MkIIIc causing frequent loss of frame sync and data. This was repaired for the next cast but still a problem persisted with the OPC; this turned out to be due to a faulty lead. Once replaced the OPC gave good data throughout the remainder of the cruise.

The 20° beam angle LADCP was swapped back to the MkIIIc CTD system frame after some casts were carried out with the 30° beam angle instrument which eventually suffered a beam failure.

The second leg of the cruise was biased towards long SeaSoar tows but a number of CTD and LHPR stations interspersed these tows.

Interfacing the OPC with the Neil Brown MkIIIc CTD - *John Smithers*

Prior to cruise D253 a technical innovation fund bid was secured to interface an Optical Plankton Counter to operate on the same single conductor wire as the CTD. The CTD operated with a 5/10 kHz FSK data transmission system and the OPC with 44/50 kHz FSK, both had to be transmitted simultaneously over the same conductor along with a third frequency of 1200 Hz, utilised to communicate with the Rosette Pylon.

To achieve this objective, a new FSK transformer was designed for the CTD to allow the auxiliary power requirements for other external instruments as well as the OPC to be handled in a more efficient manner than had been done previously. The FSK modulator board was modified to allow this to be done. The CTD was also provided with a constant current circuit to deliver 200 mA at approximately 25 volts to the OPC. A mixer circuit combined the two FSK frequencies and drove the transformer, thence the single conductor sea cable. Signal levels of the two FSK systems were adjusted to give maximum signal levels but to minimise interference with the Rosette Pylon.

Simple high and low pass LC filters allowed the appropriate FSK signals to be separated and routed to the CTD and OPC deck units. A small degree of amplification was necessary to boost the higher frequency OPC FSK signals. In conclusion, the required circuits and modifications were relatively simple to install and extended the range of oceanographic measurements that could be made.

SeaSoar Operations - *John Smithers and Jeff Benson*

The SeaSoar system used during cruise D253, FISHES, made use of the existing body shell, towing bridle and hydraulic power system as used in the past but with a totally new payload and internal arrangement (Figure 4). The hydraulic power system sat further back in the vehicle, with a nylon cylinder fitted to extend the existing tail cone. This provide enough space for two full length instrument bays within the vehicle, one above the other. The most visible change came from the necessity to gain access to both top and bottom of the vehicle. To allow this freedom of access, the SeaSoar was mounted vertically on its tail in a purpose built launch and recovery stand.

In spite of a high instrument density and little free space, the instrument payload could be fitted and removed with little difficulty. Fitting the tow cable to the bridle was just a bit more awkward and required at least 2 but preferably 3 people to carry out. During the launch and recovery of the vehicle the new vertical stand somewhat simplified the procedure although a few modifications need to be made in the future to avoid the possibility of trapped fingers and increase the ease of use etc.

The SeaSoar operations, constrained to the second leg of the cruise, were divided into three fine scale surveys in water depths ranging from 300-1600 metres. An opportunity was taken at the end of the first leg of the cruise to test the system and check it's flight capabilities. These were abortive for a number of reasons but allowed time to attempt or suggest solutions before the start of the second leg. The impeller that drives the hydraulic Seasoar hydraulic power pack had been fitted at SOC for demonstration purposes and without a key to lock it to the shaft. The quality of fit to the shaft was such that a test by rotating the impeller by hand caused the appropriate effect to the wing angle. Once launched however, the impeller merely rotated freely doing little or rather nothing at all. The vehicle was recovered and this rectified before a second deployment. This time there was still no response from the control system. Various problems with the instruments failed to produce a satisfactory test run.

On the second leg of the cruise, some modifications were made and the vehicle was eventually launched with a functioning payload. The dummy pressure case initially fitted in place of Tuba was removed. Initially there was no response from the vehicle, but this recovered, indicating that the Moog control valve in the hydraulic power pack had stuck, this may have also have been the case for the second test deployment. From this point onwards, the vehicle flew well with little roll and a slight tail down attitude. The maximum depth obtained with 700 metres of faired cable was 485 metres. Overall repeatability of each yo-yo was excellent. Some careful changes in ballast to move the centre of gravity more towards the centre of pressure of the wings could perhaps have yielded more depth.

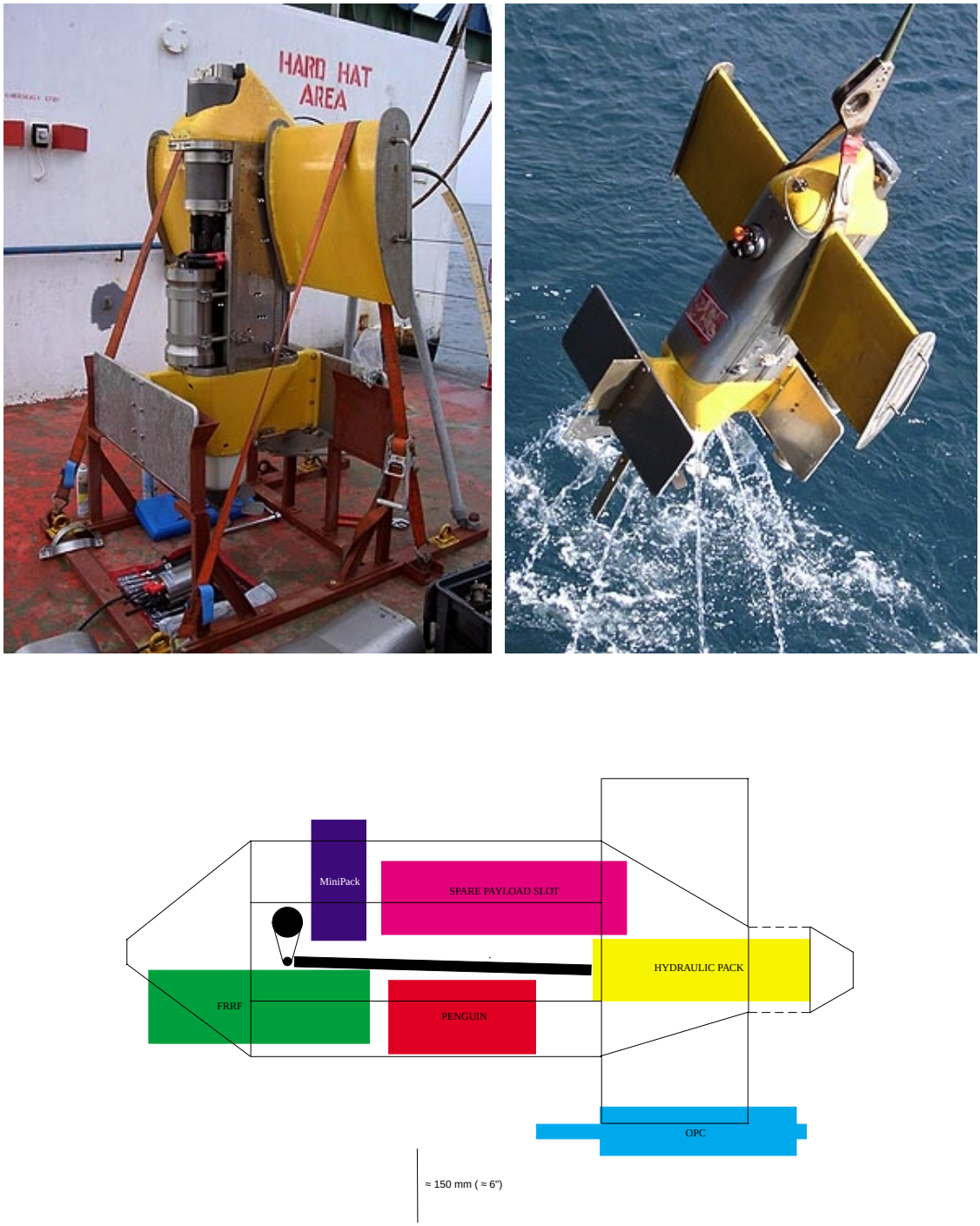

Figure 4: Two photographs of the 'new' SeaSoar system used on the FISHES cruise, and a schematic diagram of the SeaSoar payload in profile view.

The horizontal winch used for deployment and recovery worked smoothly although a certain amount of fiddling was necessary to position the scrolling gear so that it could work as designed. The deck unit and control software performed without problem.

Two incidents marred an otherwise very successful series of surveys. At the last stage of the first recovery, the SeaSoar vehicle swung and struck the stern of Discovery quite heavily. The CI FRRF sustained mechanical damage but on recovery still worked. This was replaced with a second FRRF for the second deployment. Contact with the sea-bed occurred during the second fine scale survey causing damage to the FRRF and what turned out to be more or less cosmetic damage to the OPC mounted under the tail. A third FRRF was fitted and the third survey completed without incident.

SurfMet System - *Jeff Benson*

The SurfMet system was installed for this cruise in the following configuration:

A) TSG system: housing temperature FSI OTM s/n 1374

remote temperature FSI OTM s/n 1360

housing conductivity sensor FSI OCM s/n 1376

flow-through 20cm transmissometer WetLabs/SeaTech s/n T-1005

flow-through fluorometer WetLabs s/n WS3S-117

All the above sensors are calibrated with the exception of conductivity which has its calibration stored internally. Rhopoint DGH convertors are used to give +/- 5 volts for the transmissometer and fluorometer data. The transmissometer and fluorometer were cleaned at weekly intervals throughout the cruise, with air and blank values recorded pre- and post-cleaning to monitor sensor drift.

B) Met system: air temperature/relative humidity Vaisala HMP44L s/n 1850014

barometric pressue Vaisala PTB100A s/n S361008

port PAR sensor Didcot/ELE DRP-5 s/n 30471

starboard PAR sensor Didcot/ELE DRP-5 s/n 30470

port TIR (pyranometer) sensor Kipp & Zonen s/n 994133

starboard TIR (pyranometer) sensor Kipp & Zonen s/n 994132

anemometer Vaisala WAA s/n P50421

wind vane Vaisala WAV s/n R07101

The wind speed and direction are not calibrated; all other meteorological sensors have calibrations. Met system data is collected through a Vaisala QLI50 sensor collector. All SurfMet data is polled once every second; a thirty second average is then taken and sent to the OED shipboard data collection for application of calibration constants. In addition, salinity is calculated using the housing temperature and conductivity sensors, and calibrated throughout the cruise by once hourly salinity samples.

General Data Logging and IT Support - *Rob Lloyd and Martin Beney*

The standard suit of (RVS) logging and processing hardware and software was provided for this cruise together with network support for the PSTAR processing software.

The cruise was largely problem free but for the usual difficulties in integrating a number of different mailers with the hybrid Novell Groupwise and BAS satellite link software.

An intermittent problem occurred with the Ashtek attitude sensing system that required careful watch-keeping but overall little data was lost.

An important new feature of the cruise was the provision of the JIF funded DartCom satellite data receiving system. Routine weather images were processed and used by the ships officers to supplement their existing systems. Some spectacular images were captured including a clear image stretching from the Azores to the Pole of two Atlantic depressions on the 22nd. May. From this image we were able to highlight some orographic lenticular clouds stretching 40 km downwind from the Færœ island of Suduroy. Other notable images included the Greenland ice shelf and one clear image SST representation of the Iceland Færœs front.

PENGUIN (SeaSoar) Data Logging - *Vic Cornell, Nick Crisp, James Riggs*

"**P**ractical **E**nvironmental **N**etwork for **G**rouping **U**nderwater **I**nstrumentation **N**odes"

Discovery cruise 253 has seen the first deployments of a new instrument logging system "PENGUIN". This new system provides greater data logging capacity to towed and tethered platforms such as SeaSoar and LHPR, increasing the number of instruments that can be logged and the data bandwidth available over conducting cables. The deployments have been an almost unqualified success with almost 100% reliability of the logging system and full retrieval of all data values logged by the attached instruments. The system itself is very new and we were expecting some "teething" problems. Some of these have been encountered but most have been overcome.

System Description

PENGUIN is an independent underwater data acquisition system based around an implementation of DAPS (Data Acquisition System) on the open source operating system LINUX. On cruise D253 we have deployed PENGUIN as the data collection system for both the SeaSoar vehicle and the LHPR. Penguin acquires data from instruments typically via serial interfaces. Via DAPS, it validates, timestamps and logs the data to an on board hard disk. If a network connection has been configured via the towing cable the data is made available to clients initiating ftp transfers. Software has been provided (the EMPEROR system) to automatically monitor PENGUIN and use ftp to routinely transfer all collected data to an archive area on a ship-side storage area. In addition by acting as the cabling hub for SeaSoar and other platforms PENGUIN can house power supplies and act as a power distribution and conditioning unit.

Deployments

Station No	Date	Time	Platform	Configuration
Test	150		SeaSoar	
14101	155	10:47	P2/SeaSoar	Penguin+OPC+FRRF+MiniPAK+ATT
14107	158	14:37	SeaSoar	Penguin+OPC+FRRF+MiniPAK
14119	162	04:26	SeaSoar	Penguin+OPC+FRRF+MiniPAK
14126	166	21:26	LHPR	LHPR
14128	166	04:14	SeaSoar	Penguin+OPC+FRRF+MiniPAK
14129	168	13:35	LHPR	Penguin+OPC

SeaSoar

The first deployments made were three test runs made at the end of the first leg of the Cruise. The first of the two units brought, PENGUIN_A, successfully logged OPC, CTD and FRRF. SeaSoar however would not “fly” correctly and was retrieved after 1-2 hours each time.

A more determined deployment was made at the start of the second leg. The second unit PENGUIN_B was mounted on SeaSoar, logging OPC, FRRF, MiniPAK and the on-board attitude sensor. After 2 hours of operation connection was lost with PENGUIN_B. Several things were tried including power cycling the modems. A power cycle was initiated and

connection was restored. However, the MiniPAK CTD failed to return to function despite several shutdown/restarts/power cycles and the SeaSoar was retrieved. It was this event that prompted us to introduce the power cycling and modem reset functionality detailed below.

At this point doubts were raised about the advisability of deploying PENGUIN_B in its relatively untried state and, after a prolonged period of bad weather a re-deployment was made using PENGUIN_A. The deployment was a complete success with only short (5-20 seconds) interruptions encountered and these easily overcome by PENGUIN_A re-setting its modems. Two further 3-day SeaSoar deployments were made without event, the only changes made to the system being refinements to the plotting programs used to display the data as it arrived.

LHPR

It was decided that there would be scientific merit in mounting both TUBA and the OPC on the LHPR and making a series of tows. PENGUIN would be used to log the OPC data in an "off-line" mode since it was felt that the PENGUIN data signal would, if carried on the same cable as that of TUBA, interfere with TUBA's data stream. PENGUIN could not log TUBA data directly at this time.

PENGUIN_B was mounted on the LHPR frame and networked temporarily by running a separate cable across the deck. The network link had been temporarily re-routed through the Hydraulic sea-connector on PENGUIN_B's end cap for this purpose. Once the system had been booted, and logging established, the network cable was detached and the vehicle launched. The tow and recovery went well, however on re-attaching PENGUIN_B to the network it was found to be shut down. This turned out to be the result of our failure to de-activate the network monitoring scripts used for SeaSoar tows!

A second LHPR tow as made at the end of the cruise. This time PENGUIN_B logged the OPC data without interruption.

Solutions to Problems Encountered

Connection Failures

During operation the Penguin ADSL connection has shown a tendency to temporarily loose connection. Whilst this does not cause data loss as Penguin caches data on its hard disk and transfers it asynchronously to the ship-board system, it has caused concern. Any long-term connection failure on a SeaSoar deployment would result in a retrieval since it could not be guaranteed that data logging was taking place. Also the pressure signal that PENGUIN sends up the towing cable is necessary for "flying" SeaSoar.

Scripts were written to allow PENGUIN to first reset its internal modem and then reboot itself should it discover a connection failure. This successfully allowed PENGUIN to recover from several long connection breaks. PENGUIN will now automatically shut itself down should the above methods fail to re-instate the link successfuly. Thus a full power cycle of SeasSoar could take place from the ship safely. The only possible downside to this system is one must remember to disable it in situations where PENGUIN is logging data in non-networked mode. Otherwise PENGUIN will shut itself down within 5 minutes of being removed from the network.

CTD Resets

During a full reset of the system, it was discovered that the CI MiniPAK would not return to service after a simple power cycle. Only a sequence of two power cycles separated by about three second would return it to active logging. This caused us to undertake a review of Penguin's power management strategy. It was suggested that relays could be installed and controlled through I^2C from PENGUIN's parallel port. This was successfully implemented for the MiniPAK CTD and power resets are now possible through the "mpower" script.

Gnuplot.

It is very useful during SeaSoar deployments, to be able to visualise the data collected in almost real time since problems and collection errors can be easily noted from changes in the data patterns. Since DAPS logs data in an ASCII data stream we experimented with GnuPlot, an open source package which is often bundled with LINUX. Despite the fact that Gnuplot is quite basic and only allows a single property to be plotted on a single line, quite useful plots were produced and scripts written which would update them, on screen, periodically.

This achieved functionality similar to that of the software used with the previous Neil Brown CTD based SeaSoar vehicle.

Physical Characteristics

PENGUIN is housed within a titanium acetyl pressure case and has proved, in the field, extremely robust. It has survived one impact by SeaSoar with the ship's stern during the recovery stage of the second deployment and one "dredging" event where SeaSoar brought back some sample of the Iceland-Færœs Ridge.

In the first event, the FRRF was rammed into the top of PENGUIN_A's pressure case where the connectors are attached. Some deformation of the connector blocks occurred but this was temporary and no other damage was sustained.

In the second event SeaSoar hit the seabed wedging a large number of small rocks in the OPC slit and between the OPC and the SeaSoar tail wing. PENGUIN_A again appeared to be undamaged and continued logging, again the FRRF bore the brunt of the damage.

6. SCIENTIFIC INVESTIGATIONS

Lowered CTD Data - *Raymond Pollard, Stuart Cunningham, Penny Holliday, Naoise O'Reilly*

CTD Measurements

During this cruise two types of CTD instrument were used: a Neil Brown (DEEP04) MkIII CTD and a Sea-Bird 9/11 *plus* (SBE). DEEP04 is an instrument that has been accurate and reliable and used regularly since its purchase in 1993, while the SBE is a new instrument to us. Therefore, this cruise was used to gain experience of the SBE (operation, data logging and processing) and to directly compare its performance with the familiar (tried and tested) DEEP04.

Introduction to Neil Brown CTD data processing

Raw CTD and bottle firing data were logged to the CTD acquisition PC and passed to the SOC Data Acquisition and Processing System (DAPS). DAPS ran on a SUN-Ultra 5 workstation with a 16 serial-port box for receiving data inputs. DAPS performed the role of the RVS Level ABC system, including a one second de-spiking and averaging routine.

DEEP04 has, historically, been a relatively stable and accurate instrument: the pressure sensor has small hysteresis, less than 0.6 dbar and has consistently shown differences in full scale pressure from one calibration to the next of less than 1.0 dbar; the temperature sensor has also been relatively stable with an average rate of change of 0.4 m°C/year since 1993.

Processing Path

The following cshell scripts were used to process the CTD and bottle data. In the following ###### is a five digit Discovery station number. The numbering convention for D253 was such that each station could have a series of casts, where #1 signified the primary CTD cast, #2 a net haul and #3 a repeat CTD cast if more water was required for the primary productivity stations. In the following files, the main CTD cast is given the station number (eg 13989), with bottle samples numbered 1 to 24. Repeats CTD casts (#3) are numbered 3#### (eg 33989) and the bottle samples numbered 25 to 48. On the two occasions when 2 main CTD casts were done

(stations 14034 and 14066) the second CTD cast files were numbered 034 and 066 eg ctd034.1hz.

CTD Path

>*ctd0*: Read in raw 1hz CTD engineering data from DAPS and created a PSTAR file: File out -> ctd#####.raw. Also, read in the winch data. File out -> win#####

>*ctd1*: Applied sensor calibrations to the raw data using the PEXEC program ctdcal. The calibration coefficients were read from calibration file d253.ctd04.cal. This calibration file was modified during the cruise as the conductivity calibration was refined. New versions of the file had station numbers inserted in the file name to indicate which stations the modified calibration applied to. File out -> ctd#####.cal, .1hz (1hz calibrated down and up cast file), .10s (10s averaged 1hz file; used to merge onto firing times to compare with the sample salinity data).

>*ctd2*: Produced a 2db gridded downcast file from the .1hz file. File out -> ctd#####.2db.

Firing Path

>*fir0*: Read in bottle firing data (time and firing code) from DAPS. File out -> fir#####.tim.

>*fir1*: merged winch data onto the firing file. File out -> fir#####.wir

>fir2: merged the 10s CTD data onto the firing data. File out -> fir#####.ctu.

>*fir3.press*: Ran PEXEC program pbotle. This extracted records from the downcast 2db file that matched the upcast bottle firing data; this was used to calibrate CTD oxygens. File out -> fir#####.cud.

Sample Path

> *makeblanks*: created empty sample files ready to receive CTD firing data, bottle salinities and other chemistry data. File out -> sam#####

>*pat.exec, sal.exec, chl.exec, nut.exec, oxy.exec*: used to ftp sample bottle files from a Mac, remove extraneous characters, read into pstar file (pascin). The script names referred to reversing instruments, salinity, chlorophyll, nutrients and oxygens respectively. Files out -> pat#####.bot, sal#####.bot, chl#####.bot, nut#####.bot, oxy#####.bot.

>*paspat, passal, paschl, pasnut, pasoxy*: Used PEXEC program ppaste to paste salinity sample data into the sample file.

>*pasfir.rtp*: Used PEXEC program ppaste to paste upcast CTD data (10s average) at the bottle firing times into the sample file; paste downcast 2db CTD data corresponding to bottle fires, for oxygen calibration. Variables in the sam##### file were prefixed by d for down and u for up.

>*makeresid*: This exec calculated bottle conductivity (botcond) = F(botsal, upress, utemp) where upress and utemp were upcast CTD values matched from the ctd.10s file at the time of bottle fires and botsal was bottle salinity. It also calculated differences between reversing instruments and CTD upcast data, and between bottle oxygen and CTD oxygen downcast data. File out -> res#####. This script was used by NPH in preference to the alternative "botcond.exec" (SCU) which only calculated conductivity residuals. The latter script wrote new variables to the sam#####, causing subsequent problems with incompatible variable names for gridding and on occasion caused corruption of files which were being written to simultaneously by 2 users.

>*ctdtimes.exec and ctdpos.exec*: The combination of these two scripts picked out the start, bottom and end time of each CTD cast, wrote them to a pstar file and merged in the latitude, longitude and water depth for each time. The lat, lon and depth at the bottom of the CTD cast was pasted into the header of all CTD, firing and sample files. File out ->tim#####.a.

<u>*Calibration*</u>

Temperature

Temperature raw counts were first scaled by (1) then calibrated using (2),

$$T_{raw} = T_{raw} \times 0.0005 \tag{1}$$

$$T_{cal} = 0.12019 + 0.99930 \times T_{cal} \tag{2}$$

Temperature response was accelerated to match conductivity by (3),

$$T = T + 0.25 \times \frac{\partial T}{\partial t} \tag{3}$$

where 0.25 was chosen to minimise salinity spiking.

Pressure

Raw pressure counts were scaled by (4) then calibrated using (5),

$$P_{raw} = 0.1 \times P_{raw} \tag{4}$$

$$P_{cal} = -34.5 + 0.107373 \times P_{raw} \tag{5}$$

Conductivity

Raw conductivities were scaled by (6) then calibrated using (7), (8) or (9) according to station number,

$$C_{raw} = 0.001 \times C_{raw} \tag{6}$$

Stations 13965 to 13999 $C_{cal} = -0.0332096 + 0.96230015 \times C_{raw}$ (7)

Stations 14000 to 14026 $C_{cal} = -0.0352633 + 0.96224496 \times C_{raw}$ (8)

Stations 14064 to 14130 C_{cal}=-0.0162905+0.9546438xC_{raw} (9)

Immediately before station 14063 (a station subsequently abandoned) a new conductivity cell (L53) was fitted to try to eliminate the systematic hysteresis between down and up (salty) theta/S profiles.

This was followed by the cell material deformation correction (10)

$$C = C \times \left[1 + \alpha\left(T - T_0\right) + \beta\left(P - P_0\right)\right] \tag{10}$$

where the coefficients for the cell material were: $\alpha = -6.5E-6C^{-1}$, $\beta = 1.5E-8dbar^{-1}$, $T_0 = 15°C$ and $P_0 = 0dbar$.

Equations (7), (8) and (9) were determined as a best fit of (bottle conductivities - upcast CTD conductivities) versus bottle conductivities across groups of stations that by eye, had similar slope and offset. Residuals versus pressure were also examined and it was concluded that the residuals were best fit in conductivity space (rather than pressure). After calibrating the raw

conductivity data using (7), (8) and (9), a small residual station by station offset was removed. Salinity was recalculated, and the salinity residuals after final calibration are shown in Figure 5.

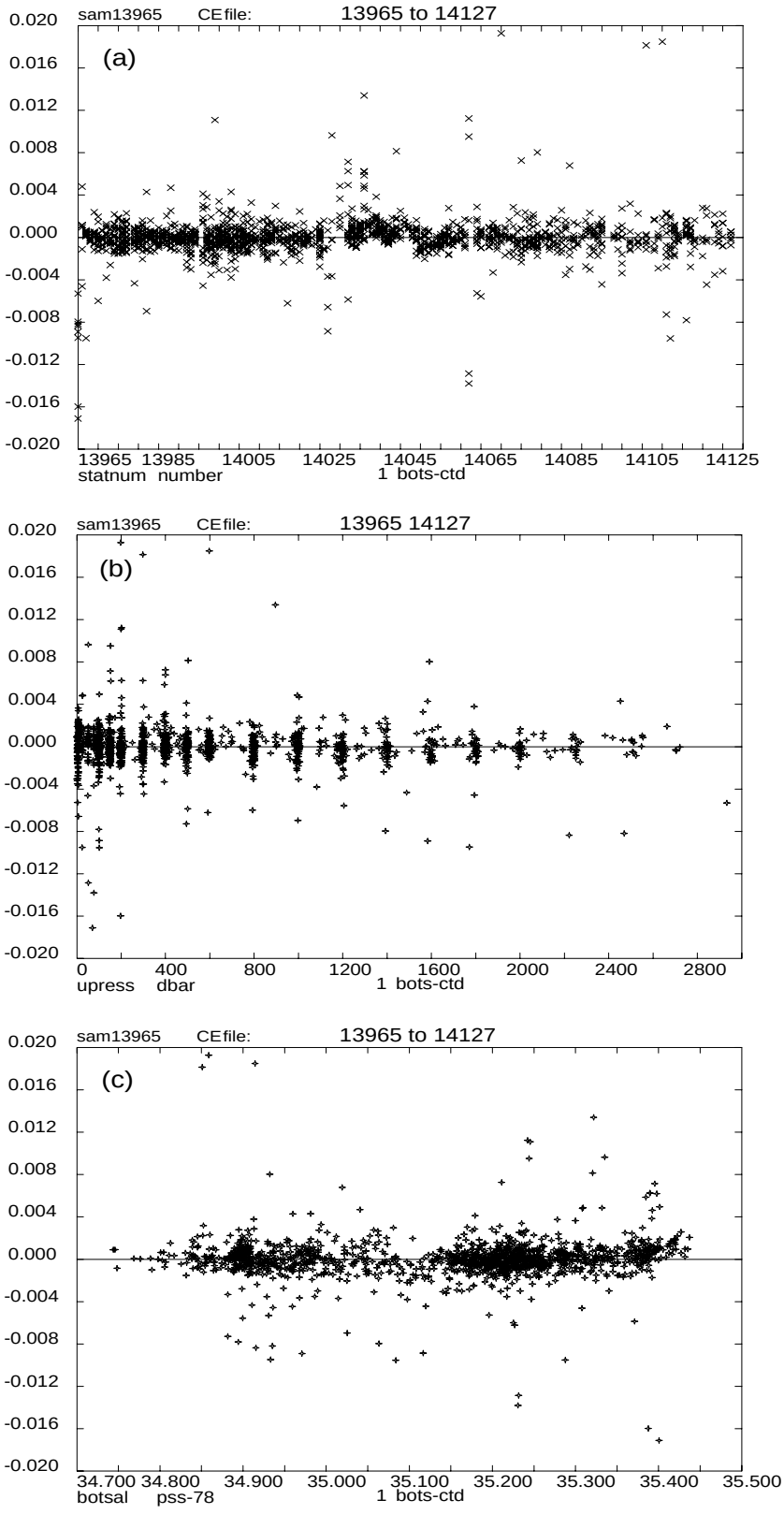

Figure 5: Neil Brown MkIII salinity residuals (bottle salinity - upcast ctd salinity) plotted against (a) station number, (b) pressure and (c) bottle sample salinity.

Statistics of the remaining salinity residuals were:

Stations	Mean	Standard Deviation	n (limits ±0.03)
13965 to 13999	-0.0003	0.002	412 of 433
14000 to 14026	-0.0001	0.001	308 of 320
14064 to 14130	0.0001	0.002	413 of 431

(see later for details of SeaBird stations 14027-14062)

Transmittance, Fluorescence, Altimetry

Transmittance and fluorescence were converted to voltages through the calibration of the analogue CTD channels (11).

$$volt = -5.62440 + 1.7166419 \times 10^{-4} (volt)_{raw} + 3.0839868 \times 10^{-12} (volt)^2_{raw} \qquad (11)$$

Altimetric raw data were converted to height off bottom by (12).

$$alt = -271.412911 + 8.260713 \times 10^{-3} (altraw) + 6.740444 \times 10^{-10} (altraw)^2 \qquad (12)$$

Oxygen

No attempt was made to properly calibrate the CTD oxygen sensor with the bottle samples. A nominal calibration was applied to allow plotting on reasonable scales, but a careful calibration was not attempted before the end of the cruise. The new Pascal oxygen sensor was deployed on all the DEEP04 stations, the only calibration carried out however was to instrument volts (11).

Neil Brown CTD Data Problems

As documented on a few preceding cruises Neil Brown CTD DEEP04 had developed a significant hysteresis in salinity between down and upcasts, with the upcast salty relative to down (Cunningham et al., 2000; Holliday, 2000). The typical hysteresis produced an error of up to 0.004 in salinity a few hundred meters after the bottom of the down cast (Figure 6). The reasons for this were thought to be in the conductivity sensor as in situ calibration of the temperature sensor and laboratory calibration of the pressure sensor had not shown any problems. However, this hysteresis persisted despite the trial of a number of different conductivity cells and it therefore remains something of a puzzle.

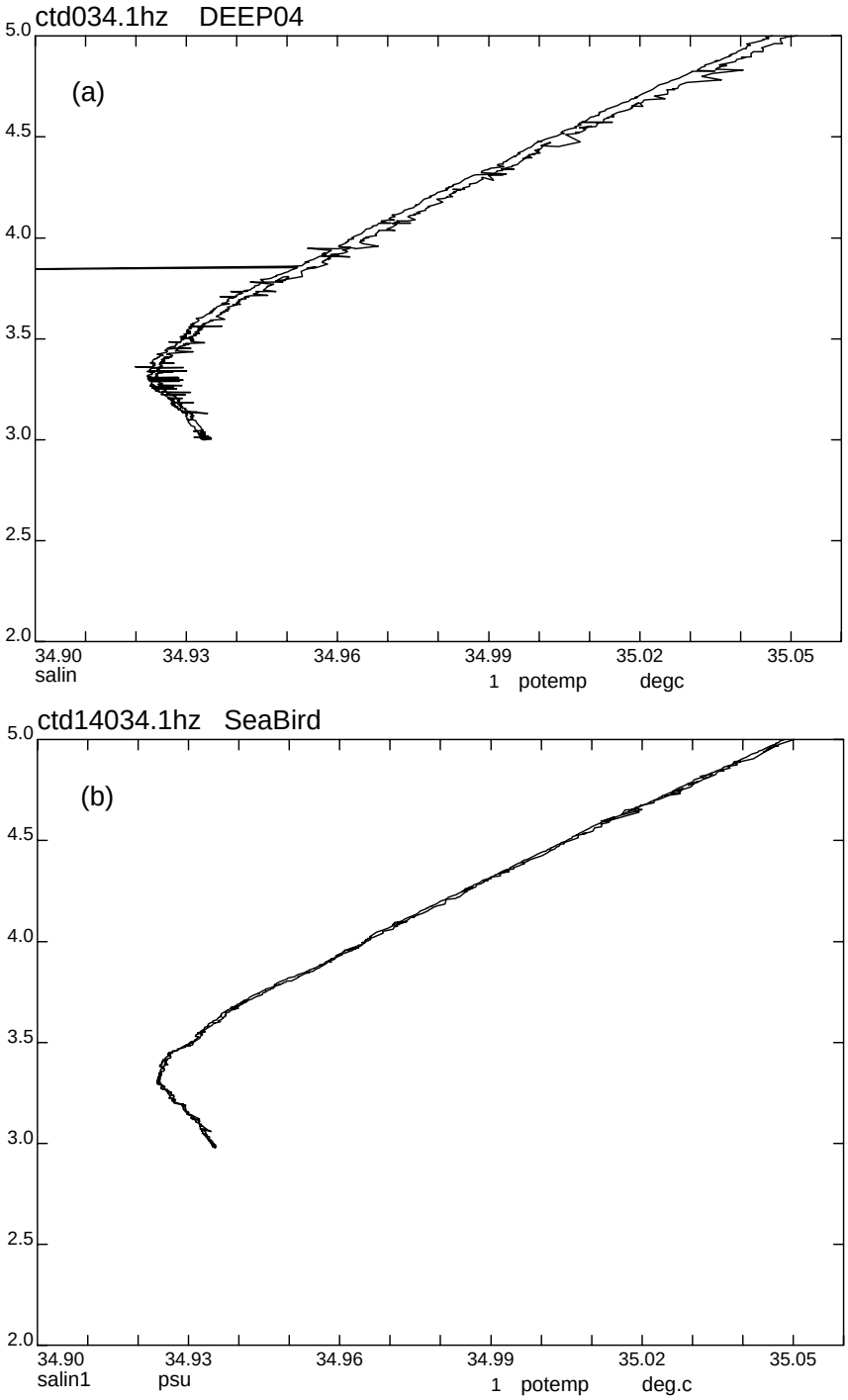

Figure 6: Repeat hydrography; down/up-cast theta-S plot for the deep water at station 14034, from the 1Hz data. Two plots are shown: (a) shows the NB DEEP04 profiles and (b) shows the SeaBird profiles. The NB DEEP04 is noisier and the upcast is about 0.004 salty relative to the down cast.

SeaBird SBE 9/11 plus instrumentation

Within the UK National Marine Equipment Pool (NMEP) the stock of older Neil Brown CTD's (a mixture of pre-WOCE and WOCE upgraded instruments) were gradually being replaced. The instrument of choice in the wider oceanographic community was the Sea-Bird 9/11*plus* for high accuracy and precision deep-sea oceanography. RRS *Discovery* cruise 253 was an ideal first opportunity to try one of the new (to NMEP) Sea-Bird 9/11*plus* instruments and learn how to process and calibrate the data; it also presented an ideal transitional opportunity to compare the accuracy and precision of the SBE to the older Neil Brown MkIII CTD DEEP04 by repeat stations in deep water.

Processing Path

Where possible, the processing of the SBE CTD data followed closely the path and naming conventions of the DEEP04 CTD processing. Differences are highlighted below.

The SBE CTD had dual conductivity and temperature sensors. We did not extended the processing to consider or handle the duplicate measurements. Throughout, we used the primary variables cond1 and temp1 for calibration and these variables appeared in the sample files unaccompanied by their duplicates. During each cast it was noted that the differences between the duplicate sensor pairs was small. Preprocessing of the data was done using SBE processing programmes on a PC. These were set up to run using DOS batch processing. The processing of the SBE data is explained in detail in the SBE 9/11 data acquisition software manual (http://www.seabird.com/pdf_documents/documents.htm).

> *process###.bat* where ### is the last three digits of the station number. This process ran the following SBE routines, using input File: D253_###.dat and working file D253_###.cnv:

>datcnv -iD253_###

>wildedit -iD253_###

>celltm -iD253_###

>filter -iD253_###

>asciiout -iD253_###

>rossum -iD253_###

creating ASCII output files:D253_###.ros, .bl, .btl,con, .dat, .hdr, .asc and binary output file: D253_###.cnv. All files were archived until their significance for final processing had been

determined. A 2500m cast took 6 minutes and 41 seconds to process, and this time could be expected to scale with water depth.

The following short notes, looking at the individual SBE processing routines in a little more detail, were taken from the SBE manuals; the latter should be consulted for a full description of the instrument and algorithms.

< datcnv, converted the raw data to pressure, temperature and conductivity and parameters obtained from auxiliary sensors such as dissolved oxygen current, dissolved oxygen temperature and light transmission. The following equations converted the sensor frequency outputs to calibrated data.

Temperature

$$T_{cal}(ITS-90)°C = \left(\frac{1}{\left\{ g + h\left[l_n\left(f / f_0 \right) \right] + i\left[l_n\left(f / f_0 \right) \right]^2 + j\left[l_n\left(f / f_0 \right) \right]^3 \right\}} \right) - 273.15 \qquad (13)$$

where l_n was the natural log function, f was the output frequency in Hz, $f_0 = 1000$ was an arbitrary scaling used for computational efficiency. The temperature calibrations were performed on 6 March and 1 March 2001 for the primary and secondary sensors respectively. Fitted temperature residuals were less than 0.00009°C with the following calibration coefficients for (13).

coefficient	primary	Secondary
g	$4.40360373.10^{-3}$	$4.42585928.10^{-3}$
h	$6.48784093.10^{-4}$	$6.84179508.10^{-4}$
i	$2.32857082.10^{-5}$	$2.43170152.10^{-5}$
j	$2.05881294.10^{-6}$	$1.98973198.10^{-6}$

Conductivity

The conductivity sensors were calibrated over a range of 3 to 6 Sm^{-1} using natural seawater; a water sample at each point was compared to IAPSO standard seawater using a Guildline AutoSal. The calibration equation was,

$$C(Sm^{-1}) = \frac{g + hf^2 + if^3 + jf^4}{10(1 + \delta T + \varepsilon P)} \tag{14}$$

where f was the instrument frequency (KHz), T was temperature (°C), P was pressure (db), $\delta = -9.57 \times 10^{-8}$ was the bulk compressibility and $\varepsilon = 3.25 \times 10^{-6}$ was the thermal coefficient of expansion of the borosilicate cell.

The primary and secondary conductivity cells were calibrated on 6 and 20 March 2001 respectively. Conductivity residuals (Sm^{-1}) were all less than 0.00004, in a seven point calibration, with the following conductivity calibration coefficients.

Coefficient	primary	Secondary
g	-10.5041834	-10.5025701
h	1.63101173	1.54527667
i	$-1.13122928.10^{-4}$	$-2.51475759.10^{-4}$
j	$1.01138491.10^{-4}$	$1.04102654.10^{-4}$

Pressure

Pressure was measured by a DIGIQUARTZ pressure transducer with quartz crystal pressure sensing and thermal compensation. Pressure was calibrated from,

$$P = A\left(1 - \frac{B_0^2}{B^2}\right)\left[1 - D\left(1 - \frac{B_0^2}{B^2}\right)\right] \tag{15}$$

where B was the pressure period (μs), A, D and B_0 were given by

$$A = A_1 + A_2 T + A_3 T^2 \tag{16}$$

$$D = D_1 + D_2 T \tag{17}$$

$$B_0 = B_1 + B_2 T + B_3 T^2 + B_4 T^3 + B_5 T^4, \tag{18}$$

where T was temperature (°C) and the calibration coefficients were as follows.

Coefficient	
A1	-40933.35
A2	-0.1005887
A3	0.0110412
D1	0.030176
D2	0
B1	29.92572
B2	$-3.202788.10^{-4}$
B3	$3.72467.10^{-6}$
B4	$2.87034.10^{-9}$
B5	0

We have not reported oxygen but primary instrument calibrations were available for the same period as the pressure, temperature and conductivity calibrations.

< wildedit: checked for and marked wild data. The standard deviation of blocks of data N scans long was calculated and data more than 2 standard deviations (sd) from the mean were flagged bad. The process was repeated twice, on the second pass data more than 20 sd from the mean were flagged bad.

< celltm, carried out a conductivity thermal mass correction. A recursive filter removed conductivity cell thermal mass effects from the measured conductivity. In areas of steep temperature gradient a thermal mass correction could be expected in the order 0.005 PSU, and negligible elsewhere. The algorithm used was,

$$dT = T_{t+1} - T_{t-1} \tag{19}$$

$$ctm_t = -\left(b \times ctm_{t-1}\right) + \left(a \times {dC}/{dT} \times dT\right) \tag{20}$$

$$C_{corr} = C_t + ctm_t \tag{21}$$

where, $a = 2\left\{\frac{\alpha}{\left(2+\left[\text{sample interval}\times\beta\right]\right)}\right\}$, $b = 1-\left(\frac{2a}{\alpha}\right)$ and $dC/dT = 0.1\left(1+0.006\left[T-20\right]\right)$;

with typical values of $\alpha = 0.03$ and $1/\beta = 7.0$ for a SBE 9/11 plus TC ducted conductivity cell (3000 rpm pump).

< filter; low pass filtered conductivity and pressure with a time constant of 0.03 s and 0.15 s respectively. The filter was applied forwards and backwards through the file to eliminate phase shifts.

< asciiout: Output the header portion of data to .hdr and the data portion to .asc, according to a preset file format.

< rossum, produced formatted ascii output of bottle firing data and could include a specified number of CTD scans and variables at each bottle fire. NB the CTD data cycles extracted at this point were not used for calibration. For calibration purposes, CTD data at bottle stops were been taken from the later 10 s averaged CTD file.

SBE CTD path through PSTAR

The following cshell scripts were used to process the SBE CTD and bottle sample data. Throughout, ###### was a five digit Discovery station number.

>*sbctd0*: Read in calibrated 24hz CTD data from ascii files and created PSTAR files. Calculated time in seconds from jday (day of year): output file -> ctd#####.raw. This also read in the winch data: output file -> win#####

> *sbctd1*: Created 1 s and 10 s averaged files from the 24 Hz files. Some simple editing of data ranges was also performed. Output files -> ctd#####.1hz (1Hz calibrated down and up cast file), .10s (10 s averaged 1Hz file; used to merge onto firing times to compare with the sample salinity data).

>*sbctd2*: Produced 2db averaged downcast files; this was not implemented during the cruise.

>sbctd3: Produced full profile theta/S and deep theta /S plots from 1 Hz averaged data.

SBE bottle Firing Path

>*sbfir0*: Read in bottle firing data (time and firing code) from bottle firing file .ros. Calculated time in seconds from jday (day of year): output files -> fir#####.tim.

>*sbfir1*: merged winch data onto the firing files: output files -> fir#####.wir

>*sbfir2*: merged the 10 s averaged CTD data onto the firing data: output files -> fir#####.

There was no processing path set up for oxygen calibration during D253.

Sample Path

The path for processing bottle sample data was as for the Neil Brown DEEP04 CTD processing described above. The only difference was in the pasting of the CTD data into the sample files:

>*sbpasfir*: Used PEXEC program ppaste to paste upcast CTD data (10 s average) at the bottle firing times into the sample files. Variables in the sam##### files were prefixed by d for down.

Calibration

As for the Neil Brown DEEP04 instrument, SBE 9/11 plus (botcond-ucond) residuals versus botcond, station number and pressure were plotted. These showed that the SB had remarkable stability and held its performance relative to the pre-cruise calibration better than the Neil Brown DEEP04. The residuals increased by about 0.001 $mScm^{-1}$ with depth or decreasing conductivity.

The statistics of these salinity residuals were:

Stations	Mean	Standard Deviation	n (limits ±0.03)
14027 to 14062	0.0005	0.003	343 of 358

Digital reversing thermometers and pressure sensors

On the majority of CTD stations (both Neil Brown and SBE) reversing thermometers and pressure sensors were fired on bottles 1 and 4. The instruments used were:

Stations	Bottle 1	Bottle 4
13965	T795, P6394	T1684, P6571
13966 – 14011	T1684, P6571	T995, P6394
14012 - 14025	T1684, P6571	
14027	T1684, P6571	T995, P6394

14028 - 14031		
14032 - 14130	T1684, P6571	T1545, P6534

The continuity of the reversing instruments across the two CTDs provides a useful indication of the difference between the CTDs. In fact the results were very encouraging, with no significant difference between the CTDs in temperature (Figure 7).

Stations	CTD Inst.	RevT-CTDT		RevP-CTDP	
		mean	SD.	mean	SD
13966 to 14011	NB Deep04	0.0003	0.0038	-0.8544	3.6697
14028 to 14062	SBE 9/11	-0.0015	0.0032	-3.0539	1.8494
14064 to 14130	NB Deep04	0.0010	0.0033	-0.3064	1.6115

Comparison of Neil Brown DEEP04 and Sea-Bird 9/11 plus CTDs

Stations 14034 and 14066 gave us an opportunity for an intercomparison between the Neil Brown and the SeaBird CTD systems. Only station 14034 has been closely analysed at this time (Figure 6).

Station 14034 was 2200 m deep. Above 1400 m there was a lot of natural variability in the water properties between the two casts. Fully calibrated 1 Hz averaged downcast profiles were gridded on potential temperature. Differences in pressure, temperature, conductivity and salinity were determined on potemp intervals. Above 1400 m large differences in all these parameters were clearly apparent. However, below 1400 m differences in pressure, temperature and conductivity were small and compensating. Furthermore, the difference in salinity exhibited no trend from 1400 m to 2200 m. In conclusion the Neil Brown DEEP04 and the SBE 9/11 plus measurements were the same.

Final processing macros

The following executable C-shell scripts resided in /data61/ctd:

calibrate_cond.exec: This exec applied a conductivity offset to Neil Brown DEEP04 CTD stations 13695 to 14026. Salinity and potential temperature were recalculated. Conductivity corrections were applied to the 1Hz data and new 10 second averaged files were created from the calibrated 1Hz files.

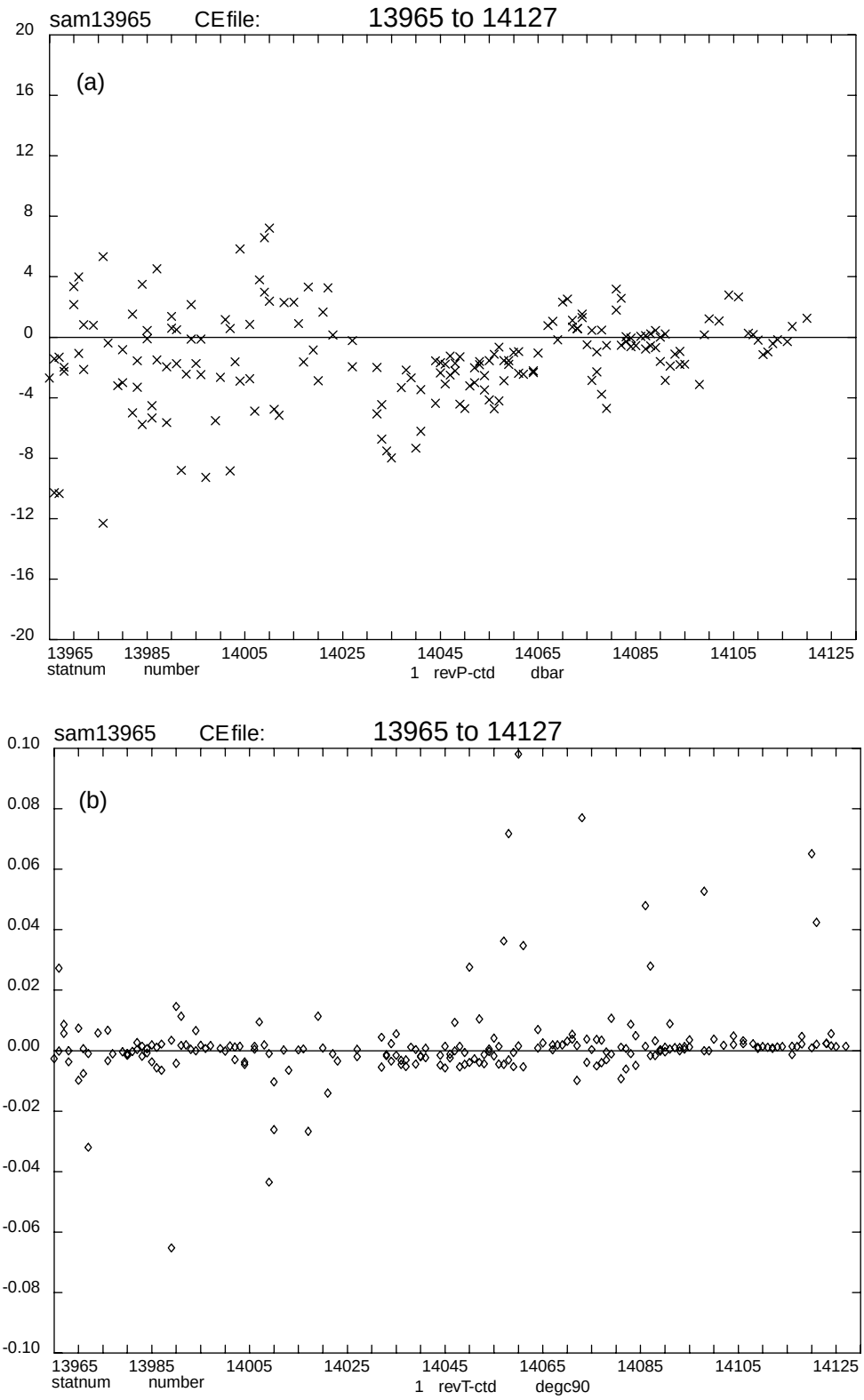

Figure 7. Difference between reversing instruments and (a) CTD pressure, (b) CTD temperature.

reprocessctdexec: This exec re-ran the CTD processing to pass changes to conductivity and other derived variables down through the processing path to reach the sample file. Steps were:

ctd2 (created new 2db file) ->fir2 (merged 10 second averaged file with fir.wir to give fir.ctu) ->fir3.press (determined downcast values that matched upcast bottle stops for O_2 calibration, fir.ctu to fir.cud) ->pasfir.scu (NB: this version of pasfir searched /ctd for the firing files! it then pasted upcast and downcast variables from fir.cud into the sample file). This exec was also used to apply different conductivity slope and offset corrections by re-running versions of ctd1 for different groups of stations. The different versions of ctd1 used different calibration files with the different conductivity calibrations.

For stations 14064 onwards:

stat#####: A number of scripts that applied the small conductivity calibration offsets to the 1Hz data files, and carried the calibrated data through the rest of the processing (ctd2, fir2, fir3.press, pasfir.rtp, makeresid). This was an alternative script written to replace the preceding scripts, and it effected the same changes.

The following executable C-shell script resided in /data61/bottle:

botcond.exec: For calibrating conductivity in a sample file. This exec calculated botcond as a function of (botsal,upress,utemp); and then calculated botcond-upcond.

The following executable C-shell scripts resided in /data61/seabird:

batch.sbctd0.exec

batch.sbctd1.exec

batch.sbfir0.exec

batch.sbfir1.exec

batch.sbfir2.exec

batch.sbpasfir.exec

batch.sbwin0.exec

these execs ran the relevant basic processing execs on groups of files.

calibrate_cond.exec: applied an offset and slope correction to cond1 in the 1Hz files. It re-computed potemp and salin and created a new 10 second averaged data file.

Self-Contained CTD Data - *John Allen and Xabier Irigoien*

A self contained 'stand alone' end cap for the Chelsea Instruments MiniPAK CTDs had been purchased prior to the FISHES cruise. This arrived just a few hours before the ship left Southampton. This end cap replaced the 'real time' end cap and contained a rechargeable battery pack. Although the stand alone end cap would fit either of the two MiniPAK CTDs, only one instrument, serial number 210011 (see later), had been fitted with a Smart Card reader/recorder for data storage; which, strangely, was not a component of the stand alone end cap.

The stand alone end cap had been purchased so that we could fit a MiniPAK CTD on the FRRF/Net haul frame discussed in later sections. However, a number of problems were encountered with the CTD and therefore it was only fitted for the first few net stations. The limited CTD data obtained from the MiniPAK CTD, in stand alone mode, have not been processed at this time; although a visual comparison of a profile with that from the main CTD cast at the same station showed encouraging similarity.

The fundamental problem with the MiniPAK CTD in stand alone mode was that the recording of data was unreliable. On several occasions the instrument switched itself off during a CTD/net cast and no more data was recorded. Recorded data could only be downloaded by removing the end cap, thus disturbing the pressure seal, and withdrawing the Smart Card for reading in a floppy diskette Smart Card reader. Before withdrawing the Smart Card, a micro-switch was pressed to shut down the data file. The same micro-switch was used after insertion of the Smart Card to verify the format and set up the instrument for deployment; an LED sequence indicated success or failure of the set up or shut down procedure. These procedures were difficult and unreliable, frequently needing to be repeated to achieve a successful set up or shut down signal; and eventually the set up procedure failed to work permanently. The MiniPAK CTDs, including the stand alone end cap, were sent back to Chelsea Instruments for modifications following the cruise. In addition we suggested that multiple CTD casts should be recorded to separate files and not concatenated to the one data file, i.e. that the Chelsea Instruments sea switch that turns the instrument on only when it is in contact with water, should also be used to close the previous data file and open a new one.

Three Smart Card media data files exist for future evaluation,

Data file name	Start date/time	End date/time
D253966_2.csv	07.05.2001/12:17:58	07.05.2001/13:50:24
D253986.csv	10.05.2001/18:15:59	11.05.2001/04:42:25

D253014.csv	15.05.2001/05:57:09	15.05.2001/16:54:04

SeaSoar CTD Data - *David Smeed*

Data

The 'new' SeaSoar system (Figure 4), in use for the first time on FISHES, carried a Chelsea Instruments MiniPAK CTDF (Conductivity, Temperature, Depth and Fluorescence) instrument which was considerably more compact than the Neil Brown CTD instrument that had traditionally been carried in SeaSoar. The two MiniPAK CTDs taken on FISHES were new instruments and suffered a number of teething problems that have been discussed earlier in the cruise diary and the technical support sections. Following the cruise, both MiniPAK CTDs were returned to Chelsea Instruments for modifications.

During SeaSoar deployments data were recovered, in real time, from the PENGUIN data handling system on SeaSoar by ftp to create identical data files on the EMPEROR Linux PC in the main lab: this is discussed in detail in the preceding technical support section. Thus data were logged in four files, one containing the CTDF measurements, an other containing output from the pitch and roll sensors in PENGUIN and two further files for the FRRF and OPC data. The FRRF and OPC data are dealt with later in this report.

All of the variables output by the MiniPAK CTDF were calibrated using pre-set calibrations stored in the instrument firmware. The sensors sampled at 16 Hz, but the output variables were one second averages. The variables output were:

Conductivity ($mScm^{-1}$)

Temperature (°C)

Pressure (dbar)

ΔT ($°Cs^{-1}$), temperature change over the one second averaging period.

Chlorophyll (mgm^{-3})

Each of these were output at one second intervals and a time/date stamp was added by the DAPS handling software on PENGUIN. The time rate of change of temperature, ΔT ($°Cs^{-1}$)

was the difference between the first and the last sample in the one second average of temperature. Firmware calibration coefficients for the two CTDs were as follows:

MiniPAK serial no. 210011, calibration date 09/03/01,

$$press. = -1.88563 \times 10^{-9}(bits)^2 + 9.44603 \times 10^{-3}(bits) - 9.9314 \quad (22)$$

$$temp. = 3.97147 \times 10^{-11}(bits)^2 + 6.00337 \times 10^{-4}(bits) - 3.5925 \quad (23)$$

$$cond. = -6.66290 \times 10^{-11}(bits)^2 + 1.11454 \times 10^{-3}(bits) - 1.2161 \quad (24)$$

$$Chla\ conc. = 0.00260(bits) - 8.067. \quad (25)$$

MiniPAK serial no. 210012, calibration date 28/03/01,

$$press. = -1.80455 \times 10^{-9}(bits)^2 + 9.44658 \times 10^{-3}(bits) - 10.3503 \quad (26)$$

$$temp. = 5.20709 \times 10^{-11}(bits)^2 + 5.98726 \times 10^{-4}(bits) - 3.4919 \quad (27)$$

$$cond. = -6.58088 \times 10^{-11}(bits)^2 + 1.08984 \times 10^{-3}(bits) - 0.9711 \quad (28)$$

$$Chla\ conc. = 0.00205(bits) - 6.450. \quad (29)$$

Following the teething problems with the MiniPAK CTDs, discussed earlier, only CTD serial no. 210011 was used on SeaSoar during the FISHES cruise.

The pitch and roll sensors in PENGUIN recorded the variables Pitch (°), Roll (°) and T_I (°C). Where pitch and roll described the orientation of the vehicle to the vertical and T_I was an internal temperature measurement. Again a date/time stamp was added by the DAPS software. In fact these attitude variables were only logged during a test deployment.

The use of the MiniPAK CTD and the PENGUIN acquisition system necessitated a few modifications to the processing route for SeaSoar data as used on previous cruises.

Processing Steps

The following 4 C-shell scripts were run every 4 hours;

Emp_copy

Copied the latest versions of the DAPS data files from the EMPEROR PC to the shipboard SUN UNIX system over the ship's ethernet. The only difficulty that was encountered with this

step was that if EMPEROR updated its data files by ftp from PENGUIN whilst *Emp_copy* was in progress then *Emp_copy* would fail. The failure rate was dependent upon the frequency of the ftp routine. Increasing the time between ftp updates to 30 seconds significantly reduced the incidence of failure. The failure rate increased if the file sizes were larger, i.e. if *Emp_copy* were run every 36 hours then the failure rate would increase significantly even if ftp updates were only made every 30 seconds.

Pgexec0

Read the raw DAPS data into PSTAR format and added information to the PSTAR header. If the attitude sensors were logged (as was the only the case on a test deployment), then this data was merged with the CTD data. In addition time in seconds was calculated from the Jday variable used by DAPS. Note that it was necessary to use the *-square* command line option for the pexec program *pxtime*. Unless this option was specified *pxtime* rounded the time to the nearest second occasionally giving rise to two records having the same time.

Pgexec1

Because the MiniPAK outputs variables in physical units it was not necessary to use the pexec program *ctdcal*, and so this script was written to replace ssexec1. The main steps were

a) *pcalc* to apply temperature correction

b) *pintrp* to interpolate pressure across gaps in the data. Typically less than 0.3% of the data had to be interpolated

c) *peos83* to calculate salinity and density.

Note that for future deployments it would be useful to add another step to apply linear corrections to conductivity and chlorophyll.

Two copies of the output were saved, one a backup in case the subsequent processing needed to be repeated.

Pgexec2

This script was used to produce plots of the data using the programs *plotpr* and *pldot*. There were large spikes in conductivity and chlorophyll near the surface, and so all data above 2 m were rejected. Below this level, inspection of the data allowed occasional (~0.01%) spikes in conductivity to be removed using the program *plpred*.

Subsequently, 4 hour files were merged to produce a single file for each survey, which was then merged with the navigation data. Following corrections to salinity and chlorophyll described below, the data were interpolated to a 5 km by 6 dbar regular grid. The processing was repeated every day, including all data collected up until noon that day, so that it was available for assimilation by the onboard forecasting model by 5pm the same day.

Temperature Correction

It was necessary to make a correction for the small delay in the response of the CTD temperature sensor for two reasons. Firstly, to obtain a more accurate determination of temperature for points in space and time. But, more importantly to obtain the correct temperature corresponding to conductivity measurements, so that an accurate calculation of salinity could be made.

Surprisingly, according to the MiniPAK users manual the time response of the temperature and conductivity cells should have been the same. However, a lag in temperature was apparent in the data in two ways. There was a difference between up and down profiles of temperature (and hence salinity) because the time rate of change of temperature has opposite signs on the up and down casts. The second manifestation was the "spiking" of salinity as the sensors traversed maxima in the gradients of temperature and salinity. The rate of ascent and descent of SeaSoar was greater (typically up to 2.5 ms^{-1}) than that of a lowered CTD package, thus the effects of the temperature lag were more pronounced. Thus, the following correction was applied to the temperature before evaluating the salinity

$$T_{corr} = T_{raw} + \tau.\Delta T \tag{30}$$

where ΔT is defined above and τ is constant. The best value of τ was chosen so as to minimise the difference between up and down casts and noise in the salinity profile. The best value was found to be $\tau = 1$ second. This was very much larger than expected and has since been discussed with Chelsea instruments with regard to the other teething problems that we experienced with the MiniPAK instruments.

Calibration

The calibration of the MiniPAK CTD sensors was checked by comparison with the underway thermosalinograph (TSG) measurements and the lowered CTD data. A preliminary calibration based only on data from the first SeaSoar survey was completed on board as follows:

a) Using temperature and salinity data from the TSG it was established that the time lag between SeaSoar temperature measurement and the TSG remote temperature was 155 seconds. This lag correlated with the length of cable used to tow SeaSoar. The length of cable was ~700 m during each of the deployments. The time lag between the SeaSoar salinity and the TSG salinity was 115 seconds, this lag was different from the temperature lag because of the time taken for water to flow through the ship's non-toxic supply to the TSG. Note the actual time to flow from the remote intake to the TSG sensors was longer than this, but most of the this was corrected for by the TSG system software.

b) After correcting for the time lag the temporal evolution of the differences between the SeaSoar temperature and salinity and the TSG variables was examined. No significant drift in temperature or salinity was detected

c) Temperature salinity plots were compared with similar plots from lowered CTD profiles. The best fit with the lowered CTD data was obtained by adding a constant 0.16 to the salinity data.

d) A linear calibration was applied to the chlorophyll so that the minimum value was zero and the maximum values corresponded with the analysis of underway surface chlorophyll samples. The correction applied was as follows:

$$Chl_{cal} = \left(0.2 \times Chl_{raw}\right) + 0.54 \tag{31}$$

Initial analysis suggested that in a final calibration it would be necessary to take into account quenching by using the PAR data from the Fast Repetition Rate Fluorimeter.

Summary and Data Quality

The quality of the data appeared generally good. There did not appear to be any significant drift in the sensors during the cruise and an examination of profiles with near constant temperature and salinity gradients suggested the noise level in the salinity values was less than 0.01 practical salinity units (psu).

A great advantage of the inductive conductivity cell was that the occurrence of spikes and offsets due to biological fouling was virtually nil. Thus it was entirely feasible for all the SeaSoar processing to be undertaken by just one scientist.

The apparently large difference in the time response of the temperature and conductivity sensors was a concern. According to the users manual the time response of the temperature sensor was

0.3 s, and the output values of temperature and conductivity were adjusted to take account of this. In practice a significant correction to temperature had to be made. A more thorough analysis will be made after the cruise to examine the accuracy of the final salinity values.

It is recommended that laboratory calibrations of the CTD sensors are made before and after each cruise.

An example SeaSoar Processing log for D253

1. Please enter the SeaSoar file number here : _____ :

Deployment number : _____ :
Tick here if this is the start of a deployment : _____ :
Tick here if this is the end of a deployment : _____ :

2. Check status of DAPS files on /seasoar

Run the *dinfo* command three times as follows and note the current DAPS file in each case. In the last column enter "Y" if DAPS has stopped writing to the file. Enter start times only if this is the first data to be read from the file.

Command	Filename	Start time	Time of last data	End?
dinfo /seasoar min				
dinfo /seasoar att				
ls -l /seasoar/frrf				

N.b. dinfo doesn't work with the frrf file so use ls instead

3. Copy data files to /data61

The command ***penguin_copy*** will copy the above data files to: /data61/seasoar/daps_data

4. Run pgexec0

Reads in data to pexec format. Use the start and stop times for the MiniPAK file if not processing a complete 4 hours. Note the following details

SeaSoar file #		**saraw### version =**	
Start time:		**peng### version =**	
Stop time:			

5. Run pgexec1

Applies temperature correction and calculates salinity. Do create an ascii file.

Input file saraw###. Version code:	
Time constant of temp. correction:	
Output file sa253###. Version code:	

6. Run pgexec2

This exec produces 6 plots of the data. Use device mx11 to see on the screen and device htpiia4 for the hardcopies. It is not usually necessary to make additional plots. Please file the plots in the appropriate folders.

7. Comments

Profiling Floats - *Penny Holliday and Helen Johnson*

Three APEX profiling floats were deployed during the FISHES cruise; 2 in the Rockall Trough and one in the Iceland Basin. The floats were "park and profile"; that is to say that they would float at a set park pressure (in our case set at 1500 or 1750 dbar), then sink to the maximum profile pressure (2000 dbar) before surfacing. All 3 floats had been tested prior to the cruise and programmed to resurface every 10 days. Time at the surface was set to around 6 hours to minimise transportation by surface currents, but to allow time for full data transmission by Argos satellite communication.

All deployments were carried out from the port corner of the stern of the ship, as the ship steamed into the wind at 1 knot, ~0.5 miles from the subsequent CTD station. Each float was reset prior to the deployment, with timing of the reset chosen to ensure the first re-surfacing time was between 08:00 and 14:00 GMT when satellite coverage would be at a maximum. The reset process included a test for Argos transmission. Immediately prior to deployment the plugs of the conductivity cell duct and the temperature sensor cap were removed. The floats were lowered into the water by means of a rope through the hole in the mounting damper plate.

All floats had the following settings in common:

- ~45 seconds repetition rate for satellite transmission.
- 1 hour trip interval; 228 intervals down and 12 intervals up (giving 240 hours or 10 day cycling time).
- 2000 dbar maximum pressure for the profile
- Ascent rate of approximately 0.08 ms^{-1}

Float ID	Park Depth	Reset Date (Jday) and Time	Launch Time	Launch Location	CTD cast number
13353	1750 dbar	6/5/01 (126) 11:52	15:36	Rockall Trough 55° 0.04' N 12° 59.9' W	13965
13354	1750 dbar	20/5/01 (140) 13:15	16:37	Rockall Trough 57° 13.9' N 10° 02.2' W	14034
13355	1500 dbar	10/5/01 (130) 12:15	14:56	Iceland Basin 61° 29.9' N 20° 01.4' W	13981

Position and profile data from all three floats (Figure 8) were received from Brian King, back at SOC, as the cruise progressed, and some preliminary calibrations were carried out. Float 13353 moved northwards in the Rockall Trough, it covered about 100 miles over the course of 40 days and surfaced at 56° 33' N, 12° 25' W on 15/6/01 (Jday 166). Float 13354, deployed on the Ellett line, also moved northwards; it travelled about 20 miles over its first 10 days, and surfaced at 57° 30' N, 10° 04' W on 9/6/01 (Jday 160). The float deployed on the Iceland Shelf, 13355, moved approximately 80 miles to the south-east along the slope of the Reykjanes Ridge; it reached 60° 59' N, 22° 37' W by the time it surfaced 30 days later on 9/6/01 (Jday 160). Advection of the floats by surface currents appeared to be small compared with the distance they covered at depth.

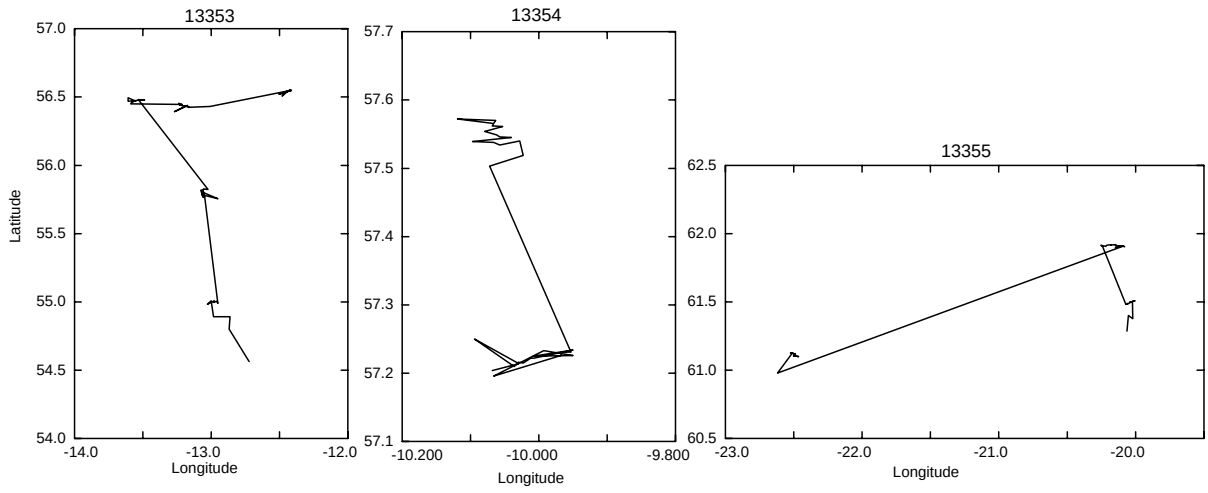

Figure 8. Tracks of the three floats deployed during leg 1 of FISHES; as at Jday 167.

Float 13353 and 13354 calibrations were checked by comparing the profile data from their first ascents with the original CTD station profiles. Temperature and salinity differences were calculated at given pressure values:

Float ID	CTD Cast Number	Measurement	Depth Range	Mean	Standard Deviation
13353	13965	Temperature	All (+/-0.2)	-0.019	0.085
		(°C)	0-1200	-0.109	0.192
			1200-bottom	0.087	0.108
		Salinity	All (+/-0.02)	-0.0061	0.0103
			0-1200	-0.0130	0.0080

			1200-bottom	0.0070	0.0121
13354	14034	Temperature	All (+/-0.2)	-0.031	0.060
		(°C)	0-1200	-0.096	0.217
			1200-bottom	-0.070	0.065
		Salinity	All (+/-0.02)	-0.0057	0.074
			0-1200	-0.0054	0.0078
			1200-bottom	-0.0067	0.0661

Statistics for float 13354 were likely to be most reliable because the float stayed close to the orginal CTD station. The greatest differences in T and S occurred in the deep thermocline (Figure 9), with the profiles in the upper and deep parts of the ocean lying relatively close together.

Salinity differences were also calculated as a function of temperature. Largest differences occurred at about 8°C in each case (Figure 10).

Float ID	CTD Cast Number	Measurement	Mean	Standard Deviation
13353	13965	Salinity	-0.0055	0.0088
13354	14034	Salinity	-0.0018	0.0057

Float 13355 was deployed in an area of intense mixing. CTD profiles here showed large amounts of interleaving at depth, which made calibration of the float profile difficult. On it's second ascent the float surfaced close to the section CE. Comparison with all CTD profiles on this line showed that the float captured general water properties well (Figure 11), but there was no obvious single CTD station to choose for calibration. The deep part of the T-S curve lay closest to that for ctd13994. The following statistics applied to temperatures below 4°C (~1400 dbar):

Float ID	CTD Cast Number	Measurement	Mean	Standard Deviation
13355	13994	Temperature	-0.011	0.056
(ascent b)				
		Salinity	0.0052	0.0079

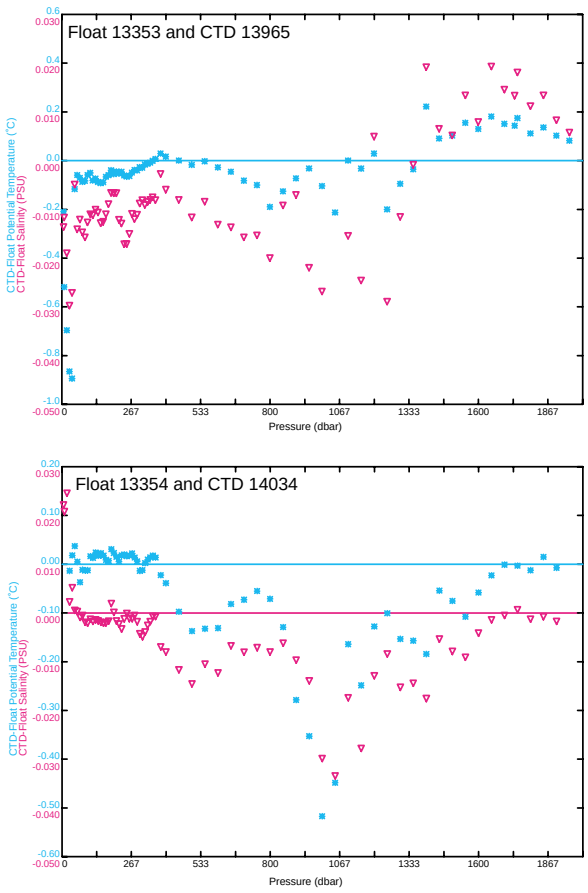

Figure 9. Salinity and temperature differences between float and CTD profiles against pressure

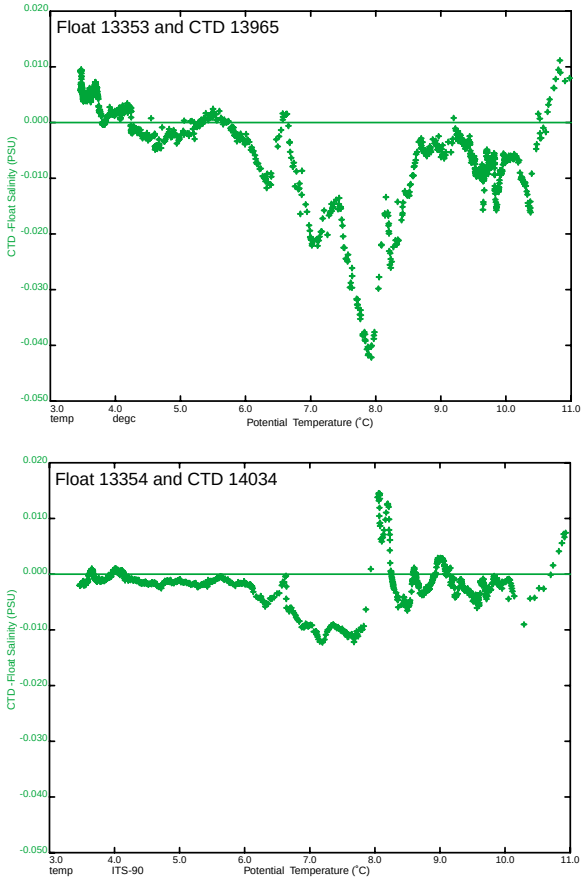

Figure 10. Salinity differences between float and CTD profiles as a function of temperature

Salinity Bottle Samples - *James Harle and Meric Srokosz*

Additional operators – Steven Alderson, Naiosé O'Reilly, John Allen, Paul Nelson, Mark Moore

Salinities – Leg 1

Salinity samples were drawn from the Niskin bottles mounted on the CTD rosette at all depths below and including100 m, and from the surface bottle. A duplicate sample was drawn from the deepest Niskin bottle and occasionally, on the deeper stations, the Niskin fired at 1000 meters. Samples were taken using 200 ml glass sample bottles; that were rinsed three times in the sample, filled to the shoulder and sealed with a disposable plastic insert and the bottle's screw cap. Samples were also taken every fours hours from, initially the ThermoSalinoGraph (TSG) outflow in the wet lab and then the FRRF outflow to calibrate the continual TSG measurements.

Situated in the chemistry lab were a model 8400A and a model 8400 Autosal salinometer both fitted with peristaltic pumps. The Constant Temperature Lab was being used for biological

experiments at un-suitable temperatures of sub 10 °C. Thus, it was decided to run both salinometers at the 24°C water bath setting as the chemistry lab temperature was fluctuating between 20°C and 25°C over the steaming period to the first station. In order to maintain some kind of stable temperature environment, hourly temperatures checks were included in the general watch keeping duties. Temperatures were regulated using a portable heater and fan, with the aim of maintaining temperatures at around 2°C lower than the bath temperature as salinometers are more efficient at heating that cooling. Once a crate of sample bottles had been filled they were moved into the chemistry lab to stand for 24 hours prior to analysis. Two out of the twelve crates bought on board had salt crystals on the inside shoulders of the sample bottles and had to be thoroughly cleaned, although this was only realised after one of the crates had been analysed (stations 13966/67/68).

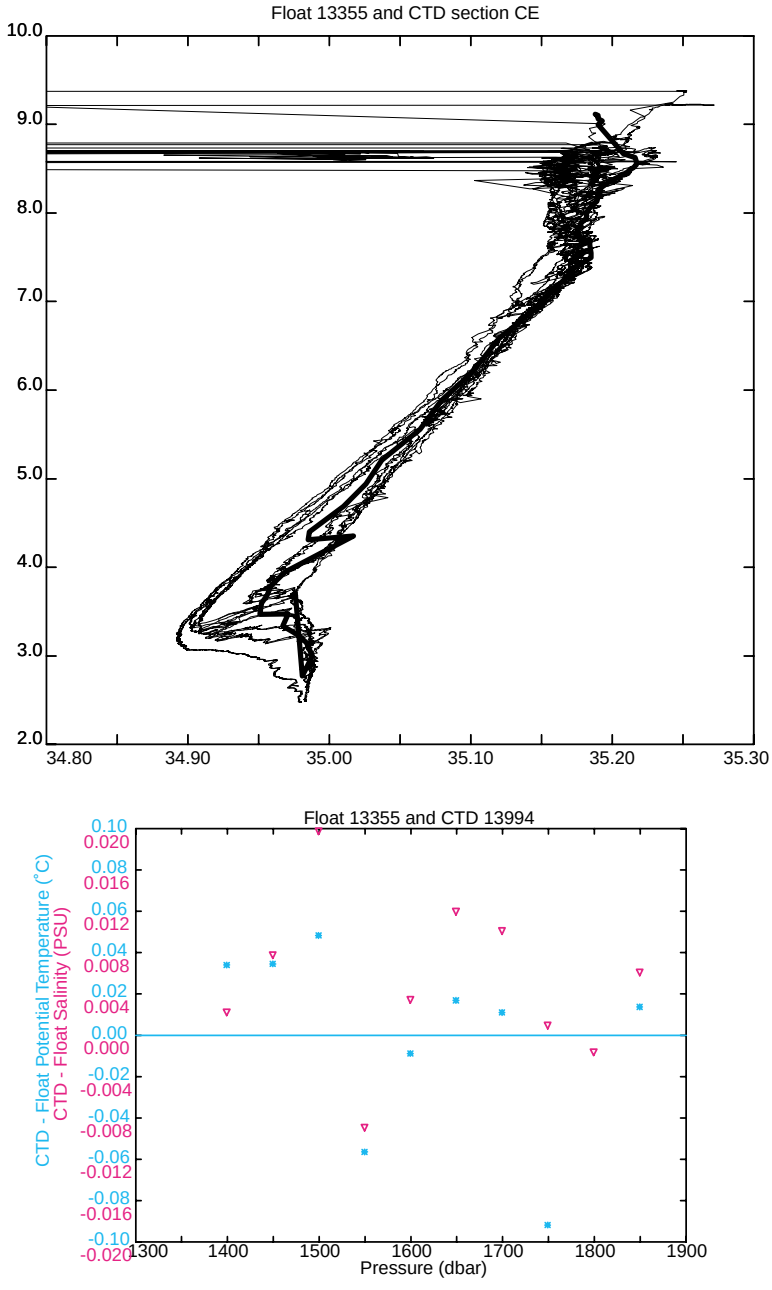

Figure 11. T-S diagram and temperature and salinity differences for float 13355 (second ascent)

Throughout the first leg of the cruise the 8400A Autosal salinometer was predominantly used. Only on three occasions was the 8400 Autosal used, these were

4/5/01 - to take over from the rapidly drifting 8400A Autosal which was subsequently flushed several times with de-ionised water. This drifting occurred during the analysis of stations 13097/98;

18/5/01 - simply to increase the turn-over rate of samples;

20/5/01 - in a comparison of the 8400A to the 8400, performed using samples from station 14025. Every fourth sample was re-analysed on the 8400 with a mean difference of 0.0001 in salinity and a standard deviation of 0.0005.

Over the duration of the first leg of the cruise the 8400A salinometer remained fairly stable and the heater lamps cycled regularly. The standby reading fluctuated between 24+5593 and 24+5602, not varying by more than 5 units in any one crate analysis. The zero reading fluctuated between 0.0000 and 0.0003. There were, however, a few minor physical problems with the salinometer;

15/5/01 the tube from the peristaltic pump into the salinometer began to leak. To solve this the tube was slid further over the insert to the salinometer and held in place with Blue-Tack.

22/5/01, the cell chamber second from the right was noticed to have what looked like particles or small air bubbles trapped between the winds of the coil. A methanol solution was used to soak the cell for 1 hour and then flushed with de-ionised water. Standard readings initially dropped by 0.00010 in 2x conductivity ratio, but soon returned to levels prior to flushing along with what we now believe to be tiny air bubbles trapped between the coils in the afore mentioned cell chamber. After consultation it was deemed to be a normal occurrence and as the stability of the readings were unchanged, measurement continued.

25/5/01, micro air bubbles were entering the cell sporadically, when the cell was filled. This persisted for a day then seemed to stop. The tubing was checked during the port call in Lerwick on the 31st May.

In addition to these incidences there were also the common problems of air bubbles within the cell (especially the chamber second from the right) and occasional poor sampling, ie salt in the bottle caps, bottles being over/under filled etc.

Standardisation was performed using IAPSO Standard Sea Water batch P139 before and after analysis of each crate of samples. There was a definite drift in the conductivity measured over

the first leg of the cruise (Figure 12). During this period a total of 145 duplicates were taken, indicating consistent sampling and analysis with a standard deviation of 0.00076 in salinity.

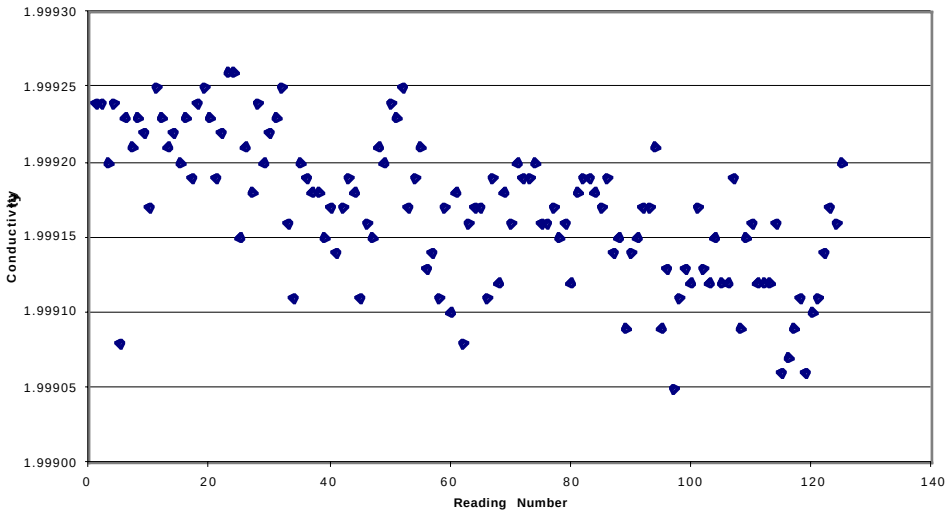

Figure 12. Variation in measured conductivity of the SSW batch P139.

Salinities – Leg 2

Salinity sampling was carried out in a similar manner to that described previously for Leg 1, with the exception that the underway sampling was hourly routinely, and half-hourly during SeaSoar surveys. The Autosal 8400A was used throughout the cruise for salinity determination, with the bath temperature set at 24°C. As for the Leg1 the chemistry lab temperatures were found to vary, generally between 20 and 23°C, occasionally as low as 19.5°C and as high as 25°C, and in one case down to 18.5°C. The portable fan and heater, plus leaving the chemistry lab door open or closed, were the means used to reduce variations in the lab temperature. To test if the variations in temperature were affecting the salinity determinations the standard seawater conductivity values from analyses during the cruise were regressed against the lab temperature. No significant correlation between the variables was found. The variations in the determined standard seawater conductivity over time were also examined. Unlike the situation on Leg 1, no significant trend over time could be discerned from the data.

It was found that crate 1 bottles appeared to have salt crystals on the inside, so this crate was not used. When half-hourly sampling was introduced for the first SeaSoar survey, and more inexperienced watch keepers were involved in the underway sampling, quite a few samples were found to be overfull, with plastic caps missing or not inserted fully. A note to the watch leaders about correct sampling procedures led to an improvement in the underway sampling. An unusual occurrence was that two bottles used for the underway sampling (89 in crate 4 on 13/6/01, day 164 and 281 in crate 12 on 15/6/01, day 166) were found to be cracked, when

brought to the lab for analysis. No explanation for this occurrence could be found, and the bottles were replaced with spares.

For one CTD station (14110) some of the sample salinities could not be reconciled with those obtained from the CTD. Other sample salinities from the same crate of bottles, analysed in the same batch, matched other CTD station data (14108, 14109). Thus it was concluded that some problem had occurred during the salinity sampling for station 14110 (possibly contamination by rain, or mismatched CTD rosette bottle numbers and sample bottle numbers).

During Leg 2, the analysis of duplicate samples indicated the mean difference between salinity determinations carried out using the Autosal 8400a was 0.000, with a standard deviation of 0.001.

Thermosalinograph and SurfMet Data - *Lisa Feighery and Glenn Nolan*

Instruments

Underway surface meteorology and thermosalinograph measurements were recorded by the RVS Surfmet system throughout Discovery cruise 253. The instruments used, together with their serial numbers and manufacturer are listed in the table below.

Instrument	Manufacturer	Serial number
OTM (temperature) Housing	FSI	1374
OTM (temperature) Remote	FSI	1360
Fluorometer	WetLabs	117
Transmissometer	SeaTech	T1005
Barometric Pressure	Vaisala	S361008
Temperature / Humidity	Vaisala	1850014
PAR (DRP-5)	Didcot/ELE	30471
PAR (DRP-5)	Didcot/ELE	30470
TIR (Pyranometer)	Kipp & Zonen	994132
TIR (Pyranometer)	Kipp & Zonen	994133
OCM (Conductivity)	FSI	1376

Sensor collector (QLI50)	Vaisala	R381005
Anemometer	Vaisala	P50421
Wind Vane	Vaisala	R07101

Processing

Processing of the underway data was undertaken daily which entailed running several PSTAR routines described below.

1. *smtexec0*: This script was used to convert the data from RVS format to PSTAR format using *datapup*. Resultant file was smt253**.raw

2. *smtexec1a*: Ensured absent surfmet data values were set to –999. The script also calculated TSG salinity using housing temperature, conductivity and a pressure value set to zero. Calibration of temperature variables was included at this point:

$$temp_h(housing) = -7.48453013\times10^{-3} + 1.00060764(\text{temp}_{\text{rawh}}) - 6.00362039\times10^{-5}(\text{temp}_{\text{rawh}})^2 + 1.11000097\times10^{-6}(\text{temp}_{\text{rawh}})^3 \quad (32)$$

$$temp_m(remote) = 2.30711152\times10^{-3} + 1.00108689(\text{temp}_{\text{rawm}}) - 9.54037439\times10^{-5}(\text{temp}_{\text{rawm}})^2 + 2.00706518\times10^{-6}(\text{temp}_{\text{rawm}})^3 \quad (33)$$

   Bestnav positions (every 30 seconds) were then merged into the file smt253** and this was subsequently averaged into a 2 minute file smt253**.av

3. *smtexec1b*: The master Ashtech file was merged with smt253**.av at this point. This allowed accurate heading data to be incorporated into the underway dataset.

4. *smtexec2*: This routine computed vessel speed and subtracted it from relative winds to obtain true wind speed and direction. Resultant file was smt253**.met

The .met files were appended to each other to create a single large data file called allmet for D253. Two further routines were run on the allmet file. Firstly *pdist* generated a distance run variable, then *pcmcal* converted the wind speed and direction into East and North components. Outliers in the East component of the wind were removed using the *datpik* routine as necessary. Finally, using the *pldot* programme, the user was able to select variables to plot on an

appropriate time and spatial scale. Figure 13 shows the underway temperature data for D253 as an example.

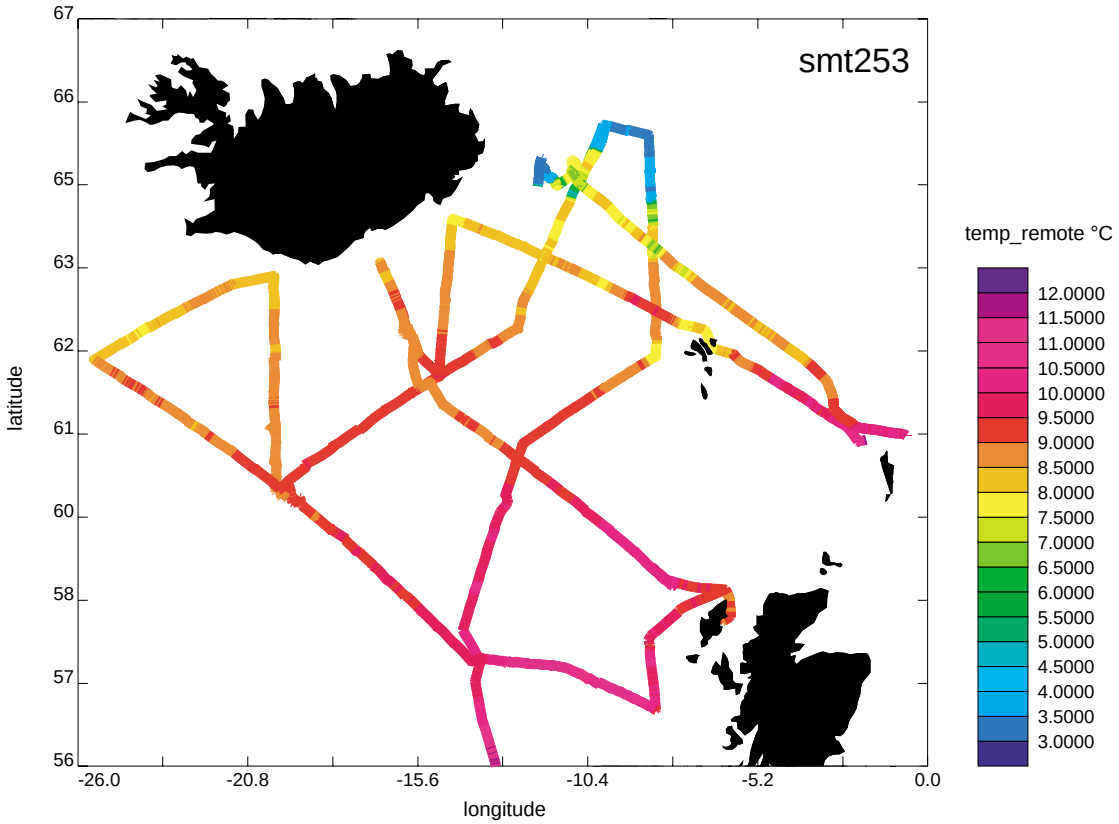

Figure 13. Underway surface temperature from the remote TSG sensor.

Salinity Calibration of Underway Data

A text file containing julian day time stamp and the corresponding bottle salinity value was imported into PSTAR format using the *pascin* routine. The new file was then merged, using *pmerge*, with the existing allmet file to directly compare underway and bottle salinity with a view to applying a calibration to the underway salinity data. It was thought more appropriate to apply the calibration to conductivity rather than salinity so the *peos83* routine was used to recalculate bottle conductivity first. At this point *datpik* was used to remove 20 obvious outliers from the bottle conductivities leaving 308 values in the dataset for the regression to be calculated. The *plreg2* routine was used to calculate a linear regression where the x value was TSG conductivity and the y value was bottle conductivity. An offset of 0.20312 and slope of 0.99228 was then applied to the TSG conductivity data using the *pcalib* routine. The salinity residuals were recalculated after application of the calibration to yield a mean residual of –0.0009 and a standard deviation of 0.0075. The final calibrated file was called allmetcal in the /data63/surfmet directory on discovery2.

Optical Plankton Counter - *Alex Mustard and John Smithers*

Two Focal Technologies Optical Plankton Counter (OPC-1T) instruments were used to determine mesozooplankton distributions during the cruise. The Deep OPC (Serial No TOW048) was mounted for the first time on both the Neil Brown CTD frame and the LHPR, and the Shallow OPC (Serial No TOW033) was used on the 'new' SeaSoar vehicle discussed earlier in section 5.

The interfacing of the Optical Plankton Counter with the Neil Brown MkIIIb CTD was discussed in detail in section 5.

Use of the OPC on the CTD

The Deep OPC was mounted on a bracket attached to the inside of the CTD frame outside the periphery of the bottle rosette system, with the sampling tunnel vertically orientated. The flow-reducing acrylic insert was not fitted to the sampling tunnel. Initial post cruise examination of the CTD mounted OPC data indicated that this position did not provide any significant obstructions to the flow. Data handling problems meant that OPC data were not collected at Stations 13965 to 14010 and 14012 to 14063 (see the CTD operations in section 5 of this report for more details). OPC data were collected at Station 14011 and at all CTDs with Discovery station numbers between 14063 and 14130.

OPC data were read into PSTAR from DAPS using script *dopcexec1.ctd*. The data were then merged with CTD pressure from the 1 Hz file and dpress/dt was calculated using the script *dopcexec2.ctd*. Further processing was not undertaken at sea, pending modification of the OPC gridding program *gropc* for CTD operations, and completed later at SOC.

OPC attenuance measurements were processed and showed close correlation with fluorescence (in the euphotic zone) and turbidity. The attenuance measured by an OPC is not a precise measurement, in this survey it varied only over 12 integer values, it is in fact a measure of the power required to keep the intensity of the light beam received across the tunnel constant. As a result the data were not detailed enough to resolve the finer structure of phytoplankton distributions in the euphotic zone. For this reason it was not recommended that attenuance be used as a proxy for phytoplankton concentration. It was important however, to verify that the attenuance was recording environmental variability because this is fundamental to an OPC's ability to detect discreet particles.

The flow through the OPC was influenced by both the winch speed (which was approximately 1 ms^{-1}) and the vertical movement resulting from the ship rolling in the swell. The dpress/dt showed that, in the relatively calm conditions during the FISHES cruise, the flow through the OPC had a mean of 1 ms^{-1}, but varied between 0.3 and 1.6 ms^{-1} as a result of the ship rolling.

When plotted against time, variability in dpress/dt had a period of about 8 seconds which was similar to the wave period of the swell.

Preliminary examination of the OPC counts showed that the zooplankton concentrations were greatest in the upper mixed layer and lowest at depth. There were also differences in the number of counts per second and the size of animals between the CTD stations on either side of the Iceland-Faeroes Front.

Use of the OPC on the LHPR

The Deep OPC was mounted on a bracket attached to the outside of the LHPR frame behind the nose cone, with the sampling tunnel horizontally orientated and parallel to the net. The flow-reducing acrylic insert was fitted in the sampling tunnel. The OPC data were logged directly to PENGUIN 2. A small software problem, operator error, resulted in the data being lost from the first deployment (Stn 14126). Data were successfully collected at Stn 14129, and were read into PSTAR using the script *dopcexec1.ctd*. Further processing to be completed at SOC after the LHPR's CTD data have been read into PSTAR.

Use of the OPC on the SeaSoar

The Shallow OPC was mounted on the underside of the rear tail plane of the 'new' SeaSoar vehicle. The flow-reducing acrylic insert was fitted in the sampling tunnel. The OPC was deployed with the SeaSoar on the three fine scale surveys of the Iceland-Faeroes Front. Data from the SeaSoar's attitude sensors, which were logged during the test deployments, showed that SeaSoar was close to horizontal during flight (see the SeaSoar operations description in section 5 of this report for more details). This indicated that the OPC's sampling tunnel was usually parallel to the flow, and the volume of water sampled could be calculated from the tunnel mouth area multiplied by the distance travelled. A more sophisticated calculation of the volume sampled accounting for the changing speed of SeaSoar would be applied to the data after the cruise.

OPC data were "corrupted" for the last two legs of fine scale survey 1 (after Jday 160.24 to the end of the survey) and for the middle section of survey 2 (Jday 163.19 to 163.83). The symptoms of this problem were the loss of the counts data and the attenuance channel reading much higher than a normal value. The time stamp remained unaffected. The reasons for these problems were not clear, but an electronic error within the OPC was suspected. OPC data were also affected by the collision of SeaSoar with the seafloor at Jday 163.96. The collision caused pebbles to be jammed into the mouth of the OPC's sampling tunnel, which reduced the volume of water sampled and consequently the number of zooplankton counted. Apart from the lower number of particle counts the instrument continued to record the expected pattern of

zooplankton distribution. It should be possible to correct these data with an offset calibration after the cruise.

OPC data were read into PSTAR from DAPS using the script *dopcexec1.ss*. The data were then merged with the distrun and pressure from the raw sawtooth SeaSoar files using *dopcexec2.ss*. The time stamps of both the OPC and SeaSoar data were reduced by 120 seconds to correct the latitude and longitude for the position of SeaSoar behind the ship. OPC counts data were required for examining mesozooplankton distributions and also for assimilation into the ecosystem model of the Iceland-Faeroes Front. These applications required different types of data, and as a result the OPC data were processed twice. The script *dopcexec3.ss* was used to grid the OPC data into the same spatial bins as the CTD data and to calculate the abundance and biovolume of zooplankton in size classes. For examining distributions, the zooplankton biovolume was computed using a spherical model and calibrated by a spheroidal calibration factor of 0.61. Both biovolume and abundance were divided into size classes of logarithmically increasing volume with mid points of 0.016, 0.063, 0.25, 1 and 4 mm^3. These are equivalent to ESD ranges of 0.40-0.64, 0.64-1.02, 1.02-1.61, 1.61-2.56 and 2.56-4.07 mm. For modelling requirements OPC biovolume was calculated using a spherical model and split into size classes of 0.25-0.5, 0.5-1.0, 1.0-2.0 and 2.0-4.0 mm ESD. The usual three dimensional files were converted into two dimensional files with each size class's abundance and biovolume as a new variable using the script *dopcexec4.ss*.

Mesozooplankton biovolume was dominated by the 0.64-1.04 and 1.04-1.61 mm ESD size classes. This OPC size spectra differed from those we had observed in other ocean regions which were dominated by the 0.4-0.64 mm size class. The size spectra was consistent with the expectations of the zooplankton community in the survey area, i.e. dominated by the large copepod *Calanus finmarchicus*. Microscope measurements of net samples determined the following ESDs for the different stages of *C. finmarchicus*: CIII 0.7-0.9 mm ESD, CIV 0.9-1.2 mm ESD, CV 1.3-1.6 mm ESD, CVI females 1.5-1.7 mm ESD. Microscope measured ESDs are usually greater than OPC measured ESDs because the latter are reduced by the orientation and transparency of the animals. Therefore the 0.64-1.02 mm ESD size class probably represented CIII and CIV *Calanus*, while the 1.02-1.61 mm ESD size class represented CV and CVI.

Preliminary results indicated that OPC biovolume was strongly correlated with the IFF frontal water where the chlorophyll concentrations were also highest. The 1.04-1.61 mm size class was confined more to the highest chlorophyll concentrations than the 0.64-1.04 mm. The net catches also revealed that CV and CVI *C. finmarchicus* (that were expected to make up the majority of the 1.04-1.61 mm size class) were most abundant in the front. Gut fluorescence analysis showed that copepods in the frontal water had an order of magnitude higher gut chlorophyll concentrations than those to the south of the frontal water.

Vessel Mounted ADCP (VM-ADCP), Navigation/Heading/Gyro - *Penny Holliday and Helen Johnson*

Introduction

Two Vessel-Mounted Acoustic Doppler Current Profilers (VM-ADCPs) were operated on D253; the 150kHz ADCP and a new 75 kHz Phased Array instrument (Ocean Surveyor). The 150 kHz ADCP was mounted in the hull 1.75 m to port of the keel, 33 m aft of the bow at the waterline and at an approximate depth of 5 m. The 75 kHz ADCP was also mounted in the hull, but 4.15 m forward and 2.5 m to starboard of the 150 kHz well.

This section describes the operation and data processing paths for both ADCPs and describes a brief comparison exercise between them. The navigation data processing is described first since it is key to the accuracy of the ADCP current data.

Navigation

The ship's best determined position was calculated by the RVS process *bestnav*. The main data source was the ships GPS Trimble 4000 system corrected for selective availability by the Racal Marine Star mark III Differential GPS system. During gaps in the GPS Trimble data, further GPS data were available from the GPS Glonass system which used both Russian and American satellite networks. In the unlikely event that no GPS system was available the Chernikeef electo-magnetic log velocity data and gyro heading were used to dead-reckon the ship's position.

Data were transferred daily from the RVS Level C bestnav file to the PSTAR absolute navigation files abnv2531 and abnv2532 (Legs 1 and 2 respectively). The gps-4000, gps_glos and gyro (gyronmea) data streams were also transferred daily.

Scripts:

navexec0: transferred data from the RVS bestnav stream to PSTAR, calculated the ships velocity, appended onto the absolute (master) navigation file and calculated the distance run from the start of the master file. Output: abnv2531 (Leg 1) and abnv2532 (Leg 2).

gyroexec0: transferred data from the RVS gyronmea stream to PSTAR, a nominal edit was made for directions between 0-360° before the file was appended to a master file.

gp4exec0: transferred data from the RVS gps_4000 stream to PSTAR, edited out pdop (position dilution of precision) greater than 5 and appended to the master file.

gpsexec0: this was identical to gp4exec0 but transferred the RVS gps_glos data stream to PSTAR.

Heading

The ships attitude was measured every second by the 3D GPS Ashtech ADU2 system. Configuration settings from previous calibrations (Trials cruise in April 2001) were used throughout the cruise. Four antenna, 2 on the boat deck, two on the bridge top, measured the phase difference between incoming satellite signals from which the ship's heading, pitch and roll were determined by ultra-short baseline navigation. The data were used to calibrate the gyro heading information.

ashexec0: transferred data from the RVS gps_ash stream to PSTAR.

ashexec1: merged the ashtech data from *ashexec0* with the gyro data from *gyroexec0* and calculated the difference in headings; ashtech-gyro (a-ghdg).

ashexec2: edited the data from *ashexec1* using the following criteria:

heading	0 < hdg < 360 degrees
pitch	-5 < pitch < 5 degrees
roll	-7 < roll < 7 degrees
attitude flag	-0.5 < attf < 0.5
measurement RMS error	0.00001 < mrms < 0.01
baseline RMS error	0.00001 < brms < 0.1
ashtech-gyro heading	-10 < a-ghdg < 10 degrees

The heading difference (a-ghdg) was filtered with a running mean based on 5 data cycles with a maximum difference between median and data of 1 degree. The data were then averaged to 2 minutes and further reduced for

-2 < pitch < 2 degrees

0 < mrms < 0.004

-10 < a-ghdg < 10 degrees

The 2 minute data were merged with gyro data files to obtain spot gyro values. The ship's velocity was calculated within the file and converted to speed and direction. The resulting a-ghdg variable was a smoothly varying trace that was merged with ADCP data to correct the gyro heading. However, during ship manoeuvres, bad weather or around data gaps, there were spikes which were edited out manually (*plxyed*).

Ashtech 3D GPS coverage was generally good. However, dropouts occurred several times on each leg; in those cases the Ashtech Unit in the Comms Room was reset. Gaps over 1 minute in the data stream are listed below.

time gap : Jday 126 15:11:36 to 126 15:12:48 (72 s)

time gap : Jday 131 04:02:20 to 131 04:07:19 (5.0 mins)

time gap : Jday 131 22:40:24 to 132 00:03:24 (83.0 mins)

time gap : Jday 132 09:17:32 to 132 09:25:24 (7.9 mins)

time gap : Jday 132 22:29:08 to 132 22:43:24 (14.3 mins)

time gap : Jday 136 06:56:56 to 136 06:58:47 (111 s)

time gap : Jday 146 08:06:07 to 146 08:25:49 (19.7 mins)

time gap : Jday 147 07:47:39 to 147 07:49:01 (82 s)

time gap : Jday 149 07:45:48 to 149 08:26:54 (41.1 mins)

time gap : Jday 151 07:52:43 to 152 19:43:00 (35.8 hrs)

time gap : Jday 153 07:10:26 to 153 08:42:08 (91.7 mins)

time gap : Jday 153 08:43:33 to 153 09:04:46 (21.2 mins)

time gap : Jday 153 12:26:34 to 153 12:31:27 (4.9 mins)

time gap : Jday 153 12:52:25 to 153 13:56:48 (64.4 mins)

time gap : Jday 153 16:38:41 to 153 17:08:49 (30.1 mins)

time gap : Jday 155 07:24:51 to 155 08:21:55 (57.1 mins)

time gap : Jday 155 21:22:18 to 155 21:37:54 (15.6 mins)

time gap : Jday 157 07:02:23 to 157 08:51:51 (109.5 mins)

time gap : Jday 157 09:41:33 to 157 11:10:19 (88.8 mins)

time gap : Jday 160 07:01:50 to 160 08:16:49 (75.0 mins)

time gap : Jday 161 06:43:11 to 161 07:52:24 (69.2 mins)

time gap : Jday 161 09:25:41 to 161 09:39:24 (13.7 mins)

time gap : Jday 163 00:20:36 to 163 00:27:24 (6.8 mins)

time gap : Jday 163 06:52:24 to 163 07:46:19 (53.9 mins)

time gap : Jday 165 00:55:00 to 165 01:01:49 (6.8 mins)

time gap : Jday 167 06:28:58 to 167 09:37:54 (3.1 hrs)

150 kHz ADCP

The 150kHz RDI ADCP was logged using IBM Data Acquisition Software (DAS) version 2.48 with profiler software 17.20. The instrument was configured to sample over 120 second intervals with 64 bins of 8m thickness, pulse length 8m and a blank beyond transmit of 8m. Early in the cruise the ADCP was switched to bottom and water track mode over shallow ground to enable calibration. For the rest of the cruise the ADCP operated in water track mode only. The two ADCPs were configured to synchronise their pings over the ensemble period, with the 150 kHz instrument as the "master" and the 75 kHz instrument as the "slave", as recommended by RDI. The result was that each ADCP had 40 water track pings in a 2 minute period. No technical problems were encountered during the cruise. A discussion about potential interference between the ADCP instruments is given below.

The main difference between the 150 kHz ADCP on D253 and previous cruises was that it had been refitted in dry dock prior to sailing and given an offset of 45° on the advice of RDI. This offset was accounted for in the DAS software which performed the beam to earth co-ordinate transformation. The other major advance was that the ADCP PC clock had been synchronised with the ship's master clock, so removing the tedious need for logging the drift of the PC clock and correcting for it in the processing (previous *adpexec1*).

Spot gyro heading data were fed into the transducer deck unit where they were incorporated into the individual ping profiles to correct the velocities to earth co-ordinates before being reduced to a 2 minute ensemble. The ADCP data were logged continually by the level C computer. From

there they were transferred once a day to the PSTAR processing system. Standard processing was used;

adpexec0: transferred data from the RVS level C adcp data stream to PSTAR. The data were split into two paths; gridded, depth dependant, data were placed into 'adp....' files while non-gridded, depth independent, data were placed into 'bot....' files. Velocities were scaled to cms^{-1} and amplitude by 0.42 to dB. Nominal edits were made on all the velocity data to remove both bad data and to change the DAS defined absent data value to the PSTAR absent value. The depth of each bin was determined from the user supplied information. Output Files: adp253##, bot253##.

adpexec2: this merged the adcp data (both files) with the ashtech a-ghdg created by *ashexec2*. The adcp velocities were converted to speed and direction so that the heading correction could be applied and then returned to east and north: noting the renamed and re-ordered variables. Output files: adp253##.true, bot253##.true.

adpexec3: applied the misalignment angle, ϕ, and scaling factor, A, to both adcp files. The adcp data were edited to delete all velocities where the percent good variable was 25% or less. Again, variables were renamed and re-ordered to preserve the original raw data. Output Files: adp253##.cal, bot253##.cal.

adpexec4: merged the adcp data (both files) with the absolute navigation file created by *navexec0*. Ship's velocity was calculated from the 2 minute positions and added to the adcp velocities. The end product was the absolute velocity of the water. Output Files: adp253##.abs, bot253##.abs.

Calibration of the 150 kHz ADCP was performed using the bottom tracking data on the Celtic shelf, and some zig-zag runs in the southern Rockall Trough early in the cruise. The values of ϕ (misalignment angle) = 3.814 (sd = 0.078) and A (scaling factor) = 0.9966 (sd = 0.002) were derived. Bottom track and water track calibrations resulted in very similar A and ϕ, but the standard deviation of the water track means were much higher due to variable current velocities over the period taken to complete the zig-zags.

75 kHz ADCP

D253 was the first scientific cruise on which the new RDI Ocean Surveyor 75 kHz Phased Array ADCP was used and thus a new processing path was written. The instrument was configured to sample over 120 second intervals with 60 bins of 16m depth, pulse length 16 m and a blank beyond transmit of 8 m. The instrument was a narrow band phased array ADCP

with 76.8 kHz frequency and a 30° beam angle. The PC was running RDI software VmDAS v1.2.012 and WinADCP v1.1.0. Gyro heading, GPS Ashtech heading, location and time were fed as NMEA messages into the software which was configured to use the Gyro heading for co-ordinate transformation. The PC software logged the PC clock time, stamped the data (start of each ensemble) with that time, and recorded the offset of the PC clock from GPS time. This offset was then applied to the data in the processing path before merging with navigation. The ADCP was fitted to *Discovery* in the forward well previously occupied by the unsuccessful ACCP and before that the ADCP prior to the 1992 re-fit. During fitting a nominal offset of 45° was intended, but the April 2001 trials cruise ascertained that the offset was in fact 60°, and this offset was accounted for in the RDI software. Bottom tracking was used early in the cruise and switched back on during the first half of Fine Scale Survey 1 for calibration calculations.

The 2 minute data were written to the PC hard disk in files with a .LTA extension, eg D253000_000000.LTA, D253001_00000.LTA etc. Sequentially numbered files were created whenever data logging was stopped and re-started. The software would close the file once it reached 48 MBytes in size (a user-specified size), though on D253 files were closed after a few days so they never became that large. The .LTA files were transferred to a networked Mac for ftp transfer to the unix directory /data62/surveyor. Broadly speaking the new processing path followed the steps outlined for the 150 kHz ADCP. In the following script description, "##" indicates the daily file number.

The calibration was established from bottom tracking data collected on long straight SeaSoar runs of Fine Scale Survey 2. The values were ϕ = 1.3578 (sd = 0.078), A = 1.0050 (sd = 0.0031), which differed to those derived from the water-track zig-zags (ϕ = 1.7376, sd = 0.9951, and A = 1.0110, sd = 0.0145). Since the bottom track calibrations had lower standard deviation, and because it had already been established that the zig-zags gave fairly large errors for the 150 kHz ADCP, it was decided to use the bottom track calibrations. See below for comparison with the 150 kHz on-station velocities.

*surexec0***:** data read into pstar format from RDI binary file (*psurvey*, new program written on D253 by S Alderson). Water track velocities written into 'sur...' files, bottom track into 'sbt....' files but the latter only if in bottom track mode. Velocities were scaled to cms^{-1} and amplitude by 0.45 to dB. The time variable was corrected to GPS time by combining the PC clock time and the PC-GPS offset. The depth of each bin was determined from the user supplied information. Output Files: sur253##.raw, bot253##.raw.

surexec1: data edited according to status flags (flag of 1 indicated bad data). Velocity data replaced with absent data if variable 2+bmbad was greater than 25% (% of pings where

>1 beam bad, thus no velocity computed). Time of ensemble moved to the end of the ensemble period (120 secs added with *pcalib*). Output files: sur253##, bot23##.

surexec2: this merged the adcp data (both files) with the ashtech a-ghdg created by *ashexec2*. The adcp velocities were converted to speed and direction so that the heading correction could be applied and then returned to east and north: note the renamed and re-ordered variables. Output files: sur253##.true, sbt253##.true.

surexec3: applied the misalignment angle, ϕ, and scaling factor, A, to both files. Variables were renamed and re-ordered to preserve the original raw data. Output Files: adp253##.cal, bot253##.cal.

surexec4: merged the ADCP data (both files) with the absolute navigation file created by *navexec0*. Ship's velocity was calculated from the 2 minute positions and added to the adcp velocities. The end product was the absolute velocity of the water. Output Files:sur253##.abs, sbt253##.abs.

Assessment of the 75 kHz ADCP

The main hurdle to be overcome in the development of the data processing path was establishing the source of the time stamp on the 2-minute ensembles. The RDI Manual was not overly helpful, but email communication with Loic Michel of RDI Europe clarified that issue, as well as the meaning of some variables. Once the correct time was being used, bottom tracking and water tracking calibrations could be calculated.

This following paragraphs outline simple comparisons of the data from the two ADCP instruments in order to draw some conclusions about the performance of the new 75 kHz ADCP. It should be noted that the author was a novice at understanding ADCP data and as such this assessment is not expected to be definitive by any means.

On-Station Profiles

The on-station data tended to be the best quality ADCP data, penetrating deepest into the water column. The on-station data for section A to D (Stations 13966 to 13985, 14027 to 14047) were selected and averaged into u and v profiles for each ADCP (covering velocities of ±40 cms^{-1}). The data were merged together and the differences in u and v calculated (75 kHz minus 150 kHz). The results (Figure 14) were very encouraging, suggesting the ADCPs agreed within the expected noise level of the instruments:

U (east) Mean = -0.175 cms^{-1}, sd = 1.539 (N = 828)

V (north) Mean = -0.058 cms^{-1}, sd = 1.780 (N = 828)

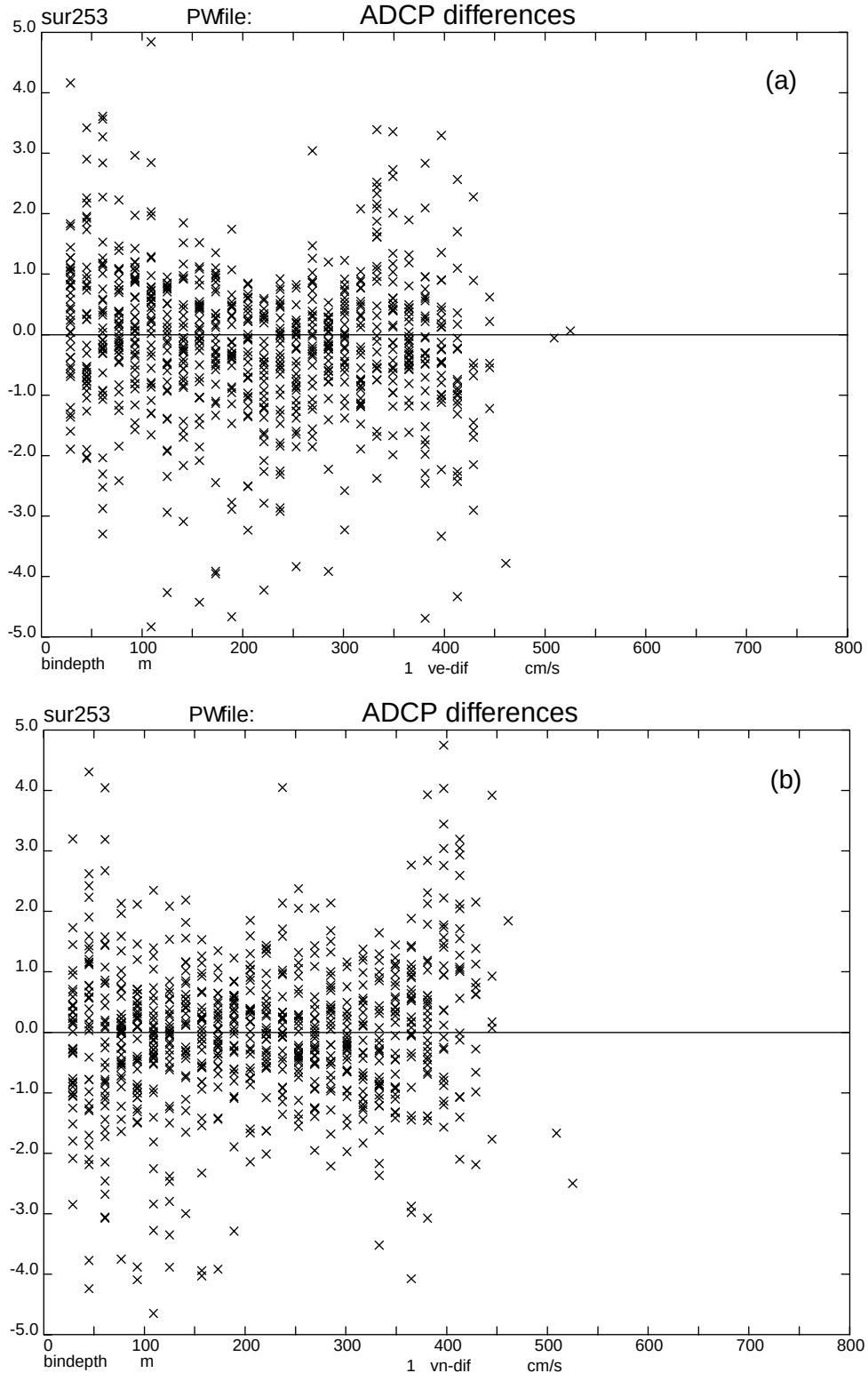

Figure 14. On-station profile differences between the 2 VM-ADCPs (75 kHz – 150 kHz); a) East component, b) North component.

Depth of Penetration

The main potential advantage of the 75 kHz ADCP was that the lower frequency meant greater depth penetration (Figures 15 and 16), though at reduced vertical resolution (16 m bins versa 8 m). During D253 the 75kHz ADCP managed to reach 700-750m on station, and 600-750m steaming in good weather. In contrast, typical maximum depths for the 150 kHz were 350-400 m under the same conditions. It was noticeable though that the 75 kHz depth penetration whilst steaming suffered very readily with the onset of anything other than calm conditions. For example in the southern Iceland Basin (Leg B to C) the 150 kHz was able to provide good data to 350 m underway, whereas at the same time the 75 kHz was only achieving 300 m. It was therefore postulated that the forward well was more prone to contamination by bubbles than the aft well, and if the 75 kHz ADCP were to become the standard ADCP for Discovery it might be appropriate to move the 75 kHz to the aft well.

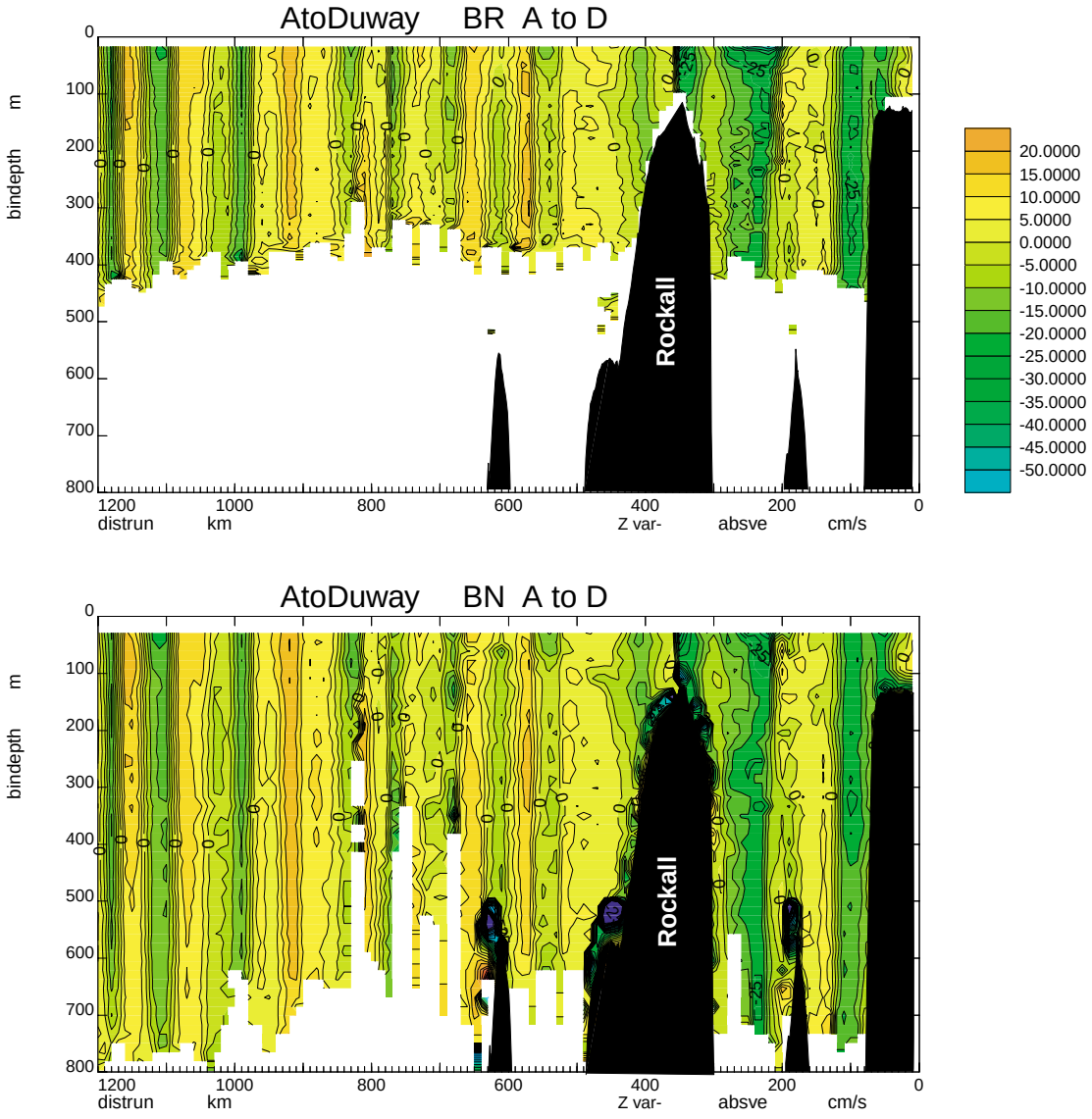

Figure 15. Contoured absolute velocities (east) for a) 150 kHz ADCP and b) 75 kHz ADCP across the Iceland Basin and Rockall Trough (A to D).

Mid-Depth Spiking

Figure 16 (north velocities) shows a curious feature that appeared common to all the 75 kHz data, and that was a spike in the 330 m bin. It turned out that these spikes occurred only during steaming passages, and were positive in the direction that the ship was travelling. Thus on the section A to D, they were most prominent in the north velocities in the Iceland Basin where the track was northwards along the 20 °W meridian. The origin of these spikes has not been ascertained, though possibilities suggested were interference with the 150 kHz pings, or wrapping of pings. The spikes were always at 330 m and did not vary with bottom depth. This problem needed further investigation after the cruise.

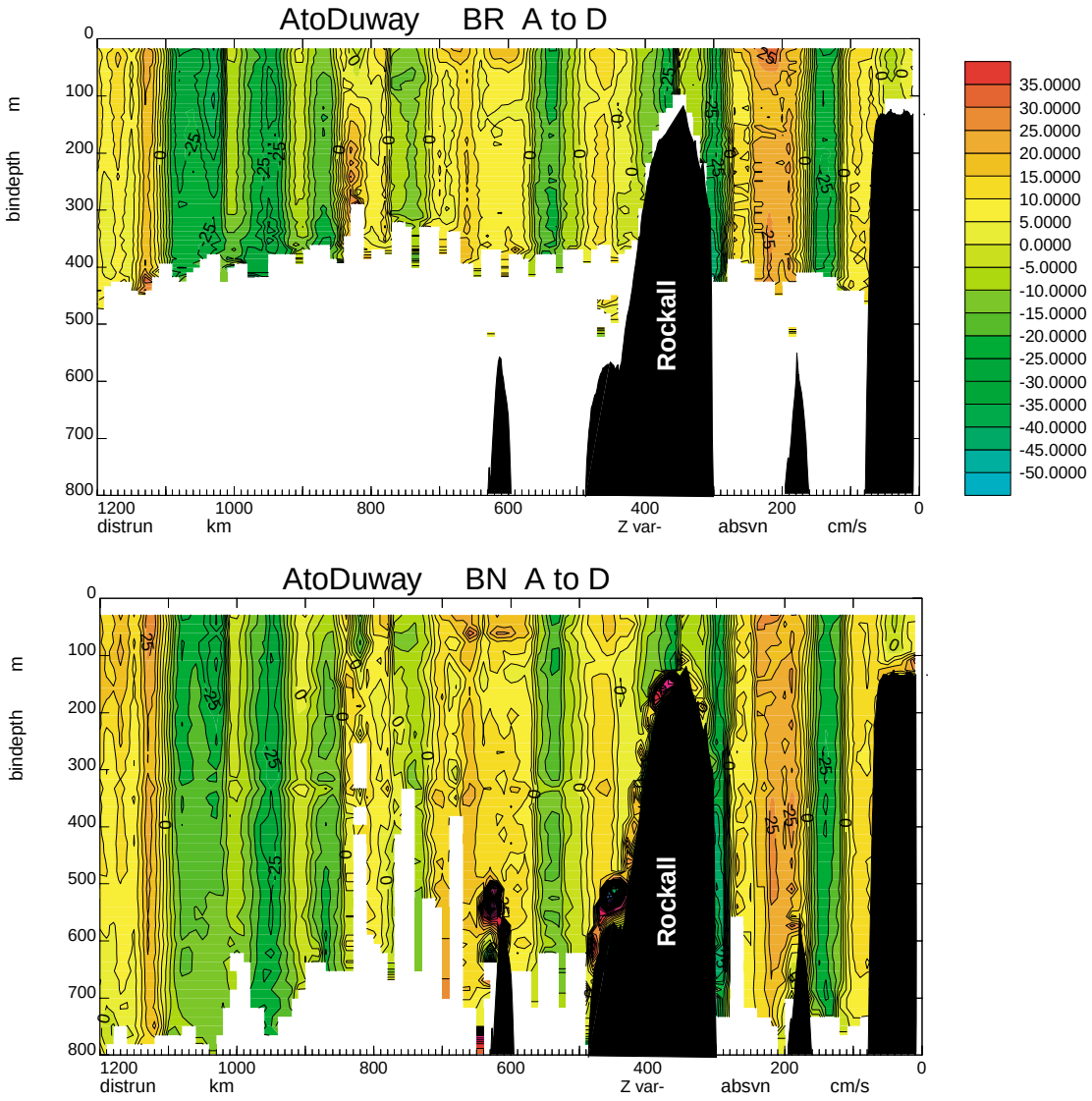

Figure 16. Contoured absolute velocities (north) for a) 150 kHz ADCP and b) 75 kHz ADCP across the Iceland Basin and Rockall Trough (A to D).

Lowered ADCP (LADCP) - *Steven Alderson, Jeff Benson, Nick Crisp, Lisa Feighery, Penny Holliday, Glenn Nolan, Naoise O'Reilly, David Smeed and John Wynar*

Introduction

The two Lowered Acoustic Doppler Current Profilers (LADCP) used on the FISHES cruise were RDI 150kHz BroadBand ADCP's (phase III) with 25 degree and 30 degree beam angles. They were mounted vertically within the CTD frames with the bottom of the transducers protected by the base of the CTD frame.

The 20 degree instrument was installed on the frame with the Neil Brown Mk III CTD at the beginning of the cruise. The 30 degree instrument was mounted on the frame with the SeaBird 9/11 plus CTD.

A few minutes before each cast, a command file was downloaded to the LADCP unit from a PC in the deck lab via a serial link. On this cruise the same command file was used for the whole cruise (an annotated listing is given in an Appendix at the end of this section).

Bottom tracking was used throughout. This reduced the number of water track pings but was justified because it allowed a second independent estimate of the bottom current to be made. At regular intervals the instrument emitted a bottom ping to test for range. Once the bottom was found the instrument recorded the velocity of the ground with respect to the package. It was hoped to use this to provide a check of the quality of the absolute velocity data calculated by the more round about route described below.

The data were recorded internally and downloaded at the end of each cast by connecting a data link to the package from the PC. RDI utilities BBTALK and BBSC were used to interrogate the profiler and to download data to the PC. Power was supplied to the profiler via the serial cable in order to conserve the battery pack.

Processing

Data were transferred to the UNIX workstations via FTP and then processed using a combination of PERL scripts and MATLAB m-files developed by Eric Firing at the University of Hawaii.

Processing was done in a number of steps which are briefly described below.

i The binary data were first scanned to find useful information from the cast such as time at the surface, time at the bottom and the number of ensembles.

ii The data were then read into a CODAS database. Magnetic variation and position were added to the database at this stage.

iii When CTD data were available the pressure temperature and salinity data were added to the database in order to correct for the variation of sound speed with depth.

iv Absolute velocities were then found by calculating horizontal velocity shear to eliminate package motion, integrating with time to calculate the barotropic terms and then merging with navigation data to remove the motion of the ship.

Bottom velocity data were not included in the processing path and had to be extracted manually from the binary file on the PC and processed separately from the water track data.

To aid processing a number of master scripts were written. These were:

dowater - performed all water data steps, from reading in the data from the RDI binary file to calculation of absolute velocity; all intermediate files in the calculation being replaced or edited for each cast so that no old information was mistakenly used.

dobottom - calculated near bottom water velocities by using bottom track data;

donav - created file of GPS data which had been edited for bad fixes by screening the resulting speed over ground velocities;

docomp - created a file merging LADCP data with on station averaged 150 kHz VM-ADCP data

dopict, dodisp - two scripts which created summary plots of LADCP and ADCP data for all stations.

Results

The following table gives the LADCP station numbers with their positions and resulting magnetic variation. Also given is the rms difference, over the depth range 100-200m, between the mean LADCP absolute velocity components and those from the 150kHz VM-ADCP whilst on station. Apart from obvious problem stations (e.g. 14035 and 14066), the differences were generally small (of order 2-3cms^{-1}), which was encouraging. More work will be required to reconcile the values further. The 75kHz VM-ADCP may provide useful future comparisons here.

Station	latitude	longitude	magnetic	20° or 30°	rms diff. east cm/s	rms diff. north cm/s
13965	55 01.10N	12 58.60W	-9.56	20	1.0963	4.0860
13967	57 48.75N	14 29.72W	-11.37	20	0.6943	0.6646
13968	58 03.14N	14 59.80W	-11.72	20	2.5486	2.5807
13969	58 17.37N	15 30.07W	-12.08	20	1.8610	1.0684
13970	58 30.64N	16 00.03W	-12.44	20	2.3005	1.5217
13971	58 43.85N	16 30.32W	-12.80	20	2.3932	1.4979
13972	58 57.52N	16 58.61W	-13.15	20	0.9865	1.7094
13973	59 10.17N	17 29.28W	-13.51	20	3.5284	1.7605
13974	59 20.06N	17 47.83W	-13.75	20	3.0283	4.5585
13975	59 29.13N	18 14.73W	-14.06	20	1.2472	4.3295
13976	59 41.22N	18 46.05W	-14.43	20	1.8154	3.7520
13977	59 53.92N	19 18.84W	-14.83	20	0.7533	1.9788
13979	60 29.39N	19 59.35W	-15.49	20	0.9802	2.8264
13980	60 58.94N	19 58.21W	-15.74	20	0.6975	4.6230
13981	61 29.84N	20 00.32W	-16.02	20	2.0606	1.2298
13982	61 59.61N	19 59.28W	-16.28	20	3.7133	3.4077
13983	62 30.40N	20 00.09W	-16.56	20	0.7897	0.8336
13984	63 00.33N	20 01.05W	-16.84	20	3.1106	3.5845
13985	63 12.77N	19 59.94W	-16.94	20	6.2338	1.8454
13986	63 05.30N	21 17.53W	-17.61	20	1.9708	1.9557
13987	62 52.85N	22 08.28W	-17.98	20	1.0027	1.8491
13988	62 40.12N	22 59.89W	-18.35	20	2.5893	2.6448
13989	62 27.31N	23 49.29W	-18.69	20	1.5302	1.1780
13990	62 13.34N	24 39.95W	-19.03	20	0.7588	2.6338
13991	61 59.23N	25 30.21W	-19.35	20	2.0507	4.3466
13992	61 44.05N	24 40.82W	-18.75	20	0.5864	2.9764
13993	61 27.66N	23 48.65W	-18.11	20	1.9603	3.5267
13994	61 11.47N	22 56.74W	-17.48	20	1.0694	4.3256
13996	60 55.14N	22 07.58W	-16.88	20	1.3462	2.3656
13997	60 39.09N	21 19.60W	-16.30	20	2.1621	5.1594
13998	60 22.60N	20 34.79W	-15.75	20	2.2973	3.2930
13999	60 04.97N	19 50.65W	-15.21	20	0.5748	0.8185
14000	60 24.63N	19 02.14W	-14.93	20	1.3340	0.7251
14001	60 42.18N	18 11.59W	-14.62	20	2.7184	1.1029
14002	60 57.50N	17 22.96W	-14.30	20	4.5100	0.6903
14003	61 14.40N	16 36.49W	-14.01	20	2.1886	0.7044
14004	61 29.69N	15 47.99W	-13.68	20	1.3926	3.1426
14005	61 44.70N	14 57.65W	-13.33	20	2.4067	0.8231
14006	62 03.91N	15 34.65W	-13.82	20	0.5577	0.4475
14007	62 28.35N	15 57.03W	-14.23	20	2.2097	5.3619
14008	62 53.84N	16 16.57W	-14.62	20	1.8199	2.3289
14009	63 17.97N	16 38.63W	-15.03	20	1.8716	2.5917
14010	63 24.87N	16 44.88W	-15.15	20	1.0484	2.2044
14011	61 38.88N	15 13.11W	-13.43	20	1.6641	0.7255
14012	61 18.94N	14 48.33W	-13.04	20	0.7570	0.9788
14013	61 05.12N	14 7.14 W	-12.56	20	0.5505	2.4976
14014	60 51.31N	13 27.59W	-12.10	20	0.7460	1.5721

14015	60	36.93N	12	45.86W	-11.62	20	2.9687	4.7571
14016	60	20.41N	12	00.42W	-11.10	20	5.0965	5.0326
14017	60	03.16N	11	13.90W	-10.57	20	5.4997	3.6505
14018	59	45.65N	10	28.89W	-10.06	20	3.4305	3.6632
14019	59	27.95N	9	43.23W	-9.55	20	0.9585	0.7802
14020	59	09.14N	8	56.67W	-9.03	20	3.2544	1.7030
14021	58	49.39N	8	12.38W	-8.54	20	4.5905	1.6896
14022	58	44.48N	7	59.49W	-8.40	20	1.0081	2.9353
14024	58	44.29N	7	59.81W	-8.40	20	3.9831	2.6971
14025	58	54.86N	8	23.52W	-8.66	20	2.8533	2.2527
14026	58	44.34N	8	00.02W	-8.40	20	2.4080	7.3576
14031	57	03.00N	9	13.00W	-8.44	30	-999	-999
14032	57	05.91N	9	25.26W	-8.55	30	3.2648	2.8379
14033	57	09.01N	9	41.42W	-8.70	30	2.6620	1.1798
14034	57	12.80N	10	3.42 W	-8.90	20,30	4.0290	7.5886
14035	57	17.36N	10	22.56W	-9.09	30	27.723	4.5007
14036	57	21.69N	10	39.15W	-9.25	30	3.8534	5.6182
14037	57	24.09N	10	51.09W	-9.37	30	2.6063	3.5565
14038	57	27.08N	11	04.77W	-9.50	30	1.6190	2.0969
14039	57	28.35N	11	18.61W	-9.62	30	2.4594	3.7948
14040	57	29.23N	11	31.93W	-9.74	30	4.1485	6.0408
14041	57	29.70N	11	50.90W	-9.90	30	3.5593	0.9082
14042	57	30.68N	12	14.63W	-10.10	30	4.0446	1.2422
14043	57	31.71N	12	37.44W	-10.30	20	8.4950	1.9764
14044	57	31.66N	12	51.75W	-10.42	20	3.0729	0.8634
14045	57	32.99N	12	59.88W	-10.50	20	1.5173	1.1147
14046	57	34.04N	13	19.97W	-10.67	20	3.6435	8.7013
14049	58	34.78N	13	51.67W	-11.35	20	1.3312	1.8000
14050	59	10.09N	13	28.99W	-11.40	20	0.7252	0.9550
14051	59	30.10N	13	15.57W	-11.42	20	1.3600	4.4669
14052	59	59.78N	12	54.88W	-11.44	20	1.2783	1.3179
14054	60	44.92N	12	23.01W	-11.47	20	1.7165	1.1022
14055	61	00.04N	11	38.25W	-11.16	20	3.4752	2.4285
14056	61	16.83N	10	47.58W	-10.82	20	2.7537	0.8907
14057	61	34.48N	09	53.05W	-10.43	20	1.8777	1.5043
14058	61	48.01N	09	07.45W	-10.10	20	1.2118	1.0006
14061	62	43.60N	08	19.68W	-10.00	20	3.9097	1.4839
14062	63	07.07N	08	22.52W	-10.18	20	1.4233	2.7211
14065	64	22.23N	08	27.63W	-10.70	20	2.7884	1.8372
14066	64	47.05N	08	29.72W	-10.87	20	15.449	16.508
14067	65	17.34N	08	32.12W	-11.09	20	2.1428	1.3658
14068	65	21.59N	09	13.55W	-11.53	20	3.5432	3.1891
14069	65	26.12N	09	55.35W	-11.99	20	1.8902	3.5832
14070	65	00.76N	10	17.02W	-12.04	20	3.7528	5.3683
14071	64	35.36N	10	41.54W	-12.11	20	1.0007	4.9051
14072	64	11.80N	11	04.57W	-12.17	20	2.4253	7.2513
14073	63	45.72N	11	28.38W	-12.22	20	5.2021	5.4139
14074	63	19.44N	11	53.74W	-12.28	20	3.8627	0.8246
14075	62	52.53N	12	21.13W	-12.35	20	2.0350	2.0678
14076	62	26.67N	12	31.53W	-12.26	20	2.1041	0.7513
14077	62	13.32N	13	21.69W	-12.64	20	0.7168	1.8965
14078	61	58.72N	14	09.81W	-12.98	20	0.6230	0.9809
14079	61	44.27N	14	57.87W	-13.32	20	5.2456	4.9847

14081	63 59.04N	14 04.21W	-13.85	20	3.9061	3.1285
14082	63 49.06N	13 12.07W	-13.26	20	2.7534	1.2526
14083	63 39.59N	12 25.41W	-12.73	20	1.3015	0.9202
14084	63 29.52N	11 40.02W	-12.22	20	1.6192	1.6068
14085	63 19.24N	10 52.68W	-11.69	20	2.5765	3.2115
14086	63 06.92N	09 58.93W	-11.09	20	3.9705	1.5873
14087	62 54.54N	09 06.00W	-10.51	20	1.0801	2.1787
14088	62 42.83N	08 21.36W	-10.01	20	6.1823	1.9920
14090	62 03.54N	05 56.00W	-8.43	20	1.9914	0.9947
14091	61 48.29N	05 05.01W	-7.88	20	0.7639	1.1684
14092	61 33.61N	04 16.16W	-7.37	20	2.4479	0.8639
14093	61 26.49N	03 51.96W	-7.11	20	1.2812	2.5313
14094	61 19.05N	03 30.27W	-6.89	20	1.3202	0.8118
14095	61 10.57N	03 03.94W	-6.61	20	0.9287	1.8701
14096	61 02.48N	02 37.30W	-6.34	20	3.0924	4.0312
14097	60 58.98N	02 24.08W	-6.21	20	0.9510	2.4215
14099	64 35.35N	10 40.15W	-12.09	20		
14100	65 00.63N	10 16.11W	-12.02	20		
14104	64 49.82N	10 46.91W	-12.25	20		
14106	64 42.04N	10 51.65W	-12.25	20		
14108	63 40.80N	10 05.00W	-11.37	20		
14109	63 46.28N	09 54.37W	-11.30	20		
14110	63 51.29N	09 44.44W	-11.24	20		
14111	63 57.36N	09 33.48W	-11.17	20		
14112	64 03.97N	09 21.76W	-11.10	20		
14113	64 09.19N	09 10.70W	-11.03	20		
14114	64 14.05N	09 00.70W	-10.96	20		
14115	64 19.44N	08 49.49W	-10.88	20		
14116	64 19.22N	08 49.73W	-10.88	20		
14117	64 24.68N	08 40.25W	-10.83	20		
14118	64 00.33N	08 00.39W	-10.28	20		
14120	64 06.81N	11 43.77W	-12.51	20		
14121	64 15.21N	11 26.75W	-12.40	20		
14123	64 22.82N	11 10.87W	-12.30	20		
14124	64 32.42N	10 55.51W	-12.21	20		
14125	64 40.97N	10 39.23W	-12.11	20		
14127	64 50.37N	10 19.17W	-11.97	20		
14130	63 55.15N	10 54.88W	-11.95	20		

Figure 17, spread over the following five pages, presents the full profile LADCP velocity components (east in black, north in red) plotted against depth and station number. A black dotted line indicates the station number and the zero of the components. One station unit is equivalent to 50 cms^{-1} of velocity. The on station 150 kHz ADCP components are over-plotted for comparison (in blue and green).

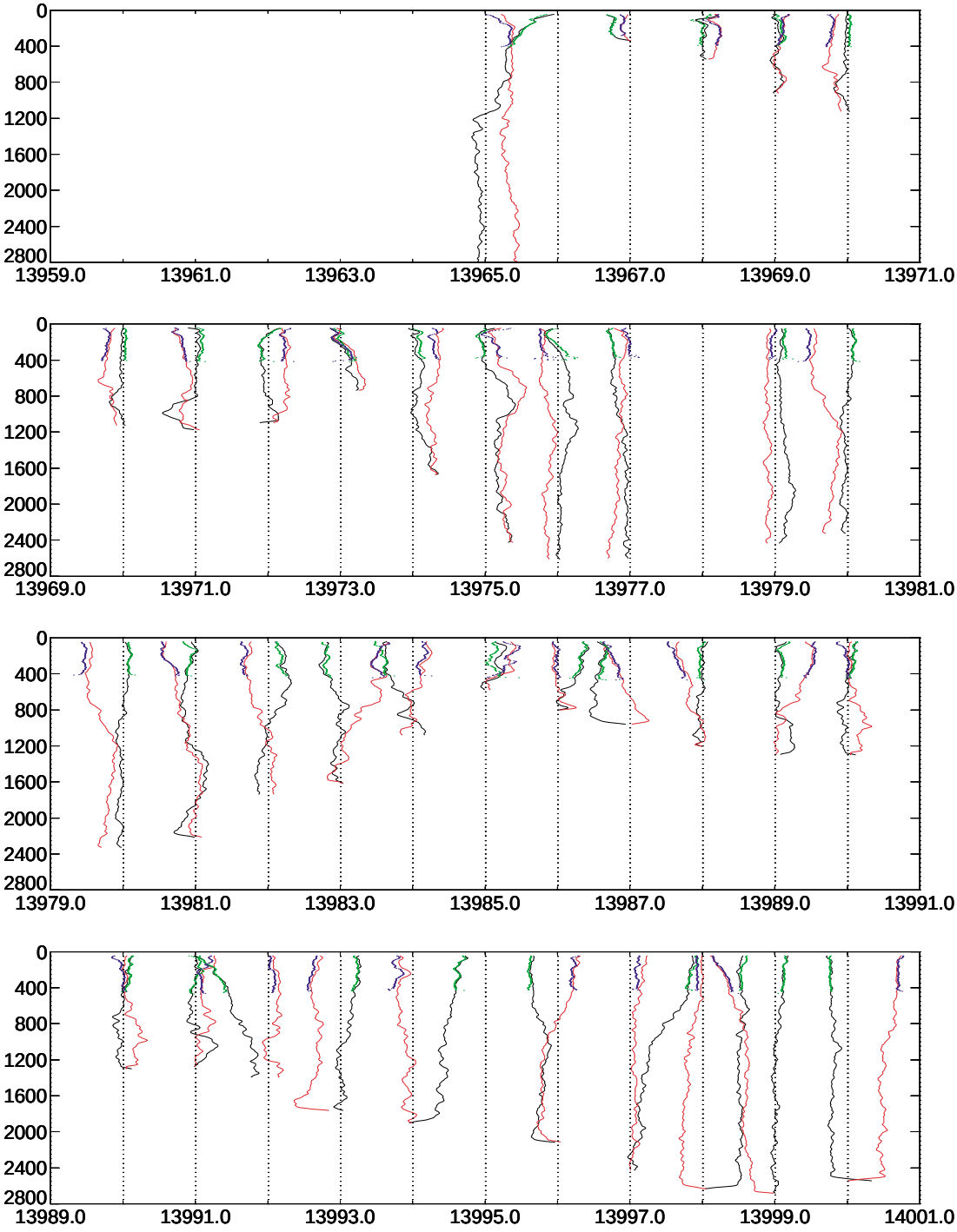
0
400
800
1200
1600
2000
2400
2800
13959.0
13961.0
13963.0
13965.0
13967.0
13969.0
13971.0
0
400
800
1200
1600
2000
2400
2800
13969.0
13971.0
13973.0
13975.0
13977.0
13979.0
13981.0
0
400
800
1200
1600
2000
2400
2800
13979.0
13981.0
13983.0
13985.0
13987.0
13989.0
13991.0
0
400
800
1200
1600
2000
2400
2800
13989.0
13991.0
13993.0
13995.0
13997.0
13999.0
14001.0

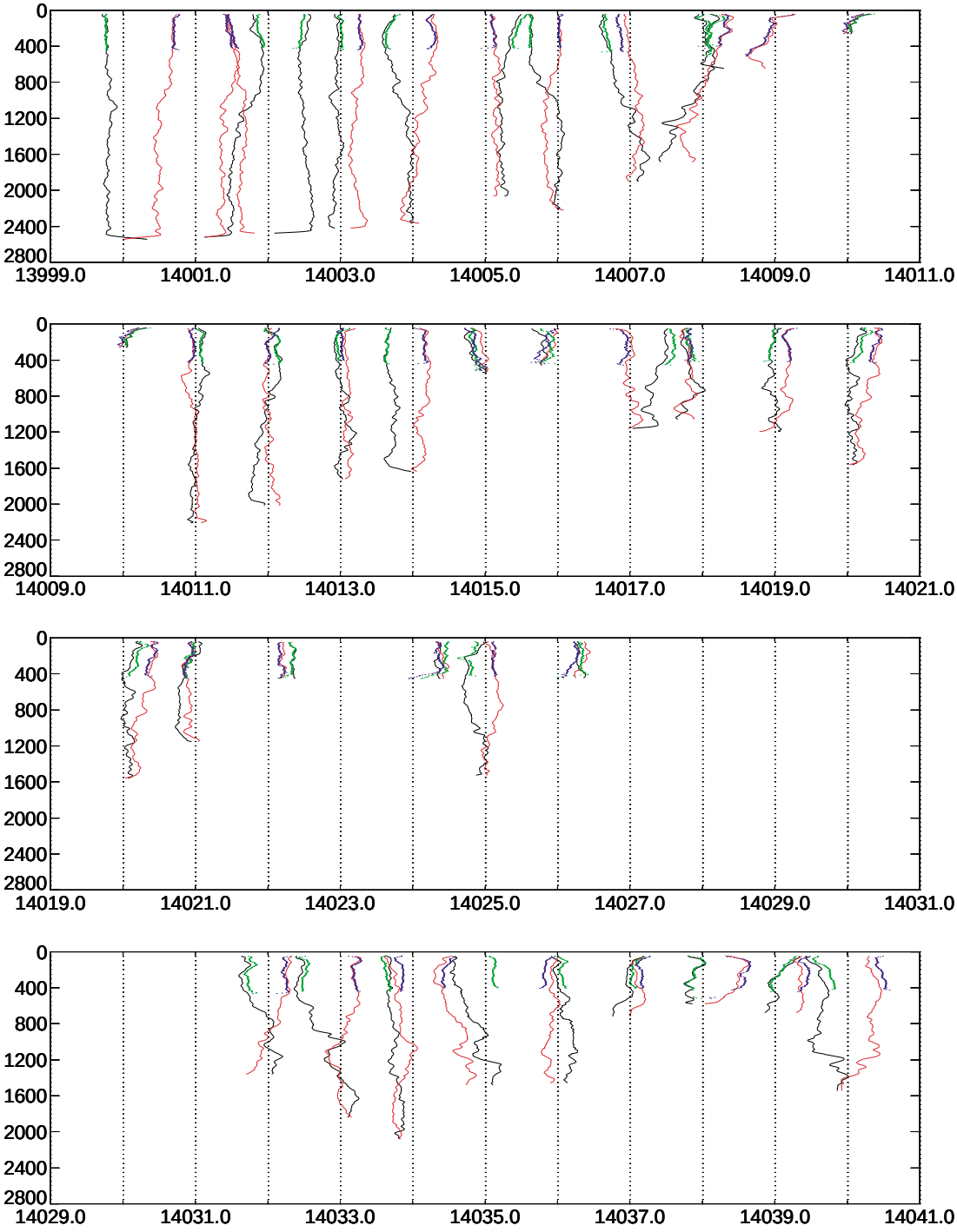
0
400
800
1200
1600
2000
2400
2800
13999.0
14001.0
14003.0
14005.0
14007.0
14009.0
14011.0
14009.0
14011.0
14013.0
14015.0
14017.0
14019.0
14021.0
14019.0
14021.0
14023.0
14025.0
14027.0
14029.0
14031.0
14029.0
14031.0
14033.0
14035.0
14037.0
14039.0
14041.0

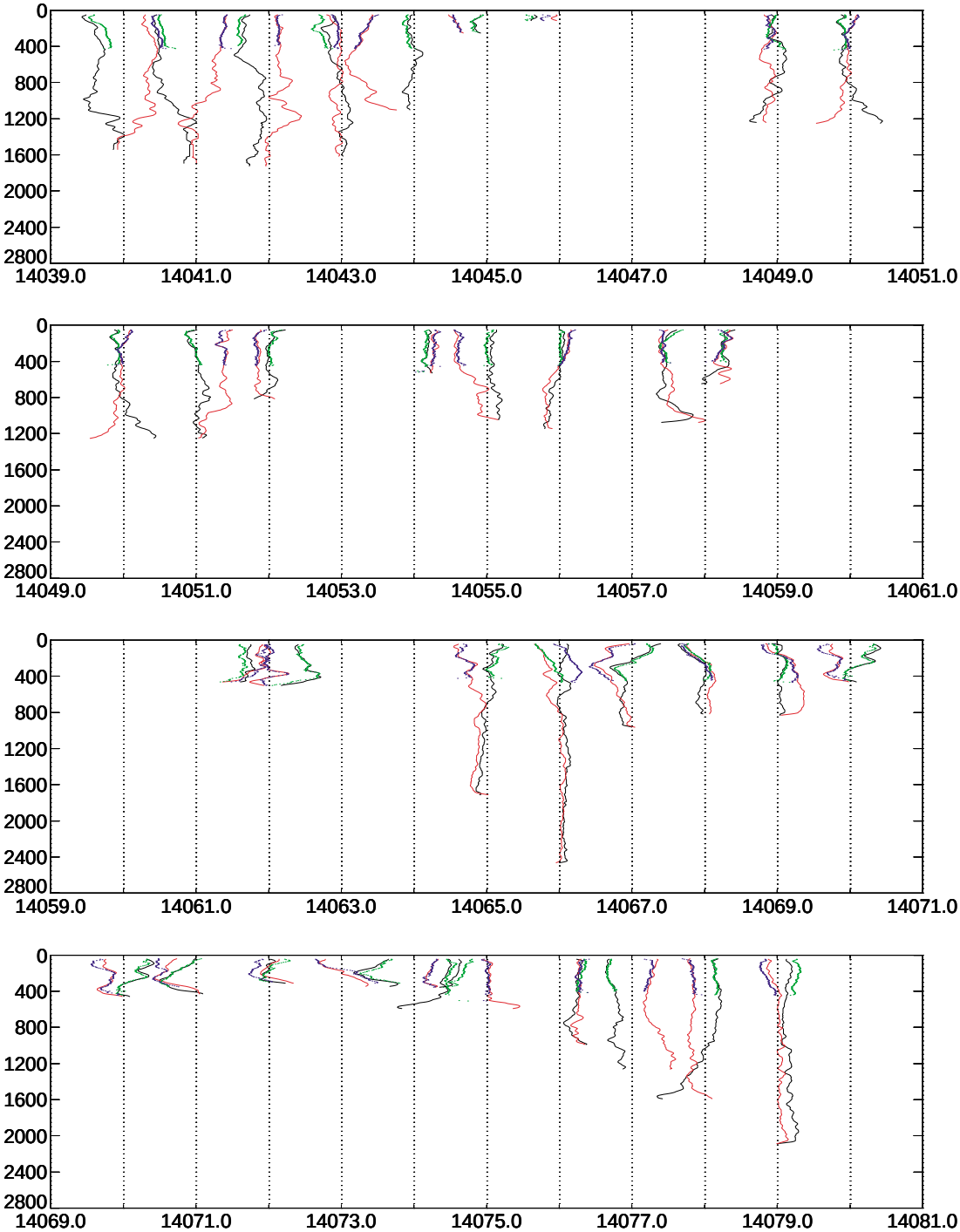
0
400
800
1200
1600
2000
2400
2800
14039.0
14041.0
14043.0
14045.0
14047.0
14049.0
14051.0
0
400
800
1200
1600
2000
2400
2800
14049.0
14051.0
14053.0
14055.0
14057.0
14059.0
14061.0
0
400
800
1200
1600
2000
2400
2800
14059.0
14061.0
14063.0
14065.0
14067.0
14069.0
14071.0
0
400
800
1200
1600
2000
2400
2800
14069.0
14071.0
14073.0
14075.0
14077.0
14079.0
14081.0

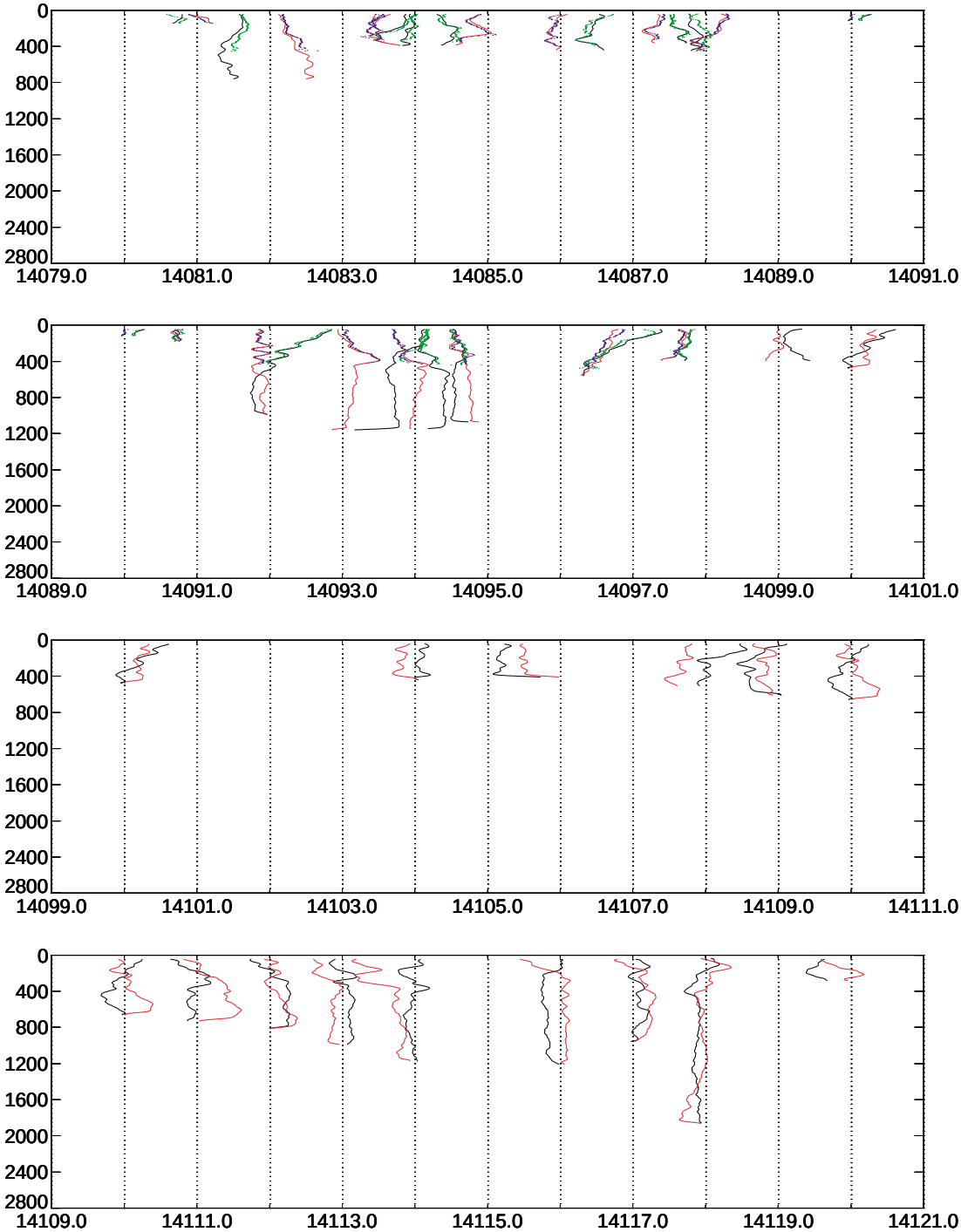
0
400
800
1200
1600
2000
2400
2800
14079.0
14081.0
14083.0
14085.0
14087.0
14089.0
14091.0
14089.0
14091.0
14093.0
14095.0
14097.0
14099.0
14101.0
14099.0
14101.0
14103.0
14105.0
14107.0
14109.0
14111.0
14109.0
14111.0
14113.0
14115.0
14117.0
14119.0
14121.0

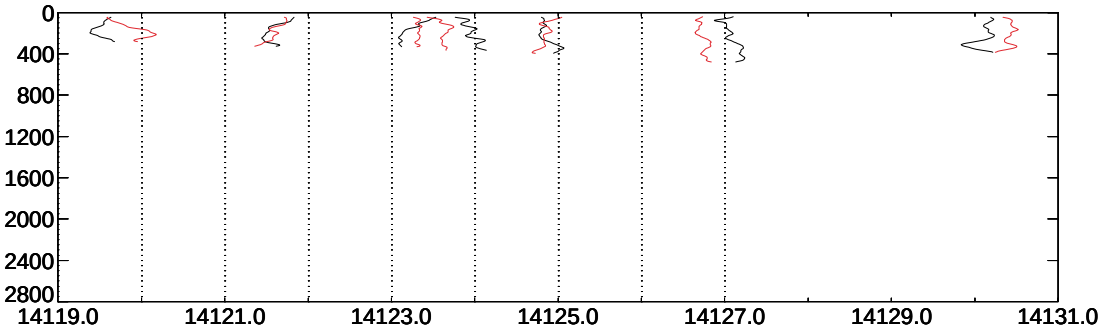

Problems

Previous use of the 30° LADCP instrument had raised questions about the resulting data quality. So-called "X-profiles" (because of the shape made by the up and downcast profiles), had been prevalent on other cruises with this instrument. This cruise was no exception. Because of the wish to use the SeaBird CTD on station 14031 and thereafter, the 30° instrument was used. The incidence of X-profiles increased; peculiarly, whatever caused this phenomenon averaged out between the up and down profiles resulting in mean east/north profiles that continued to match well with the VM-ADCP data. Apart from cast 14035, there seemed little difference in the rms LADCP-(VM-ADCP) values, presented in the table above, between the 20° and 30° instruments. However, cast 14034 was repeated with the 20° instrument for comparison purposes and revealed significant potential problems with the 30° LADCP instrument. It was recommended that this LADCP instrument should not be used again until the problems have been resolved by RDI.

Part way through leg 1 it was discovered that the data processing had been carried out with the assumption that a 30° LADCP instrument was in use throughout. The resulting differences would be small, but nevertheless the processing was repeated with the correct processing path. This was achieved by adding code to *dowater* which identified the instrument type and called the corresponding routines.

Matching with the CTD data was difficult when the latter had remnant pressure spikes since these produced large inferred package velocities. To get round this for the LADCP processing, a number of the CTD files were copied to separate files and spikes removed. The LADCP data was then reprocessed with this CTD data. No manual intervention was required in the matching process apart from this. However it did mean that when the CTD data was re-calibrated, the CTD copied for LADCP processing may not have been re-calculated.

Appendix A – LADCP Command File

Annotations are not part of the command file format.

CR1		-	reset to factory default parameters
PS0		-	print out hardware/firmware information
CY		-	
CT0		-	turn off automatic initialisation on power up
EZ	0011101	-	select sources of sensor data
EC	1500	-	manual speed of sound
EX	11101	-	coordinate transformation
WD	111100000	-	select data types to be collected
WL	0,4	-	disable water reference layer averaging (first 0)
WP	00001	-	set number of pings per ensemble
WN	010	-	set number of depth cells
WS	1600	-	set depth cell size
WF	1600	-	set depth after transmit
WM	1	-	set profiling mode (1 means set pulses with a short lag to avoid ambiguity resolving errors)
WB	1	-	set bandwidth control
WV	400	-	set ambiguity velocity when WM is 1 (400cm/s)
WE	0150	-	set error velocity threshold (150 mm/s)
WC	056	-	set minimum correlation threshold (56 counts)
CP	255	-	set power output (highest power = 255 counts)
CL	0	-	set power saving on or off (0 = off)
BP	001	-	set number of bottom track pings per ensemble
BD	25	-	set delay period before attempting to reacquire the bottom
BX	2500	-	set maximum tracking depth for bottom tracking (250 m)
BL	0,200,600	-	set bottom track reference layer boundaries (off since first number is 0)
BM	4	-	set bottom track mode (uses correlation side peak position)
TP	000100	-	set time between pings (mmss.ss)
TE	00000200	-	set time per ensemble (hhmmss.ss)
&R20			
CF11101		-	set flow control (11101 means start next data collection when ready; ping immediately when ready; send binary output; dont send via serial connection; record internally)
&?			

ADCP Backscatter/EK500 - *Nick Crisp and Sophie Fielding*

ADCP Backscatter Processing

The daily gridded files containing beam-averaged echo-intensity data from the shipboard 150 kHz ADCP were collected as usual via the normal processing route for underway current profile data (see VM-ADCP section). These amplitude data were then converted to Mean Volume Backscatter Strength (MVBS) values using the formula from RDI (RDI, 1998), incorporated into a PSTAR program *amplcal*. This program superceeded the original *amplcal* and a program called *calampl4*, and could process amplitude data in one of 2 ways:

1. Using data supplied from an ascii ampl.dat file in the format described below to utilise information such as manufacturers constants, beam calibrations, and surface temperature and salinity.

2. As above but also using in-situ temperature and salinity data from merged CTD or SeaSoar data. Changes in absorption with depth were taken into account using this method.

During the cruise the data were processed using the first method, by obtaining daily mean surface temperature and salinity data from the underway thermosalinograph (TSG), and automatically incorporating these into the ampl.dat ascii file using a C-shell script.

The ampl.dat files took the following form.

4.17e5	150 kHz system constant.
183.15, 8.95	Power into water, and dimensionless noise factor (an average of the 4 beams)
26, 10	electronics temperature and transducer temperature (the latter was replaced by our averaged value from the TSG data)
8, 8, 5	bin length, pulse length, and blank beyond transmit
7.14	lowest echo-intensity value from the 64^{th} bin from an adcp file
1	flag=1 for nominal calibration (0.42dB/count applied)

After calculating MVBS using *amplcal*, the ADCP %good variable was used as a threshold for suspect MVBS data; as with velocity processing, data with a percent good of less than 25 were replaced with absent data. Future processing will involve removing the data below the sea-floor using depth data from the EA500 echosounder.

For a more accurate calibration to MVBS after the cruise, the SeaSoar temperature and salinity data will be merged with the ADCP amplitude data so that the changes in absorption with depth can be taken into account. This is now a standard procedure when using ADCP data for MVBS at SOC, and, in fact, can be achieved with the same PEXEC program *amplcal* once the data have been merged.

EK500 Scientific Echosounder

SOC's portable 3-frequency (38 kHz, 120 kHz and 200 kHz) SIMRAD EK500 echosounder and winch were installed on the aft deck in the usual position portside of the after hold cover. The electronics and printer were installed on a shelf in the hangar, and connected to the winch junction box via the standard 25 m long cables. RGB coax cables for the monitor, installed in the main lab, were routed via suitable junction boxes in the hangar, deck-lab, and main-lab. A cable for the remote control joystick on the monitor was routed directly from the unit in the hangar to the main lab.

Prior to the cruise, the electronics were fitted with version 5.3 of the EK500 firmware. This change of firmware meant that a new calibration would have to be made, and this was planned for the second leg of the cruise.

During the last previous usage of the EK500 on RRS *Discovery* cruise 232, in the Strait of Gibraltar, the performance of a hairy-faired cable was tested, and found to be unsuitable for use at speeds over 7 knots due to the high-drag and excessive strumming of the cable. As a result of this, and due to the potential requirement for towing at up to 12 knots between CTD stations during leg 1 of the FISHES cruise, the winch was refitted with an original faired cable (using rubber fairing sections based on the design of those used on the PES fish), last used during RRS *Charles Darwin* cruise CD104 in 1998.

The fish was deployed at 15:24 on day 127, and generally left deployed during the CTD survey except for recovery at approximately weekly intervals during CTD stations to check the mechanical soundness of the tow-fish, and cable. More generally, people were keeping an eye on the angle of the tow-cable, and, of course, on the data-display and data-collection software on the monitor in the main-lab.

A test of the background noise shortly after deployment, whilst on station, was made by setting the receivers in passive mode, and monitoring noise figures in the TEST/TRANSCEIVER menu. Values of -150, -138, and -130 dB (for 38, 120 and 200 kHz respectively) were fairly typical for previous installations on *Discovery*, and enabled useful data to be collected to depths of ~750, ~170 and ~100 m respectively whilst on-station. During CTD stations, when generally steaming at up to 11-12 knots, data quality was significantly degraded, reducing the useable depth ranges to approximately half that of the values given above.

During the first recovery of the fish for an inspection on 10 May, the tail section of the tow-fish suffered some minor damage as the fish swung against the ship's hull. The spare tail was fitted immediately, and the fish re-deployed during the same CTD cast. There were no fibre-glass repair kits aboard the ship, and so precautionary arrangements were made for some to be brought to Lerwick.

It was whilst checking the tow-cable angle on 29 May just after lunch, that the cable was found trailing out at the surface with no tow-fish attached. The ship was brought to a halt immediately, and the cable was recovered. There was no damage to the tow-cable or to the fairing segments (as we have had on previous cruises, caused by long lines or other fishing gear). Inspection of the end of the tow-cable revealed that it had pulled all the way from the moulded plug on the junction box inside the tow-fish, through the towing-strut termination, such that the original hand-stripped ends of the individual conductors were still intact. The cable itself did not break, the only sign of failure was in the kevlar braid (the strength member in the tow-cable) (Figure 2). Inspection of the kevlar braid (the main strength member in the tow-cable) led to the general consensus that, possibly, the ingress of sea water into the termination had, over time, allowed abrasion and possibly allowed the growth of an enzyme, known to attack kevlar, to occur.

Inspection of the data for the last few minutes before the fish became detached, revealed no significant degradation in signal quality, suggesting that the kevlar had failed suddenly as we began to steam off station, and that the cable must have almost instantly pulled out of the underwater connector on the junction box in the fish and through the termination block.

The loss of the tow-fish had serious implications for the second leg of the cruise where the data were to be used in earnest during the repeat SeaSoar surveys, and for LHPR and TUBA comparison/intercalibration. However, this lead us to consider ways in which to maximise the use of both the multifrequency TUBA instrument, which due to technical/software issues could not be flown on the SeaSoar vehicle, and of the OPC. The reader is referred to the sections on TUBA, OPC and the LHPR for further information.

Data Acquisition and Processing

From the electronics unit in the hangar, data were transmitted over ethernet to the DAPS SUN workstation in the main lab. Here, they were logged using a SIMRAD program *record* which was run within a script to generate 2-hourly raw files of MVBS. Bottom depth data were collected in the same manner. The 2-hourly files were then averaged over 2-minute intervals and converted to PSTAR format using the program *pshow4* which was an in-house modified version of SIMRAD's *show* program.

Post processing involved appending the PSTAR files into daily files starting and ending at midnight GMT, and then editing of data below the noise floor using a PSTAR program *pnoisek*. Future processing will involve adjusting for fish-depth versus ship speed and editing data below the seafloor.

An important post-cruise note here for future work, is that there is now some excellent commercial software on the market called 'Echoview' by SonarData Pty (www.sonardata.com)

which will both log the data and enable the user to integrate regions of any size, resample the data, scroll back and forth through the entire data set, zoom in and out, apply calibration data, etc. What is less clear is how easy it is to export the data for further advanced processing and merging with other data sets in PSTAR, although we have already spoken with a representative of the company about such issues. An important, if apparently trivial, reason for moving towards use of this software, is that we could no longer get spare printer cartridges for the HP Paintjet printer used with the EK500 system, and so in future it will no longer be easy to glance back at past data.

With the loss of the EK500 tow-fish on this cruise, there will clearly be a requirement to consider replacement, not only of the tow-fish, but perhaps of the electronics (upgrading to the new EK60 electronics) and the data acquisition method.

TUBA - *Andy Harris, Alex Mustard, James Riggs and Nick Crisp*

TUBA, the Towed Undulating Bio-Acoustic Instrument, was a compact multi channel high frequency SONAR designed for the study of oceanic zooplankton abundance. The system was designed for use on towed instrument platforms such as Seasoar, and was also suitable for use on small net systems. The system used on the FISHES cruise was a second generation but still development system.

TUBA consisted of seven high frequency echosounders, working at 175, 250, 370, 640, 920, 1666 and 2200 kHz. The returns from these channels were heterodyned down to lower frequencies, which were mixed together and digitised within a Desktop Computer at the shipboard end of the cable. The data was collected and displayed on a custom built software package.

Calibration

Prior to the cruise, an attempt was made to calibrate TUBA making use of the acoustic test tank facilities at SOC. The calibration process involved the recording of data returned from standard spheres of known target strength at each frequency, and at various distances from the transducer head. It was possible to see a 250 kHz calibrated sphere on all 7 channels at a distance of 2 metres from the transducer head.

Deployment

The intention was to deploy TUBA on SeaSoar in conjunction with the new PENGUIN underwater data handling system; making use of PENGUIN's on-board high speed Analogue-to-Digital convertor card.

Due to difficulties in obtaining a software driver for this card it was necessary to make alternative arrangements for deployment of the instrument. TUBA was deployed initially on the net frame, together with the FRRF, at stations 14109 through to 14117. At station 14117 a calibration deployment was also made; i.e. a 250 kHz sphere of known target strength was suspended within the field of view of TUBA.

For these deployments, electrical connections were made to the instrument via 250 metres of 5 core cable. This was payed out and recovered by hand as the net frame was lowered and retrieved. The net/FRRF casts were made to a depth of 125 metres and returned an abundance of *Calanus Finmarchicus*, mostly 2-3mm in length and probably accounting for the majority of targets visible to TUBA.

The time domain display on the TUBA software allowed the user to discern targets within the received signal as they were detected, and during the net cast deployments it was possible to make out a number of targets, however these were generally fairly weak. Background noise was high and some post processing of the data would be necessary to further distinguish the targets from this noise floor.

A serious problem was noted with the 640 kHz channel;. no response whatsoever was detectable on this frequency. As all channels had appeared to be working on the bench with the dummy load, it was suspected that the failure of this channel was due to a problem with the transducer rather than with the electronics, but this also will require further investigation.

The second series of TUBA deployments were made on the Longhurst-Hardy Plankton Recorder (LHPR) frame, in conjunction the OPC and PENGUIN. In order to facilitate these deployments, modification was made to the PENGUIN DAPS software to act as a dumb data recorder for the OPC, and a SeaSoar style cable bridle was built for the LHPR frame in order that the LHPR could be deployed on the SeaSoar cable. This was the only suitable towing cable having a sufficient number of conducting cores to allow real time communication with TUBA.

The first LHPR deployment of TUBA presented an unexpected problem. Whereas all of the channels bar the 640 KHz had been functioning correctly during the net casts, response on the upper 5 channels during the LHPR deployment appeared seriously impaired. This was found to be caused by the increased capacitance of the SeaSoar cable, which was attenuating the higher frequencies. Despite this problem, it was possible to make out a few weak targets within the returned signal. The LHPR recorded an abundance of *Calanus* during this deployment, as well as a number of *Meganyctiphanes Norvegica*, which should have been clearly visible to a well tuned TUBA.

The cable attenuation problem was overcome after recovery of the instrument by the construction of an active filter within TUBA having reverse frequency characteristics to those in

the cable. With this filter in place, the instrument was once more set up to give similar returns from a given injected signal at each frequency. The channel gains were increased slightly in the hope that an increase in Signal to Noise ratio could be obtained. The 640 kHz channel remained dead.

The second LHPR deployment of TUBA gave better results than the first. The towing speed was lower than during the previous attempt. Due to the increased signal gains within the system, the background noise visible at the surface was significantly greater than on the first LHPR tow, and the headroom between the noise level and the clipping level was insufficient for targets to be discernible. It was realised that the low gain of the instrument had been overcompensated for, the gain this time being too high. This being the last planned TUBA deployment, the signal was reduced in amplitude by the addition of a capacitor across the shipboard end of the sea cable during deployment. This attenuated the signal sufficiently for targets to show above the noise without clipping, although clipping still took place on particularly strong targets.

Notes for Future Deployments

The previous deployments of TUBA were made in Antarctic waters, from the James Clark Ross in January of the same year (2001). *Meganyctiphanes* Krill were very abundant in the area, and these presented strong targets to the instrument.

TUBA was mounted on a large towed net, with the transducer head mounted in the centre of the aperture facing forward. It was noted at the time that targets could be seen to enter the field of view of the instrument and increase in amplitude as they approached the transducer head, remaining within the field of view for the duration of a number of TUBA pings.

On the D253 (FISHES) LHPR deployments of TUBA the head was mounted sideways, the transducers oriented perpendicular to the direction of travel. Thus any targets seen by TUBA would remain within the field of view for only a very short period of time.

The LHPR was towed at around 4 ms^{-1}, thus, given that sound travels at around 1500 ms^{-1}, by the time the reflection from a target insonified 4 metres from the head was returned, the head would have moved a distance of around 11 mm in the direction of towing.

Biology at the TUBA Net Deployment Stations

Zooplankton size spectra were produced from microscope measurements for Stations 14113, 14114, 14116 and 14117 to aid the preliminary interpretation of TUBA data. The copepod *Calanus finmarchicus* dominated the community at 14113, 14114 and 14116, accounting for more than 90% of the zooplankton captured by the net. At stations 14113 and 14114 the

copepodite stage CIV (length = 1.8-2.0 mm) was most abundant. The size spectra at station 14116 was more evenly distributed, with greater numbers of CIIIs (length = 1.3-1.6 mm), CIVs, CVs and CVIs (length = 2.2-2.7 mm). The catch at station 14117 was dominated by two species of copepod: *Metridia lucens* accounted for 60% and *Calanus finmarchicus* for 35% of the total. These species were of a similar size and at this station the spectra was dominated by CVs and CVI females of both species (length = 2.0-3.0 mm).

FRRF (Fast Repetition Rate Fluorometer) Data - *Mark Moore*

Introduction

The Fast Repetition Rate Fluorometer (FRRF) is an active fluorescence instrument which can be used to make rapid, non-destructive and *in situ* measurements of phytoplankton physiology (Kolber *et al.* 1998). Such data can then be used in bio-physical models to estimate the rate of phytoplankton photosynthesis at scales comparable to those of physical variability within the environment (Kolber and Falkowski, 1993).

Deployment Strategy

FRRF Instruments (Chelsea Instruments, CI, FASTtraka) were deployed in three modes of operation during D253.

1. Underway Sampling

One instrument was kept permanently attached to the ships non-toxic supply in order to provide a continuous record of changes in near surface phytoplankton physiology and provide a comparison and means of data quality verification with the other instruments deployed *in situ*. Power was provided to the instrument using a standard Chelsea Instruments deck box. Data from this instrument was recorded internally and downloaded every 24-48 hrs to a PC. A total of 34 files were collected (see table below). Problems encountered included the failure of one of the deck boxes due to a blown fuse, and fouling of the optical chamber. The latter problem resulted in the frequency of optical chamber cleaning being increased from once every 4-5 days at the beginning of the cruise, to every other day towards the end.

File	Date	Gain	File	Date	Gain
T1_0505	05/05/01	4	T18_2405	24/05/01	1
T2_0605	06/05/01	1	T19_2505	25/05/01	1
T3_0705	07/05/01	1	T20_2605	26/05/01	1

T4_0805	08/05/01	1	T21_2705	27/05/01	1
T5_0905	09/05/01	1	T22_2805	28/05/01	1
T6_1005	10/05/01	1	T23_2905	29/05/01	1
T7_1105	11/05/01	1	T24_0206	02/06/01	1
T8_1205	12/05/01	1	T25_0306	03/06/01	1
T9_1305	13/05/01	1	T26_0406	04/06/01	1
T10_1405	14/05/01	1	T27_0706	07/06/01	1
T11_1505	15/05/01	1	T28_0806	08/06/01	1
T12_1705	17/05/01	1	T29_0906	09/06/01	1
T13_1905	19/05/01	1	T30_1106	11/06/01	1
T14_2005	20/05/01	1	T31_1206	12/06/01	1
T15_2105	21/05/01	1	T32_1406	14/06/01	1
T16_2205	22/05/01	1	T33_1506	15/06/01	1
T17_2305	23/05/01	1	T34_1606	16/06/01	1

2. In Situ Vertical Profiling

A second instrument was used to collect *in situ* vertical profiles of phytoplankton physiological variability, the intention being for one profile to be collected at every CTD station. Unfortunately due to the need for full depth CTD profiles and a relatively low pressure rating (500 m) for the instrument casing, deployment on the CTD frame was not possible. The instrument was therefore deployed in a stand alone pre-fabricated frame combined with the zooplankton net haul frame (Figure 18).

Initially these deployments were achieved using the starboard stern crane and a small on-deck winch. Such a deployment strategy proved to be problematic, especially in rougher sea states. The decision was therefore made to move FRRF/Net deployment to the main CTD gantry using another faster winch and a length of hydrowire. Such a deployment method proved to be much more satisfactory and a total of 125 vertical profiles to a depth of 100–130 m were collected over the first and second legs of the cruise (see table below).

Figure 18. FRRF instrument deployment.

Power was provided using the CI battery packs. The instrument was interfaced with a CI pressure sensor and PAR sensor for all deployments. Data was again recorded internally and downloaded once a day on to a PC, typically following the post dawn deployment. This timing was chosen as the PAR data from the first deployment of the day required processing rapidly in order to calculate an attenuation coefficient and the % light depths for the daily primary production station.

Station	Date	Name	Gain	Station	Date	Name	Gain
13966	07/05/01	B	1	14051	22/05/01	BJ4	1
13967	07/05/01	BC1	1	14052	22/05/01	BJ5	1
13968	07/05/01	BC2	1	14053	23/05/01	BJ6	1
13969	07/05/01	BC3	1	14054	23/05/01	J	1

13970	08/05/01	BC4	1	14055	23/05/01	JH1	1
13971	08/05/01	BC5	1	14056	23/05/01	JH2	1
13972	08/05/01	BC6	1	14057	23/05/01	JH3	1
13973	08/05/01	BC7	1	14058	23/05/01	JH4	1
13974	08/05/01	BC8	1	14059	24/05/01	JH5	1
13976	09/05/01	BC10	1	14060	24/05/01	JH6	1
13981	10/05/01	IB16	1	14061	24/05/01	H	1
13982	10/05/01	IB17	1	14062	24/05/01	HR1	1
13983	11/05/01	IB19	1	14063	24/05/01	HR2	1
13984	11/05/01	IB20	1	14064	24/05/01	HR3	1
13985	11/05/01	D	1	14065	25/05/01	HR4	1
13987	11/05/01	DE2	1	14066	25/05/01	HR5	1
13988	11/05/01	DE3	1	14067	25/05/01	R	1
13989	12/05/01	DE4	1	14068	25/05/01	RS1	1
13990	12/05/01	DE5	1	14069	25/05/01	S	1
13991	12/05/01	E	1	14070	26/05/01	SG1	1
13992	12/05/01	EC1	1	14071	26/05/01	SG2	1
13993	12/05/01	EC2	1	14072	26/05/01	SG3	1
13995	13/05/01	EC3b	1	14073	26/05/01	SG4	1
13996	13/05/01	EC4	1	14074	26/05/01	SG5	1
13997	13/05/01	EC5	1	14075	26/05/01	SG6	1
13998	13/05/01	EC6	1	14076	26/05/01	G	1
13999	13/05/01	C	1	14077	27/05/01	CG8	1
14000	14/05/01	CG1	1	14078	27/05/01	CG7	1
14001	14/05/01	CG2	1	14079	27/05/01	CG6	1
14002	14/05/01	CG3	1	14082	28/05/01	MH2	1
14003	14/05/01	CG4	1	14083	28/05/01	MH3	1
14004	14/05/01	CG5	1	14084	28/05/01	MH4	1
14005	15/05/01	CG6	1	14085	28/05/01	MH5	1

14006	15/05/01	FL1	1	14086	28/05/01	MH6	1
14007	15/05/01	FL2	1	14087	29/05/01	MH7	1
14008	15/05/01	FL3	1	14088	29/05/01	H	1
14009	16/05/01	L	1	14089	29/05/01	HP1	1
14010	16/05/01	L1	1	14090	29/05/01	HP2	1
14011	16/05/01	F	1	14091	29/05/01	HP3	1
14012	16/05/01	FJ1	1	14092	29/05/01	HP4	1
14013	17/05/01	FJ2	1	14094	30/05/01	HP5	1
14014	17/05/01	FJ3	1	14096	30/05/01	HP6	1
14015	17/05/01	J	1	14097	30/05/01	HP7	1
14016	17/05/01	JK1	1	14098	30/05/01	P	1
14017	17/05/01	JK2	1	14099	04/06/01	SG2	1
14018	17/05/01	JK3	1	14100	04/06/01	SG1	1
14019	18/05/01	JK4	1	14102	04/06/01	F1P1	1
14020	18/05/01	JK5	1	14104	05/06/01	F1P2	1
14021	18/05/01	JK6	1	14108	10/06/01	F1hS	1
14022	18/05/01	K	1	14109	10/06/01		1
14023	18/05/01	K1	1	14110	10/06/01		1
14027	20/05/01	A.ADT	1	14111	10/06/01		1
14029	20/05/01	15G	1	14112	10/06/01		1
14031	20/05/01	ADS	1	14113	10/06/01		1
14033	20/05/01	ADO	1	14114	10/06/01		1
14035	20/05/01	ADM	1	14116	10/06/01		1
14038	21/05/01	ADJ	1	14117	10/06/01		1
14040	21/05/01	ADH	1	14118	11/06/01		1
14043	21/05/01	ADE	1	14123	14/06/01		1
14045	22/05/01	ADC	1	14127	15/06/01		1
14047	22/05/01	B	1				1
14048	22/05/01	BJ1	1				1

14049	22/05/01	BJ2	1		1
14050	22/05/01	BJ3	1		1

3. SeaSoar Deployment

A third FRRF instrument was flown on the SeaSoar undulating towed body during the second leg of the cruise. This instrument was powered by the PENGUIN underwater data handling unit also flown on SeaSoar. Data was recorded in real time via the RS422 ascii output option ('verbose mode') on the FRRF and using the PENGUIN/DAPS software system. The data acquisition system was found to be reliable and proved to be a highly efficient method for collecting multi-instrument data using the SeaSoar vehicle (Figure 19). The principal problem encountered during these deployments was damage to two of the FRRF instruments caused firstly by impact with the ships stern on SeaSoar recovery and secondly by impact with the seabed whilst SeaSoar was in flight.

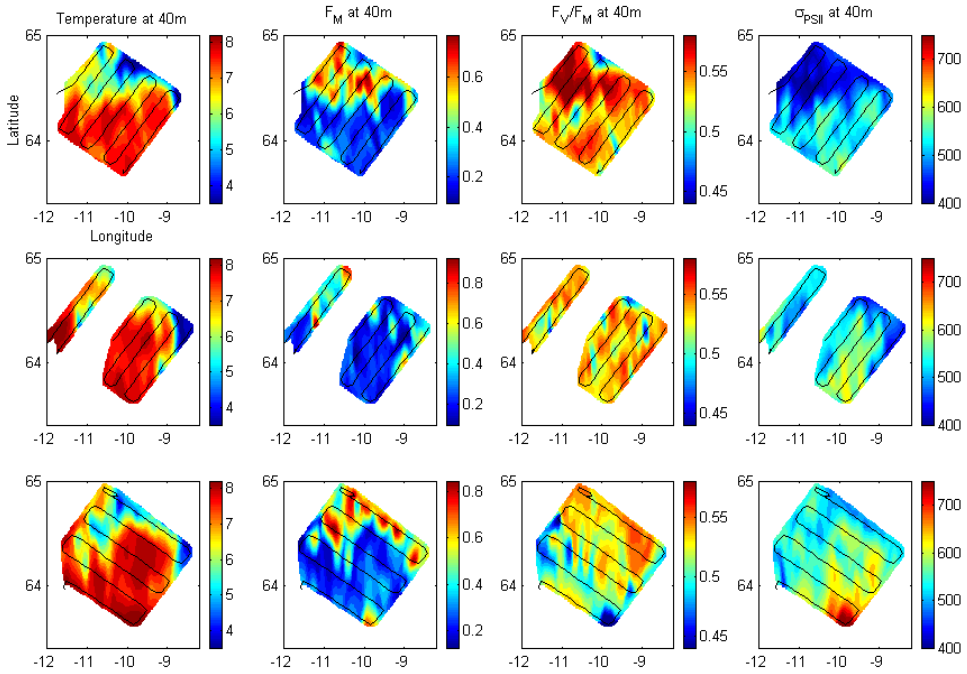

Figure 19. From left to right, temperature, fluorescence, F_v/F_M (photochemical efficiency) and σ_{PSII} (functional absorption cross section) at 40 m for all three SeaSoar surveys, top to bottom. Physiological variability associated with meso-scale physical variability is clearly apparent.

Data Handling and Analysis

All data were fitted to the biophysical model of Kolber *et al*. (1998). Data downloaded from internally recording instruments were typically analysed using the custom software provided by CI (FRS version 1.4). Results of this analysis were compared with values obtained using code written for FRRF data in MATLAB. Data collected from the instrument in the SeaSoar were analysed in sections corresponding to either 4 or 12 hours of deployment using code written in MATLAB. This data was then merged with depth from the CTD data collected using the CI MiniPAK on SeaSoar. Ascii files of CTD data were generated for the merging process which was again carried out within a MATLAB environment.

Measurements of New and Regenerated production, and of Chlorophyll-*a* concentration - *Mike Lucas, Vallia Avgoustidi and Tim O'Higgins*

Introduction

The primary aims of this study were to quantify new and regenerated primary production within the Iceland Basin and in the Iceland–Faroes frontal (IFF) region of the North East Atlantic. A central theme of the study was to provide some understanding of the biogeochemical and physical controls on the rates of primary production and how phytoplankon community structure changes in response to increasing nutrient depletion as the season advances. To accomplish these broad aims, the following specific goals were adopted -

1. measure the distribution of phytoplankton biomass and pigment composition

2. enumerate the dominant phytoplankton taxa

3. measure the rates of primary production

4. measure the size-fractionated rates of new (export) and regenerated production

5. establish the physiological parameters of photosynthesis with respect to light and nutrient (NO_3, NH_4, Si, PO_4) concentration using photosynthesis-irradiance (P. vs. E.) experiments and in situ Fast Repetition Rate Fluorometry (FRRF) approaches (discussed above)

Associated with these goals, a number of research activities conducted by other groups on board *Discovery* were particularly relevant. These were -

1. measurements of phytoplankton production using ^{14}C and ^{32}Si radio-tracer isotopes (*Louise Brown and Richard Sanders*)

2. measurements of nutrient (NO_3, NH_4, Si, PO_4) distribution (*Richard Sanders, David Hydes and Martin Johnson*)

3. measurements of ambient DOC concentrations and bacterial biomass and production (*Hugh Ducklow and Leigh McCallister*)

4. measurements of mesozooplankton abundance and grazing rates (*Xabier Irigioen and Dave Pond*)

5. measurements of upper ocean physics by CTD, and by SeaSoar deployments to which the FRRF was mounted (*Penny Holliday, Stuart Cunningham, Raymond Pollard, David Smeed and Mark Moore*)

The comprehensive, and in many cases, novel measurements listed above would afford us the opportunity to considerably advance our understanding of the mechanisms which control phytoplankton, export production and community succession associated with the spring bloom. Two of the most novel approaches were the simultaneous measurements of C, N, Si & P fixation or uptake which would provide valuable insight into the stoichiometry of phytoplankton growth. These measurements coupled with P vs E and FRRF measurements would be used not only to determine the physiological response of phytoplankton to light and nutrients, but would be used also to calibrate FRRF estimatimation of production which was still in its infancy.

The relative magnitude of new and regenerated production expressed as the f-ratio provided a measure of the potential export production for the region. The dual labelling approach also allowed an examination of the coupling between carbon fixation and nitrogen uptake (ρ) relative to that commonly predicted (6.6:1) from Redfield stoichiometry. In addition, ^{14}C and ^{15}N based P vs E parameters would provide information on the light dependency of carbon fixation and nitrogen uptake. From previous studies, we knew for example that the P vs E response to light for ρNO_3, ρNH_4 and $\rho urea$ was quite different. There was previous evidence that ρNO_3 had a greater light dependency than $\rho urea$ or ρNH_4, which had implications for the control of phytoplankton community succession between diatoms and phytoflagellates as the spring bloom gave way to nano- and picoplankton with increasing depth related light and NO_3 and Si limitation as surface waters became increasingly nutrient limited.

As phytoplankton community structure and succession was known to have a marked influence on the strength of the biological pump, this project addressed regional implications for atmospheric CO_2 draw-down, C & N cycling and climate change.

Study Area and Station Listing

Figure 3 and the following table shows the positions of the productivity stations and details of the measurements made are discussed below.

Date	Time GMT	Station No.	Latitude	Longitude	Max. depth
11 May	07:12	13984	63° 00.08' N	20° 00.60' W	1200 m
12 May	04:53	13989	62° 27.96' N	23° 49.28' W	1314 m
13 May	05:17	13995	61° 05.53' N	22° 39.72' W	1877 m
14 May	05:37	14000	60° 25.85' N	19° 03.22' W	2540 m
15 May	06:07	14005	61° 44.84' N	14° 55.21' W	2080 m
16 May	04:40	14010	63° 41.46' N	16° 44.80' W	297 m
17 May	06:40	14014	60° 51.30' N	13° 26.82' W	1642 m
18 May	05:30	14020	59° 09.19' N	08° 56.75' W	1570 m
21 May	06:14	14038	57° 27.10' N	11° 04.75' W	591 m
23 May	04:34	14053	60° 26.48' N	12° 36.56' W	303 m
24 May	06:01	14060	62° 22.22' N	08° 20.49' W	160 m
25 May	04:50	14066	64° 47.00' N	08° 29.00' W	2496 m
26 May	04:10	14071	64° 35.36' N	10° 41.53' W	416 m
27 May	05:46	14078	61° 58.72' N	14° 09.79' W	1622 m
29 May	06:00	14088	62° 42.83' N	08° 21.39' W	509 m
4 June	05:15	14099	64° 35.34' N	10° 40.11' W	429 m
5 June	05:30	14104	64° 50.03' N	10° 46.76' W	432 m
8 June	10:08	Underway water sample	64° 41.72' N	10° 14.76' W	Surface
10 June	04:03	14108	63° 40.91' N	10° 05.06' W	547 m
11 June	03:30	14118	64° 20.14' N	08° 23.27' W	1865 m
15 June	03:07	14127	64° 50.41' N	10° 19.35' W	499 m

Methods

CTD Station Sampling

Two basic types of CTD station were completed. On most mornings just after dawn, a "productivity" CTD profile to ~300m was completed and sampling bottles were closed at the depths of 97%, 45%, 18%, 8%, 3%, 1.3% and 0.1% of surface PAR (Photosynthetically Available Radiation) determined from prior deployment of the FRRF. Water drawn from bottles of the same light depth were pooled into darkened 25 litre carbuoys prior to sub-sampling for biological measurements - ie. chlorophyll-*a*, HPLC, preserved phytoplankton samples and samples for productivity measurements.

All other stations were CTD profiles to the bottom with bottles being closed at standard depths (5, 25, 50, 75, 100, 150, 200, 300m etc.). For each of the bottles within the top 300m, samples were taken for chlorophyll-*a* analyses.

Nutrient (and oxygen) samples covering the entire depth range were drawn directly from each of the rosette bottles for all CTD stations.

Underway Sampling

Surface chlorophyll-a, nutrient and and preserved phytoplankton samples were taken from the non-toxic sea water supply (originating from ~5 m depth) at 2 hour intervals throughout the cruise; interrupted only when at CTD stations. At some of the underway stations, HPLC and samples for productivity measurements were also collected.

Preserved phytoplanklton samples

At each of 3 depths in the water column at productivity stations (typically at 50%, 3% and 0.1% light depths) and at some surface underway stations, 2 x 100ml samples were preserved in 1% Lugol's Solution and 2% buffered Formalin respectively for later enumeration of phytoplankton taxa (including flagellates and ciliates) by inverted microscopy. From these counts and cell measurements, subsequent calculation of cell biovolume and carbon content would also be obtained. Note, that as Lugols is an acidic preservative, Coccolithophores would only be represented in the Formalin sample. Note too, that as it would not be possible to differentiate between heterotrophic and autotrophic ciliates and flagellates, total autotrophic cellular carbon may be overestimated (*Russell Davidson*, SOC)

Pigments: chlorophyll-a

For each CTD, production and underway station, chlorophyll-*a* samples were obtained by filtering 100 ml of sea water onto Whatman 25 mm GF/F filters to yield total chlorophyll after

24 hours extraction in 90% acetone in a dark freezer. For size-fractionated Chlorophyll-*a* determinations, a further 100ml sample was passed through a 20 µm mesh plankton screen and then filtered onto a GF/F filter to provide the < 20 µm fraction. A third 100ml sample was filtered through a 47mm, 2.0 µm Nuclepore filter; the filtrate then being passed through a 25 mm GF/F as before to retain the < 2 µm picoplankton fraction. Netplankton (> 20 µm) and nanoplankton, (< 20 µm but > 2 µm) chlorophyll values were obtained by difference. Pigments retained on the GF/F filters were read on a Turner Designs AU-10 scaling Fluorometer following the Welschmeyer (1994) protocol.

Pigments: HPLC

For each of the light depths sampled for productivity measurements, 500ml was filtered onto 25mm Whatman GF/F filters which were then frozen at -70 °C for later HPLC analyses at SOC.

Pigments: absorbance

For each of the light depths sampled for productivity measurements, 500ml was filtered onto 25mm Whatman GF/F filters which were then frozen at -70°C for later spectral absorbance measurements at SOC.

Nutrients

At each station, nitrate, nitrite, silicate and phosphate concentrations were routinely measured and are discussed later. Ammonium determinations on fresh samples were based on the fluorometric method of Holmes et al. (1999). Samples (2 x 20ml) for urea determinations were taken and frozen for later analyses at SOC using the diacetylmonoxime/sulphuric acid digestion method of Mulvenna and Savidge (1992) and modified by Goeyens et al., (1998).

Underwater irradiance and PAR

The underwater light field and percent light depths for sampling were measured and calculated (as a ratio) from the 2π light sensor deployed with the Chelsea Instruments FRRF and the shipmounted 2π PAR sensor connected to the SURFMET system.

Productivity Measurements

Rate measurements were based on 3 types of incubation experiment:-\

1. Dual labelled simulated in situ (on-deck) incubation experiments using ^{15}N and ^{13}C stable isotopes for each of the 7 light depths.

2. Simulated in situ (on-deck) ^{14}C radio-isotope tracer incubation experiments for each of the 7 light depths.

3. Photosynthesis-irradiance experiments using the chlorophyll-*a* maximum depth sample (P vs. E curves) and using ^{14}C & ^{15}N-NO_3, ^{15}N-NH_4 radio- and stable isotopes.

I. Stable isotope ^{15}N & ^{13}C incubations

15-N ($N0_3$, NH_4, urea) uptake and 13C fixation rates

For each of the production station light depths, 2.0 litre incubation volumes, in polycarbonate bottles, were supplemented with 100 µl of 1.0 µmol / 0.1 ml $K^{15}NO_3$ (98 atom%) to give a final concentration of 0.5 µmol l^{-1}; 200 µl of 0.05 µmol / 0.1 ml $CO(^{15}NH_2)^2$ (99.1 atom%) to give a final urea concentration of 0.05 µmol l^{-1} and for NH_4-N uptake experiments, two 2.0 litre volumes were spiked with 100 µl of 0.1 µmol / 0.1 ml $15NH_4Cl$ (98 atom%) to provide a final concentration of 0.05 µmol l^{-1}. To each of the nitrate incubation bottles (2.0 litres), 0.2 mmol / 0.4 ml $Na^{13}HCO_3$ was added to yield a final ^{13}C concentration of 0.1 mmol l^{-1}; ie. about 5% of ambient TCO_2 assumed to be 2 mmol. Spike concentrations of ^{15}N were adjusted so that they were maintained at approximately 10% of the ambient nutrient concentration.

The nitrate, ammonium and urea incubation bottles were placed in the simulated in situ on-deck (perspex) incubator tubes covered with neutral density screens to provide the appropriate shading. The bottles were cooled by surface sea water pumped through the tubes. The second 2.0 litre $^{15}NH_4$ bottle was immediately filtered onto a 47 mm GF/F filter which was retained and frozen for later particulate N analysis. The filtrate (900ml) was retained in a 1.0 litre glass Schott bottle to which 1.0 ml NH_4Cl (10 µmol / ml) carrier was added before freezing the sample at -30 °C for later isotopic dilution analysis at time zero (R_0). Uptake experiments were terminated after ~8 hours by filtration onto pre-ashed (450 °C for 6 hours) Whatman 47 mm GF/F filters which were retained and frozen at -20 °C for later analysis of particulate N and ^{15}N (and ^{13}C) content with a Europa Scientific 20/20 Mass Spectrometer. Prior to freezing, the dual labelled (^{15}N,^{13}C) filters were subject to 10% HCl to drive off unincorporated ^{13}C as $^{13}CO_2$. At the end of the NH_4 uptake experiment, (R_t), 900ml filtrate and carrier was retained and frozen as before for isotopic dilution measurements of NH_4 regeneration.

Nitrate and urea uptake rates were calculated according to Dugdale and Goering (1967):

$$\rho NO_3 \text{ or } \rho \text{urea} = (PE \times PN)/(R_0 \times T) \qquad (34)$$

where PE is the % ^{15}N enrichment of the PON fraction in excess of the natural abundance; PN is the particulate N concentration (mmol.l^{-1}); T is the experimental duration (hours) and R_0 is the calculated aqueous ^{15}N enrichment at time zero.

Ammonium uptake rates were similarly calculated but corrected for isotopic dilution due to ^{14}N excretion (Glibert et al. 1982):

$$\rho\mathrm{NH}_4 = (\mathrm{PE} \times \mathrm{PN})/(\mathrm{R} \times T) \tag{35}$$

where R is the exponential average enrichment,

$$R = R_0 \big/ kt\left(1 - e^{-kt}\right) \tag{36}$$

and

$$k = \frac{-\ln\left(R_t / R_0\right)}{T} \tag{37}$$

where R_0 and R_t are the measured aqueous ^{15}N enrichments at the beginning and end of an experiment.

A relative preference index (RPI) was calculated for each nutrient assimilated (McCarthy et al. 1977). For example for ammonium,

$$RPI = \frac{\rho NH_4}{\rho \Sigma N} \Big/ \frac{\left[NH_4\right]}{\left[\Sigma N\right]} \tag{38}$$

where ρNH_4 and $\rho \Sigma N$ are the uptake rates for ammonium and the sum of the rates for the three nitrogen species and where $\left[NH_4\right]$ and $\left[\Sigma N\right]$ are their ambient nutrient concentrations.

Ammonium regeneration

Aqueous ammonium in the 900 ml R_0 and R_t samples (frozen) was recovered by diffusion from the thawed samples back at the laboratory in SOC. Sufficent MgO was added to to the bottles to increase the pH to > 9.0. A 25 mm GF/F filter moistened with 50 µl 6N H_2SO_4 was suspended above the aqueous sample and the bottle re-capped. After standing for approximately 2 weeks at room temperature, > 50% of the aqueous NH_4 was recovered on the filter as NH_4SO_4. The filters were then shaken in 5 ml Milli-Q water and a sample was removed for colorimetric ammonium concentration determination.

Ammonium regeneration rates (rNH_4) were calculated from the model:

$$r = \frac{\ln(R_t/R_0)}{\ln(S_t/S_0)} \cdot \frac{(S_0 - S_t)}{T} \quad (39)$$

where R_0 and R_t are aqueous ammonium concentrations at the start and end of the experiment. Where ammonium concentrations over the experimental time remain unchanged (< 0.02 µmol l^{-1} differential) at < 1 µmol NH_4^+ l^{-1}, r is calculated from:

$$= \frac{\ln (Ro / Rt) So}{T} \quad (40)$$

Size-fractionated 13C fixation and 15N uptake

Size-fractionated uptake experiments were carried out on surface (50% underwater irradiance) communities at most of the CTD production stations. For each nutrient, three 6.0 litre samples were innoculated with ^{15}N label (NO_3, NH_4 and urea) to yield the same final ^{15}N enrichment as before. To measure carbon fixation, ^{13}C label was also added to the NO_3 incubation sample as before. Two litres (NH_4 incubation) were also spiked for aqueous NH_4 determinations and isotopic dilution measurements at time zero (R_0) as described earlier and immediately filtered onto a Whatman GF/F filter. Experiments were incubated on-deck as before. At the end of the incubation period the spiked samples for each nutrient (NO_3 + ^{13}C, NH_4, urea) were split into an intact unfiltered community (2.0 litre), a < 20 µm fraction (2.0 litre passed through a 20 µm mesh) and a < 2µm fraction (2.0 litre passed through a 2.0 µm Nuclepore filter). Each separate fraction was then filtered onto 47 mm GF/F filters and the particulate ^{15}N (and ^{13}C) enrichment determined as previously. For the NH_4 incubation experiment, 900 ml was collected from the filtrate for aqueous NH_4 measurements (R_t) as outlined before.

II. Radio-isotope ^{14}C incubations

Simulated in situ (on-deck) incubations to measure primary productivity were carried out on both legs of the FISHES cruise. On the 1st leg these were conducted by *Louise Brown* (Queens University, Belfast) and on the 2nd leg by *Mike Lucas* (SOC).

The protocols used for both legs of the cruise were the same. In summary, for each productivity CTD cast, ^{14}C productivity experiments were conducted at each of the 7 light depths in a similar maner to the stable-isotope incubations. For each depths three 80 ml polycarbonate "light bottles" and one "dark bottle" were filled with seawater and innoculated with 10 µCi / 100 µl buffered $NaH^{14}CO_3$ working stock. The "spiked" bottles were placed in the on-deck incubators for approx. 4-6 hours before the contents were filtered onto 25 mm (0.2 µm) polycarbonate Nuclepore filters to retain the phytoplankton. The filters were then fumed over 10% HCl for 20

minutes to remove unfixed inorganic ^{14}C prior to being placed in 7 ml plastic pony vials to which 5 ml Packard "Hisafe 3" scintillation cocktail had been added. Samples were counted (DPM) on a Wallac 1414 WinSpectral DSA-based liquid scintillation counter.

The precise activity of the ^{14}C spikes was determined from standards. Exactly 100 µl of the working stock was added to 10 ml Carbasorb and from this, 5 replicates of 100 µl were placed in 7 ml pony vials to which 5 ml Packard "Supermix" scintillation cocktail was added and the samples were counted on the scintillation counter together with the experimental samples.

III. Photosynthesis Iradiance Experiments (P. vs. E.)

During the second leg of the cruise only, 10 P. vs. E. incubation experiments were completed to measure the physiological response of carbon fixation (^{14}C) and nitrogen uptake ($^{15}NO_3$ and $^{15}NH_4$) to light. Each experiment consisted of 3 light boxes containing twenty 80 ml polycarbonate incubation bottles subjected to an irradiance range of approximately 1500-1.5 µE $m^{-2}s^{-1}$ for approx. 4 hours and cooled with running seawater drawn from the non-toxic seawater supply. The light gradient was obtained by using neutral density blue filters. Incubation samples were typically obtained from a single depth for each experiment corresponding to the sub-surface chlorophyll maximum; usually from the 50% light depth.

Silicate Assimilation - *Louise Brown, Graham Savidge, Richard Sanders*

The primary production and subsequent sinking of diatoms from the surface ocean is a key factor in controlling the marine silica cycle and in the carbon flux to the deep ocean, particularly in conditions associated with the end of the North East Atlantic spring bloom. Estimates of Si and C uptake by diatoms and the associated export fluxes are vital for development of marine biogeochemical models, but data on diatom production are limited for the North East Atlantic region. Conventional techniques for assessing Si uptake require the addition of ^{30}Si tracer in concentrations which are high compared to the ambient silica concentrations in North Atlantic waters, potentially resulting in increased rates of diatom production in tracer studies relative to natural conditions. However, Brzezinski and Phillips (1998) demonstrated that this problem could be overcome by using a high specific activity solution of the radiotracer, ^{32}Si, enabling rapid, high precision analysis whilst increasing ambient dissolved silica concentrations by only 3 nM.

The aim of this study was to determine rates of Si uptake and diatom production in the North East Atlantic region during and after the spring bloom, using the method of Brzezinski and Phillips (1998) modified for shipboard analysis. Si production rate profiles were obtained by collecting triplicate 280 ml water samples from a range of water depths representing 97%, 45%, 17.6%, 8.0%, 2.9%, 1.3% and 0.1% of surface light intensity, adding 0.03 µCi ^{32}Si and

incubating for six hours in on-deck incubators under simulated in situ light conditions. Dark and formalin-poisoned control bottles were also spiked and incubated for each depth. Incubations were terminated by filtration onto 0.8 µm polycarbonate filters, which were placed in 20 ml glass scintillation vials. The biogenic Si was digested from the filters with 2.5 ml 0.2 µM NaOH at 85 °C for two hours, and 10 ml of 'HiSafe 3' scintillation cocktail were added to the vial. The activity of ^{32}Si, and its daughter product, ^{32}P, was determined using liquid scintillation spectrometry. It was anticipated that phosphate uptake rates might also be determined from the ^{32}P activity. The relationship between substrate concentration and diatom production was examined by sub sampling a bulk sample from the 45% light depth and adding sufficient volumes of a 1.5 µM $NaSiO_3$ solution to increase the Si concentration in the samples by up to 20 µM, followed by tracer addition, incubation and analysis as outlined above. Stations were selected to obtain data from sites with a range of dissolved silica concentrations and anticipated primary production rates. ^{32}Si production rate profiles were measured from stations 13971, 13984, 13995, 14000, 14005, 14010, 14029, 14060, 14071, 14078, and ^{32}Si substrate concentration-uptake kinetics from 13989, 14053, 14065, 14088. In addition to the ^{32}Si uptake studies, ^{14}C production rate profiles were obtained at each of the stations listed above using the method outlined in Strickland and Parsons (1977) and incubating under the same conditions as the ^{32}Si experiments. Particulate material from each sample was also collected by filtering 250-500 ml of seawater for analysis of biogenic silica, organic carbon and phosphorus concentrations.

Nutrient Data; Nitrate, Nitrite, Silicate, Phosphate - *Richard Sanders and David Hydes*

Report on Leg 1

Samples were drawn from all depths at all stations, with the exception of stations 14024, 14025 and 14026, directly into virgin polystyrene coulter counter vials. Samples were then stored in a fridge before analysis, which was generally commenced within 12 hours. The concentrations of nitrate + nitrite, phosphate and silicate were then determined using conventional colorimetric methods using a Skalar San Plus autoanalyser with a 8503 digital interface.

This instrument was new to the SOC Nutrients Group and it took sometime to become accustomed to its idiosyncrasies. Generally the performance of the instrument improved over the course of the cruise. The photometers and heating bath were never switched off over the course of the cruise. The pump decks were lifted and the lines de-tensioned after each run and following a period of pumping Milli-Q water through the lines. The phosphate line was periodically cleaned using a 1 M aqueous solution of sodium hydroxide whenever the peak shape deteriorated to an unacceptable extent. A single cadmium column was used throughout

the cruise and the pump tubes were all changed at the beginning of the cruise and during the brief break in Stornoway for the boat transfer.

Data was acquired from the instrument using a Dell laptop computer running version 1.04 of the FlowAccess software supplied by Skalar. The ability of this software to correctly assign peak markers was poor, approximately 10% of stations required significant manual editing to produce acceptable results. Raw data files were checked on the same machine and ASCII files for each station created and exported to the ships data system via a zip drive. This part of the process did not work well. The laptop used to acquire the data could not be simultaneously used to work up previous data as this caused failure of the logging process. When loaded on two further PCs the software was unable to recognise the raw data files. This lead to a serious data backlog which was only recovered at the end of the first leg of the cruise.

Due to these delays the data was only loaded into the PSTAR system at the start of the second leg. There was not time by the end of the second leg to assess the quality of the data for the determination of water mass properties.

The run-to-run reproducibility of the Skalar system can be assessed from the value of the calibration coefficients calculated each time the analyser was run to make measurements. This data is plotted in Figure 20. The variation recorded during the first leg (summarised in the following table) was greater than during the second leg. In part this was because changes were made to the operating set up of the system at various times during the course of Leg 1. In the following table the data are grouped into three sequential groups this indicates that there was a reduction in the variability of the calibrations during the course of the first leg.

All runs	Nitrate	Phosphate	Silicate
count	43	43	44
mean	143.0	607.9	155.9
max	312.2	775.4	199.2
min	67.6	532.6	67.3
%stdev	33.9	8.0	15.3
Runs 1-15			
count	14	14	15
mean	170.8	586.5	141.5
max	312.2	620.4	181.8
min	67.6	559.6	67.3

%stdev	42.7	3.3	21.7
Runs 16-30			
count	15.0	15.0	15.0
mean	118.5	597.6	162.0
max	152.8	668.1	199.2
min	68.1	540.6	127.5
%stdev	19.8	7.1	11.7
Runs 17-44			
count	14.0	14.0	14.0
mean	141.4	640.3	164.8
max	165.9	775.4	176.6
min	115.9	532.6	140.9
%stdev	8.5	9.3	6.3

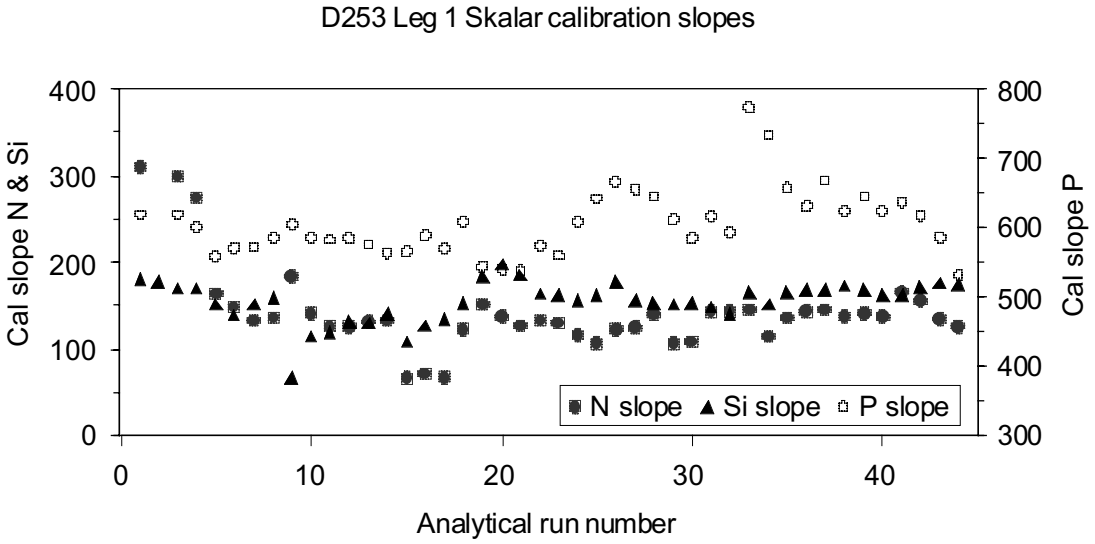

Figure 20. Plot of the calibration coefficients calculated for each of the measurement runs performed on the Skalar analyser during Leg 1 of cruise D253.

Report on Leg 2

Preparatory work prior to start of sample measurements

The work on Leg 1 was compromised in part by the poor performance of the auto-analyser. Prior to the start of running samples on Leg 2 a number of modifications were made to the configuration of the analyser to improve the performance of the instrument. These were:-

1. An error was found in the recipe for the acidified molybdate solution used on Leg 1. The amount of diluted sulphuric acid (280 ml concentrated acid in 1 litre of dilute solution) used to make up 2 litres of the reagent was reduced from 800 ml to 500 ml. Although the formation of the phospho-molybdate complex is pH dependent, the method can produce apparently good results over wide range acid concentrations. However a near doubling of the acid concentration would put the method in a region where possible variations in the flow rates of the peristaltic tubing on the pump could have created a reaction mixture in which the complex would not form.

2. A related problem was found on the silicate manifold. To correct this the tubes carrying the sample and the acidified molybdate solution were switched round. The sample was now added to the molybdate stream rather than the other way round. This is because two possible silico-molybdate complexes can be formed in acid solution (α and β). The α complex has a higher absorption coefficient. This complex is formed at lower pHs. To maintain a low pH in the reaction step the seawater sample was added to the acid reagent, the acid then was in excess throughout the mixing step.

3. The tubing to the de-bubbler shared by the silicate and phosphate sample lines was rearranged so that only the phosphate line was de-bubbled. This deceased the amount of un-segmented mixing in the silicate manifold and greatly improved the peak definition on the silicate channel. As the sample needle moved between the wash position and the sample an air bubble was drawn into the needle. This bubble was split in the stream splitter, on the nitrate manifold it was removed by the de-bubbler before the Cu/Cd column. On the silicate and phosphate manifolds it had the potential to go all the way through the system and if it was large, the de-bubbler on the analytical cell would not remove it. If it passed though the cell it blocked the light beam and produced a large spurious peak. The phosphate channel sampled at a flow rate of 0.8 ml/min while the silicate sampled at 0.4 ml/min, therefore, the bulk of the bubble would be pulled down the phosphate channel. The de-bubbler at the new design of Skalar flow cell fitted in the colorimeters worked well enough to remove the extra bubbles in the silicate line. I suspect that the same would be true even for the larger phosphate line bubble. There was not time on the cruise to test this possibility.

4. To carry out the analytical runs a separate “Table-file” was created for each run. On Leg 1 a table with the same name was used repeatedly. One possible cause of the system crashing when trying to analyse data from a previous run while making new measurements could have been software conflict when both operations tried to access the same file name “Table-file”. No crashes occurred on Leg 2 when previous runs were processed during a new measurement run.

These changes enabled the wash time to be reduced from the 90 seconds used on Leg 1 to 45 seconds on Leg 2, a 90 second sample time was used on both legs (equivalent to a saving of about 1 hour on longer measurement runs). N.B. More tuning work needs to be done onshore to reduce this to 60 seconds sample, 30 seconds wash.

Problems encountered with the Skalar software on Leg 2 were:-

1. On noisy small peaks, particularly on the phosphate channel, peak allocations were sometimes made prematurely. This was understandable and in future it could possibly be eliminated by careful adjustment of some of the peak picking settings. However a number of times this coincided with the software allocating two peaks in the same time window. This indicated a significant fault with the underlying peak picking algorithm. This error could be corrected using the post run software. This was a time consuming process. If the error occurred early in an 80 cup run it could take 20 or more minutes to reallocate all the peaks.

2. The software did not do a full calculation of the data at the end of the run. Some times when the post run results file was inspected it appeared to have done so, other times it did not. The option 'results/view/recalculate/all channels' needed to be used. The number of columns of information displayed on accessing results was unstable, some times just the calculated results were displayed, other times the result plus measured and corrected peak heights were displayed. Using 'results/options/format results' to select these channels brought these columns back to the screen. The instruction manual suggested that the options selected would be saved and the information would be present that way in future – this was not so (Inst. Manual Chapter 4.3.4).

3. Once the peak height allocations had been checked and the data had been recalculated it was then exported so that it could be worked on in an Excel spreadsheet. This had to be done by exporting a text file 'results/view/export/ text file'. If the option to export an Excel file was used, the Excel file generated by Flow Access contained hidden columns of data. The consequence was that Excel crashed if an attempt was made to cut and paste data from the Flow Assess generated Excel file into another Excel spread sheet.

4. The instruction manual suggested it was possible in the post processing software to set up a dummy channel in which further calculations on the data could be carried out. This option was drawn in the appropriate window, but was "greyed out" and not usable. If it had been available peak overlap corrections could have been done automatically to improve the accuracy of the data (Inst. Manual Chapter 4.3.5).

5. The instruction manual also suggested it was possible to save examples of the plots of the "real time" data peaks to a file for transfer to other documents but this option was also not active (Inst. Manual Chapter 4.2.2). In practice it only seemed possible to save a low definition JPG file of the whole run. So details of peaks shape and baseline noise were lost. A separate run would need to be done to achieve a hard copy of useful details. Note: This was done for the last measurement run 010617c1, and the output is presented in the appendix of this report.

Observations of System Performance

System performance on Leg 2 was monitored by:-

1. Maintaining records of:- (i) the baseline at the start of each measurement run, (ii) the gradient of the calculated calibration equation (a linear fit forced through the origin), (iii) the R^2 value of the regression calculation used to derive the calibration equation, (iv) the average difference between duplicates on each measurement run.

2. Running all underway samples in duplicate and a minimum of three CTD bottle samples per station also in duplicate. All duplicate measurements were tabulated and the difference and absolute difference between duplicates was calculated. The difference was compared to the WOCE expected precision.

Calibration Records

Introduction

The extinction coefficient of the coloured dye formed in each of the nutrient reactions is a physical constant. When the analyses are performed manually it is possible to predict from this value the absorbance of a given concentration of nutrient before the analysis is carried out. When measurements are made using an auto-analyser this is not possible because the reactions are not taken to the end point of full colour development.

On an auto-analyser the amount of colour developed per unit concentration of nutrient on any measurement run would be expected to be constant for a given set-up of the chemistry of the system. This is not true in practice because – (i) the rate of the colour forming reactions will be

determined by the ambient temperature of the laboratory, the samples and the reagent solutions (ii) temperature will also effect the properties of the peristaltic pump tubes so that the volume pumped changes and the concentration of the reaction mixture will change as a result, (iii) the volumes of flow in the pump tubes will also change as the tubes ages (iv) the tolerance to which pump tubes are manufactured means that the volumes pumped are only reliable to within about 10%, (iv) the colorimeters are single channel instruments so the light output changes as the lamps and detectors warm up and age (v) the chemical reagents themselves can age – this may produce noise from particles of precipitates or a baseline shift where the solution becomes coloured as it ages (Note: the reagents are normally in sufficient excess that the colour development itself should only be effected where deterioration of one or more reagents is extreme), (vi) in the particular case of the determination of nitrate a significant variable can be the performance of the Cadmium column which is used to reduce nitrate to nitrite before carrying out the colour forming reaction. This is perhaps the least stable component of an auto-analyser system.

Results

The variations of the calibration coefficients of the three methods on the 35 measurement runs done during Leg 2 are summarised in the following table. The phosphate measurement channel performed very well on this cruise. The standard deviation of the calibration was 0.8 % relative to the mean value. This was within the 1% variation that could be expected when an auto-analyser system is running well. Variation of the silicate calibration was 2.3 %. From experience I would have expected the silicate calibration to show a smaller variation than the phosphate method. This experience is based on systems which have a heating bath on both channels. I suspect the good result for phosphate was because this channel had the heating bath and silicate did not. Due to the cold weather outside the ship on this cruise, temperatures in the *Discovery* deck lab were quite variable. The variation in the nitrate calibration calculated for all runs was large at 8.8%. When the variation was calculated for the station from run 9 onwards after the column had been repacked the variation fell to 3%.

Summary data for all CTD bottle samples measured during Discovery Cruise D253.

Leg 1

	Nitrate	Phosphate	Silicate	N:P
count	1601	1601	1563	1601
max	23.47	4.41	20.31	26.96
min	0.08	0.04	0.00	1.60

median	12.94	0.84	6.20	15.25
average	12.32	0.83	6.19	15.12

Leg 2

	Nitrate	Phosphate	Silicate	N:P
count	339	339	340	339
max	14.74	1.00	12.39	24.96
min	0.83	0.10	0.07	7.27
median	12.75	0.86	6.44	14.65
mean	11.05	0.76	5.86	14.74

N.B. Measurement runs should be done on shore in a controlled temperature laboratory to look at the influence of temperature on the colour yield on the different channels. Appropriate temperatures would be 10°, 20° and 30° C.

In Figure 21a, b, c and d, the % difference between the calibration factor for each run and the mean of all the values for all the runs is plotted against run number. The variation in the phosphate calibration appeared to be random (Figure 21a). As did the variation in nitrate once the performance was considered without the data from the first 8 runs (Figure 21b and c). The variation in silicate showed a jump that was consistent with the re-tubing of the pump before run 22.

Figure 21. (Over the page) Shows the record of the variation in the slope of the calculated calibration factor for each measurement run, presented as the percentage difference of the individual slope to the mean of all the calibration factors for that analysis:- (a) Phosphate, (b) Nitrate - all data, (c) Nitrate omitting first 8 stations, (d) Silicate.

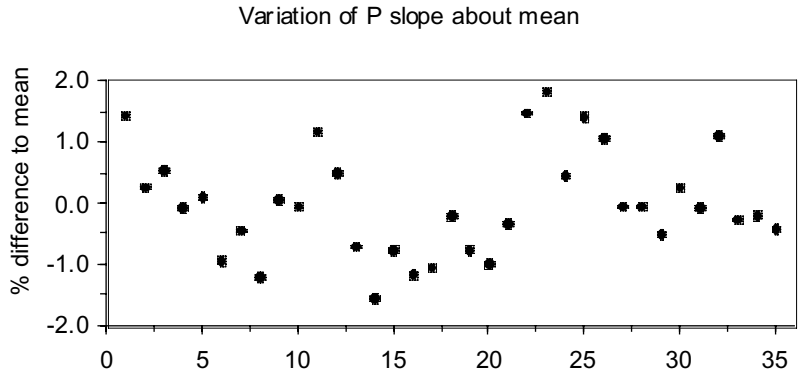
Variation of P slope about mean
% difference to mean
2.0
1.0
0.0
-1.0
-2.0
0
5
10
15
20
25
30
35

(a)

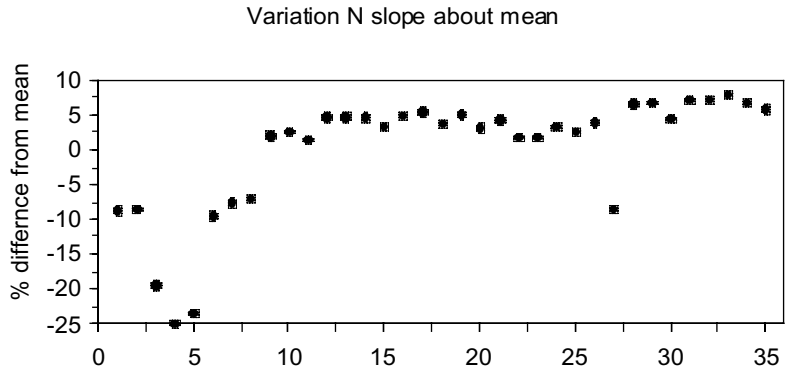
Variation N slope about mean
% differnce from mean
10
5
0
-5
-10
-15
-20
-25
0
5
10
15
20
25
30
35

(b)

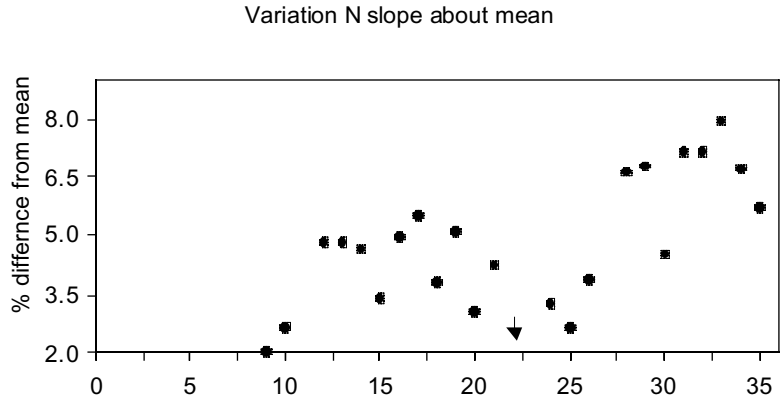
Variation N slope about mean
% differnce from mean
8.0
6.5
5.0
3.5
2.0
0
5
10
15
20
25
30
35

(c)

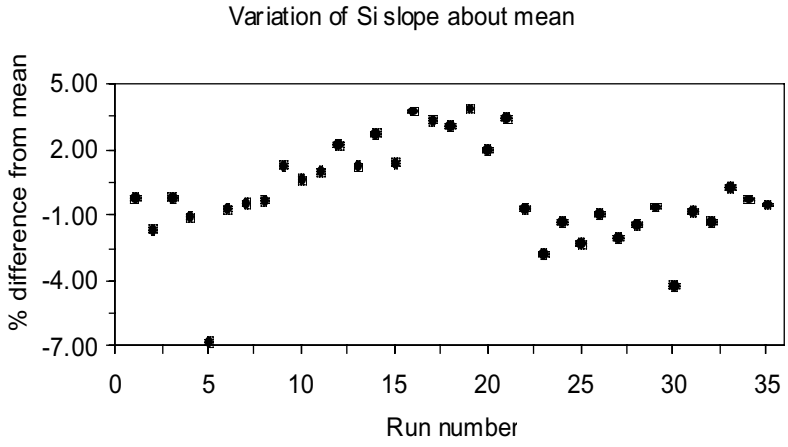
Variation of Si slope about mean
% difference from mean
5.00
2.00
-1.00
-4.00
-7.00
0
5
10
15
20
25
30
35
Run number

(d)

In Figure 22, the changes in the baseline heights for the three channels are plotted. Movement of the value of baseline of the nitrate channel was small. There was a clear drop in the phosphate baseline at runs 21 and 22. This might be explained both by the fact that the reagent bottles were topped up before run 21 and the machine was re-tubed before run 22. There was significant upward trend in the silicate baseline. This may have been due to deterioration of the acidified molybdate reagent.

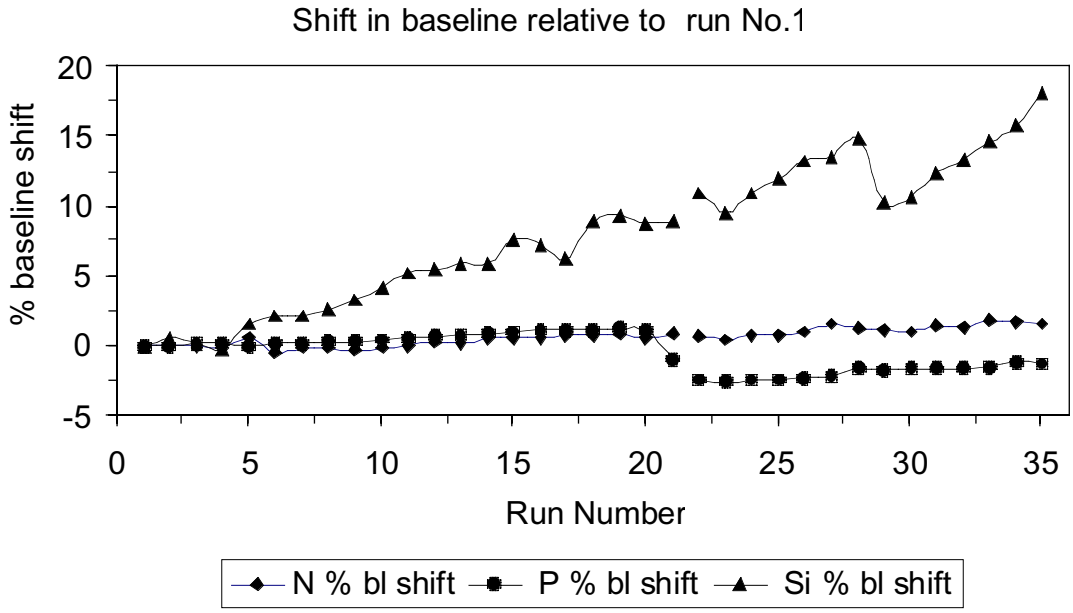

Figure 22. Graph showing consistency of the measurement of the sodium chloride (40g/l) wash at the start of each measurement run. The value plotted is the % difference between the value for the run and the value recorded for the first run of samples.

N.B. Measurements on shore should continue these observations to see what changes occur when the analyser is repositioned and supplied with fresh reagent solutions, and then look at changes with ageing solutions.

Estimates of analytical precision based on measurements of samples in duplicate

N.B. Accuracy of data: Currently we have no assessment of the accuracy of the measurements made on Leg 2. On Leg 1, an assessment was made by comparison of the working standards to measurements of 'Sagami' nutrient standards. The 'Sagami' standards were fully used up on Leg 1. Accuracy of the data from both Legs needs to be evaluated by:- (i) Comparison to archived data from the sampled water masses (ii) Exchange of sub-samples of the standards used on the cruise with other laboratories (possibly NIOZ and Scripps ODF). On return to

SOC as part of this exercise the calibration of the pipettes and volumetric flasks used on the cruise need to be checked, and standards compared to freshly prepared standards.

The average difference between duplicates on each measurement run.

All the underway samples and a minimum of three samples from the deeper bottles closed on each CTD cast were measured in duplicate. Each run consisted of halves separated by the measurement of the 'drift' solution (standard 3) as an unkown then as a 'drift' (from which the software estimated change in calibration) and then two cups of wash solution (from the second of which the software estimated any changes in position of the baselines there might have been). Samples were run in numerical order in each half of the run. After each run, using an Excel spreadsheet, the actual difference (second measurement subtracted from the first, therefore negative value equalled higher second measurement) and also the absolute difference between the pair of values for each sample were tabulated. The average value of the differences for each set of measurements was then found. If the differences were random due to noise in the system then the average of the actual difference should tend to zero. If the values of the actual differences tend to equal the absolute difference then there is a consistent source of error such as a real (or perceived) drift in sensitivity that the software was not correcting accurately.

The data for the average differences is plotted in Figure 23. The values for nitrate (Figure 23a) were consistent and lower after the cadmium column was repacked prior to run 9. The average differences were close to zero suggesting no systematic error. The values for phosphate (Figure 23b) were consistent throughout the leg apart from high values on runs 20 and 21 (two runs of CTD samples on which only 3 and 6 duplicates were measured). The actual difference was about half the absolute difference. This offset may have been caused by an increase in colour yield, through the run, that was not accounted for by the software. It may have been due to an increase in overlap between peaks as the run progressed, (during this cruise apart from the very busy day 161 the system was cleaned with deionised water between each run and with Decon-90 at the end of each day). The values for silicate (Figure 23c) were less consistent. They suggested that between runs 12 and 22 errors were mostly random but towards the end of the cruise the there was an upward drift in sensitivity through the run that was not accounted for by the software.

N.B. After the cruise some of the raw data should be reanalysed to see to what extent the software is correctly assessing drift in the system.

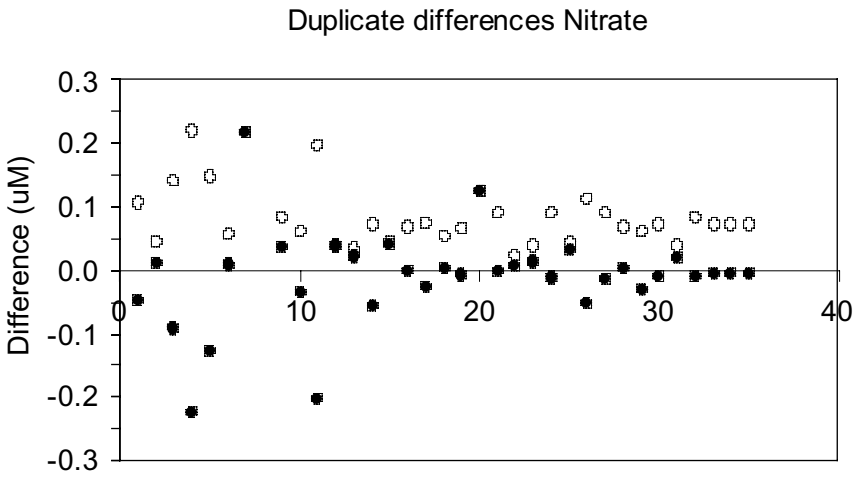

(a)

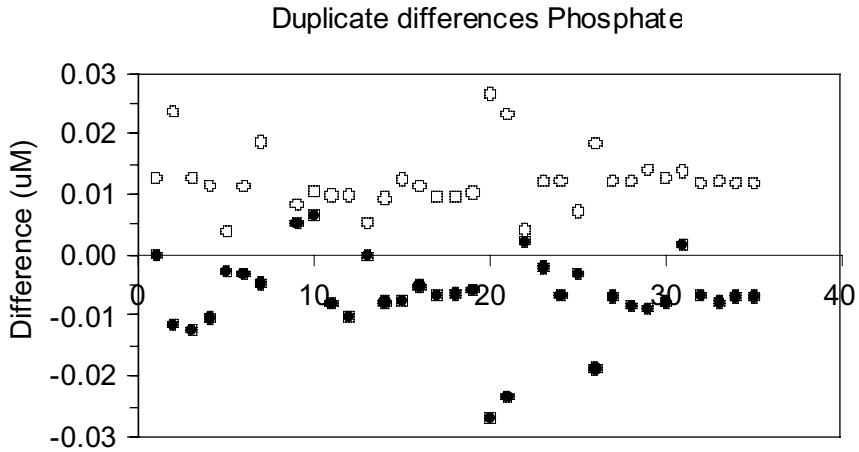

(b)

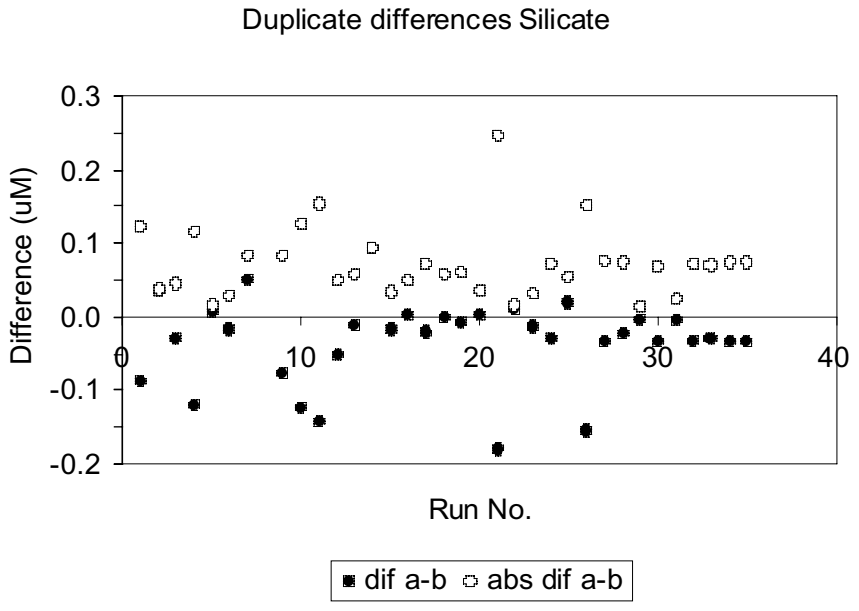

(c)

Figure 23. Graphs showing the variation in the mean of actual differences between duplicates and of the absolute value of the difference. The mean is the mean for each measurement run. (a). Nitrate, (b) Phosphate and (c) Silicate.

The values of the absolute differences between duplicates were tabulated in an Excel spread sheet and compared to the criteria that the WOCE methods manual considered might be achievable. The criteria used in this test were:- grade 1 for Nitrate and Silicate was for a duplicate difference less than 0.25 %, grade 2 was less than 0.5 %, of the full scale value of the calibration (20 uM in each case). For Phosphate the corresponding grade levels were 0.5 % and 1 %. For Nitrate the scores were 46 % and 77 %, Silicate 57 % and 77 %, and for Phosphate 75 % and 81%. The differences are plotted in rank order in Figure 24. The distribution of the errors was similar for each nutrient.

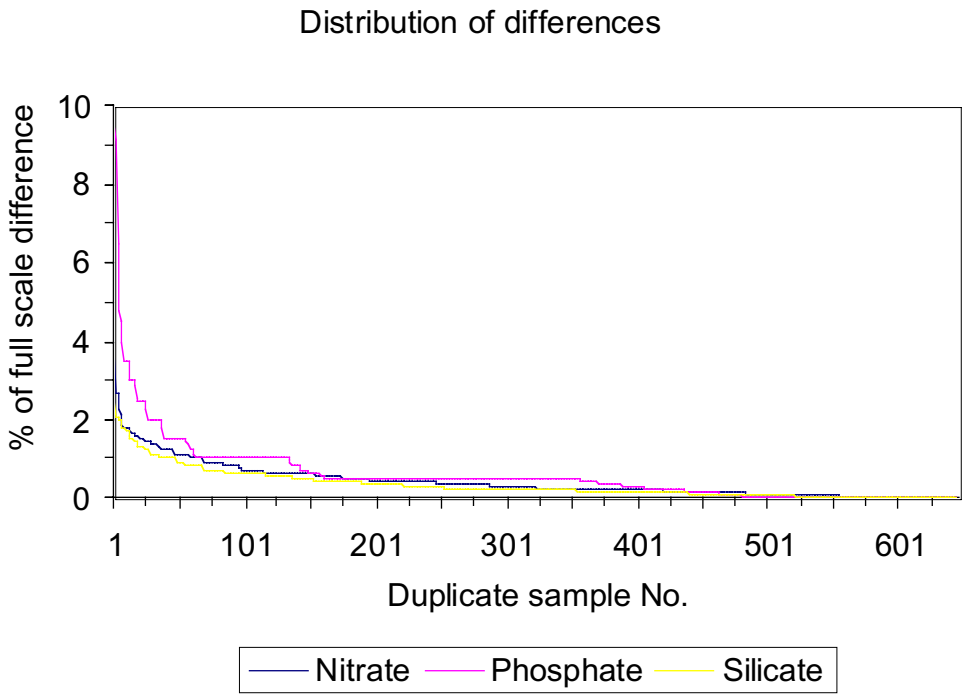

Figure 24. Value of absolute difference in duplicate values for each sample expressed as a % of the full scale of the calibration range of the measurements plotted in rank order.

Other Quality Control Measurements

The other QC measurements made on Leg 2 of D253 were that on the first run of each day a standard solution containing nitrite in place of nitrate was run to access the reduction efficiency of the Cd/Cu column, and a sample of OSI Low Nutrient Seawater was run to test the consistency of low concentration measurements. The value for the nitrite standard which had a concentration of 12.5 µM was 11.83 ± 0.1, for measurements with the repacked column. This gave the column an efficiency greater than 100 % and suggested the column was over reactive

with some reduction of nitrite in addition to nitrate occurring. The values for the OSI-LNS were Nitrate 0.32 ± 0.05, Phosphate -0.01 ± 0.01, Silicate 0.98 ± 0.02.

Preliminary Assessment of Results From D253 / leg 2

CTD Bottle Samples

A total of 340 samples were measured from bottles closed on CTD casts at 22 stations. The range of values obtained were given earlier in the table above. These can also be compared to the range obtained from the 1600 samples determined from the bottles closed during leg 1 also presented earlier. The range of values measured on leg 2 are more in keeping with historical measurements from this area.

Throughout most of the world's ocean the ratio of nitrate to phosphate is relatively constant (in solution the "chemist's" Redfield ratio is 15). In Figure 25a the nitrate and phosphate data from leg 2 are plotted. Regression analysis gave an equation [Nitrate] = 14.574[Phosphate] + 0.0353 µM (Nitrate) with an R^2 = 0.9822. The spread of data was much tighter than that achieved during leg1.

In Figures 26a and b the data for silicate and nitrate are plotted against one another. In leg 2 (Figure 26a), the change in the Silicate to Nitrate ratio between over flow water and shallower waters was clearly visible. In the data from Leg 1 (Figure 26b), the data was so scattered that this change was completely obscured.

In Figures 27a and b the concentrations of nitrate and silicate are plotted against depth of the sample. There was a wide variability in the concentration of nitrate above depth of 500 m. Below 500 m concentrations of nitrate were constant. Concentrations of silicate were variable at all depths (Figure 27b). The presence of overflow water of relatively high silicate concentration could be clearly seen at about 500 m depth at some stations.

The Redfield ratio became more scattered towards the surface (Figure 27c). Although values of both Nitrate and Phosphate decreased towards the surface the increase in variation was greater than the increase in the likely error of the N:P estimate. At the surface the range of values was very wide. In Figure 28, the N:P ratio is plotted against the concentration of silicate. This shows that the highest N:P ratio was associated with the lowest Silicate values which were in turn associated with a phytoplankton population that had shifted from being dominated by diatoms to one dominated by phaeocystis.

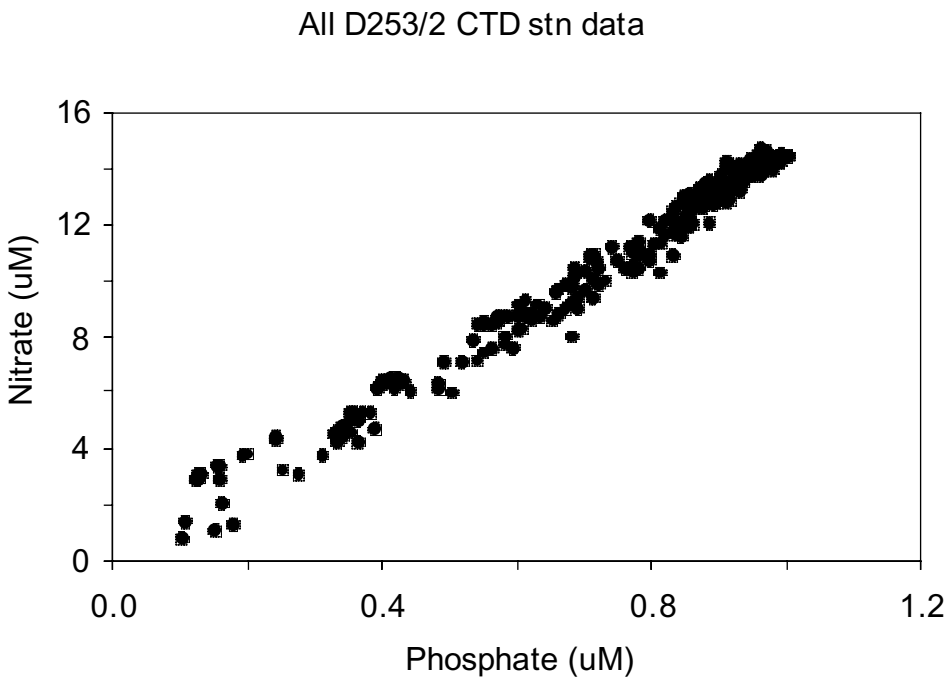

(a)

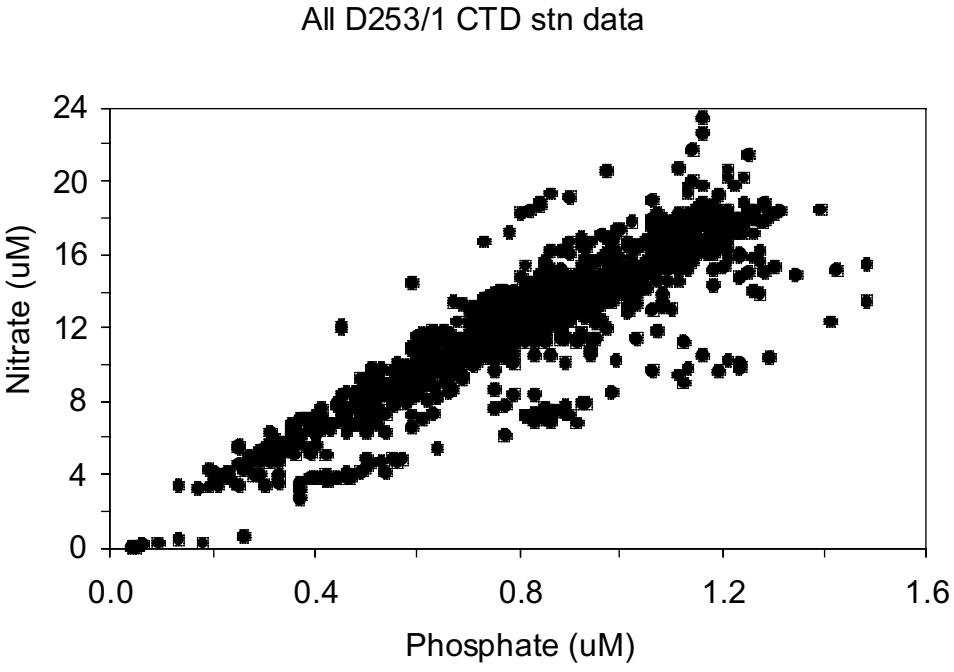

(b)

Figure 25: Plots of concentration of nitrate against phosphate measured in samples from CTD rosette bottles on legs 1 and 2; (a) leg 2 data, (b) leg 1 data.

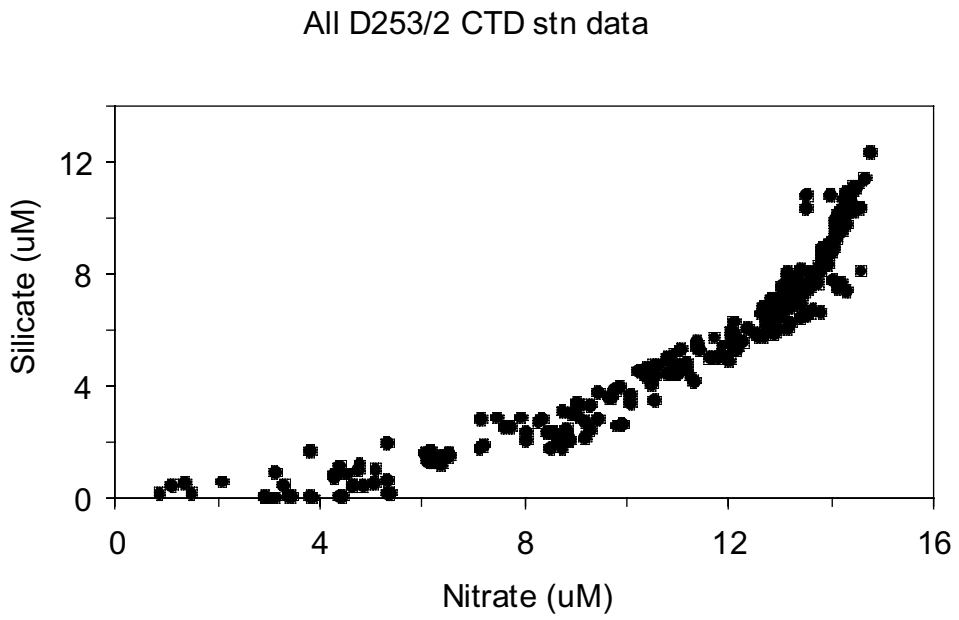

(a)

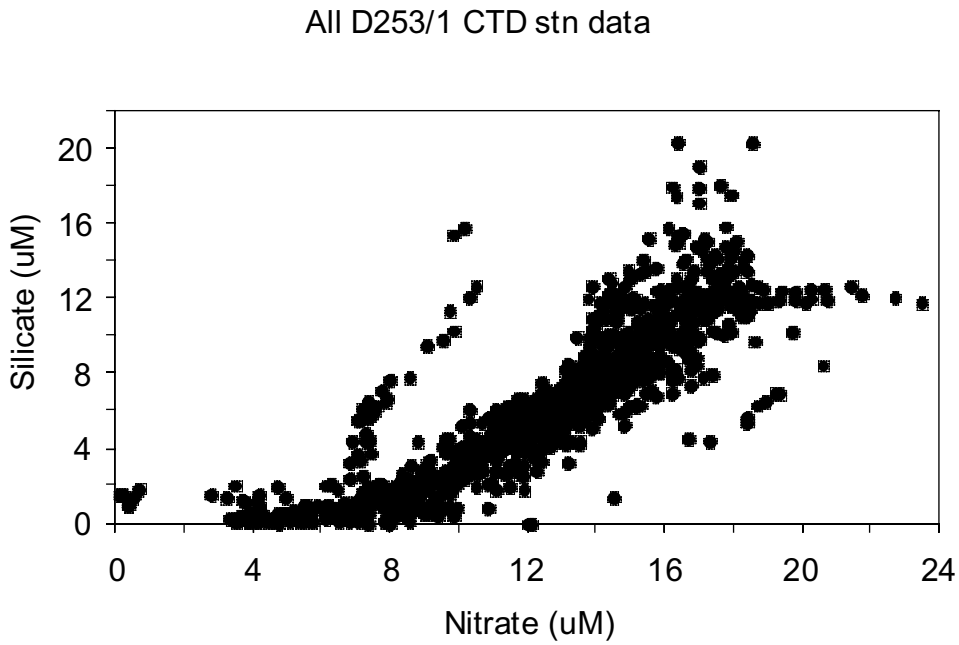

(b)

Figure 26. Plots of concentration of silicate against nitrate measured in samples from CTD rosette bottles on legs 1 and 2; (a) leg 2 data, (b) leg 1 data.

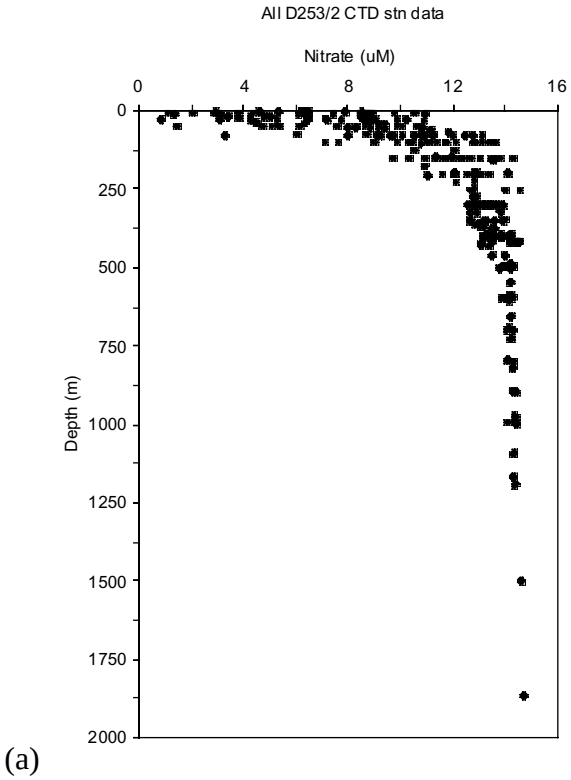

(a)

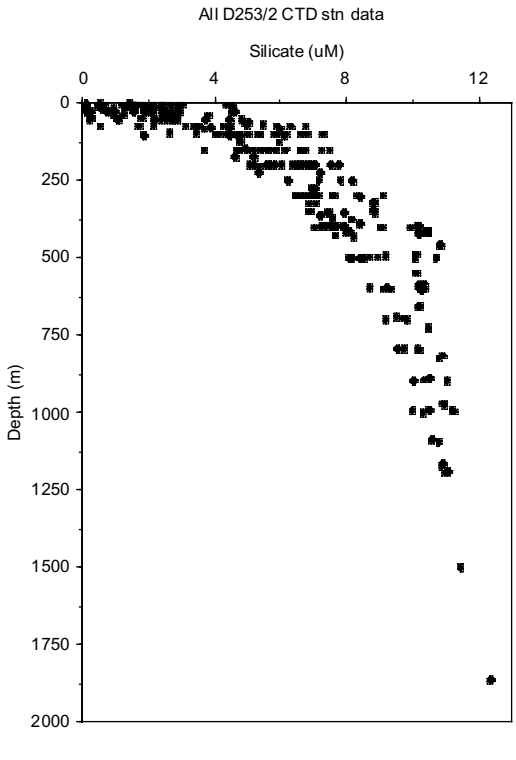

(b)

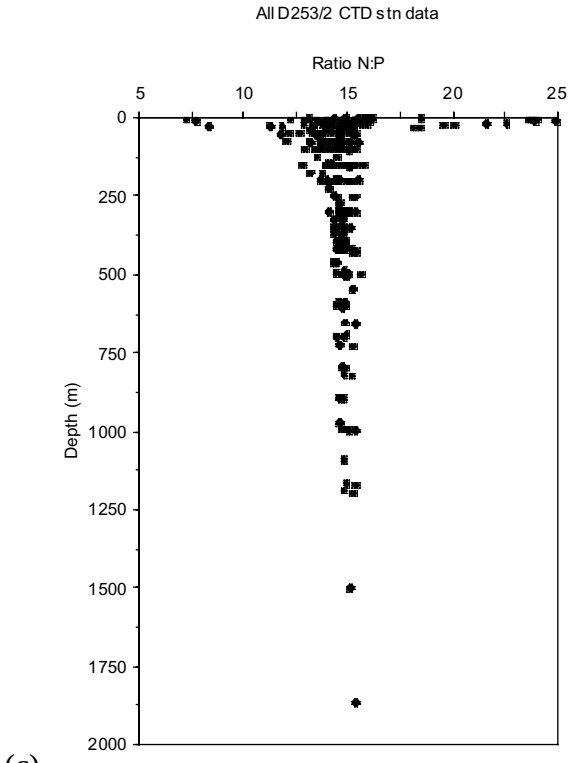

(c)

Figure 27. Depth related distribution of concentration of Nitrate, Silicate and of the ratio of concentration of Nitrate to Phosphate, for CTD bottle data for leg 2; (a) leg 2 Nitrate against depth, (b) leg 2 Silicate against depth and, (c) ratio of concentrations of Nitrate to Phosphate against depth.

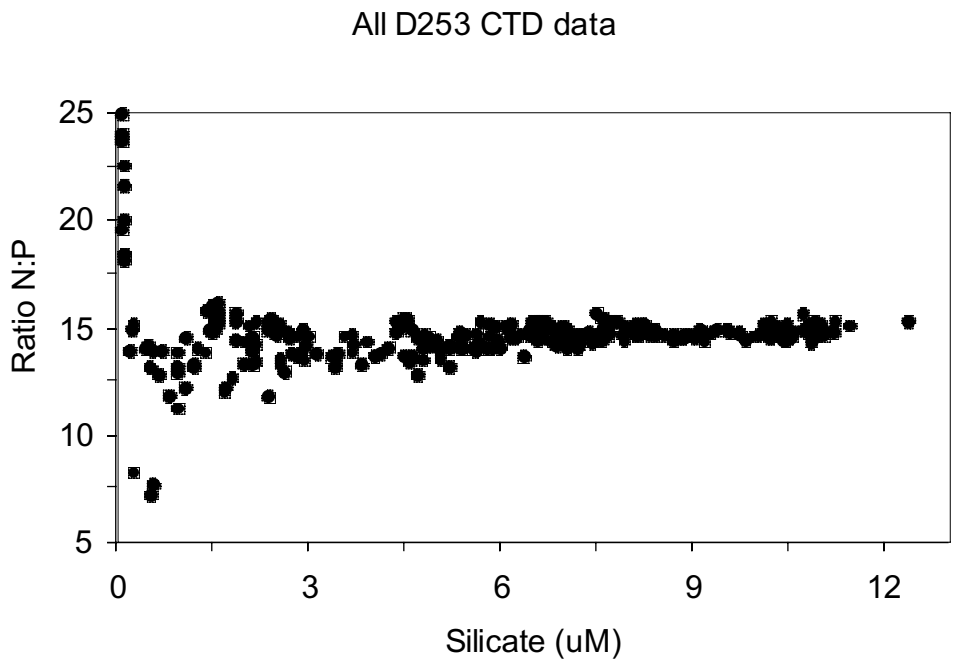

Figure 28. Plot of the ratio of N to P against the concentration of silicate in the same sample.

Underway Samples Collected During the three SeaSoar surveys

During the Seasoar surveys, at approximately half hourly intervals, samples were collected for the determination of nutrients (and chlorophyll and salinity) from the ships "non-toxic" seawater supply in the Wet Lab. The data for the three surveys are summarised as the maximum, minimum, median and mean values in the following table, and the variation in concentrations of phosphate and silicate against the concentration of nitrate are plotted in Figure 29. Both the table and Figures 29 show that the spread of values were similar on all three surveys.

Summary of nutrient data comparing values obtained from samples of surface seawater collected at half hourly intervals during the three SeaSoar surveys.

	Time	Nitrate	Phosphate	Silicate
	Survey 1			
count	221	221	221	221
min	153.21	0.48	0.11	0.28
max	161.07	12.02	0.79	5.38
median		8.42	0.57	2.23
mean		7.74	0.53	2.39
	Survey 2			
count	144	144	144	144
min	161.42	0.76	0.13	0.18
max	165.39	11.41	0.74	5.17
median		9.12	0.58	2.93
mean		8.11	0.54	2.92
	Survey 3			
count	113	113	113	113
min	165.94	1.25	0.09	0.07
max	168.52	10.87	0.68	4.66
median		8.14	0.52	2.80
mean		7.40	0.49	2.75

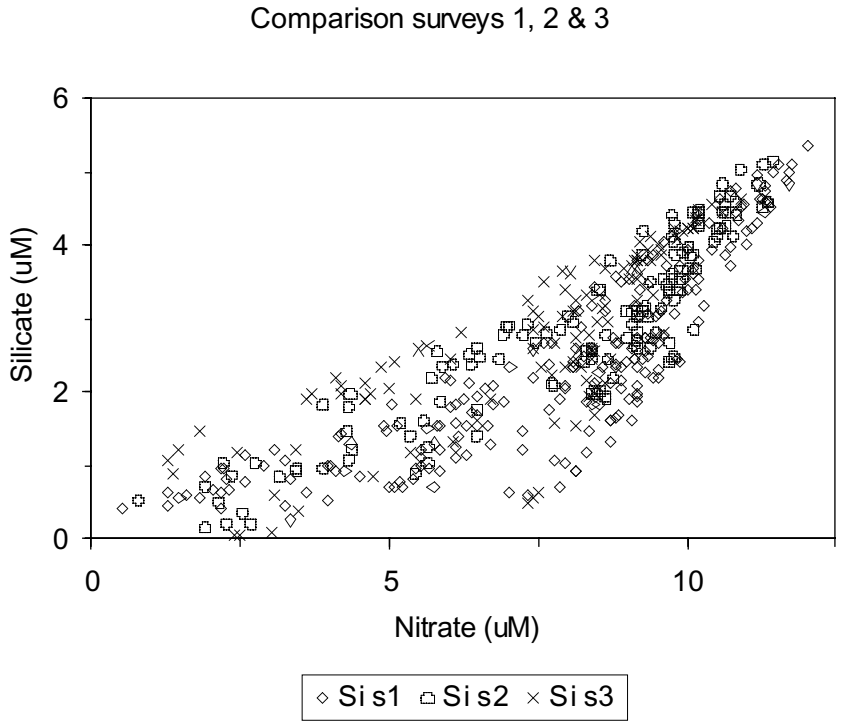

(a)

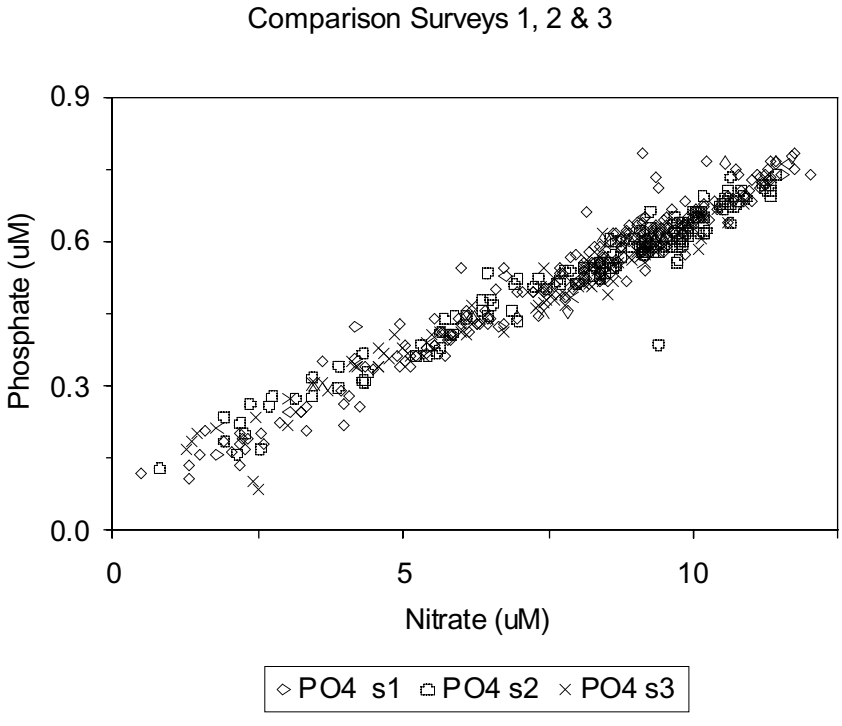

(b)

Figure 29. Plots of the co-variation of concentrations silicate and phosphate against nitrate comparing findings during each of the three SeaSoar surveys; (a) variation of Silicate and Nitrate, (b) variation of Phosphate and Nitrate.

Appendix

The final condition of analyser the end of D253 Leg2

The “Real Time” plots from the last run of the analyser run 010617c and a photograph of the analyser set up in the deck laboratory immediately prior to shutting down on 18 June 2001.

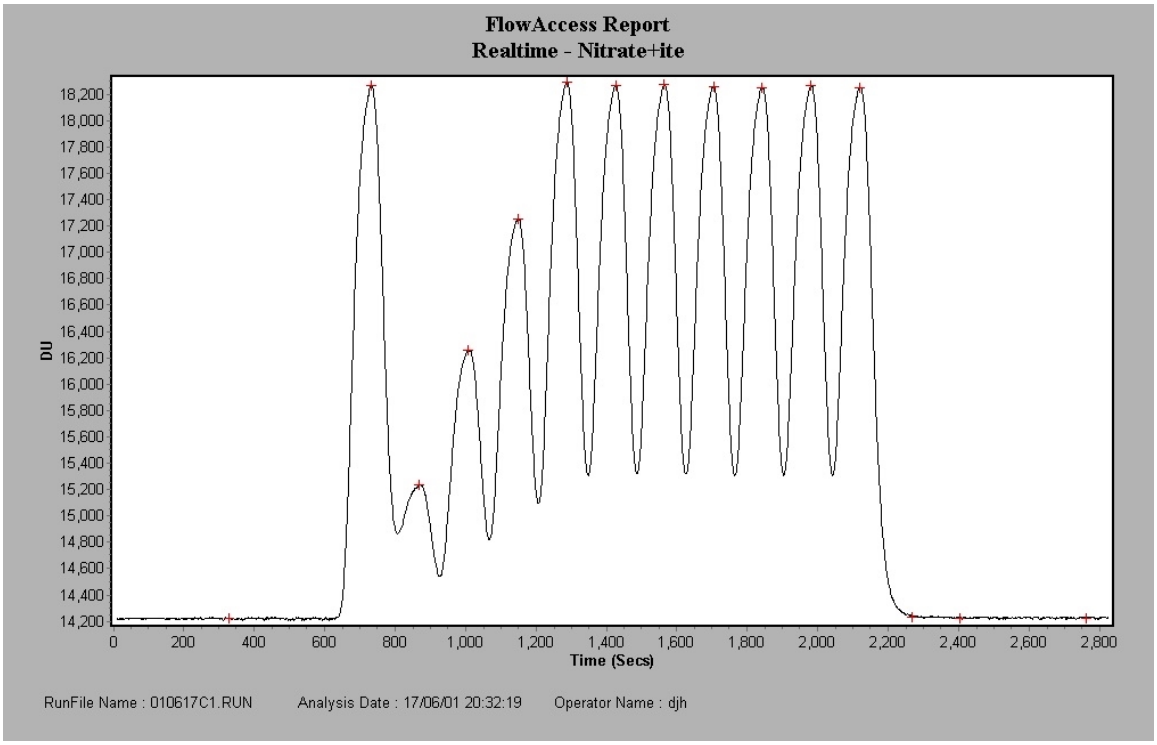

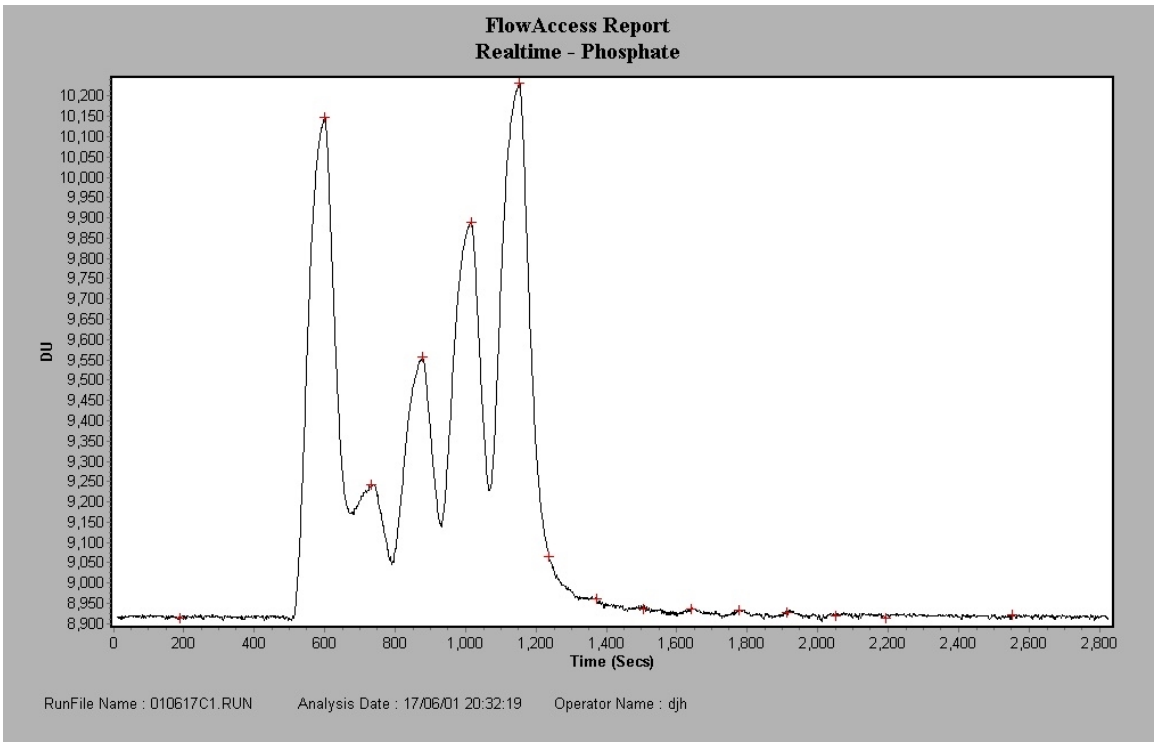

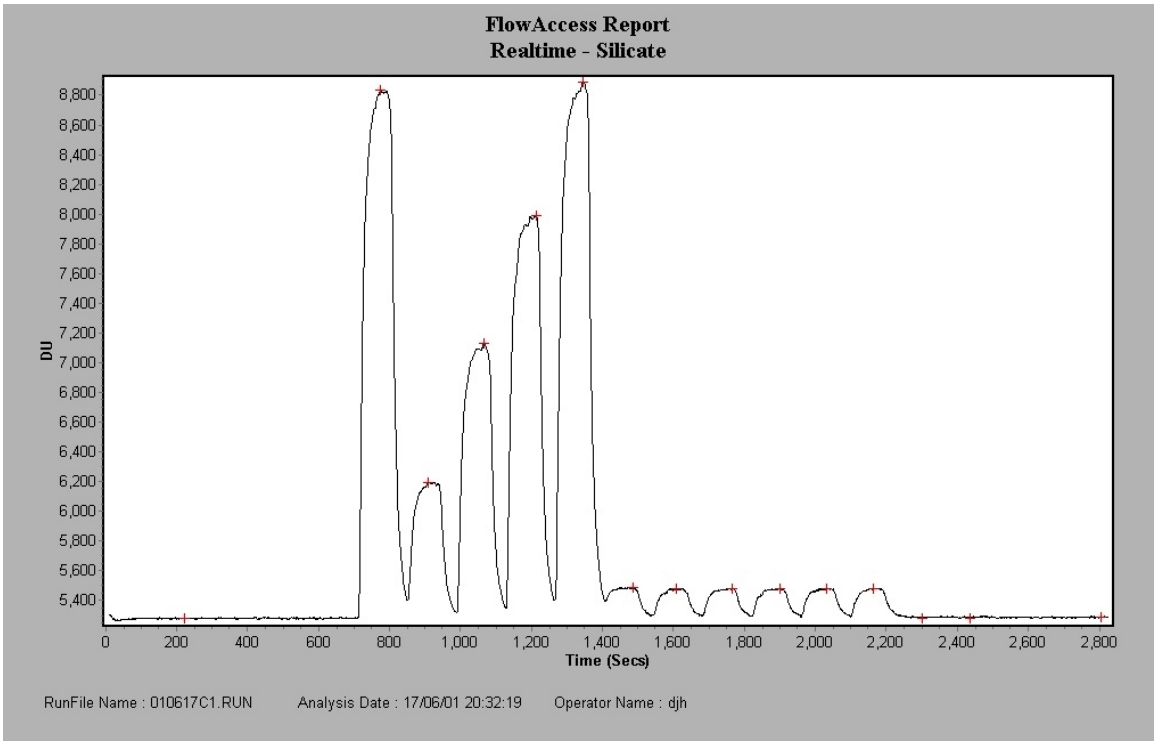

Picture. View along port side bench of Deck Laboratory during Discovery Cruise D253 leg2.

Dissolved Oxygen Concentration - *Sophie Fielding*

At CTD stations, dissolved oxygen samples were typically the first sample drawn from each niskin bottle, except at the productivity stations (early morning) where they were drawn after an ammonia sample. Between 1 and 3 duplicate samples were taken on each CTD cast. The samples were drawn through short pieces of silicon tubing into clear, pre-calibrated, wide necked glass bottles. Each sample was fixed immediately, on deck, with manganese chloride and alkaline iodide dispensed using precise repeat Anachem™ bottle top dispensers. Samples were shaken on deck for approximately half a minute, and if any bubbles were detected in the samples at this point a new sample was drawn. The samples were transferred to the chemical laboratory, where they were shaken again thirty minutes after sampling and stored under water until analysis.

The temperature of the water in the niskin bottles, at the time of sampling, was measured using a hand held electronic thermometer probe. The temperature was used to calculate any temperature dependant changes in the sample bottle volumes. It should be noted that all three hand held temperature probes were unreliable throughout the cruise, providing variable accuracy.

Samples were analysed in the chemical laboratory, starting two hours after their collection, following the procedure outlined in Holley and Hydes (1995). The samples were acidified immediately prior to titration and stirred using a magnetic stir bar set at a constant spin. The Winkler whole bottle titration method with amperometric endpoint detection (Culberson and Huang, 1987), with equipment supplied by Metrohm, was used to determine the oxygen concentration. The spin of the stir bar was affected by the movement of the ship and by the uneven bases on some of the glass bottles, leading to less effective stirring of the sample and thus longer titration times, although this probably did not effect the accuracy of the endpoint detection.

The normality of the thiosulphate titrant was checked against an in house potassium iodate standard of 0.01 M at 20 ºC at the beginning of each eight hour shift and incorporated into the calculations. A total of five standards were used throughout the duration of the cruise. Blank measurements were also determined at the start of each run to account for the introduction of oxygen with the reagents and impurities in the manganese chloride, as described in the WOCE Manual of Operations and Methods (Culberson, 1991). Thiosulphate standardisation was carried out by adding the iodate after the other reagents and following on directly from the blank measurements in the same flask. Changes in the thiosulphate normality are shown in Figure 30. The thiosulphate normality precision for each batch was poor, this may have been influenced by the highly variable temperature of the chemical laboratory (18-25 ºC). The temperature of the laboratory was noted for each analytical run and was included in the calculation of the thiosulphate normality.

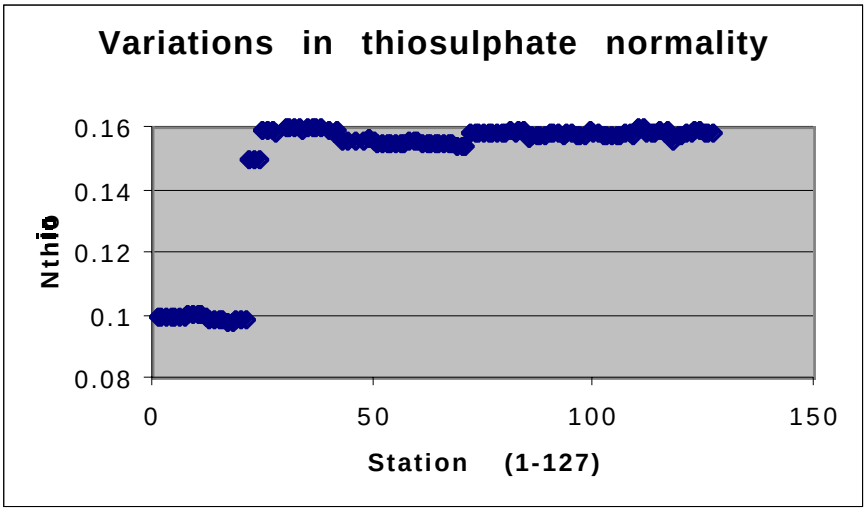

Figure 30. Variations in thiosulphate normality.

Absolute duplicate differences for each station are shown in Figure 31 for a sample size of 97 pairs of duplicate measurements. The average duplicate difference was 2.12 µmol l^{-1} (± 2.64).

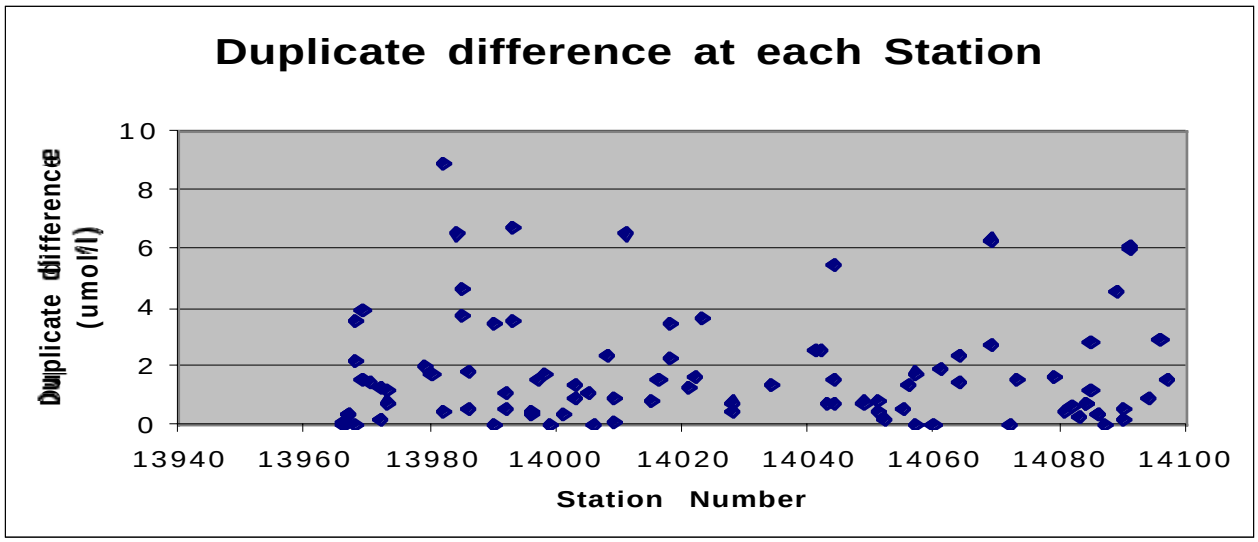

Figure 31. Oxygen duplicate difference at each station.

Problems

The temperature of the chemical laboratory ranged between 18 and 25°C throughout the cruise. The temperature of the laboratory was noted for each analytical run.

On station 14039#1 it was noticed that the metrohm system was not titrating to the end point. The whole system was replaced, including the electrode. In addition new reagents and titrates were made up.

On station 14057#1 the anachem dispenser used for the $MnCl_2$ clogged. The dispenser was replaced and a new one used for the rest of the cruise.

DOC/DON Measurement - *Hugh Ducklow, Leigh McCallister and Dennis Hansell*

Biological productivity in the biosphere results in synthesis and release of organic matter in solid, liquid and gas phases, of which the solid phase is the most conspicuous (terrestrial biomass). The dissolved organic matter (DOM) phase however, may be the most dynamic, since large fluxes of DOM driven by rapid bacterial turnover of labile small molecular weight compounds, and breakdown of polymeric forms dominate global respiration on land and in the ocean. DOC also constitutes the largest pool of organic matter in the ocean. Marine DOC can be discriminated into 3 or more pools by their relative turnover times, ranging from minutes to millennia. Of particular importance is an intermediate-sized pool with turnover times on the order of weeks to months, the *semilabile pool*. In the ocean, net production of semilabile DOC constitutes about 15-20% of the global marine new production, thus forming an important cog in the biological carbon pump.

Breakdown of semilabile DOM is slow, and its contribution to bacterial metabolism is hard to estimate. The semilabile pool accumulates over seasonal timescales. The slow decomposition of semilabile DOM allows advective transport over regional to basin scales, and permits export into the deep ocean at the major sites of intermediate and deep water formation, including the NE Atlantic.

The process of DOM transport toward export regions has been inferred mostly from a few sections showing surface accumulation of enhanced DOC concentration and penetration to depth. Decomposition during flow from source regions to export sites has not been studied, nor has the accompanying transport of dissolved organic nitrogen and phosphorus (DON and DOP). Our goal in the FISHES cruise was to infer the transport of accumulated DOC, DON and DOP during the spring phytoplankton bloom in the NE Atlantic Ocean, the region previously studied in the JGOFS North Atlantic Bloom Experiment.

To this end, we sampled the full water column (ca 150–2600 m) for DOC, DON and DOP along the L-F-J-K and M-H-P lines (Figure 1). These lines were chosen for sampling because they were bounded by land masses and/or shallow topography. Transport (Mol $m^{-3}s^{-1}$) would be calculated from the concentration fields observed for each element and circulation as diagnosed by FISHES colleagues. We also sampled, at reduced frequency (9 stations), along the B-J-H-R1 line to examine north-south and cross-frontal gradients in dissolved organic matter species. DOM samples would be analysed post cruise in Dennis Hansell's lab in Miami using established JGOFS Protocols.

Bacterial biomass and production rates were measured approximately daily in coordination with primary production determinations, at the stations given in the following table. Bacterial biomass would be determined later both by video image analysis of epi-fluorescent microscope imagery and by flow cytometry using the VIMS Coulter ALTRA instrument. Production rates were assayed using daily 3H-thymidine and 3H-leucine incubations. Biomass and production were measured at standard depths or productivity light-depths between the surface and 1000 m.

BP	Station	Date	Depth
1	BC5	08 May	990
2	BC11	09 May	150
3	IB14	11 May	1000
4	BE4	12 May	1000
5	EC3'	13 May	1000
6	CG2	14 May	1000
7	CG6	15 May	150
8	L	16 May	800
9	JK4	18 May	1000
10	ADS	20 May	125
11	ADJ	21 May	584
12	BJ6	23 May	294
13	JH6	24 May	159
14	HR5	25 May	2600
15	CG7	27 May	1000
16		28 May	

At Stations C and HR6 we performed short term seawater culture experiments to determine the timescale and extent of lability of ambient surface layer DOC. Samples were incubated for 5-10 days and assayed for DOC concentration and bacterial abundance. Finally, large-volume (200 litre) incubations were performed at both stations to determine the ^{14}C age of the DOC fraction utilised and incorporated into bacterial biomass. Following 3-4 days growth in the inoculated 0.2 µm filtered water, bacterial biomass was harvested on filters and frozen for accelerator mass spectroscopic analysis of the natural abundance of ^{14}C.

Ammonia Concentration - *Martin Johnson*

Seawater ammonium concentrations were measured using the OPA fluorescence method outlined by Holmes *et al* (1999). It was originally intended that regular surface samples would be taken throughout the cruise, and that one depth profile would be measured each day. Due to time constraints, only a few surface samples were taken, and effort was concentrated on the daily depth profiles of ammonium concentration. The results were of a high precision and, in general, well duplicated.

Some alterations were made to the method: instead of using the working reagent in a 10ml:30ml ratio with the sample, a ratio of about 1ml:30ml was used. This was done in order to make the working reagent last longer, but it also appeared to reduce the baseline fluorescence and therefore the detection limit. This may have been due to the absence of the ammonia pollution that is observed in the lab on land. The smaller amount of working reagent also meant that the incubation time for the inoculated samples needed to be increased, from the recommended 2-3 hours to as much as 12 hours. The fluorescence plateau was increased by similar proportions. Exact sample volumes are not important except for the standard additions (see below).

Calibration was achieved by standard additions to a set of samples (usually sampled from the Niskin bottle fired nearest the surface), sample volume was measured using a syringe. For the first week of the cruise, a 50 µmol l^{-1} stock standard solution made up with milli-Q water was used. This was not ideal because of the matrix effects caused by the salinity difference between samples and standards. This was negated to some extent by using standard additions, but it was decided that it would be wise to make up a new "salty" standard. After collection of some deep seawater (very low ammonium concentration) and production of a new 50 µmol l^{-1} stock standard, a series of comparisons between the standards was conducted, and the earlier results were normalised to the new standards. The calibrations were excellent (Figure 32) and the

response of the fluorometer was very stable over the time it took to run a set of samples (~1 hr per 25 samples), although it did vary slightly from day to day.

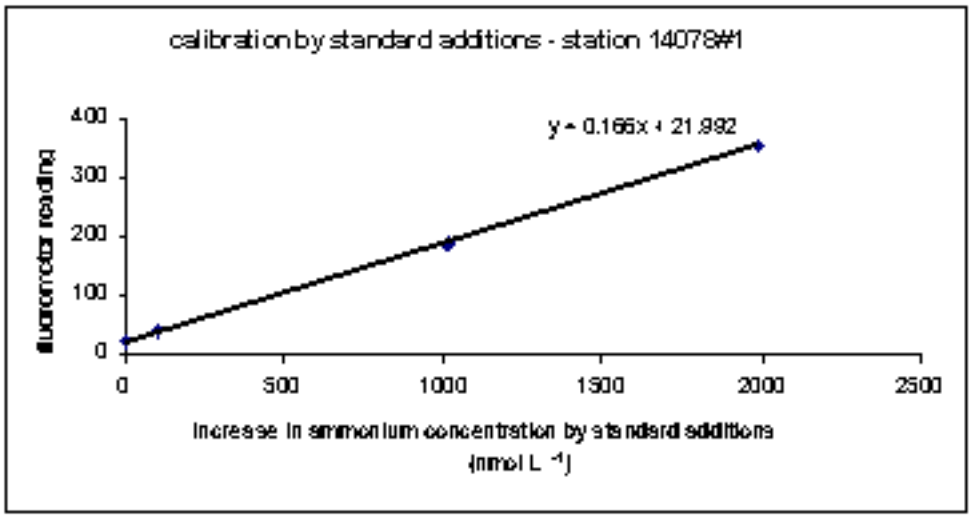

Figure 32. Calibration of Ammonium determination by standard additions.

Samples were taken from the stations listed in the table below. Measured concentrations varied from 5 nmol l^{-1} in deep waters to as much as 1.1 µmol l^{-1} at depths of maximum regeneration. Surface water concentrations varied by an order of magnitude between the two most extreme stations.

Stations sampled	Profile/Surface	Surface concentration (nmol l^{-1})
13970#1	surface	223
13977#1	profile	223
13984#1	profile	164
13989#3	profile	47
13993#1	surface	55
13995#1	profile	133
14000#1	profile	607
14000#3	profile	550
14005#1	profile	342
14005#3	profile	339
14010#1	profile	268

14014#1	profile	690
14020#1	profile	344
14021#1	profile	550
14022#1	bottom 3 depths	n/a (observation of re-suspension event)
14025#1	profile	540
14026#1	bottom 5 depths	n/a (as 14022#1)
14029#1	profile	36
14038#1	profile	119
14040#1	surface	93
14048#1	surface	128
14053#1	profile	337
14060#1	profile	451
14066#1	profile	645
14066#3	profile	401
14071#1	profile	378
14078#1	profile	93
14088#1	profile	56

Contamination, as with all ammonium methods, was a matter of serious concern. Disposable latex gloves were worn as much as possible (4 boxes containing 100 gloves each were brought, and they were nearly all gone after 2 weeks!) as the most serious contamination comes from people's fingers! All equipment was washed and then soaked in Decon and then rinsed and soaked in milli-Q before use (plastic boxes were used for this on the ship). In spite of all the precautions, contamination still occurred. There was a 'contamination baseline' of a few nmol l^{-1}, but also one-off contaminations occurred regularly (maybe once or twice per profile). These were quite easy to identify, as they were generally increases of tens or hundreds of nmol l^{-1}.

In all, a very interesting and detailed data set was collected, and the method proved extremely successful. There had been some talk during the cruise about attempting to automate the process in the nutrient auto-analyser style, which could potentially increase surface sample resolution and eliminate some contamination problems.

Osmium Samples - *John Allen and Richard Sanders*

On two stations water samples were taken for the later determination of the concentration of the trace element, Osmium, by *Kevin Burton* of the Open University. The two stations were IB13 (13979) and IB17 (13982). One litre polycarbonate sample bottles were filled from 12 Niskin bottles selected to make a suitable vertical water profile for each station. The sample bottles were capped and then placed upside down in the cut off bottom half of plastic 2 litre carbonated drinks bottles half filled with water from the same Niskin bottle. The assembled bottle combinations were then placed in individual zip lock plastic bags.

CFC Samples - *Richard Sanders and Stuart Cunningham*

CFC samples were taken for *Stephen Boswell* (GDD) in order to test the efficiency of a new sampling method. Samples were drawn at 5 depths in duplicate from *Discovery* station 14066 into copper tubes, sealed immediately and returned to SOC for subsequent analysis.

Longhurst Hardy Plankton Recorder (LHPR) Tows - *Sophie Fielding*

The LHPR is a vehicle designed to be towed in a single V-shaped profile through the upper 450 m of the water column. It has a large aluminium frame, with a polypropylene tail fin, which houses a conical net. A nose cone at the front of the frame channels water through the 333 μm conical net to its cod-end. The cod-end contains two spools of gauze which wind round a take-up spool every two minutes, sandwiching a sample of zooplankton between them, thus allowing semi-discrete samples. Attached to the frame, one each side, are two cylinders containing a rechargeable battery pack and the electronics for driving the cod-end, monitoring the sensors (in our case these were a Seabird conductivity meter, temperature probe, depth sensor and flowmeter) and communicating with the surface. To assist the sampler to dive a 45 kg depressor weight is attached to the underside front and a drogue streams from the back of the frame to assist stability.

On this cruise the LHPR was run in two modes; using a conducting cable with full communications to the surface and in internal logging mode.

Conducting cable mode:

A TOBI swivel was used to connect the main conducting warp to the LHPR sensor unit. In the main laboratory the conductors were connected to the LHPR deck unit and via that to a computer using the COM 1 port. The programme *PROLHPR* (Spartel) (run on the PC) displayed in real time, the depth, temperature, salinity, wind-on function and flow throughout the tow. The gauze wind-on could be switched on and off at will, in this case the gauze wind-on

was switched on when the LHPR was at the surface at the beginning of the tow and switched off at the end of the tow before recovery of the vehicle onto the deck. The maximum time in the water was limited to the amount of gauze on the wind-up spools and the charge life of the batteries.

Using the conducting warp, deployment of the LHPR was from the main A frame over the stern of RRS *Discovery*. Wire was payed out until the LHPR was just below the surface and the LHPR held there for five minutes to allow at least two wind-on's of the gauze. The wire was then payed out at a maximum rate of 30 m/minute until the LHPR was at ~300 m. During this the ships speed was increased from the deployment/recovery speed of 1.5 knots to ~4.5 knots. The LHPR was then held at maximum depth for 10 minutes before hauling in at 30 m/minute. Upon retrieval, the cod-end was removed from the frame. The third spool, holding the sandwiched zooplankton, was placed in a bucket containing 4% formaldehyde and then both net and cod-end were washed in preparation for the next tow.

Internal logging mode:

For the last two LHPR tows it was decided to mount TUBA (see earlier section) and the OPC on the LHPR frame. TUBA required 4 cores in a conducting cable to transmit data, hence it was necessary to tow the LHPR using the SeaSoar multi-conducting cable rather than the single conductor main conducting warp. In addition the OPC could not use the same conducting cable as TUBA without interference in data transmission. Therefore PENGUIN was also mounted on the LHPR frame to log the OPC data. Brackets were made to mount the OPC, TUBA and PENGUIN at the front end of the LHPR frame, in line with the existing sensor and battery cylinders and close to the towing bridle to minimise drag and maintain the horizontal position of the LHPR in the water. A new towing bridle also had to be made to allow for the SeaSoar style cable termination. This was the first time that the LHPR had been towed from a SeaSoar cable.

Using the SeaSoar cable, deployment of the LHPR was from the main A frame and the SeaSoar block, over the stern of RRS *Discovery*. As the conducting cable was already in use for TUBA data, the LHPR was run in internal logging mode. The maximum duration of the LHPR tow in this mode was 180 minutes (the data holding capacity of the sensor cylinder before overwriting), including deployment and recovery: to err on the side of caution the tows were limited to around 150 minutes. A delay of 6 minutes before the first wind-on of the gauze was added to allow time for deployment. Again the LHPR was held just below the surface for 5 minutes to allow the gauze to wind-on several times before the cable was payed out at ~15 m/minute. The cable out was limited to just less than the depth of water to prevent the LHPR from grounding on the sea bed (as the behaviour of the LHPR with the additional sensors was unknown). The LHPR was held at the bottom for 10 minutes before hauling in at 15 m/minute, stopping for 10 minutes every 50 metres of cable in. Retrieval of the LHPR on to the ship deck and preservation of the

samples followed the same method outlined above. With the additional weight and drag of extra sensors the towing speed was reduced to a maximum of 3.5 knots. The low drag of the faired SeaSoar cable provided a much greater deployment depth for a given length of cable payed out.

Summary of LHPR tows

A total of four deployments were made with the LHPR (see table below). On each deployment, the LHPR was towed though a sea surface temperature and salinity anomaly, identified from the TSG data. There were three problems that occurred. During the first deployment, station 14103, the flowmeter did not work. On retrieval of the LHPR the flowmeter was turned upside down and during pre-haul tests it worked. However on its second deployment, station 14115, the flowmeter again failed, this time ~5 minutes into the tow. It was believed that the connection of the cable to the flowmeter was becoming loose under pressure, and for the third deployment the cable was taped in place using self-amalgamating tape. This seemed to do the trick! Additionally the gauze wind-on, displayed using the *PROLHPR* programme appeared to have stayed on during the first 30 minutes of the tow, not settling until the LHPR was at 120 m depth. The effect of this would only be evident on examination of the gauze on return to SOC. During the third deployment, station 14126, when the LHPR was run in internal logging mode, all parts worked correctly. However, it was unclear whether TUBA was observing targets and the OPC did not log to PENGUIN as a result of a software setup glitch (discussed in an earlier section). For the final deployment, station 14129, each instrument behaved correctly: due to the adverse weather (Sea state ~6) the towing speed was reduced to 2.5 knots.

Station No	Jday	Time deployed	Time recovered	Towing speed
14103	156	00:40	~02:15	4.5 (knots)
14115	161	17:20	~19:35	4 (knots)
14126	165	21:23	~23:40	3.5 (knots)
14129	168	13:32	~15:40	2.5 (knots)

Mesozooplankton Species Abundance, Size Fractionation and Lipid Concentration -
Alex Mustard, Xabier Irigoien, David Pond and Tim O'Higgins

Leg 1: Mesozooplankton Analysis Overview

The objective of the mesozooplankton group was to study the population structure of *Calanus finmarchicus* in the Iceland basin, its reproductive rates, the feeding rates of the early stages and the lipid content of the overwintering stages.

Population structure:

50 µm mesh wide WP2 nets were to be used in vertical tows from 100 m to the surface. Unfortunately the two 50 µm nets were lost at the beginning of the cruise and the samples were collected with a 200 µm net. Therefore earlier naupliae stages of *Calanus* will not be represented in the samples and the early copepodites will be underestimated. A total of 109 samples (see table below) were collected and fixed (4 % formaldehyde) for counting during leg 1 of FISHES.

Station	Abundance	Egg production	Feeding	Lipids (stage V)	Lipids (egg production)	Lipids Deep Chl. Max.	Comments
13966	√						net broken
13967	√						
13968	√						
13969	√						
13970	√						net broken
13971	√						200 m
13972	√						
13973	√	√		√			
13974	√		√	√			
13975							suspended because weather
13976	√						
13977							
13978		√	√	√			
13979							
13980							
13981	√	√	√				move to middle deck crane
13982	√						
13983	√						
13984	√						
13985	√	√		√			
13986	√			√			
13987	√	√	√	√			

13988	√	√	√				
13989	√						
13990	√						
13991	√	√					
13992	√						
13993	√						
13994							
13995	√	√	√				
13996	√						
13997	√	√	√				
13998	√						
13999	√			√			
14000	√						
14001	√						
14002					√		
14003	√	√	√				
14004	√						
14005	√						
14006	√						
14007	√	√	√				
14008	√	√					
14009	√						
14010	√						
14011	√	√	√		√		
14012	√						
14013	√						
14014	√						
14015	√			√			
14016	√	√	√			√	
14017	√						
14018	√						
14019	√						
14020	√						
14021	√			√			
14022	√					√	
14023	√					√	
14024						√	
14025						√	
14026							
14027	√						
14028							
14029	√						
14030							

14031	√						
14032							
14033	√						
14034							
14035	√			√			50 m repaired
14036							
14037							
14038	√						
14039							
14040	√						200 m
14041							
14042	√						
14043							
14044							
14045	√						
14046	√						
14047	√						
14048	√		√				
14049	√			√			
14050	√						
14051	√						
14052	√						
14053	√						
14054	√						
14055	√		√	√			
14056	√		√	√			
14057	√			√			
14058	√						
14059	√						
14060	√						
14061	√	√		√	√		
14062	√	√	√	√			
14063	√	√		√			
14064	√	√	√				
14065	√	√					
14066	√						
14067	√						
14068	√						
14069	√	√					
14070	√	√					
14071	√						
14072	√	√		√			
14073	√	√			√		

14074	√	√					
14075	√						
14076	√						
14077	√						
14078	√						
14079	√						
14080							
14081							
14082	√			√			
14083	√						
14084	√	√					
14085	√						
14086	√						
14087	√						
14088	√						
14089	√						
14090	√						
14091	√						
14092	√			√			
14093	√						
14094	√	√	√				
14095							
14096	√						
14097							
14098	√						

Reproductive rates:

Egg production and hatching rates were measured at 25 stations. Fifteen to thirty females were individually incubated in 60 ml jars for 24 hours. To measure hatching rates after 24 hours, the females were removed and the eggs incubated for an additional 48 hours before fixation.

Feeding rates:

A total of 16 incubation experiments were carried out to measure feeding rates of naupliae and CI of *Calanus* and occasionally *Oithona*. A mixture of 200 ml bottles some containing animals, some not (controls), were incubated for 24 hours before fixation with 1% acidic lugol. Microplankton would be counted under the microscope back in the laboratory at SOC and the ingestion estimated following Frost's equations.

Lipid content:

Between 6 and 12 individual stage V *Calanus finmarchicus* were collected from 20 stations and were preserved for subsequent lipid analysis. Four egg production experiments, each involving 10 female *C. finmarchicus*, were conducted: and at 5 stations the deep chlorophyll maxima (500-1000m) was sampled for particulate lipids.

Mesozooplankton Net Sampling During Leg 2

Mesozooplankton samples were collected during the second leg of the cruise at each CTD station (see table below) to examine the species, stage and size structure of the zooplankton community, and to provide undamaged animals for gut fluorescence measurements and egg production incubations.

Station No	Nets Used (µm)	Abundance	Size Spectra	Gut Fluorescence	Egg Production	Hatching Rate
14099	200	X		X	X	
14100	200, 500	X	X	X	X	
14102	500	X		X	X	
14104	500	X		X		
14106	500	X		X	X	
14108	500	X		X	X	
14109	500	X		X		
14110	500	X		X		
14111	500	X		X		
14112	500	X		X	X	
14113	500	X	X	X		
14114	500	X	X	X	X	
14116	500	X	X	X	X	
14117	500	X	X	X	X	
14118	50, 200, 500	X		X	X	
14120	500	X	X	X	X	X
14121	500	X	X	X	X	X
14123	500	X		X	X	X
14124	500	X	X	X	X	X
14125	500	X	X	X	X	X
14127	500	X		X	X	X
14130	500	X				

The 200 µm net used during the first leg of the cruise was replaced with a 500 µm mesh conical net (aperture diameter 50 cm) because the high concentrations of phytoplankton (particularly diatom chains, primarily *Chaetoceros* spp, and mucus colonies of *Phaeocystis*) around the front caused the net to clog. However, even the 500 µm net was clogged at some stations. The net was deployed from the CTD winch gantry (Figure 18), mounted on swivels beneath the Fast Repetition Rate Fluorimeter (FRRF). The Towed Undulating Bio-Acoustic (TUBA) instrument was also mounted above the net at stations on Jday 161 (see the TUBA section of this report for more details).

The Mesozooplankton Community Structure

The copepod *Calanus finmarchicus* (CIV, CV and CVI) dominated the zooplankton community in net catches both in terms of biomass and abundance. The 500 µm net did not reliably retain copepodite stages earlier than CIII, and when used, the 50 µm net revealed that naupliae (expected to be *Calanus*) and the small copepod *Oithona* were numerous. Microscopic size spectra measurements were made at selected stations to help assess Optical Plankton Counter (OPC) and TUBA data. Preliminary examination of the zooplankton community indicated that CIV and CVs dominated in the warmer Modified North Atlantic Water (in the south of the survey region) with few CVI females present. In the frontal water CV and CVIs accounted for a larger proportion of the total. Although the survey was to the south of the front, cold northern water was encounted at two stations. In addition to *C. finmarchicus*, this Nordic Water was typified by the copepods *Metridia* sp. (probably *M. longa*) and *C. hyperboreus* and noticeably purple-combed ctenophores. The frontal community was the most diverse with amphipods, chaetognaths, medusae and euphausiids present. The increased species richness in the front suggested that this is an ecotonal community. All samples were fixed in 4% formaldehyde for more detailed analysis later at SOC.

Gut Fluorescence

A sub-sample of each net catch was taken and immediately placed in the -70°C freezer for gut fluorescence analysis. Each sample was then defrosted in low light, and different stages of the dominant zooplankton were picked and placed into 10 ml of acetone for chlorophyll extraction. For *Calanus finmarchicus* between 25-30 CIV, 15-25 CV and CVI females were placed in each vial. The vials were then placed in the -20°C freezer, and left to extract for between 20 and 24 hours. The chlorophyll concentrations were determined fluorometrically in the same way as for filtered chlorophyll samples (see primary productivity and chlorophyll section of this report). Preliminary results showed that gut chlorophyll concentrations per animal were an order of magnitude higher in the fontal water than in the warmer water to the south. Gut clearance rates were not measured but will be defined using constants determined by the water temperature at

each station (Irigoien, 1998). This will enable the ingestion rate of the copepods to be determined.

Egg Production

Egg production incubations were performed on individual female *Calanus finmarchicus* at 16 stations during the second leg of the cruise. Each female was incubated in a 60 ml jar for 24 hours. At 6 stations (F2bS-F2b4) on the fine scale surveys' line b (Jday 165) the jars were incubated for a further 48 hours to examine egg hatching rates. All incubations were fixed (4% formaldehyde) for analysis at SOC.

Benthic Sampling !

A small number of unexpected benthic samples were collected during the second SeaSoar survey ! These have been preserved in 4% formaldehyde.

Bacterioplankton Diversity - *Alex Mustard*

The objective of this work was to collect samples suitable for flow cytometry studies of bacterioplankton diversity, for *Mike Zubkov* at the Plymouth Marine Laboratory. These samples were collected opportunistically, when time allowed. For this reason, the samples were only collected at nine stations: 13992, 13998, 14002, 14007, 14007, 14011, 14017, 14022 and 14033.

A vertical profile of samples was obtained by sampling the CTD Rossette Niskin bottles. Water was drawn from each of the bottles above 300 m (5, 25, 50, 75, 100, 150, 200 and 300 m) and also Niskin 2, which represented the deepest water at each station, away from the influence of the benthic boundary layer.

1.8 ml of seawater from each depth was pipetted into 2 ml microcentrifuge sample tubes, and inoculated with 90 µl of PFA. The seawater and PFA were then mixed using the headspace bubble. The sample tubes were labelled and placed into the refrigerator at a temperature of between +2 °C and +4 °C for 24 hours. On one occasion (Stn. 14017), a change of the fridge temperature to -10 ˚C resulted in the samples being frozen almost immediately after inoculation. After 24 hours in the fridge, the samples were frozen and stored at -20 °C for the remainder of the cruise.

Remotely Sensed Data Acquisition - *Meric Srokosz and Martin Beney*

Sea surface temperature (SST) data and ocean colour derived chlorophyll data were obtained from AVHRR and SeaWiFS respectively. They were acquired at the Dundee satellite receiving station, processed by RSDAS in Plymouth, and sifted at SOC (to find cloud free imagery of

cruise area) before being transmitted to RRS Discovery within 24 hours of acquisition (except at weekends). During Leg 1 of the cruise the SeaWiFS chlorophyll images, though partially cloudy, showed the development and decline of the spring bloom in different parts of the survey area, and were found to correspond to the shipboard observations.

Particularly clear SST and chlorophyll images (Figures 33 and 34) of the Iceland-Faeroes Front (IFF) were obtained on 23rd May showing both interesting dynamics - frontal meandering and eddies – and associated with these, a chlorophyll bloom on the north side of the IFF. These images were partly the reason why the IFF was chosen as the survey area for Leg 2. Although no completely clear images of the IFF were obtained during Leg 2 of the cruise due to cloud cover, several partial images showed the development of the physical and biological structures at the front and matched both the in situ observations and model predictions.

We are grateful to Lisa Redbourn and Cristina Peckett at SOC, and Peter Miller of RSDAS, who ensured that the relevant imagery reached us at sea promptly. We thank NASA for allowing us access to SeaWiFS data in real-time during the period of the cruise.

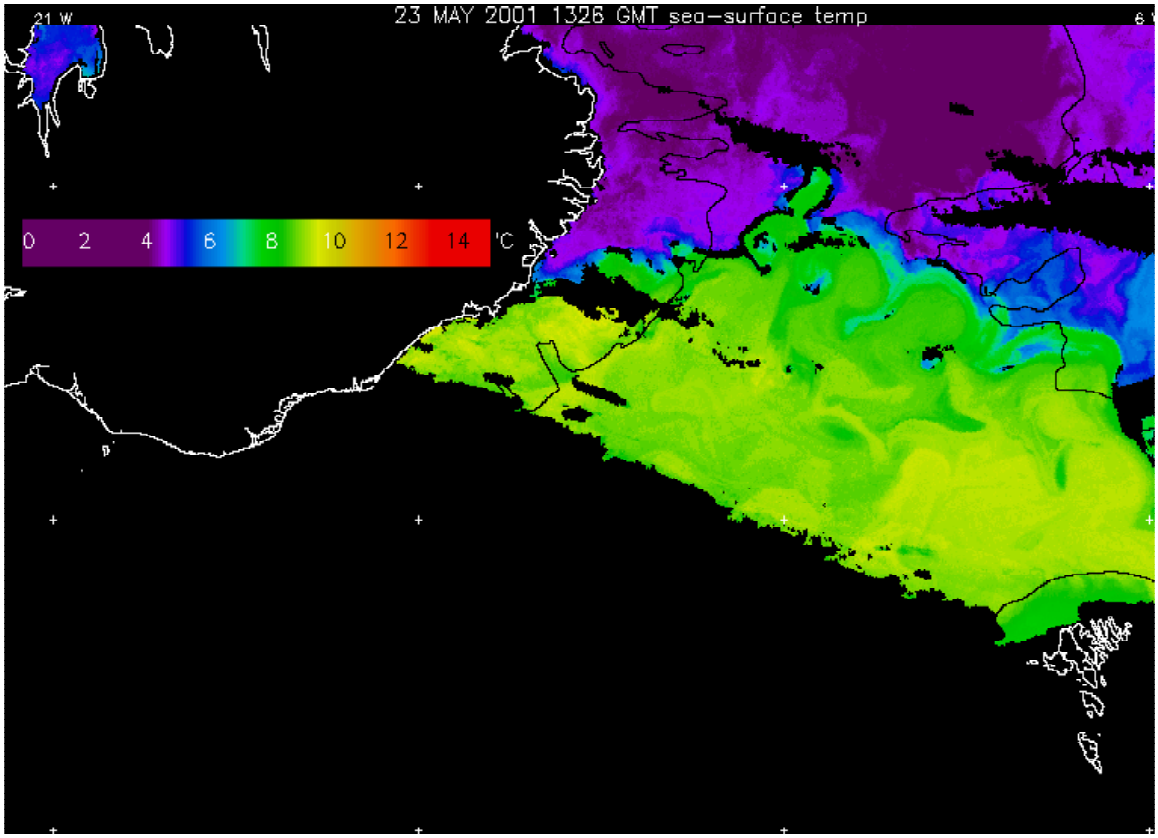

Figure 33. AVHRR SST image of the IFF, 23rd May 2001 (courtesy of RSDAS).

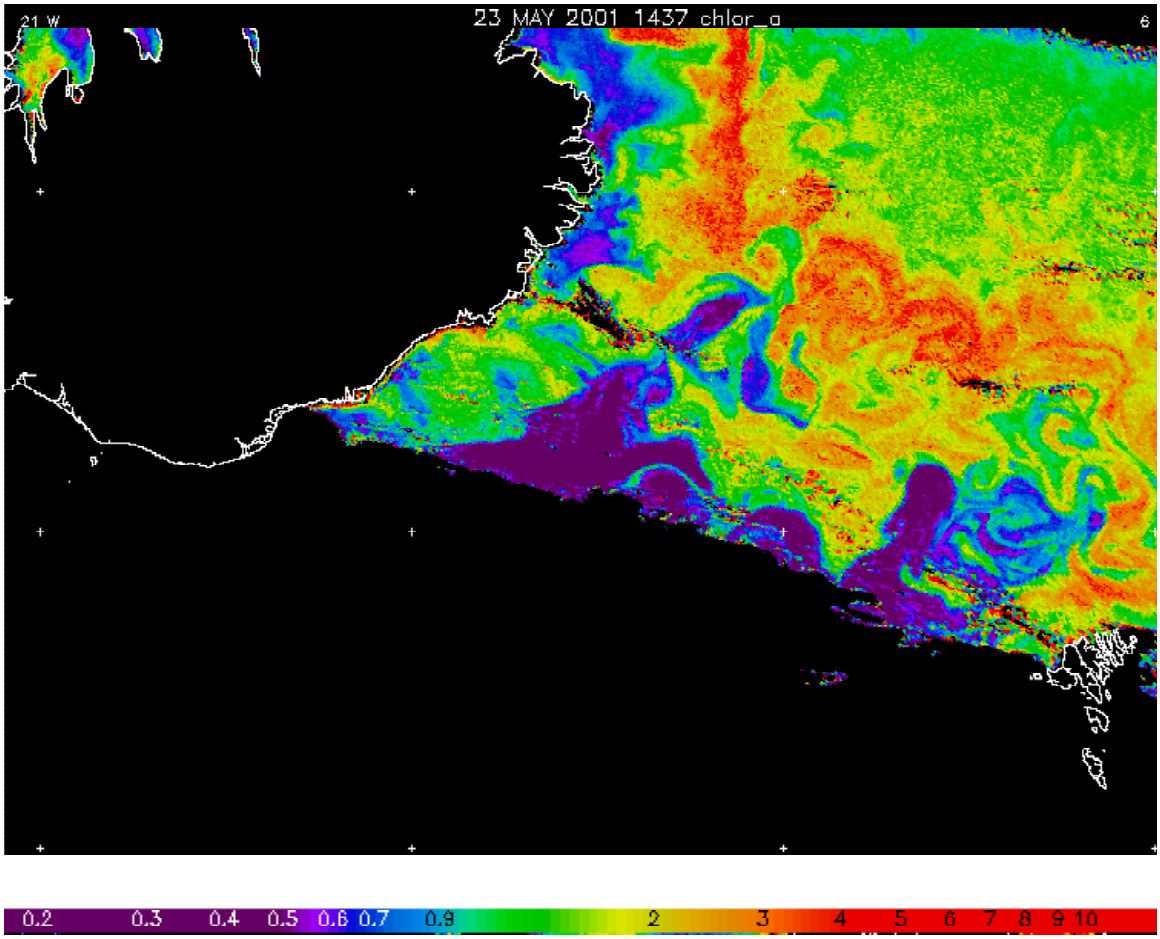

Figure 34. SeaWiFS chlorophyll image of the IFF, 23rd May 2001 (courtesy of RSDAS)

In addition to the above means of acquiring AVHRR data, we were also able to experiment with a new ship system for receiving the data directly from the NOAA polar orbiting satellites. RRS *Discovery* had recently been fitted with a Dartcom HRPT system for the reception and processing of AVHRR data. The data acquired by this provided some insight into the dynamical processes at the front, but the SST algorithm was in error by several degrees. Nevertheless, it was possible to detect frontal meanders and eddies from the relative changes in temperature output by the system. It would be worth investing some future effort in improving the processing algorithms that the system uses, in order to improve SST retrieval. This could be done with the help of RSDAS, who are experienced in processing AVHRR data.

Atmospheric Aerosols - *Paul Nelson*

Atmospheric inputs are now recognised as an important input to the coastal and open ocean. These inputs can be highly episodic, and occasional high-deposition events may have significant

effects on the phytoplankton community. These inputs become even more significant considering that nitrate deposition over the UK has more than doubled over the last 50 years.

During the FISHES cruise, samples of rain, aerosols and air were taken in an attempt to investigate the chemical characteristics of these high-deposition events and as a trial run for a larger project to investigate the significance of atmospheric nitrogen inputs into the northern North Sea, part of the NERC thematic GANE (Global Nitrogen Enrichment) project.

Sampling equipment was deployed on the highest part of the ship that was most accessible, this being the bridge roof, colloquially known as 'Monkey Island'. The sampling equipment needed to be situated at this level to avoid the possible influence of sea spray. Ideally sampling only occurred when the ship was head to wind to avoid contamination from the ships stack. However, due the nature of the cruise and, the optimum sampling time for the aerosol collection and the filter packs being 8-12 hours, this wasn't strictly followed. All sample analysis will be carried out at labs at the University of East Anglia (UEA).

Aerosols were sampled using a Volume Flow Controlled (VFC) aerosol collector with a 3 stage size segregated impactor head and Whatman™ 41 cellulose filters. The size segregation would provide information on the possible origin of the aerosol. Mineral dust tending to be larger than anthropogenic and biologically produced aerosols. Samples would be analysed for ammonium, nitrite, nitrate and organic nitrogen compounds. Samples were placed in plastic bags, (at a later stage when plastic bags became sparse, 50 ml centrifuge tubes were used) then stored in a dry dark area.

Rainfall was sampled using manual wet only collection. This consisted of two large plastic funnels with 120 ml bottles screwed into the bottom, the funnels were attached to the front railing of monkey island and covered until the onset of rain. Once the samples were collected they were capped, doubled bagged and then frozen. Rainwater would be analysed for the same species as the aerosols plus the major cations and anoins (Ca^{+}, K^{+}, Mg^{+}, Na^{+}, Cl^{-}, SO_4^{2-}, PO_4^{3-} and SiO_4^{4-}).

Gaseous ammonia and nitric acid was intended to be sampled using two methods; annular denuders and filter packs. Filter packs can introduce artefacts so denuders were preferable. However, denuders are usually deemed not suitable on a moving ship. Thus the two methods where to be compared. However, this was not possible due to the denuders being damaged at an early stage of the cruise, therefore only filter packs were used during this cruise. The sorption reagents used for ammonia and nitric acid respectively were a 2% solution of oxalic acid in a methanol/glycerol mixture and a 1% solution of sodium carbonate in a methanol/glycerol mixture. The filters were placed in 5 ml plastic vials then frozen.

Problems

As stated above sampling with the denuders was not possible. The design of the denuders brought on this cruise were more suited for land based studies than for boat work. A simpler design of denuder would have been more appropriate, however, flow rate and sorption efficiencies might then have been adversely compromised.

On a number of days sampling was not possible as it was deemed unsafe to be on monkey island during rough conditions (e.g. 27/05/01). These were not too numerous to effect the sampling coverage.

AutoFlux Meteorology - *Penny Holliday and Steven Alderson*

Autoflux – Experiences of a Watch-Keeper

Although the Autoflux package was designed to be self-contained, during this "proof-of-concept" period watch-keepers were asked to keep an eye on the system to look for failures and shortcomings. As it happens there were a few of those, and this section describes them and makes suggestions for system improvements.

The most obvious initial difficulty was with the Orbcomm system; the method by which data messages were sent back to base by satellite transmission. Tests performed prior to the cruise suggested the system was functioning, but once we were underway it became clear that no messages were getting through. The Orbcomm program window suggested messages were being sent, and gave all the indications that it was seeing satellites, however, no messages were received at SOC. After many unsuccessful attempts to reset the Orbcomm box by powering it down, the decision was made to replace the unit in Lerwick. A new unit was duly dispatched with the personnel joining the ship for Leg 2: and, after a period during which registration was completed, the new unit began sending data back to SOC. A small glitch occurred during days 163-165 when Orbcomm sent the same message repeatedly. Re-starting the Orbcomm program did not result in new messages, but a reboot of the workstation and hence complete re-start of the entire system seemed to sort things out. The cause of the error was never established, but the suspicion lies with a sustained period of no navigation fixes causing problems with the Autoflux calculations.

Once a day the IfM H_20/CO_2 sensor was given a cleansing squirt of fresh water by flipping a switch on the control unit. The reservoir of freshwater was small, and, since the balmy weather enjoyed on Leg 1 meant that little rainfall was collected, after about 2 weeks the squirting was dry. We suggest a larger reservoir for long cruises, or some way to easily refill with fresh water.

Early in the cruise the issue of time syncronisation provided much entertainment. Autoflux received GPS position and time information, and the time sync program adjusted the workstation clock to match the GPS time. In theory the GPS time could occasionally be a duff one, and the program would bring up a dialogue box asking the user if they wanted to correct the workstation time if there was a difference of greater than 10 seconds. In practice this box appeared very frequently, and the temptation to press "Yes" was too strong in the early days. In that case the time adjustment, far from being the 10 secs alluded to in the box, seemed to be more like 1000 secs over a long period of time. The time sync program ignored the resulting huge time difference, and the only safe option was to reboot the workstation and manually adjust the time. Our suggestion would be to remove the tempting box, and/or to check that when a time adjustment of 10 secs is made, that the correct offset is applied by the software.

The Autoflux package included a gyro compass situated on the bench in the main lab. To one side of the compass were all the Autoflux paraphernalia, to the other side was a PC, and behind it the SeaBird CTD deck unit. Somewhere around the middle of Leg 2 some observant watch-keepers noticed that the heading was incorrect. On closer inspection it became obvious that the gyro compass wandered freely over a range of about 30° over a few seconds during steaming, and may be as much as 100° away from the true heading.

After listing all these problems, however, it is worth mentioning that the Autoflux package was almost entirely self-sufficient and did run very smoothly. We cannot comment on the quality of the data, but the scripts processing the data appeared to be successful throughout the entire cruise, a remarkable achievement in itself.

Data Assimilation - *Ekaterina Popova, and Meric Srokosz*

As part of the second leg of the FISHES cruise an attempt was made to predict in real-time both physical and biological ocean processes at the meso-scale on-board the ship. The aims were a) to allow better understanding of asynoptically acquired data, and b) to attempt to optimise the cruise sampling strategy in near real-time. The area chosen for the three repeated surveys in Leg 2 was the Iceland-Faeroes Front (IFF). The IFF has been the subject of previous real-time forecasting attempts (Robinson et al., 1996) but this was the first attempt to include biological forecasting.

Data Assimilated

The primary tool used for acquiring data for assimilation into the model was the SeaSoar. It provided calibrated data on temperature (T), salinity (S), chlorophyll-*a* (chl-*a*) and mesozooplankton (size classes 250-500, 500-1000 and 1000-2000 μm), which were assimilated into the model. Additionally, nitrate data from half-hourly underway sampling (water intake at

5m) and CTD stations were assimilated. Between the three SeaSoar surveys, a number of CTD casts and vertical net hauls were carried out. Primary production experiments provided values that were used to constrain the biological model, and the net hauls gave insight into the zooplankton present (as the OPC only provided bio-volume estimates).

Surface Forcing Fields

The surface fluxes necessary to force the model were obtained from ECMWF 10 day forecast fields. The parameters used were; both components of the wind stress, latent and sensible surface heat flux, evaporation and precipitation, surface solar and thermal radiation. In addition, the 10 m wind velocity was also obtained, and this proved useful in understanding the local conditions at sea (though it was not necessary for forcing the model). For the first 72 hours of the forecast, the data were provided 3 hourly, thereafter 6 hourly. The data were available on a 0.5° latitude-longitude grid covering the area of interest. The data were obtained from ECMWF by via the BADC (British Atmospheric Data Centre). The data were extracted from the noon forecast of the previous day and e-mailed to RRS *Discovery* by 10:30 GMT. An attempt was made to automate this process so that forecasts could be received at the ship daily, but this did not work. Therefore the forecasts were forwarded manually on the Monday, Wednesday and Friday of each week of the cruise. This provided adequate forcing data from the on-board model predictions. While these data may not be crucial for short period (10 day) dynamical forecasts, they were important for determining the mixed layer dynamics that influence the biology.

During the cruise there were two periods of strong winds and it was found that the ship measured wind speed was typically 1.5 times stronger than the ECMWF forecast wind. This meant that the ECMWF wind stress during these periods may have been too small (approximately half the true value). This will have affected the predicted mixed layer dynamics and hence the biological predictions.

Model

Our basic forecasting tool onboard RRS *Discovery* was the Harvard Ocean Prediction System (HOPS). The physical module of the HOPS (Robinson, 1996) was based on a primitive equation (PE) open boundary model under hydrostatic, Boussinesq and rigid lid approximations. The assimilation methodology used was an intermittent optimal interpolation scheme. The biological model used was based on the model of Fasham et al. (1990) reduced to five variables: phytoplankton (P), zooplankton (Z), nitrate (N), ammonium (A), and detritus (D).

The zooplankton, Z, compartment presented a significant problem because in the original model it described fast growing zooplankton, which include microzooplankton and possibly the smallest class of mesozooplankton (up to about 500 µm). During the cruise some parts of the

area were dominated by large diatoms, most likely experiencing strongest grazing pressure from mesozooplankton larger than 500 µm. This was supported by net hauls, that showed these areas had the largest biomass of zooplankton of 500-4000 µm size class. The rest of the survey area was dominated by small phytoplankton (mainly less than 20 µm as was seen from fractionated primary production measurements) and had the lowest biomass of all sizes of mesozooplankton. In such areas microzooplankton would be the dominant grazer. Lack of microzooplankton measurements made it difficult to model an area dominated by small phytoplankton cells, as a microzooplankton field would be required to initialise the model. Results from a few sensitivity experiments were compared with available data on chl-*a*, mesozooplankton, nitrate and fractionated primary production. These showed that the best zooplankton modelling strategy was as follows. The zooplankton compartment, Z, should include microzooplankton and the smallest mesozooplankton class (250-500 µm) measured by the OPC. Mesozooplankton of 500-2000 µm size class were also available from the OPC measurements and were introduced into the model as a sort of 3D external forcing field (Z_L) which could be advected and diffused along with the other biological variables but did not have its own biological dynamics. Such an approach was justified by the low growth rate (compared with phyto- and microzooplankton) of larger species of mesozooplankton, which would be expected to be negligible over the time scale of our prediction (less than 2 weeks). Introduction of such an additional zooplankton field allowed us to model the grazing pressure of the mesozooplankton on smaller zooplankton and phytoplankton, as well as the excretion of ammonium.

To overcome the lack of data on microzooplankton for model initialisation and data assimilation of Z, we made an assumption that its biomass was negatively correlated with mesozooplankton (which in its turn was positively correlated with phytoplankton biomass). A set of sensitivity experiments showed that the best fit to all available biological measurements could be obtained if initial and assimilation Z fields were calculated in the UML from the following equation

$$Z = Z_{250-500} + \left(\frac{1 - Z_L}{4} \right) \tag{41}$$

where $Z_{250-500}$ was the biomass of mesozooplankton of 250-500 µm size class. For two more model variables (D and A) there were no measurements to create initialisation and assimilation fields. As these did not play a major role in the ecosystem dynamics on our prediction time scale, ammonium concentration (A) was taken as 5% of nitrate, and detritus concentration (D) as 10% of phytoplankton (based on Fasham, 1995).

The model domain (Figure 35) was centred on the survey area at 64.2 °N, 10 °W with an eastward rotation of 30°. The horizontal resolution was 2.5 km on a 71×55 grid, with 49 terrain following depth levels providing a resolution of 5 m in the upper 55 m and about 200 m near the bottom in the deepest part of the area. A time step of 5 minutes was used. With this spatial and temporal resolution a 10 day coupled physical and biological model run with sequential data assimilation took about 5 hours on a Sun Ultra 10 workstation (786 Mbyte memory, 440 Mhz UltraSparc IIi processor, 2×9 Gbyte disks). Objective analysis of the data and preparation of the initialisation and assimilation fields took about 3 hours. This time-scale (~8 hours) proved to be optimal at sea and made daily forecasting possible during the three SeaSoar surveys when daily updates to the data were acquired.

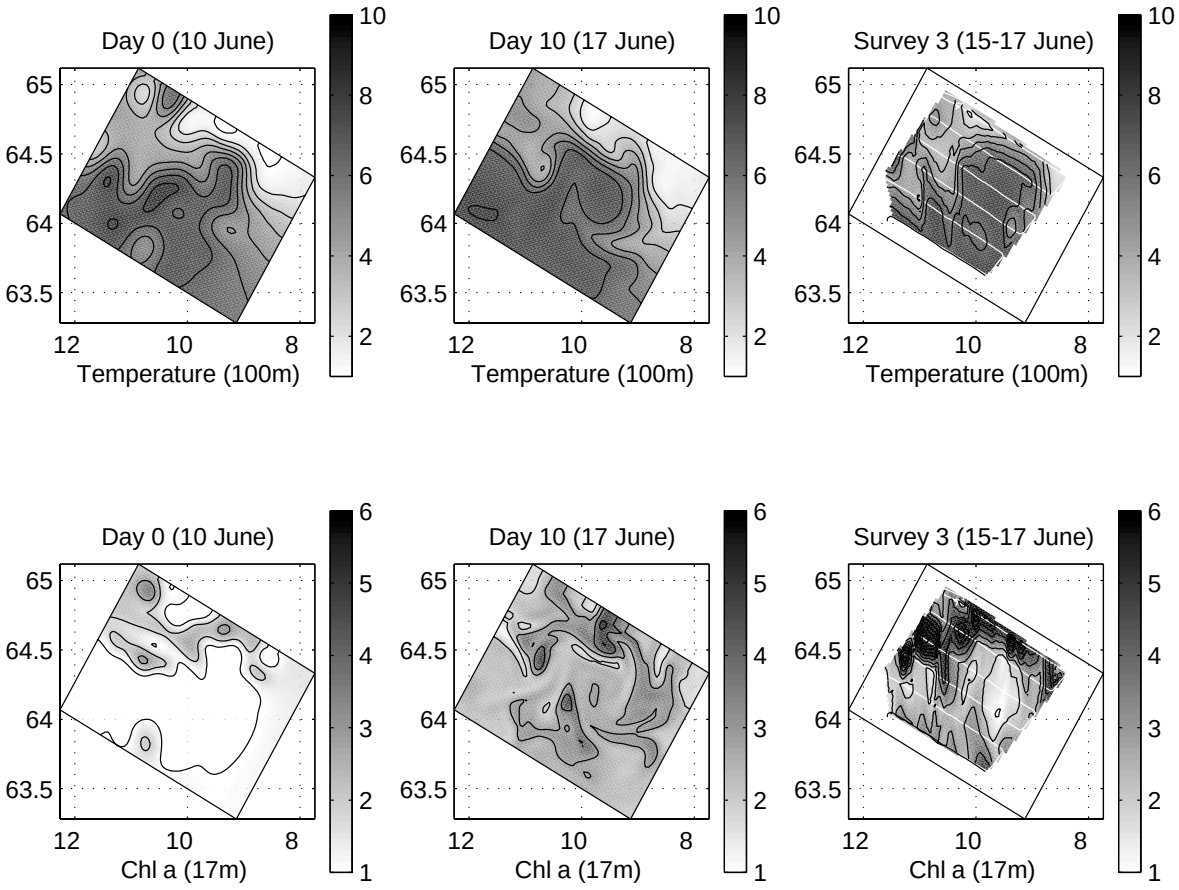

Figure 35. Left – model initialised fields for temperature (100m) and chlorophyll-a (17m). Middle - model predicted fields for same variables on day 10 (June 17). Right – Observed values of variables during SeaSoar survey 3 (15-17 June).

The model was initialised with objectively analysed data collected during the first survey. Day 158 (7 June) was designated as model day 0 (Figure 35). During the first 24 hours of the model run, T, S and biological tracers were held fixed to allow adjustment of the initial velocity field

obtained from geostrophic balance to the T and S fields. The first 15 days forecast was issued within 12 hours after completion of the first SeaSoar survey. This forecast was updated when data from the second SeaSoar survey became available. All data from the second SeaSoar survey were sequentially assimilated into the model between days 4 and 6.5. The results of this forecast for day 10 (17 June) corresponding to end of the third SeaSoar survey and thus data collected during the third SeaSoar survey are also shown in Figure 35.

Results

Figure 35 clearly showed the success of the model in predicting the warm anti-cyclonic, almost detached, meander centred at ~64.2 ˚N, 9.5 ˚W, and some of the colder intrusions from north of the IFF. The biological prediction (here for chlorophyll-*a*) captured the minimum value in the centre of the eddy, but underestimated the values in the colder water to the north. Probably, this was due to the fact that the larger mesozooplankton grazing parameter was set somewhat too high in the model. Note that the larger mesozooplankton were abundant in the colder waters to the north, but almost non-existent in the warmer water to the south, hence the better chlorophyll-*a* prediction there. The results could have been easily improved by changing the mesozooplankton grazing rate.

Survey Optimisation

The output from the model was used to optimise the survey strategy for the third SeaSoar survey, see the discussion in the following section.

Conclusions

Overall, the data assimilation and then prediction of both biology and physics at sea in near real-time can be considered to have been a success and to have met the initial aims of the study (see above). Therefore this approache provides a useful sea-going tool for interdisciplinary studies of physics and biology. It was, as far as we are aware, the first successful prediction of biological processes at the meso-scale in the open ocean.

Techniques for Optimal Environment Sampling (TOES) - *Michel Rixen, John Allen, Steven Alderson, Vic Cornell, Ekaterina Popova and Meric Srokosz*

RRS *Discovery* cruise D253, FISHES, was opportunistically used by TOES, a project which aimed to develop techniques for optimal environmental sampling. The 3 consecutive SeaSoar surveys during the second leg of the cruise, were initially designed according to previous knowledge of the Iceland-Færœs frontal area. However, recently published work within the TOES project had shown that the usual sampling strategies, i.e. with sampling legs across the

front, might not be ideal in all cases (Allen et al. 2001). Indeed they might result in significant distortion of the true field by modifying the apparent wave number of dominant instability modes, and thus lead to incorrectly diagnosed dynamic parameters. Several methods had also been proposed to correct *a posteriori* these biases (Rixen et al. 2001). The purpose of the present study was to optimise the sampling according to a real-time *a priori* knowledge of the dynamics of the area.

A preliminary study was based on a SST satellite image (23rd of May) provided by PML (*P. Miller*), the most recent cloud-free image of the area at that time. A sequence of images was then constructed by assuming a wave speed of 0.09 ms^{-1}. Qualitatively, the optimal solution obtained was similar to the results described hereafter.

Optimal interpolation data assimilation of the first two SeaSoar surveys into a 3D PE model (HOPS model, discussed in the previous section) provided a sequence of fields, which were then sub-sampled according to typical snake-like sampling patterns, with free ship time, ship velocity, station time, number of stations, leg length and separation, rotation, shear and translation, left-right and upside-down flip (Figure 36). These stations were then objectively analysed and the resulting fields were compared to a model snapshot at jday 167 12:00, corresponding to the middle time of SeaSoar survey 3. The cost function used was the RMS field difference over the whole area between this snapshot and the reconstructed field.

The sampling strategy free parameters were optimised by genetic algorithms. Starting with an initial random population, the fittest solutions were selected, crossed-over and mutated, by biological analogy, until convergence to a minimum cost. This method also had the important advantage of being initialisation independent. The station number was set to 200 to limit computation and the time on station twas set to 0. The optimal solution found showed that legs should be orientated along the front, and that the whole ship time (2.5 days) and full speed (4 ms^{-1} with SeaSoar) needed to be used. Leg length covered the whole domain and the separation obtained (20 km) was slightly less than for the first two surveys. Computation time was less than 45 minutes which made the technique suitable for operational purposes.

Several sensitivity tests had shown that the solution was robust and consistent for the different hydrodynamic and biological parameters. Moreover, a similar optimisation using a cost function dependent on gradients or curvature of the reconstructed field also led to similar sampling strategies, although the solution was, as expected concentrated in the more dynamic northern area.

Consequently, it was decided to perform the third SeaSoar survey with legs oriented along the front (Figure 3). The optimal survey was then slightly modified to cover the whole sampling

area, as the luxury of knowing *a priori* that the southern part of the survey may be dynamically quiescent could have been a modelling artefact.

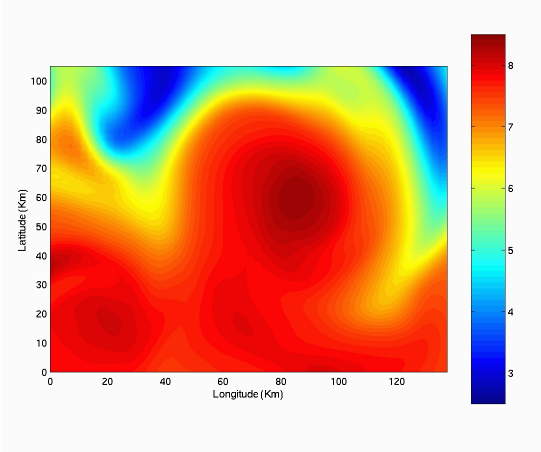

(1)

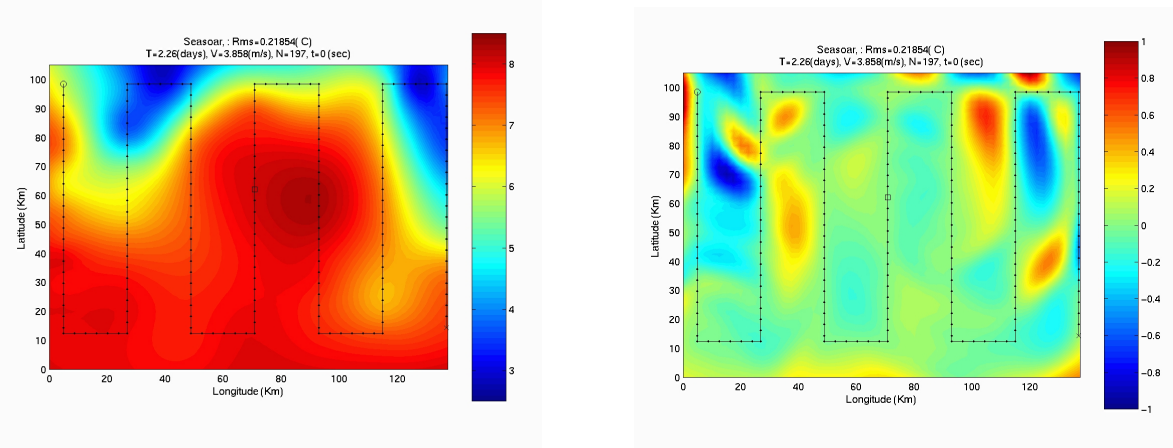

(2)

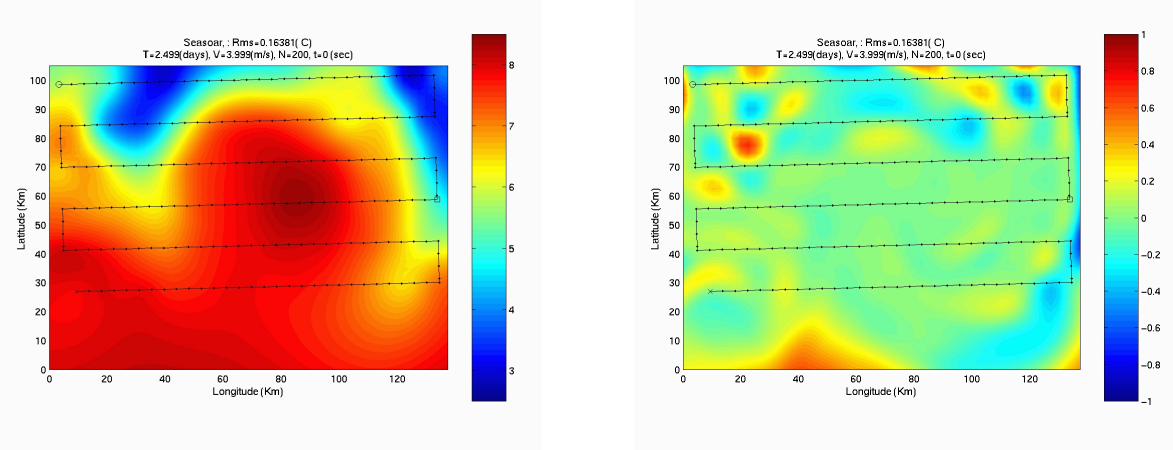

(3)

Figure 36. From top to bottom: (1) model snapshot (temperature) at jday 165, 12:00; (2) classical sampling strategy (with legs across the front) optimised for all parameters, but no rotation allowed; (3) fully optimised sampling strategy: legs are along front. Figures on the right show the error between the model output and the corresponding derived temperature field on the left.

7. DISCUSSION OF EARLY RESULTS

Jane Read, Raymond Pollard, Louise Brown and John Allen

Many detailed surveys have been made in the subpolar North Atlantic during the past decade. However, descriptions of the circulation vary in their pattern and magnitude. Satellite studies and eddy resolving ocean models indicate that eddies may dominate mean currents in some regions, effectively aliasing traditional basin scale ocean observations. However the region is important climatically and biologically. It is an area of cooling and deep winter mixing. Zooplankton distributions (specifically the copepod *Calanus finmarchicus*) are heavily constrained by the circulation. Thus it is an important area to understand dynamically.

Surveys made in the subpolar North Atlantic in 1996 (Pollard et al. 1999) and during leg 1 of this, the FISHES cruise in 2001, were designed to investigate the pathways of the North Atlantic Current and distinguish areas of eddy activity, particularly in the region between Iceland and Scotland. An upper ocean SeaSoar survey (0-400 m) with scattered full depth CTD casts was made in Oct-Nov 1996 (Vivaldi'96). Extending from west of Ireland and Scotland to East Greenland it showed clear current paths of warm stratified water flowing into the region and deep winter mixed sub-polar mode water to the east and in the north Iceland Basin. However the vertical extent of mode water was greater than the SeaSoar could survey. Thus this second survey during leg 1 of the FISHES cruise, using full depth CTD casts was made in May-June to investigate the end of winter distribution of mode water. FISHES 2001 concentrated on the region between Iceland, the Færœs and Scotland. Early results showed a large area of weakly stratified water extending 500-600 m vertically and spreading westwards from the Scottish shelf edge between the Rockall-Hatton and the Færœ Plateaux out into the Iceland Basin. Circulation was weak and no clear current paths were apparent, but topography clearly influenced the distribution of mode water.

There was considerable influence of water from the Greenland/Norwegian Seas in the FISHES survey area. The overflow water entered via the Færœ Shetland Channel and over the Iceland Faroes Ridge. This descended rapidly to the bottom, so underlying the Labrador Sea Water (LSW) over most of the deep basin. It also mixed with surface mode waters (which extended to several hundred metres deep) so it could be inferred also in the T/S relation of water on the N and W flanks of the Iceland Basin, especially along the Reykjanes Ridge.

Another interesting result was that very little evidence could be found of flow in from the south into the north Iceland Basin. In contrast, Vivaldi 1996 (Pollard et al. 1999) found something like 12 Sverdrup (Sv) flowing up from the south, evidenced by a clear Sub-Arctic Intermediate Water (SAIW) signature a few hundred metres deep.

The silicate uptake incubation experiments were a particularly novel aspect to the research carried out during FISHES leg 1. Early analyses indicated Si uptake at low light levels and in the dark suggesting limited light dependence to the mechanism. Water column integrated Si uptake values for non-bloom conditions were typical of values reported for the Southern Ocean but the uptake values for stations in near bloom conditions were high. Furthermore, mean euphotic zone $Si(OH)_4$ concentration appeared to provide an indicator of diatom bloom progress. Si uptake rates were highest at Si concentrations > 2 µM. P-max (primary productivity) was also highest at $Si(OH)_4$ > 2 µM leading to further confirmation that diatoms were therefore the key species at the peak of the spring bloom.

For the second leg of FISHES, RRS *Discovery* cruise 253, we demonstrated truly responsive mode multi-disciplinary operational oceanography. During the first leg of the cruise we had directly observed rapid variations in zooplankton biomass (Figure 37) across the Iceland Færœs Rise associated with the sharp changes in water mass characteristics associated with the IFF. Ocean colour satellite images (Figure 34) also indicated that the spring bloom had begun in the vicinity of the IFF but was probably spent further south; the latter had been confirmed by the observations of diatom biomass sinking out of the surface layers during leg 1 of the cruise (Figure 38). The satellite images also indicated that mesoscale meandering of the IFF was at least as pronounced in ocean colour as in infra-red images (Figure 33); suggesting that biological patchiness was dominated by physical processes over the Iceland Færœs Rise.

Figure 37. Zooplankton samples, separated by just tens of kilometres across the IFF, changed colour like traffic lights. Amber to the south of the front, green within the frontal jet and red in the chilly Nordic waters to the north (right to left).

In response, a SeaSoar survey region was determined from the satellite images and a regional multidisciplinary numerical model was initialised at the beginning of the second leg of the

cruise, whilst steaming. The numerical model output indicated that the meandering eddy like structures observed in the satellite images were the result of instability of the IFF and that an along front sampling interval of no coarser than 15 km would be necessary to resolve the dominant scale of instability. SeaSoar fine scale survey 1 (FSS1) was therefore designed to have 15 km spacing between conventional cross-front parallel legs carried out in a downstream direction relative to the along front flow. Data from FSS1 were then assimilated into the numerical model as quickly as they could be processed and roughly calibrated. The model forecasts were then used to choose a suitable line for LHPR tows and, CTD and net sampling stations, within the time constraint of 24 hours between SeaSoar surveys.

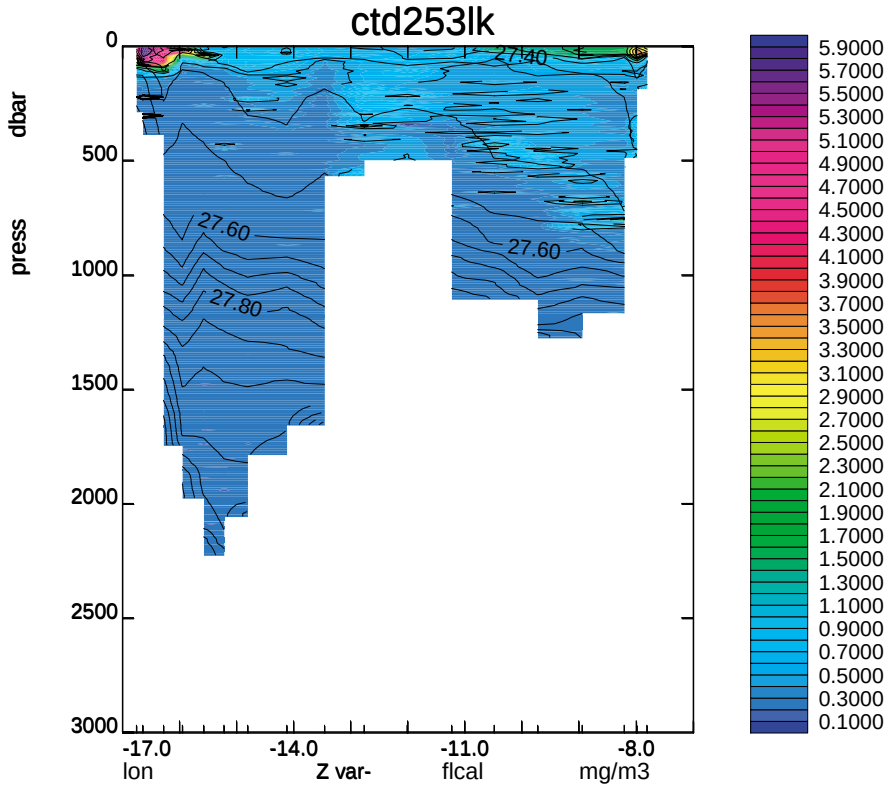

Figure 38. Contoured uncalibrated fluorescence data for leg LK of the leg 1 CTD survey, density contours are over-plotted for reference. A sinking layer of phytoplankton is clearly indicated to depths in excess of 700 m.

The numerical model forecasts and satellite images confirmed that the propagation speed of the wave like meanders and eddy structures along the IFF was much less than the effective along front sampling speed of our SeaSoar survey: i.e. FSS1 was quasi-synoptic with regard to the mesoscale instability of the IFF (Allen et al. 2001). Using a genetic algorithms technique to develop a survey strategy through the forecast model output, optimising sampling according to the mapping error in horizontal temperature gradients, we were able to show that an upstream survey pattern would not increase sampling error and that a less conventional survey of more widely spaced parallel legs in line with the mean direction of the frontal jet could significantly

reduce sampling error. Therefore, FSS2 was designed as an upstream repeat of FSS1 with an extra leg at the beginning, i.e. eastern end, of the survey.

Once again, data from FSS2 were assimilated into the numerical model as quickly as they could be processed and roughly calibrated. And, the model forecasts were then used to choose a suitable line for LHPR tows and, CTD and net sampling stations, within the time constraint of 24 hours between SeaSoar surveys. The genetic algorithms development of an optimised survey pattern continued to propose a survey of parallel legs in line with the IFF and therefore FSS3 was determined objectively by this means. To our knowledge this was the first time that an objective approach to optimise sampling strategies according to forecast mapping error has been applied in real-time during an oceanographic observational programme. This was a significant achievement for our TOES project (Techniques for Optimising Environmental Surveys) and a good demonstration of the operational oceanographic capability of the SOC and the UK's oceanographic community as a whole.

Early analysis shows a striking difference in the dynamical processes observed at the mesoscale during leg 2 of FISHES and a previous similarly detailed SeaSoar survey of the IFF in the summer of 1990. During RRS *Charles Darwin* cruise CD51, the mesoscale instability at the IFF was dominated by small (15-30 km), cold, cyclonic eddies and meanders, and, it was deduced, so too was the eddy transport (Allen et al. 1996). In contrast, both the forecast modelling and the repeated SeaSoar surveys during leg 2 of the FISHES cruise have shown the instability of the IFF to be dominated by 50-60 km anticyclonic meanders from the warm side of the front. CD51 took place considerably later in the year of 1990, and a strong surface mixed layer existed across the IFF in that data set which was not present during FISHES. This meant that there was a significant biological consequence to the observed dominance of anticyclonic meanders during FISHES; the surface waters were weakly stratified to over 100 m within the anticyclonic meanders and on the southern side of the IFF in general, holding back the spring bloom which had already begun on the north, cyclonic, side of the front.

Acknowledgements

As I began to compile these acknowledgements I quickly realised that they were to form a sizeable tome in their own right. This confirmed my previous convictions that the overwhelming success of RRS *Discovery* D253 was principally due to the outstanding teamwork achieved by the officers, crew, engineers and scientists involved in the cruise. This was a multidisciplinary cruise with a particularly full sampling schedule; the cruise fully met its objectives due to the significant enthusiasm, patience and professionalism of all the officers and crew.

Rhys Roberts, Bob Keogh, and Ritchie Phipps formed a invaluable team on board the FISHES cruise that requires special mention. Supporting 24 hour CTD station work with associated

biological net hauls in a tightly packed cruise scheduled required a significant time management effort to avoid wasted time swapping between hydro and pennant winch operations whilst maintaining high safety standards. The number of CTD stations achieved, more than 130 stations in 23 days, is a direct credit to their efforts. Further to this, significant engineering for real time platform development was provided by *Rhys, Bob and Ritchie* during the cruise. This was particularly helpful during the second leg of the cruise following a suggestion that the Longurst Hardy Plankton Recorder (LHPR) could be towed from the SeaSoar cable. Having a multi-cored conducting cable provided the opportunity to acquire data from both an Optical Plankton Counter (OPC) and the TUBA acoustic instrument concurrently with the traditional net sampling mechanism. Thus a bridle extension was manufactured to take a SeaSoar style termination and three instrument clamp systems were designed and built in approximately 4 days. This was an achievement that they should feel justly proud of and which has pushed our observational research capabilities forward.

John Smithers particularly thanks and sends his best wishes to all aboard RRS *Discovery* for making this, his last cruise before retirement, a most enjoyable experience and for the help and friendship given over many years.

Regarding those back at SOC, our thanks to *Bob* (*Ace) Wallace* and *Kevin Saw* for their experience and invaluable contributions without which PENGUIN and the 'new' SeaSoar would not have been ready for this cruise. *Kevin Saw* draughted the revised SeaSoar body, the new launch/recovery frame and the pressure case and internal frame for the new PENGUIN data handling unit; interfacing closely with the scientists and engineers involved in the project. In addition he organised construction and the ordering of components, negotiating for sensible costings where necessary. I ask you to note that the starting point here was putting the original SeaSoar into a CAD package as few formal drawings were in existence to begin with. *Ace Wallace* then built up the two revised SeaSoar bodies, using his wealth of past experience to suggest modifications where necessary. *Ace* was instrumental in the design of the launch/recovery frame and the decision to try stiff aluminium tail planes. The revised SeaSoar flies better than anyone can remember SeaSoar flying in the past. An attitude sensor indicated near level flight when ascending or descending and typical roll angles of ± 3°. For the first time in ~25 years the revised vehicle now appears to fly in a level position with ascending and descending simply achieved through wing angle, as originally designed, rather than with the body following the wing angle possibly creating near stall conditions. As a result the vehicle payload is significantly increased and the depth achieved on a given cable length has been increased (485 m on <700 m of cable out).

As PSO, I send my personal thanks to *Pam Talbot* for taking on the majority of the mundane organisational jobs prior to both legs of the cruise and keeping in close touch with us at sea. These complicated multi-disciplinary, multi-institutional cruises simply couldn't function

without well organised secretarial and administrative support. My thanks also to *Cristina Peckett and Lisa Redbourn-Marsh* for their part in keeping us supplied with satellite data, *Jane Read* for handling FISHES data requests in the months following the cruise, and *Louise Allen* for collating most of the individual components of this report.

Our thanks to *Luca Centurioni* and *Brian King* for preparation of the floats prior to the cruise.

We thank the DERA for their support of a number of staff involved in FISHES through the opportunistic exploitation and development of the TOES Joint Grant Scheme project.

Finally, if I have forgotten anyone, I apologise. I am tired, this report has taken a lot of preparation, but the quality of the various inputs has justly deserved my time and I hope that future readers are as excited as I am by the breadth of observations presented here.

John Allen

References

Allen, J. T., D. A. Smeed and A. L. Chadwick (1994). Eddies And Mixing at the Iceland Færœs Front. *Deep Sea Research 1*, **41**, No. 1, pp. 51-79.

Allen, J. T., D. A. Smeed, A. J. G. Nurser, J. W. Zhang and M. Rixen (2001). Diagnosing vertical velocities with the QG omega equation: an examination of the errors due to sampling strategy. *Deep Sea Research 1*, **48**, 315-346.

Allen J. T. and D. A. Smeed (1996) Potential vorticity and vertical velocity at the Iceland Færoes Front. *Journal of Physical Oceanography*, **26**, 2611-2634.

Astthorsson O. S., I. Hallgrimsson and G. S. Jonsson (1983) Variations in zooplankton densities in Icelandic waters in spring during the years 1961-1982. *Rit Fiskideildar*, **7**, 73-113.

Bacon S. (1997) Circulation and fluxes in the North Atlantic between Greenland and Ireland. *Journal of Physical Oceanography*, **27**, 1420-1435.

Bersch M., J. Meincke and A. Sy (1999) Interannual thermohaline changes in the northern North Atlantic 1991-1996. *Deep-Sea Research*, **46**, 55-75.

Brown C. W. and J. A. Yoder (1994) Coccolithophorid blooms in the global ocean. *Journal of Geophysical Research*, **99(C)**, 7467-7482.

Bryant (1999) TASC Model-data integration workshop in Trondheim. *Globec News*, **5**, 14-15.

Brzezinski, M.A., and Phillips, D.R. 1998 Evaluation of 32Si as a tracer for measuring silica production rates in marine waters. *Limnology and Oceanography* **42(5)**, 856-865

Crisp N. A., V. Cornell, J. T. Allen and S. G. Alderson (2000). TOES-Techniques for optimising environmental sampling. Southampton Oceanography Centre, Research and Consultancy Report No. 49, 71pp.

Culberson, C. H. and S. Huang (1987). Automated amperometric oxygen titration. *Deep-Sea Research*, 34, 875-880.

Culberson, C. H. (1991). 15pp in the WOCE Operations Manual (WHP Operations and Methods) WHPO 91/1, Woods Hole.

Cunningham, S. A. et al. (2000). RRS "Discovery" Cruise 242, 07 Sep-06 Oct 1999. Atlantic - Norwegian Exchanges. Southampton Oceanography Centre Cruise Report No. 28, 128 pp.

Dam H. G. and W. T. Peterson (1988) The effect of temperature on the gut clearance rate constant of planktonic copepods. *Journal of Experimental Marine Biology and Ecology*, **123**, 1-14.

Dugdale, R. C. and J. J. Goering (1967) Uptake of new and regenerated forms of nitrogen in primary productivity. *Limnol. Oceanogr*. **12**, 196-206.

Fasham M.J.R., Ducklow H.W. and McKelvie S.M. 1990 A nitrogen-based model of plankton dynamics in the oceanic mixed layer, *J. Mar. Res*., 48, 591-639.

Fasham M.J.R. 1995 Variations in the seasonal cycle of biological production in subarctic oceans: a sensitivity analysis, *Deep-Sea Res* I, 42, 1111-1149.

Fielding, S., N. Crisp, J. T. Allen, M. C. Hartman, B. Rabe and H. S. J. Roe (2001). Mesoscale subduction at the Almeria-Oran front. Part 2: biophysical interactions. *Journal of Marine Systems*, [in press].

Fraser J. H. (1961) The plankton of the Iceland-Færœ Ridge. *Conseil Internationale Exploration de la Mer*, **149**, 179-182.

Gislason A. and O. A. Astthorsson (1998a) Variability in the population structure of *Calanus finmarchicus* in Icelandic waters in spring. *ICES Journal of Marine Science*, **55**, 811-813.

Gislason A. and O. S. Astthorsson (1998b) Seasonal variations in biomass, abundance and composition of zooplankton in the subarctic waters north of Iceland. *Polar Biology*, **20**, 85-94.

Glibert, P. M. et al., (1982) Isotope dilution models of uptake and remineralization of ammonium by marine phytoplankton. *Limnol. Oceanogr*. **27**, 639-650.

Goeyens, L. et al., (1998) A room temperature procedure for the manual determination of urea in seawater. *Est. Coast. Shelf. Sci*., **47**, 415-418.

Gudmundsson K. (1998) Long-term variation in phytoplankton productivity during spring in Icelandic waters. *ICES Journal of Marine Science*, **55**, 635-643.

Hansen B., K. M. H. Larsen, S. Østerhus, W. Turrell and S. Jónsson (1999) The Atlantic Water inflow to the Nordic Seas. *International WOCE Newsletter*, **35**, 33-25.

Holley, S. E. and D. J. Hydes (1995). Procedures for the determination of dissolved oxygen in seawater. JRC Internal Document 20, 38 pp.

Holliday N. P., R. T. Pollard, J. F. Read and H. Leach (2000). Water mass properties and fluxes in the Rockall Trough; 1975 to 1998. *Deep-Sea Research I*, **47**(7), 1303-1332.

Holliday, N. P. (2000). CTD data quality on RRS "Discovery" Cruise 242, September-October 1999. Southampton Oceanography Centre Internal Document No. 62, 28pp.

Holligan P. M., E. Fernández, J. Aiken, W. M. Balch, P. Boyd, P. H. Burkill, M. Finch, S. B. Groom, G. Malin, K. Muller, D. A. Purdie, C. Robinson, C. C. Trees, S. M. Turner and P. van der Wal (1993) A biogeochemical study of the coccolithophore, *Emiliania huxleyi*, in the North Atlantic. *Global Biogeochemical Cycles*, **7**, 879-900.

Holmes, R. M. et al., (1999) A simple and precise method for measuring ammonium in marine and freshwater ecosystems. *Can. J. Fish. Aquat. Sci*., **56**, 1801-1808.

Houck, C.R., Joines, J.A. and Kay, M.G. (1995). A genetic algorithm for function optimisation: a MATLAB implementation, NCS-IE TR 95-09 (http://www.ie.ncsu.edu/mirage/GAToolBox/gaot/).

Irigoien, X., (1998) Gut clearance rate constant, temperature and initial gut contents: a review. *Journal of Plankton Research*. **20**: 997-1003.

Kolber, Z. S., O. Prasil and P. G. Falkowski, P.G. (1998). Measurements of variable chlorophyll fluorescence using fast repetition rate techniques: defining methodology and experimental protocols. *Biochimica et Biophysica Acta*, **1367**, 88-106.

Kolber, Z. S., and P. G. Falkowski, P.G. (1993). Use of active fluorescence to estimate phytoplankton photosynthesis in situ. *Limnology and Oceanography*, **38**(8), 1646-1665.

Mackas D. and R. Bohrer (1976) Fluorescence analysis of zooplankton gut contents and an investigation of diel feeding patterns. *Journal of Experimental Marine Biology and Ecology*, **25**, 77-85.

Martin A. P., I. P. Wade, K. J. Richards and K. J. Heywood (1998) The PRIME eddy. *Journal of Marine Research*, **56**, 439-462.

McCarthy, J. J. et al., (1977) Nitrogenous nutrition of the plankton in the Chesapeake Bay. 1. Nutrient availability and phytoplankton preferences. *Limnol. Oceanogr*. **22**, 996-1011.

McCartney M. S. and L. D. Talley (1982) The Subpolar Mode Water of the North Atlantic Ocean. *Journal of Physical Oceanography*, **12**, 1169-1188.

Morales C. E., A. Bedo, R. P. Harris and P. R. G. Tranter (1991) Grazing of copepod assembladges in the north-east Atlantic: the importance of the small size fraction. *Journal of Plankton Research*, **13**, 455-472.

Mulvenna, P. F. and G. Savidge (1992) A modified manual method for the determination of urea in seawater using diacetylmonoxime reagent. *Est. Coast. Shelf Sci.*, **34**, 429-438.

Orvik K. A., Ø. Skagseth and M. Mork (1999) Atlantic inflow to the Nordic Seas in the Svinøy section. *International WOCE Newsletter*, **37**, 18-20.

Pollard R. T., J. F. Read, N. P. Holliday and H. Leach (1999) Circulation and mode waters of the North Atlantic subpolar gyre in 1996. *International WOCE Newsletter*, **37**, 21-27.

Pollard R. T., M. J. Griffiths, S. A. Cunningham, J. F. Read, F. F. Pérez and A. F. Ríos (1996) Vivaldi 1991 - A study of the formation, circulation and ventilation of Eastern North Atlantic Central Water. *Progress in Oceanography*, **37**, 167-192.

Pollard R. T., U. Bathmann, C. Dubischar, J. F. Read and M. Lucas (2000) Zooplankton distribution and behaviour in the Southern Ocean from surveys with a towed Optical Plankton Counter. *Deep-Sea Research*, submitted.

Pollard R. T. and L. A. Regier (1992) Vorticity and vertical circulation at an ocean front. *Journal of Physical Oceanography*, **22**, 609-625.

RD Instruments, 1998: Field Service Technical Paper 003 (FST-003) Calculating Absolute Backscatter in Narrowband ADCPs, 01 MAY 1998

Read J. F. and R. T. Pollard (1992) Water masses in the region of the Iceland Færoes Front. *Journal of Physical Oceanography*, **22**, 1365-1378.

Read J. F. (2001). CONVEX-91: Water masses and circulation of the Northeast Atlantic subpolar gyre. *Progress in Oceanography*, **48**, 461-510.

Read J. F. and R. T. Pollard (1999) ACSOE-MAGE-NAE A long lived eddy in the Iceland Basin, 1998. WOCE North Atlantic Workshop, Kiel.

Read J. F., R. T. Pollard and U. Bathmann (2000) Physical and biological patchiness on an upper ocean transect from South Africa to the ice edge near the Greenwich Meridian. *Deep-Sea Research*, submitted.

Rixen, M., Allen, J. T., and Beckers, J.-M. (2001a). Non-synoptic versus pseudo-synoptic data sets: an assimilation experiment. in: Three-dimensional ocean circulation: lagrangian measurements and diagnostic. *Journal of Marine Systems*. 29(1-4), 313-333.

Rixen, M., Allen, J. T., and Beckers, J.-M. (2001b). Diagnosing vertical velocities using the QG omega equation: a relocation method to obtain pseudo-synoptic data sets. *Deep-Sea Research*. I, 48(6), 1347-1373.

Rixen, M., Beckers, J.-M., Brankart, J.-M. and Brasseur, P. (2000b). A numerically efficient data analysis method with error map generation. *Ocean Modelling*. Vol 2 (1-2), 45-60.

Rixen, M., J.-M. Beckers and J.T. Allen. (2001) Optimising sampling strategies by genetic algorithms. In 'International Liege Colloquium on Ocean Dynamics': Assimilation methods in coupled bio-physical 3D PE models.

Robertson J. E., C. Robinson, D. R. Turner, P. M. Holligan, A. J. Watson, P. Boyd, E. Fernandez and M. Finch (1993) The impact of a coccolithophore bloom on oceanic carbon uptake in the N.E. Atlantic during summer 1991. *Deep-Sea Research*, **21**, 297-314.

Robinson A.R. 1996 Physical processes, field estimation and an approach to interdisciplinary ocean modelling, *Earth_Sci. Rev*., 40, 3-54.

Robinson A.R., Arango H.G., Miller A.J., Warn-Varnas A., Poulain P.-M. & Leslie W.G. 1996 Real-time operational forecasting on shipboard of Iceland-Faeroe Front variability, *Bull. AMS*, 77, 243-259.

Roe H. S., G. Griffiths, M. Hartman and N. Crisp (1996) Variability in biological distributions and hydrography from concurrent Acoustic Doppler Current Profiler and SeaSoar surveys. *ICES Journal of Marine Science*, **53**, 131-138.

Sakshaug E. and D. Slagstad (1991) Light and productivity of phytoplankton in polar marine ecosystems: a physiological view. *Polar Research*, **10**, 69-85.

Sandwell, David T. (1987). Biharmonic spline interpolation of GEOS-3 and SEASAT altimeter data, *Geophysical Research Letters*, 2,139-142, 1987.

Saunders P. M. (1990) Cold outflow from the Færœ Bank Channel. *Journal of Physical Oceanography*, **20**, 29-43.

Saunders P. M. (1996) The flux of dense cold overflow water southeast of Iceland. *Journal of Physical Oceanography*, **26**, 85-95.

Smith W. H. F. and D. T. Sandwell (1997) Global seafloor topography from satellite altimetry and ship depth soundings. *Science*, **277**, 1956-1962.

Stefánsson U. and J. Olafsson (1991) Nutrients and fertility of Iceland waters. *Rit Fiskideildar*, **7**, 1-56.

Strickland, J.D.H. and Parsons, T.R. 1977 A Practical Handbook of Seawater Analysis. Fisheries Research Board of Canada, pp267-278

Talley L. D. (1999) Mode waters in the subpolar North Atlantic in historical data and during the WOCE period. *International WOCE Newsletter*, **37**, 3-6.

Thórdardóttir T. (1984) Primary production north of Iceland in relation to water masses in May-June 1970-1980. *ICES Comm. Meeting Biol. Oceanogr. Comm*, **L:20**, 1-17.

Tintoré J., D. Gomis, S. Alonso and G. Parrilla (1991) Mesoscale dynamics and vertical motion in the Alboran Sea. *Journal of Physical Oceanography*, **21**, 811-823.

Tyrrell T. and A. H. Taylor (1996) A modelling study of Emiliania huxleyi in the NE Atlantic. *Journal of Marine Systems*, **9**, 83-112.

van Aken H. M. and G. Becker (1996) Hydrography and through-flow in the north-eastern North Atlantic Ocean: the NANSEN project. *Progress in Oceanography*, **38**, 297-346.

Welschmeyer, N. A. (1994) Fluorometric analysis of chlorophyll-*a* in the presence of chlorophyll-*b* and phaeopigments. *Limnol. Oceanogr*. **39**, 1985-1992

White M. A. and K. J. Heywood (1995) Seasonal and interannual changes in the North Atlantic subpolar gyre from Geosat and TOPEX/POSEIDON altimetry. *Journal of Geophysical Research*, **100**, 24931-24941.

Zhang, J.W. and Nurser, A.J.G., (2000). Eddy/Mixed-layer interactions at a front. *Journal of Geophysical Research*. 105(C9), 21851-21868.